THE ROLE OF NATURAL ORGANIC LIGANDS IN TRANSFORMATIONS OF IRON CHEMISTRY IN SEAWATER AND THEIR EFFECT ON THE BIOAVAILABILITY OF IRON TO MARINE PHYTOPLANKTON.

LOUISA NORMAN

Submitted in fulfilment of the requirements for the degree

of Doctor of Philosophy in Science,

Plant Functional Biology and Climate Change Cluster,

School of the Environment,

University of Technology, Sydney

June 2014

CERTIFICATE OF AUTHORSHIP/ORIGINALITY

I certify that the work in this thesis has not been submitted for a degree nor has it been submitted as part of the requirements for a degree except as fully acknowledged within the text.

I also certify that the thesis has been written by me. Any help that I have received in my research work and the preparation of the thesis itself has been acknowledged. Furthermore, I certify that all information sources and literature used are indicated in the thesis.

Louisa Norman

ACKNOWLEDGEMENTS

This thesis is dedicated to my parents and my sister who have provided unconditional love and support from the other side of the world for the past 4 years. I don't think any of us ever imagined that the very average high school student would now be sitting here writing the acknowledgements for her Ph.D thesis. Thank you for shaping me into the person I am today as it has allowed me to push myself further than I ever thought possible.

Special thanks are given to my supervisors; Professor Christel Hassler for imparting her wealth of knowledge to me and for her encouragement throughout this process. Her enthusiasm for her research is inspiring. To Assoc. Professor Martina Doblin, for her guidance and motivation which have been invaluable, particularly in the latter stages of this journey. Professor David Waite who provided facilities and intellectual support that were instrumental to the success of part of this thesis, and to Professor Greg Skilbeck for his intellectual contribution to the finished product. My appreciation for what you all have contributed has no measure.

Thank you to Drs Andrew Bowie, Laurie Burn-Nunes, Edward Butler, Nagur Cherukuru, Michael Ellwood, Jason Everett, Carol Mancuso Nichols, Veronique Schoemann, Sutinee Sinutok, Ashley Townsend, and Isabelle Worms, Professors Vera Slaveykova and Grant McTainsh, and Lesley Clementson, Alicia Navidad, Charlotte Robinson, Claire Thompson, Roslyn Watson who have provided support in the form of analysis, data and methodologies that allowed this thesis to come to fruition. Your individual contributions are acknowledged within this thesis.

Thank you to the staff and students at the UNSW Water Research Centre in the School of Engineering for their help and friendship during my few months there. Special thanks are given to Dr An Ninh Pham who, when faced with a biologist in chemists' clothing, provided all the guidance and support I needed to make iron redox chemistry just that bit easier. I sincerely appreciate his time and kindness.

Thanks also are given to the staff and students at the Institut F.-A. Forel, Université de Genève for their encouragement and friendship during my stay in Geneva; particularly Sophie Moisset, Sonia Blanco Ameijeras, Rebecca Flueck and Giulia Cheloni who welcomed me so warmly into their circle.

Warmest thanks are given to all my colleagues within C3 here at UTS. Special thanks are extended to Drs Katherina Petrou and Daniel Nielsen for their friendship, patience, laughs and 'winesday'; to Charlotte Robinson, Kirralee Baker, Dale Radford, Joh Howes and Isobel Cummings, you are all truly amazing people; to Dr Andy Leigh and Peter Jones for their kindness and encouragement, and the provision of a stress reliever in the form of their cat, Chai; and to Professor Peter Ralph and Carolyn Carter who were incredibly kind and supportive when I returned from sea a wounded soldier, and lastly to the wonderful technical staff.

Throughout this research I have been in receipt of financial support from a number of sources and I would like to thank the University of Technology for the provision of an IRS scholarship, and the Australian Research Council which provided the research funds and a stipend that allowed this project to happen (Discovery Project DP1092892 and LIEF grant LE0989539).

And finally, to those endless cups of tea that I have consumed. I have used it to drown sorrows, celebrate achievements; to revive and relax…..it is a most remarkable beverage.

PUBLICATIONS

Publications resulting directly from this thesis:

Chapter 1:
Norman, L., Cabanes, D., Blanco-Ameijerias, S., Moisset, S., Hassler, C.S. 2014. Iron biogeochemistry in aquatic systems: from source to bioavailability. *Chemia.* 68, 764 – 771.

Chapter 4:
Norman, L., Worms, I.A.M., Angles, E., Bowie, A.R., Mancuso Nichols, C., Pham, A.N., Slaveykove, V.I., Townsend, A.T., Waite, T.D., Hassler, C.S. The role of bacterial and algal exopolymeric substances in iron chemistry. *Mar. Chem*. **In press.**

Chapter 4:
Hassler, C.S., **Norman, L**., Mancuso Nichols, C., Clementson, L.A., Robinson, C., Schoemann, V., Watson, R.J., Doblin, M.A. Exopolymeric substances can relieve iron limitation in oceanic phytoplankton. *Mar. Chem*. **In press.**

TABLE OF CONTENTS

LIST OF FIGURES

bacterioplankton, is represented separately (FeSidTr). Other non-specific uptake pathways (endocytosis, direct permeation and an ion channel) are shown. Once inside the microorganism, Fe (Fe_{int}) reacts with intracellular biological ligands (L_{bio}, e.g. Chlorophyll-*a*), is stored (e.g. vacuole, ferritin) or is involved in cellular homeostasis via gene regulation (grey arrow with ± symbol). Release of Fe biological organic ligands (L_{rel}, such as EPS and siderophores) can exert a feedback in the control of both Fe chemistry and bioavailability. Dotted, dashed and full arrows represent aggregation/disaggregation, transfer, and chemical reaction (complexation, redox), respectively. (From Hassler et al, 2011b).

Fig. 2.1. Sea surface temperature (SST) and Chlorophyll-*a* (μg L^{-1}) plots showing the study area and sampling locations for natural humic substance-like material and nutrient enrichment experiments. Natural samples were collected from at variety of watermass types (river plume, inner shelf, outer shelf, and oceanic (cold-core cyclonic eddy (CCE) and East Australia Current (EAC)), and seawater collected for the nutrient experiments was sampled from the EAC and CCE.

Fig. 2.2 Calibration curve used for the comparison of methods to determine the concentration of electrochemically detected humic substance-like (HS-like) material. Suwannee River Fulvic Acid (SRFA) was used as the HS-like standard in concentrations between 20 and 480 μg L^{-1}. i_p represents the peak height in nA of electrochemically detected Fe′-reactive organic material. Errors = SD of triplicate samples.

Fig. 2.3 Relationship between the concentration of humic substance-like (HS-like) material (log transformed), and Chl-*a* fluorescence (CTD derived) from samples taken during the SS2010-V09 Tasman Sea voyage (*RV Southern Surveyor*, 15th to 31st October 2010, austral spring). Samples were collected at 5 m, 15 m, and the depth of the chlorophyll maximum from water masses comprising river plume, inner shelf and outer shelf waters, and oceanic waters. Panel A indicates the weak positive relationship with Clarence River plume samples included (circled on the plot), Panel B indicates the relationship with these samples excluded.

Fig. 2.4 Relationships between the concentration of humic substance-like (HS-like) material, reduction peak position (E_p, V vs Ag/AgCl electrode) or sensitivity with temperature, salinity, Chl-*a* fluorescence (CTD derived), and turbidity (light transmission) from samples taken during the SS2010-V09 Tasman Sea voyage (*RV Southern Surveyor*, 15th to 31st October 2010, austral spring). Samples were collected at 5 m, 15 m, and the depth of the chlorophyll maximum from water masses comprising river plume, inner shelf and outer

shelf waters, and oceanic waters. Due to extremely high HS-like concentrations from the Clarence River Plume this data was log transformed to allow for clearer graphical representation. Clarence River Plume samples are circled on the plots.

Fig. 2.5 Concentration of macronutrients (ammonia (NH_4), nitrate + nitrite (NO_X), silicic acid ($Si(OH)_4$), and phosphate (PO_4), μmol L^{-1}) in experimental bottles measured at T0 and after 72-h shipboard, nutrient-enrichment experiments undertaken during the SS2010-V09 Tasman Sea voyage (*RV Southern Surveyor*, 15th to 31st October 2010, austral spring). The experiments were conducted in 200–210-μm filtered seawater collected from the depth of the chlorophyll maximum at two sites in the Tasman Sea; East Australia Current (EAC, 29 1 °S 154 3°E), and a cold-core eddy (CCE, 32 2°S 153 8°E). T0 = unamended seawater at the start of the experiment. The treatments were; unamended control (Con), nitrate (N, 10 μM), nitrate + inorganic Fe (NFe, 10 μM + 1 nM), silicate (Si, 10 μM), mixed nutrients (Mix; NO_3 + Fe + Si + P, 10 μM + 1 nM + 10 μM + 0.625 μM), Suwannee River fulvic acid exposed to light (FAL, 200 μg L^{-1}), Suwannee River fulvic acid dark incubation (FAD, 200 μg L^{-1}). Daily additions of nutrients were given to the East Australia Current incubations, and a single initial nutrient addition was given to the cold-core eddy incubations. Errors = SD of triplicate incubations except for EAC FAD where errors represent half interval (range) of duplicates incubations.

Fig. 2.6 Concentration of dissolved Fe (dFe, nM) measured at the conclusion of two 72-h shipboard nutrient-enrichment experiments undertaken during the SS2010-V09 Tasman Sea voyage (*RV Southern Surveyor*, 15th to 31st October 2010, austral spring). The experiments were conducted in 200–210-μm filtered seawater collected from the depth of the chlorophyll maximum at two sites in the Tasman Sea; East Australia Current (EAC, 29 1 °S 154 3°E), and a cold-core eddy (CCE, 32 2°S 153 8°E). Treatments were as per Fig. 2.5. Samples for the analysis of dFe were taken from replicates 1 and 2 of each treatment, therefore duplicate data points are shown for each treatment and experiment.

Fig. 2.7 Cell abundance (cells mL^{-1}) of bacteria (A), and picophytoplankton *Prochlorococcus* (B), *Synechococcus* (C), small eukaryotes (D) and large eukaryotes (E) measured by flow cytometry at T0 and at the conclusion of two 72-h shipboard nutrient-enrichment experiments undertaken during the SS2010-V09 Tasman Sea voyage (*RV Southern Surveyor*, 15th to 31st October 2010, austral spring). The experiments were conducted in 200–210-μm seawater collected from the depth of the chlorophyll maximum at two sites East Australia Current (EAC, 29 1 °S 154 3°E), and a cold-core eddy (CCE, 32 2°S 153 8°E). T0 = unamended seawater at the start of the experiment. Treatments were as per Fig. 2.5. Error = SD of

triplicate incubations except for EAC FAD where errors represent half interval (range) of duplicate incubations. Note differences in y-axis scale.

Fig. 2.8 Concentration of total chlorophyll-*a* (TChl-*a*, mg m^{-3}) measured at T0 and at the end of two 72-h shipboard nutrient-enrichment experiments undertaken during the SS2010-V09 Tasman Sea voyage (*RV Southern Surveyor*, 15th to 31st October 2010, austral spring). The experiments were conducted in 200–210-µm filtered seawater collected from the depth of the chlorophyll maximum at two sites East Australia Current (EAC, 29 1 °S 154 3°E), and a cold-core eddy (CCE, 32 2°S 153 8°E). T0 = unamended seawater at the start of the experiment. Treatments were as per Fig. 2.5. Error = SD of triplicate incubations except for EAC FAD where errors represent half interval (range) of duplicates incubations.

Fig. 2.9 Concentration of biomarker pigments (mg m^{-3}) measured at T0 and at the end of two 72-h shipboard nutrient-enrichment experiments undertaken during the SS2010-V09 Tasman Sea voyage (*RV Southern Surveyor*, 15th to 31st October 2010, austral spring). The experiments were conducted in 200–210-µm filtered seawater collected from the depth of the chlorophyll maximum at two sites East Australia Current (EAC, 29 1 °S 154 3°E), and a cold-core eddy (CCE, 32 2°S 153 8°E). T0 = unamended seawater at the start of the experiment. Treatments were as per Fig. 2.5.

Fig. 2.10 Carbon (C) fixation rates measured from ^{14}C incubations at the end of two 72-h shipboard nutrient-enrichment experiments undertaken during the SS2010-V09 Tasman Sea voyage (*RV Southern Surveyor*, 15th to 31st October 2010, austral spring). The experiments were conducted in 200–210-µm filtered seawater collected from the depth of the chlorophyll maximum at two sites East Australia Current (EAC, 29 1 °S 154 3°E), and a cold-core eddy (CCE, 32 2°S 153 8°E). T0 = unamended seawater at the start of the experiment. Treatments N, NFe, and FAL were as per Fig. 2.5. Error = SD of triplicate incubations.

Fig. 2.11 Concentration of electrochemically detected humic substance-like (HS-like) substances measured at the conclusion of two 72-h shipboard nutrient-enrichment experiments undertaken during the SS2010-V09 Tasman Sea voyage (*RV Southern Surveyor*, 15th to 31st October 2010, austral spring). The experiments were conducted in 200–210-µm filtered seawater collected from the depth of the chlorophyll maximum at two sites, East Australia Current (EAC; 29 1 °S 154 3°E), and a cold-core eddy (CCE; 32 2°S 153 8°E). T0 = unamended seawater at the start of the experiment. Treatments were as per Fig. 2.7. The concentration of HS-like material is expressed as Suwannee River Fulvic Acid equivalents

(SRFA eq) in μg L^{-1}. Error = SD of triplicate incubations except for EAC FAD where errors represent half interval (range) of duplicates incubations.

***** Significantly higher HS-like concentration compared to all other EAC treatments, except FAL and FAD ($p = 0.003$).

† Significantly higher HS-like concentration compared to CCE T0 and control ($p = 0.007$).

‡ Significantly lower HS-like concentration compared to CCE T0 and control ($p = 0.014$).

Fig. 2.12 Relationships between the concentration of humic substance-like (HS-like) material and Silicic acid ($Si(OH)_4$), phosphate (PO_4) and dissolved Fe (dFe) at the conclusion of a 72-h shipboard nutrient-experiment undertaken during the SS2010-V09 Tasman Sea voyage (*RV Southern Surveyor*, 15th to 31st October 2010, austral spring). The experiment was conducted in 200–210-μm filtered seawater collected from the depth of the chlorophyll maximum in the East Australia Current (EAC; 29 1 °S 154 3°E). Treatments were as per Fig. 2.5. Panel A = $Si(OH0)_4$ all data; Panel B = treatments where $Si(OH)_4 < 0.7$ μmol L^{-1}; Panel C = treatments where $Si(OH0)_4 > 20$ μmol L^{-1}; Panel D = PO_4 all data; Panel E = PO_4 enrichment treatment (Mix) excluded; Panel F = dFe all data; Panel G = dFe-enrichment > 10 nM (Mix treatment) excluded. High concentrations, subsequently excluded, are circled to highlight (panels A, D, and F).

Fig. 3.1 Cruise track from the Primary productivity induced by Iron and Nitrogen in the Tasman Sea (PINTS) voyage (RV *Southern Surveyor*, Jan-Feb 2010). Transect stations are shown as circles and process stations as diamonds. Profiles presented in this chapter were from two process stations P1 (30.0 °S, 156.0 °E, also Stn 5) and P3 (46.2 °S, 159.5 °E, also Stn 12) and from Stn 14, 44.6 °S, 149.4 °E. Stn 14 was a reoccupation of process station 3 from the SAZ-Sense expedition (*Aurora Australis*, January–February 2007). Water for the Fe-enrichment experiments was collected stations P1 and P3. Thicker solid lines indicate the East Australian Current (EAC), Tasman Front (TF), and EAC
Extension. The dashed line represents the path of the subtropical front (STF) (From Hassler et al., 2014).

Fig. 3.2 Seawater depth profiles of dissolved nutrients nitrate + nitrite (NO_X; panel A), reactive phosphorus (PO_4; panel B), and silicic acid ($Si(OH)_4$; panel C), measured at stations P1 (30.0 °S, 156.0 °E,), P3 (46.2 °S, 159.5 °E,) and Stn 14 (44.6 °S, 149.4 °E) collected during the PINTS voyage (RV *Southern Surveyor*, Jan-Feb 2010).

Fig. 3.3 Seawater depth profiles of total chlorophyll-*a* (TChl-*a* μg L^{-1}) measured at stations P1 (30.0 °S, 156.0 °E, depths 15 to 125 m), P3 (46.2 °S, 159.5 °E, depths 15 to 80 m) and Stn 14 (44.6 °S, 149.4 °E, depths 15 to 50 m) collected during the PINTS voyage (RV *Southern Surveyor*, Jan-Feb 2010).

Fig. 3.4 Seawater depth profiles (15 to 1000m) from process stations P1 (30.0 °S, 156.0 °E), and P3 (46.2 °S, 159.5 °E) and Stn 14 (44.6 °S, 149.4 °E) collected during the PINTS voyage (RV *Southern Surveyor*, Jan-Feb 2010). Concentration of dissolved Fe (dFe, nM) and the concentration of electrochemically detected Fe′-binding organic ligands (SumL, nM) and their calculated conditional stability constant (Log $K_{Fe'L}$) are presented together with the concentration of humic substance-like (HS-like) material. HS-like material is expressed as Suwannee River Fulvic Acid (SRFA) μg L^{-1}.

Fig. 3.5 Relationship between the concentration of Fe-binding organic ligands (ΣL) and the conditional stability constant (Log $K_{Fe'L}$) for process station P1 (30.0 °S, 156.0 °E), process station P3 (46.2 °S, 159.5 °E) and Stn 14 (44.6 °S, 149.4 °E). Samples were collected during the PINTS voyage (RV *Southern Surveyor*, Jan-Feb 2010; Hassler et al., 2014).

Fig. 3.6 Relationships between the concentration of total chlorophyll-*a* (TChl-*a*) and Fe-binding organic ligands (ΣL), TChl-*a* and ligand conditional stability constant (log $K_{Fe'L}$) at depths between 15 and 125 m at process station P1 (30.0 °S, 156.0 °E), and TChl-*a* and ΣL at depths between 15 and 50 m, humic substance-like (HS-like) material and SumL at depths between 15 and 300 m and at Stn 14 (44.6 °S, 149.4 °E). Samples were collected during the PINTS voyage (RV *Southern Surveyor*, Jan-Feb 2010; Hassler et al., 2014). HS-like material is expressed as Suwannee River Fulvic Acid (SRFA) equivalent in μg L^{-1}.

Fig. 3.7 Relationships between dissolved Fe (dFe) concentration (nM) and macronutrients nitrate + nitrite (NO_X), phosphate (PO_4) and silicic acid ($Si(OH)_4$) (μmol L^{-1}) at process station P3 (46.2 °S, 159.5 °E) at depths between 15 and 300 m. Samples were collected during the PINTS voyage (RV *Southern Surveyor*, Jan-Feb 2010; Hassler et al., 2014).

Figure 3.8 Concentrations of dissolved Fe (dFe, nM) and relative concentration (%) of labile Fe (Fe_{Labile}) associated with Fe enrichment experiments using phytoplankton communities collected from two sites in the Tasman Sea, P1 (30.0 °S, 156.0 °E, panels A and C) and P3 (46.2 °S, 159.5 °E, panels B and D) during the PINTS voyage (RV *Southern Surveyor*, Jan-Feb 2010). The data presented comes from unamended seawater (T0) and after 4-d incubation in samples with and without the addition of Fe and organic ligands. Treatments measured after 4-d incubation comprised an unamended control (Con), inorganic Fe only (2 nM, Fe),

desferrioxamine B ([15 nM], DFB), glucuronic acid ([15 nM], GLU), natural pelagic bacterial exopolymeric substances ([0.8 nM], EPS), fulvic acid ([100 μg L^{-1}], as Suwannee River Fulvic Acid, FA), and two treatments containing Australian desert dust (D1, 2009 Brisbane dust storm, and D2, red composite, both from the Buronga region, NSW) which were predicted to release ~2 nM Fe. DFB, EPS, GLU and FA treatments were all enriched with 2 nM inorganic Fe. Closed symbols indicate samples with phytoplankton present, open symbols indicate samples where phytoplankton were absent (0.2 μm filtered, single incubations). Error bars represent half-interval of duplicate samples; where no error bars are present the data presented is from a single sample.

Figure 3.9 Concentration of organic ligands and calculated conditional stability constants (log $K_{Fe'L}$) associated with Fe-enrichment experiments using phytoplankton communities collected from two sites in the Tasman Sea, P1 (30.0 °S, 156.0 °E, panels A and C) and P3 (46.2 °S, 159.5 °E, panels B and D) during the PINTS voyage (RV *Southern Surveyor*, Jan-Feb 2010). The data presented comes from unamended seawater (T0) and after 4-d incubation for samples with and without the addition of Fe and organic ligands. Treatments were as per Fig. 3.8. Closed symbols indicate samples with phytoplankton present, open symbols indicate samples where phytoplankton were absent (0.2-μm filtered, single incubations). Where two ligand classes were detected, stronger ligands are indicated by a red symbol and weaker ligands by a blue. Error bars represent half-interval of duplicate samples; where no error bars are present the data presented is from a single sample.

Figure 3.10 Concentration of humic substance-like material (HS-like), expressed as Suwannee River Fulvic Acid equivalents (SRFA eq) in μg L^{-1}, associated with Fe enrichment experiments using phytoplankton communities collected from two sites in the Tasman Sea, P1 (30.0 °S, 156.0 °E, panel A) and P3 (46.2 °S, 159.5 °E, panels B) during the PINTS voyage (RV *Southern Surveyor*, Jan-Feb 2010). The data presented comes from unamended seawater (T0) and after 4-d incubation for samples with and without the addition of Fe and organic ligands. Treatments were as per Fig. 3.8. Closed symbols indicate samples with phytoplankton present, open symbols indicate samples where phytoplankton were absent (0.2-μm filtered, single incubations). Error bars represent half-interval of duplicate samples; where no error bars are present the data presented is from a single sample. Note difference in y-axis scale.

Figure 3.11 Changes in total chlorophyll-*a*, (TChl-*a*) (A) and F_V/F_M (B) from Fe-enrichment experiments after 4-d incubation with and without the addition of organic ligands. Water for the experiments was collected from two sites in the Tasman Sea, P1 (30.0 °S, 156.0 °E)

and P3 (46.2 °S, 159.5 °E) during the PINTS voyage (RV *Southern Surveyor*, Jan.-Feb. 2010). Treatments were as per Fig. 3.8 Error bars represent the half interval of duplicate samples. T0 values not shown; see Table 3.1.

Figure 3.12 Total Chl-*a* concentrations (TChl-*a*) of size fractionated phytoplankton communities from Fe-enrichment experiments after 4-d incubation with and without the addition of organic ligands. Pico-, nano-, microphytoplankton were defined by sequential filtration as > 0.7–2 µm, 2–10 µm, ≥10 µm, respectively. Water for the experiments was collected from two sites in the Tasman Sea, P1 (30.0 °S, 156.0 °E) and P3 (46.2 °S, 159.5 °E) during the PINTS voyage (RV *Southern Surveyor*, Jan-Feb 2010). Treatments were as per Fig. 3.8 Error bars represent the half interval of duplicate samples. Dashed lines represent a comparison of the Fe-ligand complexes with Fe addition only.

Figure 3.13 Size-fractionated biomarker pigment data (measured by HPLC) from Fe enrichment experiments after 4 d incubation with and without the addition of organic ligands. Pico-, nano-, microphytoplankton were defined by sequential filtration as > 0.7–2 µm, 2–10 µm, ≥10 µm, respectively. Water for the experiments was collected from the depth of the fluorescence maximum at two sites in the Tasman Sea, P1 (30.0 °S, 156.0 °E) and P3 (46.2 °S, 159.5 °E) during the PINTS voyage (RV *Southern Surveyor*, Jan.-Feb. 2010). Treatments were as per Fig. 3.8.

Figure 4.1 Molar mass distribution fractograms of exopolymeric substances (EPS) obtained by FFF-RI-UV-ICPMS using a linear decrease in cross-flow rate. Differential refractive index relative intensity, absorbance measured at λ = 254 nm (upper panel of each sub figure), and ^{56}Fe relative intensity (lower panel of each sub figure) from EPS isolated from Antarctic sea ice bacteria, sub-Antarctic zone bloom (SAZ bloom) and axenic algal cultures (*Phaeocystis antarctica* and *Emiliania huxleyi*) . The grey zone following 40-min elution time illustrates the end of applied cross flow and the end of the fractionation corresponding to elution of compounds > 950 kDa as determined using PSS molecular weight calibration.

Figure 4.2 ^{56}Fe eluograms (lower panel of each sub figure) showing hydrodynamic radius (nm) of components of exopolymeric substances (EPS). For comparison refractive index relative intensity (lower panels), absorbance measured at λ = 254 nm (UV, upper panels), and fluorescence (fluo, upper panels) are shown. EPS were isolated from Antarctic sea ice bacteria, sub-Antarctic zone bloom (SAZ bloom) and axenic algal cultures (*Phaeocystis antarctica* and *Emiliania huxleyi*).

Figure 4.3 ^{56}Fe eluogram after *in silico* deconvolution of Fe distribution associated with Antarctic sea ice bacterial EPS. Maximum Fe signal intensity (red line) associated with components with hydrodynamic radii (R_h) of ~29 nm. Three further prominent components measured with R_h of ~ 26 nm, 40 nm and 60 nm (green lines).

Fig. 4.4 The solubility of Fe in the presence or absence of bacterial or algal exopolymeric substances (EPS) in both the colloidal (0.02 um to 0.2 um) and soluble (<0.02 um) size fractions. EPS isolates were from an Antarctic sea ice bacteria, a natural phytoplankton bloom from the sub-Antarctic zone (SAZ bloom), and from axenic algal cultures of *Phaeocystis antarctica* and *Emiliania huxleyi*. An experimental control solution of inorganic Fe only is also presented. Experimental medium was synthetic seawater (pH 8.0). Error bars indicate half interval, n=2.

Fig. 4.5 The effect of Fe associated with EPS (Fe-EPS) on the growth of the Southern Ocean diatom, *C. simplex,* over 187-h incubation at 4 °C and at 50 µmol photons m^{-2} s^{-1}. Growth curve in terms of cells numbers (A) and maximum quantum yield (F_V/F_M, B) are presented. Fe concentration in the Tasman Sea surface seawater (seawater) medium was 0.56 nM. The growth of *C simplex* in the presence of Fe bound to EPS was compared to both inorganic Fe and seawater control. Additions of EPS and inorganic Fe provided an additional 1 nM Fe to the seawater medium. EPS isolates were from an Antarctic sea ice bacteria, a natural phytoplankton bloom from the sub-Antarctic zone (SAZ bloom), and from axenic algal cultures of *Phaeocystis antarctica and Emiliania huxleyi*. Error bars indicate standard deviation, *n*=3.

Fig. 5.1 Relative concentration of 10 µM TAC-Labile Fe (Fe_{Labile}) as a percentage of the total dissolved Fe measured in the 0.2-µm and 0.02-µm filtered fractions of experimental samples from two replicate experiments simulating the wet deposition of Australian mineral dust into the Southern Ocean. The dust used was collected during a large dust storm over Brisbane, QLD., and resuspended in rainwater collected in the Tasman Sea (31° 35.849'S 178° 00.00'E, GP13 GEOTRACES voyage, 27/05/2011) before being exposed to UV + visible light (UV, 2000 µE), visible light only (VIS, 2000 µE), or kept in darkness (Dark). Resuspended, treated dust was added to synthetic seawater to give a dust enrichment of 0.5 mg L^{-1}. Where no bars are present the concentration of Fe_{Labile} was below detection limit (0.05 nM) after synthetic seawater Fe correction.

Fig. 5.2 Concentration of Fe'-binding organic ligands (nM; A) and conditional stability constants (Log $K_{Fe'L}$; B) in the 0.2-µm and 0.02-µm-filtered fractions of experimental

samples from two replicate experiments simulating the wet deposition of Australian mineral dust into the Southern Ocean. Treatments were as per Fig. 5.1. Ligand concentration and Log $K_{Fe'L}$ were calculated using total dissolved Fe concentrations.

Fig. 5.3 Concentration of electrochemically detected Fe'-binding humic substance-like material (HS-like; μg L^{-1} SRFA equivalent) in unfiltered, 0.2-μm and 0.02-μm filtered fractions of experimental samples from two replicate experiments simulating the wet deposition of Australian mineral dust into the Southern Ocean. Treatments were as per Fig. 5.1. Errors = standard deviation of triplicate samples. Where no bars are present the concentration of HS-like was below detection limit (1.49 μg L^{-1} SRFA Eq.).

Fig. 5.4 Concentration of total hydrolysable saccharides (reported as μM C) measured in 0.2-μm and 0.02-μm filtered experimental samples from two experiments simulating the wet deposition of Australian mineral dust into the Southern Ocean. Treatments were as per Fig. 5.1. Error = standard deviation of triplicate samples.

Figure 5.5 The effect of Fe associated with Australian mineral dust on the growth of the Southern Ocean diatom *C. simplex* over 326 h incubation period at 4 °C and 50 μmol photons m^{-2} s^{-1}. Growth curves (A), Cell volume, μm^3 (B) and F_V/F_M (C) were compared to an inorganic Fe (1 nM) incubation. The dust used was collected during a large dust storm over Brisbane, QLD., and resuspended in rainwater collected in the Tasman Sea (31°35.849'S 178°00.00'E, GP13 GEOTRACES voyage, 27/05/2011) before being exposed to UV + visible light (UV, 2000 μE), visible light only (VIS, 2000 μE), or kept in darkness (Dark). Resuspended, treated dust was added to synthetic seawater to give a dust enrichment of 0.5 mg L^{-1}. Error = standard deviation of triplicate samples.

LIST OF TABLES

µm filtered seawater collected from the depth of the chlorophyll maximum at two sites A) East Australia Current (EAC; 29 1 °S 154 3°E), and B) cold-core eddy (CCE; 32 2°S 153 8°E). The treatments included in these analyses were; unamended control, nitrate (NO_3, 10 µM), nitrate + inorganic Fe (NO_3 + Fe, 10 µM + 1 nM), silicate (Si, 10 µM), mixed nutrients (Mix; NO_3 + Fe + PO_4, 10 µM + 1 nM + 0.625 µM).

Table 2.5 Instrument sensitivity and position of the reduction peak position ($E_{p,}$ V vs Ag/AgCl electrode) derived from the determination of humic substance-like (HS-like) material. Samples analysed were from nutrient-enrichment experiments at T0 (unamended seawater) and after 4 d incubation in samples with and without the addition of nutrients. The experiments were conducted in 200–210-µm filtered seawater collected from the depth of the chlorophyll maximum at two sites A) East Australia Current (EAC, 29 1 °S 154 3°E), and B) a cold-core eddy (CCE, 32 2°S 153 8°E). Treatments were as per table 2.4.

Table 2.6 Concentration range of humic-substance like (HS-like) material measured using cathodic stripping voltammetry by Laglera et al. (2007) and Laglera and van den Berg (2009).

Table 3.1 Depth of chlorophyll maximum (Cmax), and in situ concentration of total chlorophyll *a* (TChl-*a*), nutrients (silicate (Si), nitrate + nitrite (NO_x), phosphate (PO_4)), and F_V/F_M from process stations P1 (30.0 °S, 156.0 °E), and P3 (46.2 °S, 159.5 °E). Water was collected at the depth of the fluorescence/chlorophyll-*a* max (Cmax) from these two stations to conduct Fe-enrichment experiments during the PINTS voyage (RV *Southern Surveyor*, Jan-Feb 2010).

Table 3.2 Daily uptake of dissolved Fe (dFe, nM) from Fe enrichment experiments at the conclusion of a 4-day incubation in samples with and without the addition of organic ligands. Water for the experiments was collected from two sites in the Tasman Sea, P1 (30.0 °S, 156.0 °E) and P3 (46.2 °S, 159.5 °E) during the PINTS voyage (RV *Southern Surveyor*, Jan-Feb 2010). Treatments measured after 4-d incubations comprised an unamended control (Con), two treatments containing Australian desert dust (D1, 2009 Brisbane dust storm, and D2, red composite from the Buronga region) which were predicted to release ~2 nM Fe, inorganic Fe only (2 nM), and organic ligands desferrioxamine B (DFB [15 nM]) natural pelagic bacterial exopolymeric substances (EPS, [0.8 nM]), glucuronic acid (GLU [15 nM]), and fulvic acid (FA, [100 µg L^{-1}], as Suwannee River Fulvic Acid). DFB, EPS, GLU and FA treatments also contained 2 nM inorganic Fe. Unfiltered = incubations where phytoplankton were present, filtered = incubations where phytoplankton was absent (0.2-µm filtered).

Errors are the half interval of duplicate samples. Where no errors are stated the values are from a single sample.

Table 3.3 Instrument sensitivity (expressed as Suwannee River Fulvic Acid equivalents (SRFA eq) in μg L^{-1}) and the reduction peak potential ($E_{p,}$ V vs Ag/AgCl electrode) from the determination of humic substance-like (HS-like) material from Fe enrichment experiments at T0 (unamended seawater) and after 4-d incubation in samples with and without the addition of organic ligands. Water for the experiments was collected from two sites in the Tasman Sea, P1 (30.0 °S, 156.0 °E) and P3 (46.2 °S, 159.5 °E) during the PINTS voyage (RV *Southern Surveyor*, Jan-Feb 2010). Treatments were as per Table 3.2. Unfiltered = incubations where phytoplankton were present, filtered = incubations where phytoplankton absent (0.2-μm filtered). Errors are the half interval of duplicate samples. Where no errors are stated the values are from a single sample.

Table 3.4 Variability in instrument sensitivity between experimental treatments after 4-d incubations in samples with and without the addition of organic ligands. Water for the experiments was collected at process station P3 (46.2 °S, 159.5 °E) in the Tasman Sea during the PINTS voyage (RV *Southern Surveyor*, Jan-Feb 2010). Treatments were as per Table 3.2. Statistically significant differences ($p \leq 0.05$) are highlighted in bold type.

Table 4.1 Constituents of synthetic seawater used for humic substance-like analysis. Based on AQUIL media as per Price et al. (1989) using major salt only. Final pH = 8.00

Table 4.2 Composition of exopolymeric substances (EPS) isolated from an Antarctic sea ice bacteria, a natural sub-Antarctic zone bloom (SAZ bloom) and axenic algal cultures (*Phaeocystis antarctica* and *Emiliania huxleyi)*. Relative concentration (%) of protein, uronic acid and neutral sugars present are shown together with total hydrolysable saccharides (reported as mmol C g^{-1} EPS).

Table 4.3 Mass distribution parameters for differential refractive index (DRI), UVD, and ^{56}Fe in the low molar mass (LMM) region of the respective signal fractograms exopolymeric substances (EPS) isolated from Antarctic sea ice bacteria, sub-Antarctic zone bloom (SAZ bloom) and axenic algal cultures (*Phaeocystis antarctica* and *Emiliania huxleyi*). *Mw* = weight average molar mass, *Mn* = number average molar mass, *Mp* = maximum peak intensity. Calculation for molar mass dispersity ($Đ_M$), $Đ = Mw/Mn$.

Table 4.4 Concentration of macronutrients (NO_X, NO_2, NH_3, PO_4) present in exopolymeric substances (EPS) isolated from Antarctic sea ice bacteria, a sub-Antarctic zone bloom (SAZ

bloom) and axenic algal cultures (*Phaeocystis antarctica* and *Emiliania huxleyi*). Data reported as nmol g^{-1} EPS.

Table 4.5 Concentration of trace metals present in exopolymeric substances (EPS) isolated from sea ice bacteria, a natural sub-Antarctic zone bloom (SAZ bloom) and axenic algal cultures (*Phaeocystis antarctica* and *Emiliania huxleyi*). Data reported as nmol g^{-1} EPS. <DL = below detection limit.

Table 4.6 Fe biogeochemistry associated with exopolymeric substances (EPS) isolated from an Antarctic sea ice bacteria, a natural sub-Antarctic zone bloom (SAZ bloom) and axenic algal cultures (*Phaeocystis antarctica* and *Emiliania huxleyi*). The overall % of labile iron (Fe_{Labile}) and the concentration of ligands associated with strong binding affinities ([L_1]), weaker binding affinities ([L_2]) and the sum of all ligands ([sumL]), together with the calculated conditional stability constant relative to inorganic iron (log $K_{Fe'L1}$, log $K_{Fe'L2}$ or log $K_{Fe'sumL}$) is presented. Electrochemically detected humic substance-like (HA-like) material is also shown and expressed as Suwanee River Fulvic Acid (SRFA) equivalents. Results are from a sample set measured after 24 h equilibration, and a further set measured after 9 weeks. Both sets were equilibrated at 4 °C in the dark.

Table 4.7 Pseudo-first-order rate constant (k' s^{-1}) and half-life ($t_{½}$) for Fe(II) (30 nM) oxidation at ambient laboratory temperature (22 °C) and 4 °C in 0.2-µm filtered seawater only (pH 8.09 ± 0.02) and in the presence of model saccharides and isolated natural bacterial and algal exopolymeric substances (EPS). Model ligands = Dextran (DEX, polysaccharide) in concentrations 50 – 500 nM (Ligand-to Fe-ratio, L: Fe 1.66 to 16.6), and Glucuronic acid (GLU, monosaccharide) in concentrations 50–5000 nM (L: Fe 1.66 to 166). EPS isolates = Antarctic sea ice bacteria, natural phytoplankton bloom from the sub-Antarctic zone (SAZ bloom), axenic algal culture of *Emiliania huxleyi*. EPS were added at a concentration to give L:Fe of 1.66. Seawater only n = 12 (22 °C) and 6 (4 °C), all ligands n = 3 for both temperatures.

Table 4.8 The effect of Fe associated with EPS (Fe-EPS) on the growth of the Southern Ocean diatom, *C. simplex,* over 187-h incubation at 4 °C and 50 µmol photons m^{-2} s^{-1}. Fe concentration in the Tasman Sea surface seawater medium was 0.56 nM. The growth of *C simplex* in the presence of Fe bound to EPS was compared to both inorganic Fe and seawater control. Growth rate (µ d^{-1}, calculated between 48-h and 118-h when all incubations were in exponential growth phase), final biomass at 187-h (cells ml^{-1}), and the bioavailability (in %) of Fe-EPS relative to inorganic Fe (assumed 100% bioavailable) is presented. Additions of Fe-EPS and inorganic Fe provided an additional 1 nM Fe to the seawater medium. EPS

isolates were from an Antarctic sea ice bacteria, a natural phytoplankton bloom from the sub-Antarctic zone (SAZ bloom), and from axenic algal cultures of *Phaeocystis antarctica and Emiliania huxleyi.* Errors represent the standard deviation of triplicate samples.

Table 5.1 Constituents of synthetic seawater (SS) based on AQUIL media as per Price et al. (1989) using major salts only. Final pH = 8.00. Background dissolved Fe = 0.73 ± 0.02 nM, n = 4

Table 5.2 Concentration of macronutrients (phosphate (PO_4), silicic acid ($Si(OH)_4$; µM) and trace metals (Iron (Fe), zinc (Zn) and copper (Cu); nM) present in filtrates of experimental samples simulating the wet deposition of Australian mineral dust into the Southern Ocean. The dust used was collected during a large dust storm over Brisbane, QLD., and resuspended in rainwater collected in the Tasman Sea (31°35.849'S 178°00.00'E, GP13 GEOTRACES voyage, 27/05/2011) before being exposed to UV + visible light (UV, 2000 µE), visible light only (VIS, 2000 µE), or kept in darkness (Dark). Resuspended, treated dust was added to synthetic seawater to give a dust enrichment of 0.5 mg L^{-1}. Data for single 0.2 µm and 0.02 µm filtered samples are presented. **Bold type** = Exp 2, non-bold type = Exp 3. Errors for PO_4 and $Si(OH)_4$ are the standard deviation of triplicate samples. Fe, Zn and Cu data is from a single sample. Concentrations measured in the dust treatments are the combined contribution of rainwater and dust. < DL = below detection limit.

Table 5.3 Fe size fractionation (soluble < 0.02-µm, colloidal 0.02- to 0.2-µm and particulate > 0.2-µm) of Fe associated with rainwater and Australian continental dust in experimental samples from two replicate experiments simulating the wet deposition of Australian mineral dust into the Southern Ocean. Solubilities of each size fraction are calculated using the total acid leachable concentration (372.1 nM) of Fe present in 0.5 mg L^{-1} dust. Treatments were as per Table 5.2. Relative concentrations (%) are presented. **Bold type** = Exp I, non-bold type = Exp II.

Table 5.4 Relative size distribution (%) of humic substance-like (HS-like) material in experimental samples from two replicate experiments simulating the wet deposition of Australian mineral dust into the Southern Ocean. Particulate = > 0.2-µm, Colloidal = 0.02- to 0.2-µm, soluble = < 0.02-µm. Treatments were as per Table 5.2. **Bold type** = Exp 2, non-bold type = Exp 3.

Table 5.5 Relative retention of Fe on C_{18} resin of Fe associated with Australian mineral dust. For comparison model ligands (humic acid (HA); desferrioxamine B (DFB), 15 nM; DTPA, 100 nM; glucuronic acid (GLU), 100 nM) are presented. Experimental medium was

synthetic seawater (pH 8.0). UV- and Dark-treated dust enrichments are presented. Unfiltered, 0.2-µm filtered and 0.02-µm filtered were measured to assess the nature of the organic ligands in each size fraction.

Table 5.6 The effect of Fe associated with Australian desert dust on the growth of the Southern Ocean diatom *C. simplex.* Bioavailability (%) of Fe associated with Australian mineral dust relative to inorganic Fe (assumed 100% bioavailable) measured after 24-h. Growth rate (µ d^{-1}, calculated between 136 h and 232 h when all incubations were in exponential phase) and final biomass after 326 h incubation period at 4 °C and 50 µmol photons m^{-2} s^{-1} are also presented. Treatments were as per Table 5.2. Error = standard deviation of triplicate samples.

SUMMARY

It is widely accepted that the complexation of iron (Fe) with organic compounds is the primary factor that regulates Fe reactivity and its bioavailability to phytoplankton in the open ocean. Despite considerable efforts to unravel the provenance of the many organic ligands present in the 'ligand soup' much of this pool remains largely unresolved and the ligands remain grouped into either strong (L_1) or weak (L_2) types. The Tasman Sea and Southern Ocean are areas of particular interest as both regions are subject to Fe limitation or co-limitation and are likely to be severely affected under climate change scenarios. The predictions of dryer conditions in central Australia suggest that the Tasman Sea may be subject to changes in the intensity and frequency of atmospheric dust deposition and, in consequence, enhanced Fe deposition into the surface waters. This thesis aims to improve our knowledge of a) how natural organic ligands affect Fe solubility, chemistry, and bioavailability, and b) which forms of Fe are available to phytoplankton.

Natural seawater samples (surface and profiles to 1000m) revealed that electrochemically detected HS-like material, which are thought to make up a proportion of the weaker L_2 class of ligands, account for a very small fraction of the Fe-binding organic ligand pool. The distribution of HS-like material in coastal, shelf and offshore regions associated with the EAC does not exhibit a nearshore to offshore (high to low) concentration gradient, likely because of low riverine HS-like input. Higher concentrations of HS-like material were generally found at, or adjacent to, the chlorophyll maximum (Cmax). However, little correlation with chlorophyll-*a* (Chl-*a*) was observed and so these higher concentrations are more likely linked to degraded algal material and microbial activity rather than direct primary productivity. Perturbation experiments using water collected offshore in the EAC and a cold core cyclonic eddy (CCE) indicated that the *in situ* utilisation and production of HS-like material, and its character, differ depending on the phytoplankton and microbial communities present, and reflect the biological activities of these different communities, as well as photochemical transformations. The addition of a model HS (Suwannee River fulvic acid) enhanced Chl-*a* concentration in both communities, particularly in the EAC, likely due to the remineralisation of Fe and other nutrients via photochemical and bacterial transformation of this material.

Seawater depth profiles from the northern and southern Tasman Sea indicate Fe limitation (or co-limitation) at the stations sampled. Dissolved Fe (dFe), organic ligand concentrations and conditional stability constants were consistent with previous studies (showing the

presence of mostly L_2 ligands) with higher ligand concentrations and conditional stability constants close to the Cmax. Ligand concentration, as previously reported, is in excess of dFe throughout the water column, although no correlation between dFe and ligand concentration was observed.

Fe-enrichment experiments using two contrasting phytoplankton communities investigated how the communities respond, in terms of biomass and community structure, to inorganic Fe delivered alone or bound to an organic ligand (siderophore, saccharides, bacterial exopolymeric substances (EPS)) or dust-borne Fe from two dust samples (D1 and D2) originating from the Australian continent. Overall, Fe bound to a strong Fe-binding siderophore was much less available to both phytoplankton communities; whereas, Fe bound to bacterial EPS (lowest conditional stability constant) induced the greatest increase in overall phytoplankton biomass. Dust D1 did not have the highest rate of dFe uptake, or result in the greatest increase Chl-*a*, but did induce the greatest shift in community structure. Whilst one ligand (L_2) was measured in most incubations, both L_1 and L_2 ligands were detected in the D1 and inorganic Fe incubations, indicating *in situ* biological production of Fe-binding ligands (i.e. siderophores or EPS) in response to Fe addition and an added ligand component from the dust. The greater response of the phytoplankton to the EPS and D1 led to further laboratory experiments.

Analysis of 4 EPS isolates (1 bacterial, 1 mixed natural community, and 2 microalgal laboratory cultures) showed that both bacterial and algal EPS contain functional components known to bind Fe (uronic acid, saccharides). The bacterial EPS was made up of mainly high molecular mass components, whereas the algal EPS were of low molecular mass. Most EPS contained components that were measured as both L_1 and L_2 ligands, with the L_1 ligands having an affinity for Fe close to that of bacterial siderophores. EPS greatly enhanced Fe solubility in seawater, however, it may also accelerate Fe(II) oxidation, and thus, Fe(II) removal from the system. Other trace elements and macronutrients were associated with the EPS that may be accessible to phytoplankton and could help to relieve nutrient limitation. Bioaccumulation experiments indicated that Fe bound to all EPS used was highly bioavailable to the Southern Ocean diatom *C. simplex* (50 to > 100%) relative to the bioavailability of inorganic Fe (assumed 100% bioavailable). This enhanced bioavailability was likely due to increased Fe solubility, and possible formation of more bioavailable forms of Fe.

Further experiments using dust D1, and rainwater collected in the Tasman Sea, revealed that despite low fractional solubilities (< 1%), the dust represents, potentially, an important

source of Fe and other vital macronutrients and trace elements. Both the rainwater and dust were associated with ligands in the L_2 class that helped to maintain the solubility of Fe. Light exposure, particularly UV, can a) have a substantial effect on the Fe chemistry of the Fe-laden dust, lowering the conditional stability constant and altering the size distribution of both Fe and ligands (including saccharides and HS-like material), and b) improve the bioavailability of dust-borne Fe to *C. simplex*.

The perturbation experiments in the EAC, CCE and north and south Tasman Sea demonstrated that organic ligands play an important role in regulating the nutrient dynamics of marine systems. They show that the bioavailability of Fe to phytoplankton is dependent on the various Fe species and Fe sources (i.e. inorganic Fe, organically bound, dust-borne), and that this differs between phytoplankton size fractions and from one bacterio- or phytoplankton species to another. The Tasman Sea and Southern Ocean receive, possibly increasing, periodic inputs of atmospheric dust from the source region of D1, which initiated a substantial community shift in perturbation experiments. However, the impact that dust-borne Fe will have on a natural phytoplankton community will be dependent on the duration and intensity of the dust deposition event, and the nutritive state and community structure of the resident phytoplankton. Bacterial siderophores have previously been suggested as key players in Fe biogeochemistry, however, in remote regions bacterial and algal EPS could play a significant role in the biogeochemical cycling of Fe and other nutrients, and their contribution should also be considered to further our understanding of the dynamics of Fe-limited oceans.

CHAPTER 1:

GENERAL INTRODUCTION

Note

This introduction has contributed to a manuscript published in Chemia (Norman et al. 2014, vol 68, p. 764 – 771). The manuscript is titled 'Iron biogeochemistry in aquatic systems: from source to bioavailability' and authors are; Louiza Norman, Damien Cabanes, Sonia Blanco-Ameijeiras, Sophie Moisset, Christel S. Hassler.

1.0 Introduction

Phytoplankton play a major role in marine systems as their biological functioning affects the biogeochemical cycles of a number of macro- and micronutrients (carbon (C), silicon (Si), sulphur (S), nitrogen (N), iron (Fe), etc) (Fig. 1.1). By the process of photosynthesis phytoplankton are responsible for up to 40% of atmospheric CO_2 biological fixation (referred to as primary productivity), transforming inorganic C into organic forms that sustain the marine food web (Falkowski, 1994; Falkowski et al., 1998). Part of this organic C will be respired by the phytoplankton and bacteria, recycled through the food web, and exported deep into the ocean by sedimentation processes (Chisolm, 2000). Phytoplankton, therefore, affect global C cycling and play an important role in the regulation of Earth's climate.

Primary productivity in many natural waters is limited by the availability of nitrogen (N) and phosphate (P) (Mahowald et al, 2005). However, around 40% of the world's oceans exhibit low chlorophyll concentrations despite nutrient concentrations and light levels being at least adequate for growth (Mahowald et al, 2005; Duggen et al., 2010). These regions are termed 'high nutrient, low chlorophyll' (HNLC) and include the equatorial Pacific, subarctic Pacific, and the Southern Ocean. John Martin's "iron hypothesis" was the first to postulate that Fe was limiting the growth of phytoplankton in HNLC regions (Martin & Fitzwater, 1988; Martin et al., 1991; Martin et al., 1994). Since then numerous bottle assays, and large-scale natural and artificial Fe fertilisation experiments have demonstrated that the primary factor leading to low phytoplankton biomass in HNLC waters is the limitation of Fe accessible for utilisation to bacterio- and phytoplankton (see de Baar et al., 2005; Boyd et al., 2007; Boyd & Ellwood 2010 for reviews). Fe limitation is not restricted to HNLC regions. Areas of the Atlantic Ocean and the Coral Sea exhibit reduced primary productivity due to low nutrient concentrations, specifically N (Moore et al., 2009; Law et al., 2011), and are termed 'low nutrient, low chlorophyll (LNLC) regions. In these regions Fe could become a co-limiting factor due to its crucial role in N assimilation and N_2 fixation (Moore et al., 2009).

Fe is one of the most important micronutrients required for the growth of phytoplankton, as it is involved in key metabolic functions such as photosynthesis, respiration and N assimilation (Falkowski et al., 1998; Sunda, 2001; Morel & Price, 2003). As it is the fourth most abundant element (Taylor, 1964), one would expect that Fe concentrations would reflect this, however, the solubility of Fe is extremely low in contemporary well

oxygenated seawater (Stumm & Morgan, 1996; Millero, 1998; Liu & Millero, 2002; Jickells et al., 2005) resulting in sub-nanomolar concentrations in most open ocean systems. This low Fe abundance influences the cycling of other elements (see above), thereby impacting on biological growth, primary productivity, phytoplankton biodiversity, community structure, and, on a larger scale, ecosystem functioning and CO_2 fixation (Price et al., 1994; Sunda & Huntsman, 1995; de Baar & La Roche, 2003; Boyd et al., 2007).

Fe exerts a huge control over ocean primary productivity and carbon sequestration (Boyd & Ellwood, 2010), but the relationship between Fe chemistry and the biology of surface waters is a complex and dynamic one. As such, the parameters which define the forms of Fe that are accessible for the growth of phytoplankton, referred to as bioavailable Fe, are still poorly understood. It is little wonder that, in the last 30 years, Fe biogeochemistry has received such a great deal of attention.

Determining what controls the availability of Fe to phytoplankton is one of the main challenges in understanding how Fe limits oceanic primary productivity and biodiversity. Fe cycling is influenced by both its chemistry and biology; it is a balance between input, biological uptake and recycling, and Fe sedimentation. We know that > 99% of dissolved Fe is bound to organic ligands (Gledhill & van den Berg, 1994; Wu & Luther, 1994; van den Berg, 1995; Rue & Bruland, 1995), but these compounds have been poorly characterised, and there is a paucity of literature regarding their environmental role on Fe cycling. Studies relating to the dynamics of Fe (or indeed all micronutrients) in Australian waters, notably the Tasman Sea and the Southern Ocean, are scarce. Both regions have high economic, sociological, and environmental value. Climate change prediction models indicate that the Tasman Sea may experience one of the highest increases in oceanic temperature (Hobday et al., 2008), which is likely to impact primary productivity, and, in turn, the valuable fishing resources of this area. When one considers that approximately one third of the Australian population lives along the coast of the Tasman Sea, any variability seen in the marine system will eventually impact on the human population. In addition, due to its cold temperature, circulation patterns affecting the Pacific, Indian and Atlantic Oceans, and its HNLC waters, the Southern Ocean is also an important sink for C which affects the global C cycle (Marinov et al., 2006, 2008; Lumpkin & Speer, 2007).

Several climate models predict a global lowering of pH in marine waters in response to increased pCO_2 leading to ocean acidification (IPCC, 2007). The fate of Fe-limitation in acidifying oceans still remains unclear as Fe will become more soluble at lowered pH, but will be more strongly bound to organic ligands (Breitbath et al., 2010). How a changing

environment will alter the nature of biologically produced organic ligands, the rate of production and complexation, and essentially the bioavailability of Fe are largely unknown. Therefore, in order to understand future scenarios, one must first gain a better understanding of current conditions.

It has been identified that there is a need to focus on the impact of excess organic ligands on Fe solubility and bioavailability, and on the efficiency of Fe biogeochemical cycling to produce bioavailable forms of Fe (Breitbarth et al., 2010). Furthermore, the identification of the sources of Fe which are accessible for the growth of phytoplankton is of paramount importance as this is critical to our understanding of how Fe controls phytoplankton biodiversity and productivity, and in turn the functioning of marine systems.

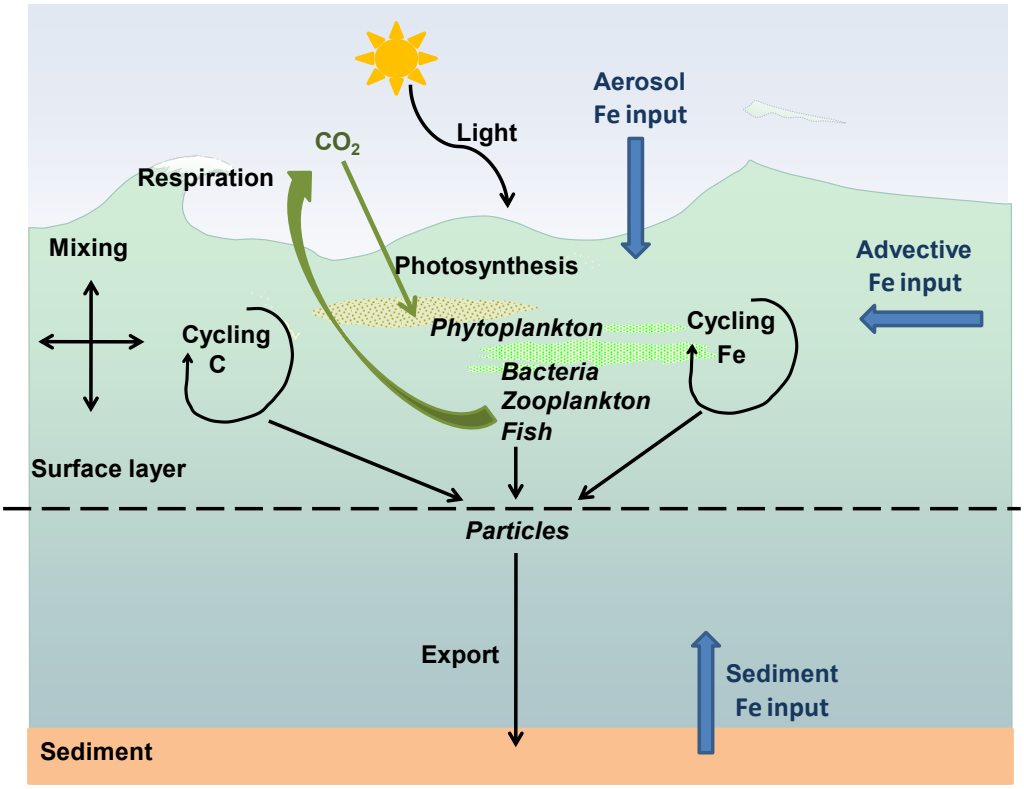

Figure 1.1 Schematic of the links between iron (Fe) and Carbon (C) cycling. Iron (Fe) enters the oceans via a number of sources, i.e. aerosol input (dust, ash), advective processes (horizontal transport of coastal water masses), upwelling of sediments. Fe is a vital micronutrient for phytoplankton as it is involved in the processes of photosynthesis and primary productivity. During photosynthesis phytoplankton fix atmospheric CO_2, thereby transforming inorganic carbon into organic forms which are transferred through the entire marine food web. Some of the organic carbon is respired by phytoplankton and bacteria, recycled through the food web, and exported to the sediments. During these processes Fe will be recycled and exported. Processes in bold black, iron inputs in blue, carbon processes in green, biological interactions in italics (From Norman et al., 2014).

1.1 Fe in the Ocean

In large areas of the oceans dissolved Fe (dFe) concentrations in surface waters are extremely low, often < 1 nM (de Baar & de Jong, 2001). Some variability can be observed with much higher concentrations being recorded in continental shelf regions (up to 7.4 nM, Martin et al., 1990), and sub-nanomolar concentrations in Southern Ocean (Parekh et al., 2004; Boye et al, 2001, de Jong et al, 2008; Lannuzel et al., 2008). Dissolved Fe concentrations are also variable between surface and deep ocean waters, with averages across the global oceans of 0.07 nM at the surface, and 0.76 nM at depth (Table 1.1). Fe has

a nutrient-like vertical distribution in the oceans with low concentrations at the surface, resulting from biological uptake, and increasing concentrations with depth (Johnson et al., 1997) due to remineralisation and scavenging (Johnson et al., 1997; Vraspir & Butler, 2009). Although, as pointed by Boyd and Elwood (2010), this nutrient-like behaviour does not seem to fit with the short residence time of Fe in the ocean (70–140 years, Bruland et al, 1994) relative to ocean circulation (~ 1000 years), or with other particle-reactive elements with short residence times that are strongly scavenged by particles and rapidly lost by sedimentation processes, such as aluminium (100–200 years, Orians & Bruland, 1985) and lead (20–80 years, Schaule & Patterson, 1981), which show a decrease in concentration with depth (Schaule & Patterson, 1981; Johnson et al., 1997; Boyd & Elwood, 2010). It is likely that the complexation of Fe with a variety of organic ligands in surface waters, which increase Fe solubility and retard scavenging, may be at least partially responsible for this behaviour (Johnson et al., 1997). Fe is distributed into dissolved (< 1-nm to 0.45-μm) and particulate (> 0.45-μm) size fractions, with the larger fractions settling faster. As such, the distribution of dFe in oceanic waters is as a result of complex interactions between Fe input, Fe chemistry (size, effect of organic ligands and redox reactions) and biological activity.

Table 1.1 Range of measured dissolved and particulate iron (Fe(III)), organic ligand concentration, and measured stability constants (log K) in different ocean basins.

	Dissolved Fe (nM)	Particulate Fe (nM)	[Ligand] (nM)	log $K'_{Fe\text{-}L}$	log $K'_{Fe^{3+}\text{-}L}$	Reference
	0.02 - 0.1(s)					Martin & Gordon, 1988
	0.6 - 0.8 (d)					Martin et al., 1989
Subarctic Pacific	0.02 (s)	> 1.0	0.48	11.3 - 12.5	*21.3 – 22.5**	Kondo et al., 2008
		0.1 -0.2				Bruland et al., 1994
		0.1 - 0.3				Johnson et al., 1997
	0.2 (s)					Rue & Bruland, 1995
North pacific	0.67-0.77 (d)		**L_1**: 0.44 **L_2**: 1.5	**L_1**: 13 **L_2**: 11.5	***L_1**: 23 **L_2**: 21.5**	Rue & Bruland, 1995
	≤0.05 (s)					Coale et al., 1996
Equatorial	0.05 (s)					Gordon et al., 1997
Pacific	0.02 - 0.04 (s)	0.1 - 0.5	**L_1**: 3.1 **L_2**: 1.9	**L_1**: 12.6 **L_2**: 11.8	***L_1**: 22.6 **L_2** 22.5**	Rue & Bruland., 1997
	0.5 - 2.4 (s)					Measures & Vink, 1999
Arabian Sea	1.25 - 2.63 (s)		0.22 - 3.8		21.6 - 22.4	Witter et al., 2000b
	1.8 (s)					Gledhill & van den Berg, 1994;
	0.15 (s)		3.5-4.8	18.8-19.7		Wu & Luther, 1995
	0.43-0.66 (s)		0.45 - 0.6			Cullen et al., 2006
North Atlantic	0.42 ± 0.05 (d)		**L_1**: 1.14 ± 0.09 **L_2**: 2.11 ± 0.002	**L_1**: 13 **L_2**: 11.6	23.22	Cullen et al., 2006
South Atlantic	0.05 - 0.3					de Jong et al, 1998
	0.05-0.51 (s)		0.18-1.39 (s)		21.0-22.7 (s)	Boyé et al., 2001
	0.33 ± 0.18 (d)		0.70 ± 0.20 (d)		21.4-23.0 (d)	Boyé et al., 2005
	0.06-0.09 (s)	0.49-0.93	0.60-0.79		21.8-22.0	Frew et al., 2006
Southern Ocean			**L1**: 0.42 ± 0.10 **L2**: 0.75 ± 0.20		**L1**: 22.97 **L2**: 21.5	Ibisanmi et al.,2011

** For consistency values in italics have been converted from the original data (log $K'_{Fe\text{-}L}$ to log $K'_{Fe^{3+}\text{-}L}$). A conversion factor of 10^{10} has been applied in accordance with Hudson et al 1994.*

1.2 Sources of Fe

Fe sources are numerous, and their relative importance to the observed Fe concentration varies regionally and seasonally. Fe reaches marine waters via atmospheric aerosols (Duce & Tindale, 1991; Jickells & Spokes, 2001; Jickells et al., 2005; Mahowald et al., 2005), riverine input, melting of sea ice (Loscher et al., 1997; Lannuzel et al., 2008), icebergs (Loscher et al., 1997), and glacial ice (Raiswell et al., 2006, 2008), continental margins (Johnson et al., 1999, 2003; Lam et al., 2006; de Baar et al., 1995), anoxic sediments, and recycling by organisms from viruses to whales (Barbeau et al., 1996; Maranger et al., 1998; McKay et al., 2005; Strzepek et al., 2005; Johnson et al., 1994; Wilhelm & Suttle., 1999; Poorvin et al., 2004, 2011; Smetacek, 2008; Nicol et al., 2010; Lavery et al., 2011). In the Tasman Sea and Southern Ocean the major Fe sources are atmospheric dust input, input from continental margins and upwelled Fe, recycled/remineralised Fe and seasonal input from sea ice and icebergs.

1.2.1 Aerosol Fe input

Globally, the largest input of Fe into the oceans comes from atmospheric aerosol/dust deposition (Duce & Tindale, 1991), although exceptions to this may be upwelling areas or coastal regions with large river inputs (Coale et al., 1996). It is estimated that approximately three times as much dissolved Fe enters the oceans via atmospheric deposition than via rivers (Duce & Tindale, 1991).

Atmospheric dust comprises both mineral (crustal) material, derived from arid and semi-arid regions (Duce & Tindale, 1991; Jickells & Spokes, 2001; Jickells et al., 2005; Mahowald et al., 2005), and anthropogenically sourced material, such as products from biomass burning, and industry (Luo et al., 2008; Mahowald et al., 2009). The proportions in which mineral material and anthropogenic material, and thus Fe, occur vary regionally. For example, in the North Atlantic, anthropogenically sourced Fe can account for approximately 70 % of the soluble Fe present in surface waters near Bermuda, but just 12 % of soluble Fe in surface waters near Barbados, where mineral dust appears to dominate (Sholkovitz et al., 2009). Overall, the spatial distribution of dust inputs are not uniform. It is estimated that the Northern Hemisphere receives 6–22-times greater dust deposition (m^{-2}) (Mackie et al., 2008), and eight times greater input of Fe than the Southern Hemisphere, mainly due to the large desert and semi-arid source regions in Asia, North Africa, India, and the Arabian peninsula (Duce & Tindale, 1991; Jickells et al., 2005). It is

suggested, however, that despite the comparatively small Southern Hemisphere dust input, the resulting impact on oceanic primary productivity may be disproportionately large due to the close proximity of HNLC regions such as the Southern Ocean (Mahowald et al, 2005).

Dust input to the South Pacific and Southern Ocean regions is thought to come from Australian deserts (Duce & Tindale, 1991; Jickells *et al*., 2005), although there are very few studies for this area. The seasonal variability of winds and precipitation means that dust deposition, and therefore Fe supply, is of an episodic nature, with a peak in dust deposition during the austral summer. Transportation of dust from Australia takes two major pathways: a NW path over the Indian Ocean, and SE path, which has three separate trajectories, NE over the Coral Sea, SE over the Tasman Sea and south over the Southern Ocean (Mackie et al., 2008). All of the SW dust paths have similar source regions and are most active between December and March, with the largest supply of dust being to the Southern Ocean (Mackie et al., 2008). Australian arid regions are relatively more humid when compared to African and Asian regions, and generally more densely vegetated (Mackie et al., 2008). In addition, Australia's complex geology has created a range of soil types, each with variable wind erosion properties (McTainsh et al., 1990; Mackie et al., 2008). It is thought that these factors give rise not only to an even more pronounced episodic supply of dust from Australia (Mackie et al., 2008), but also variability in the Fe content of the dust due to varying mineralogies (Fung et al., 2000; Cropp et al., 2013).

1.2.2 Fe from Upwelling and Continental margins

In HNLC regions and oligotrophic waters, the flux of upwelled Fe has been found to be significant, and in some cases, the dominant source of Fe (Morel & Price, 1998). It is estimated that the upward flux of Fe in the equatorial Pacific is around ten times that of the atmospheric contribution (Coale et al, 1996). In the Southern Ocean, upwelled Fe is more than five times that of atmospheric deposition (de Baar et al, 1995) and represents a significant source of Fe to Antarctic waters, particularly in the region south of the Antarctic Polar Front (APF; Watson, 2001; de Baar et al, 1995). However, in the subarctic Pacific atmospheric sources appear to be dominant and the ratio is reversed (~1:10) (Price & Morel, 1998; Watson, 2001).

Reduced continental margin sediments are a likely source of significant Fe input to many ocean regions, including the subarctic and North Pacific (Johnson et al., 1999, 2003; Lam et

al., 2006), and the Atlantic sector of the Southern Ocean (de Baar et al., 1995). This input comes from both resuspension of sediments and the decomposition of organic matter from the shallow waters of the continental shelf (Johnson et al., 1999; Elrod et al., 2004). The advection of continental sediments by the APF, as part of the Antarctic Circumpolar Current (Löscher et al., 1997), and the southward advection of enriched subtropical waters from shelf sediments in the sub-Antarctic Zone (SAZ; Sedwick et al., 2008; Bowie et al., 2009; Pollard et al., 2009: Hassler et al., 2012) are important sources of Fe for these regions of the Southern Ocean as the entrainment of particles from the continental shelf can be accompanied by high concentrations of dissolved, possibly bioavailable, Fe (Lam et al., 2006).

Upwelling of nutrient-rich water from the continental shelf to the continental slope occurs at the 'separation zone' ($\backsim$ 32° S) of the East Australian Current (EAC; Roughan and Middleton, 2002, 2004). Fe shelf sediments are known to support primary production in coastal waters (Hutchins & Bruland, 1998) and so the reported strengthening of the EAC (Ridgway and Hill, 2009) may increase sediment suspension at the continental shelf thereby enhancing Fe, and other nutrients, in the coastal region of Eastern Australia. However, depending on the direction of winds and currents, Fe originating from continental shelves can also be transported to surface waters many 100s of km off the coast (Elrod et al, 2004; Lam et al., 2006). Thus, the complex physical circulation of the EAC shelf waters may push possibly Fe-rich suspended sediment further from the coast.

1.2.3 Biological recycling

Like many other macro- and micronutrients, Fe can be biologically recycled within the water column. Recycling can occur through grazing activities (Barbeau et al., 1996; Maranger et al., 1998; McKay et al., 2005; Strzepek et al., 2005), and lysis of cells (either photochemically or through the activity of marine bacteria and viruses; Johnson et al., 1994; Wilhelm & Suttle., 1999; Poorvin et al., 2004, 2011). Questions still remain regarding the species of Fe that are produced, and the apparent bioavailability to phytoplankton, although laboratory experiments conducted by Sarthou et al. (2008) suggest that the recycled Fe generated from grazing by copepods are inorganic Fe species. Laboratory (Hutchins et al., 1993; Barbeau et al., 1996) and field experiments (McKay et al., 2005; Strzepek et al., 2005) indicate that Fe regeneration rates are rapid, occurring on time scales of hours to days. Barbeau et al (1996) suggest that protozoan grazing activity can transform previously particulate or colloidal forms of Fe to dissolved and/or

bioavailable forms, whilst Poorvin et al (2004) demonstrated that Fe recycled via viral-lysis of bacterioplankton is highly bioavailable. Estimates as to the percentage of the Fe demand that is satisfied by grazer- and viral-mediated recycling vary considerably at between 20-100% (Poorvin et al., 2004; McKay et al., 2005; Strzepek et al., 2005; Sarthou et al., 2008). The upper estimates are unlikely to be consistent year round and recycled Fe alone is probably not sufficient to fully support primary productivity in the open oceans (McKay et al., 2005, Sarthou et al., 2008). However, in oligotrophic waters (i.e., the EAC), and remote oceans (i.e., the Southern Ocean) regenerated Fe is likely to be an extremely important source to Fe-limited phytoplankton communities.

1.2.4 Sea ice and icebergs

Nutrient limitation is widespread in the HNLC waters of the Southern Ocean, but despite Fe-limitation, seasonal phytoplankton blooms are observed in Antarctic surface waters, suggesting that Fe is supplied from a source(s) other than upwelling or atmospheric deposition. Large seasonal accumulations of phytoplankton are observed at the bottom of ice sheets, where there is free exchange of nutrients with the underlying seawater, and often at the receding ice edge (Smith and Nelson, 1985), as the sea ice begins to melt.

In Antarctica, sea ice is formed from Fe-deficient water, and one would assume that the sea ice would also be Fe-deficient (Thomas, 2003). However, like many other nutrients (N and P for example) Fe can accumulate in sea ice in concentrations one or two orders of magnitude higher than that of the underlying seawater (sea ice 2.6 – 26 nM, Lannuzel et al., 2007). For N and P, this is not just a case of the nutrients being concentrated in the ice from the underlying water, but is also due to microbial remineralisation and recycling of these nutrients (Thomas et al, 2010). It seems reasonable to suggest that this may be the case also for elevated concentrations of Fe observed in sea ice.

Lannuzel et al. (2008) showed that 70% of the accumulated Fe could be released to surface waters through brine drainage over a period of just 10 days as the ice starts to warm and melt. A release of this kind may represent a significant enough iron flux to promote the onset of a spring phytoplankton bloom or at the very least sustain an existing bloom in Antarctic waters. Similarly, localised enhanced chlorophyll-*a* (Chl-*a*) concentrations have been measured in the vicinity of free drifting icebergs (Smith et al., 2007), suggesting that iceberg-hosted sediments, which often contain nanoparticulate Fe oxyhydroxides may also be a source of bioavailable Fe (Raiswell et al., 2006 & 2008).

The seasonality of Fe input to the ice covered regions of the Southern Ocean corresponds very well to the formation of large phytoplankton blooms. Although the input of Fe from sea ice and icebergs is considered marginal on a global scale, regionally it is likely to be extremely important in terms of primary productivity.

1.3 Chemical species, forms, and redox processes of Fe in seawater

Unlike other bioactive trace metals (i.e. Zn, Cd, Ni) which are present almost entirely in their dissolved phase, Fe is present in both dissolved (< 0.1-nm – 0.45-µm) and particulate (> 0.45-µm) phases, with the particulate phase having a concentration that is similar or larger than the dissolved fraction (Price & Morel, 1998). A significant fraction of dissolved Fe is in fact colloidal, likely both inorganic and organic colloids (Wells, 1998; Chen et al., 2003; Boye et al., 2010) and so the dissolved phase is therefore further split into soluble (< 1-nm) and colloidal (0.1-nm – 0.45-µm). However, depending on the filter type, and pore size of the filters commercially available for sample preparation, these are often operationally defined as < 0.02 µm for soluble Fe and 0.02- to 0.2-µm or 0.02- to 0.45-µm for colloidal Fe. To complicate matters further the speciation of Fe, and indeed many other metals, is controlled by the redox state (Fe(II) or Fe(III)), and the complexation with a variety of biologically produced organic ligands (Hutchins et al., 1999; Barbeau et al., 1996, 2001; Vraspir & Butler, 2009) (Fig. 1.2)

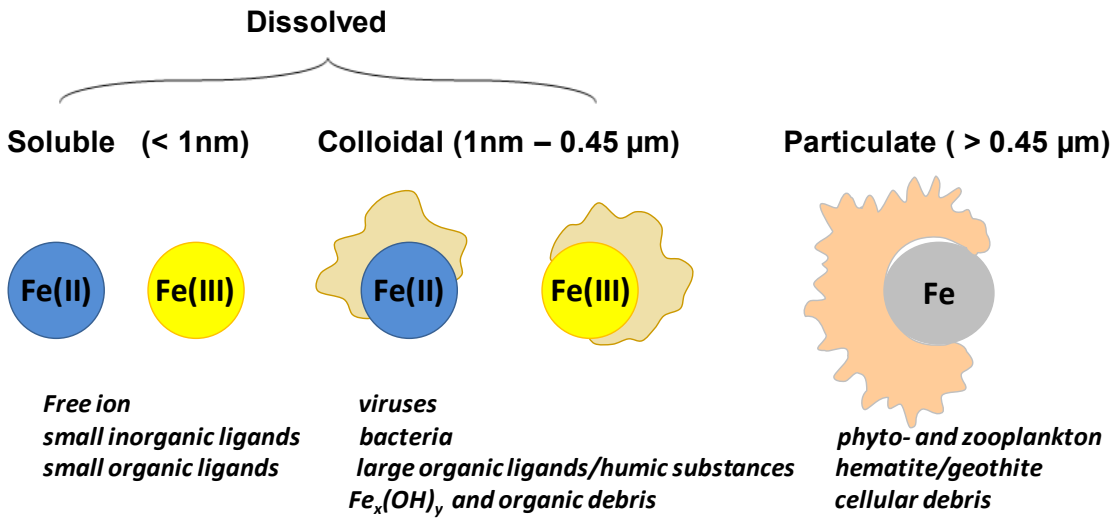

Figure 1.2 The various size fractions, species, and associated biology and NOM of iron that exists in marine waters (From Norman et al., 2014).

Fe(II) undergoes rapid oxidation in well-oxygenated surface waters, exhibiting a half-life of minutes at the normal pH of seawater (~ 8) (Miller et al., 1995; Rose & Waite., 2002; Pham & Waite, 2008). Generally, the predominant form of Fe in seawater is, therefore, the more thermodynamically stable Fe(III) (Rose & Waite 2002), which is present as either inorganic Fe(III) (Fe(III)′) or organically complexed Fe(III) (Kuma et al., 1996, Rose & Waite, 2003). In the presence of organic ligands, the solubility of Fe(III) is in the order of 0.2 – 0.6 nM in surface waters (Kuma et al., 1996; Millero, 1998), and reaches minimum values (0.15 – 0.2 nM) at depths between 50 and 200 m (Kuma et al., 1996). In the absence of organic complexation, however, Fe(III)′ is highly insoluble (Sunda & Huntsman, 1998), and will rapidly hydrolyse and form colloidal Fe oxyhydroxides (Kuma et al., 1998; Liu & Millero, 2002). These oxyhydroxides then dehydrate further and crystallise to Fe oxides such as goethite and hematite (Crosby et al., 1983; Kuma et al., 1996), which are stable but much less available for algal uptake (Kuma & Matsunaga, 1995). The Fe oxide which is formed is highly dependent on the conditions under which the Fe initially enters the marine system (Waite, 2001).

Competitive ligand exchange-adsorptive cathodic stripping voltammetry (CLE-AdCSV) has been developed from the CSV technique to allow further determination of the concentration and stability constants of Fe-ligand complexes (Croot & Johansson, 2000). More recently a modified CLE-AdCSV method has been used to determination the concentration and complex stabilities of Fe-humic substance complexes (Laglera et al., 2007, Laglera & van den Berg, 2009). Since its first use in 1994 (Gledhill and van den Berg, 1994), the CLE-AdCSV technique revealed that > 99% of dFe present in the oceans is complexed to natural organic ligands, the implication of which is vanishingly small observed concentrations of inorganic Fe (Fe'; Gledhill & van den Berg, 1994; Wu & Luther, 1994; van den Berg, 1995; Rue & Bruland, 1995; Wells et al., 1995).

It had been suggested that this ligand complexation may be a contributing factor to the limited growth of phytoplankton in HNLC regions (Boye et al., 2001). However, further experimental and modelling work have shown that organic complexation is extremely important for maintaining solubility (Kuma et al., 1996; Lui & Millero., 2003; Chen et al., 2004) and enhancing the bioavailability of Fe to bacterio- and phytoplankton (Hutchins et al., 1999; Maldonado and Price, 2001; Rose & Waite, 2003; Chen et al., 2004; Maldonado et al., 2005; Tagliabue & Arrigo, 2006; Hassler et al., 2011a, b), as soluble complexed Fe is not scavenged but remains accessible in surface waters for prolonged periods (Whitfield, 2001) .

The reduction and oxidation of iron can occur through a number of processes whether present as Fe(III)′ or Fe(II)′, or as Fe(III) or Fe(II)-ligand complexes (Fig. 1.3). These processes include direct mediation through the photochemical reduction of colloidal iron (Waite & Morel, 1984) or Fe(III)-organic ligand complexes (Barbeau et al., 2001, 2003), or direct biological reduction via biological ferrireductase. Indirect reduction pathways come from the production of the reductant superoxide via the photodegradation of natural organic matter (NOM) (Rose & Waite., 2005, 2006, Garg et al., 2007) or from microbial excretion products (Marshall et al., 2005; Rose et al., 2005).

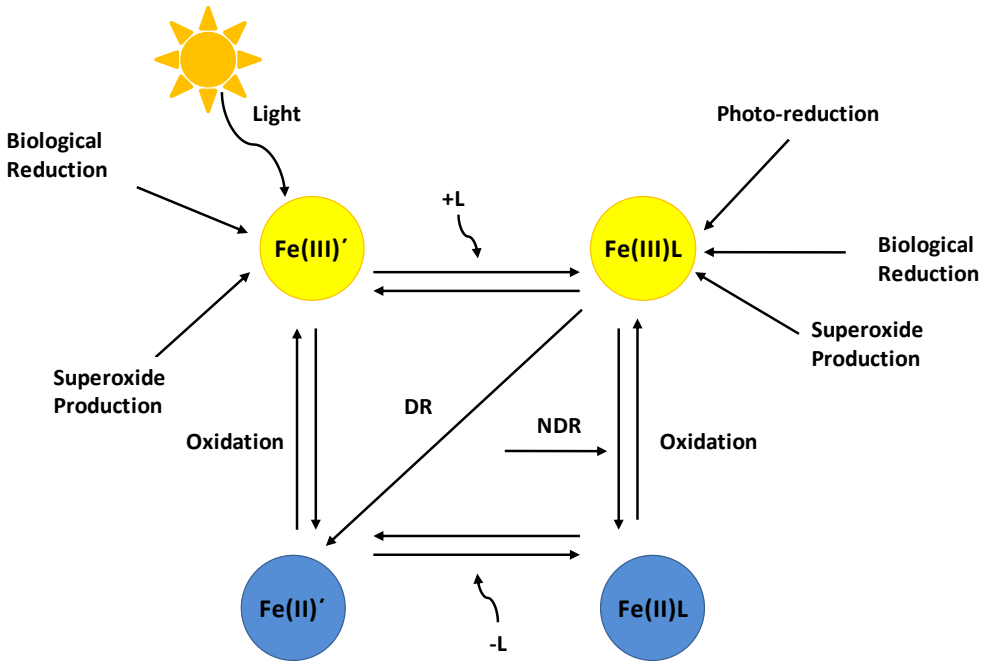

Figure 1.3 Iron exists in the ocean mainly as Fe(III), either as inorganic Fe(III)′, or bound to organic ligands (Fe(III)L). Organically bound Fe(III) is the predominant form (> 99%). Both Fe(III)′ and Fe(III)L can be reduced by the action of sunlight (photoreduction, production of superoxide by NOM), or by biological activity (biological reduction, i.e. ferrireductase, and biological production of superoxide). Iron reduction can induce the dissociation of Fe(III)L (e.g dissociative reduction, DR), or generate Fe(II)L (e.g. non-dissociative reduction, NDR). The Fe(II)L complexes are weaker than Fe(III)L complexes and will easily dissociate to Fe(II)′. In oxygenated water the Fe(II)′ is then rapidly reoxidised by O_2 to Fe(III)′ (From Norman et al., 2014).

Chromophore-containing humic substances are highly susceptible to photodegradation; however, this is not the case for all organic ligands. Siderophores which contain hydroxamate groups are photochemically stable whether free or bound to Fe. Those

containing catecholate groups will photooxidise when free but are stable when bound to Fe, whereas for siderophores containing α-hydroxy carboxylate groups the opposite is true (Barbeau et al 2003).

Fe(III) bound to organic ligands may undergo one of two reduction processes, dissociative reduction (DR), and non-dissociative reduction (NDR) (Garg et al., 2007). During NDR Fe(III) is reduced to Fe(II) but the ligand is remains intact, so the Fe-ligand complex does not dissociate. However, during DR the Fe(III)-ligand is reduced to Fe(II)-ligand and, if the resulting Fe(II)-ligand is weak, dissociation (likely photodissociation) will occur forming Fe(II)′ (figure 1.3: Garg et al., 2007; Hassler et al. 2012). Any Fe(II)′ not taken up by microorganisms will then be rapidly oxidised by oxygen and hydrogen peroxide to form Fe(III)′.

In general, soluble organic ligands form much weaker complexes with Fe than colloids (Boye et al., 2010), and Fe(II) complexes are weaker than Fe(III) complexes (Sunda & Huntsman, 1998). This suggests that the soluble organic complexes and Fe(II) may be more bioavailable than Fe(III) complexes and colloidal Fe (Sunda & Huntsman., 1998), and in fact, strong colloids may be a route of Fe removal from surface waters (Boye et al., 2010). Fe redox processes are influenced by the Fe species and organic ligands present, and the chemical environment of the surrounding waters. This is likely to determine the stability and reactivity of the complexes formed, and the regime of Fe cycling.

1.4 Fe Bioavailability

Bioavailable Fe is the part of the Fe pool present in an aquatic system which is biologically accessible to microorganisms and can sustain their growth. Put simply, Fe bioavailability controls phytoplankton biomass and the species composition of the phytoplankton assemblage, which in turn influences the community food web (Wells et al., 1995; Hassler et al., 2011a). The complex and dynamic behaviour of Fe in surface waters, its speciation, and redox chemistry means that the parameters which control Fe bioavailability are still poorly understood.

Typically, it is assumed that dissolved Fe(III)′ and Fe(II)′, and some dissolved organically complexed Fe(III) are bioavailable (Hutchins et al., 1999; Visser et al., 2003; Shaked et al., 2005; Salmon et al., 2006). Fe solubility measurements have often been used to infer bioavailability; but the two terms are not interchangeable. Dissolved Fe(II) is not always bioavailable to diatom species (Visser et al., 2003, Maldonado et al., 2006, Hassler,

unpublished data) and organically complexed Fe is not universally available to both bacterioplankton and eukaryotic phytoplankton (Hutchins et al., 1999; Maldonado et al., 2005).

The bioavailability of Fe, and other trace metals, is dependent on physical (diffusion, Hudson & Morel, 1993), biological (transport across cell membranes or uptake, Sunda & Huntsman., 1998; Worms et al., 2006), and chemical factors (dissociation kinetics of metal complexes and the various chemical forms of Fe, Wells et al., 1995; Sunda & Huntsman, 1998; Worms et al., 2006) both within the cell and in the environment immediately adjacent to the cell (Worms et al, 2006) (Fig. 1.4). The Fe requirement and uptake strategies of phytoplanktonic communities differ considerably (Shaked et al., 2005; Sunda & Huntsman, 1995), so a pool of Fe that is bioavailable to one species will not necessarily be available to another (Hassler et al., 2011a). Fe biological requirement for growth is also important as it defines the control that Fe bioavailability exerts on the structure of the phytoplankton community, and the threshold of the bioavailable Fe concentration under which phytoplankton induce high affinity transporters to increase Fe uptake rates (e.g. Maldonado and Price 1999). For example, coastal phytoplankton usually have a higher Fe requirement for growth than oceanic species (Sunda & Huntsman, 1995). Chemical speciation has a major influence on Fe bioavailability (Sunda & Huntsman., 1998; Hutchins et al., 1999; Maldonado et al., 2005), however, photochemical reactions (Barbeau et al., 2001; Amin et al., 2009; Buck et al., 2010), and the biological cycling of Fe (Strzepek et al., 2005; Sarthou et al., 2008) also play a role. The complexities and mechanisms of Fe bioavailability to bacterio- and phytoplankton have been described by Hassler at al. (2012).

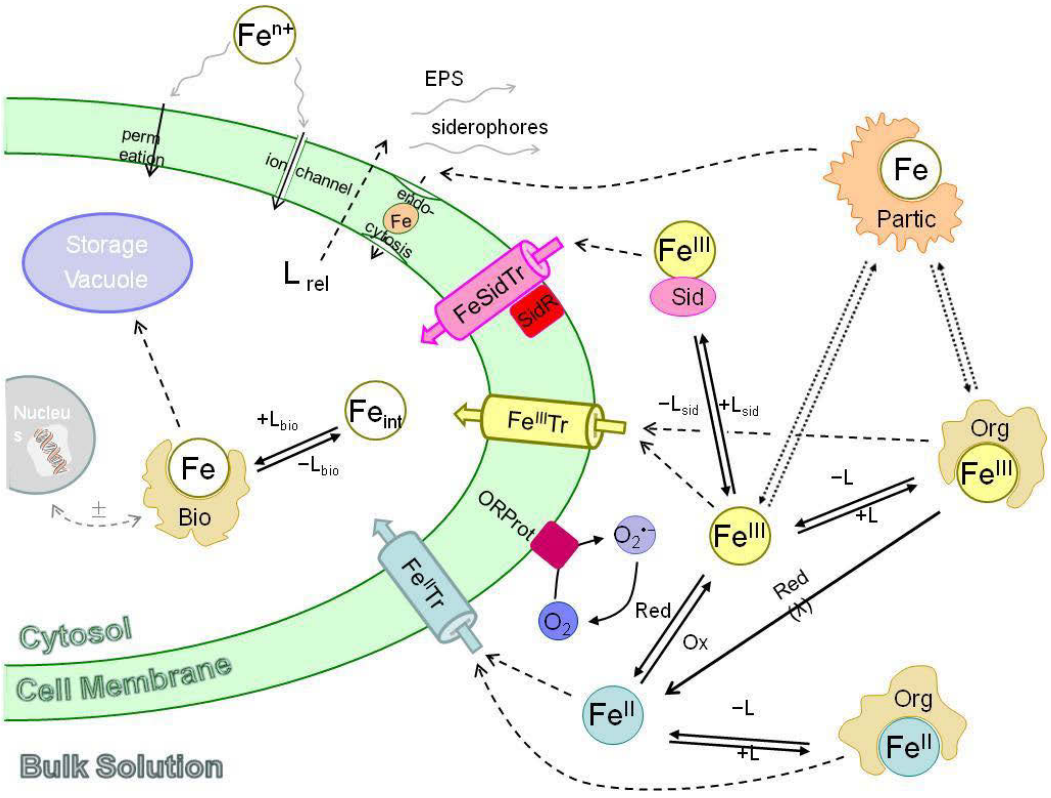

Figure 1.4 Schematic of the complex interplay between iron (Fe) chemistry and biology in defining its bioavailability to marine microorganisms. In surface water, Fe is mainly associated with particles (Partic), and with dissolved or colloidal organic ligands (L_2, e.g. exopolysaccharides, EPS; L_1 Sid, siderophores). Association with these compounds will define Fe chemical speciation and its reactivity towards the biota. Fe binding strength and reactivity is also affected by its redox chemistry (Red for reduction and Ox for oxidation), with Fe(II) usually forming the weakest complexes. Both biology (via surface reductase protein, ORProt) and light (λ) favour Fe reduction and subsequent transport with Fe(II) or Fe(III) transporters (FeTr) mainly present in eukaryotic phytoplankton. Highly specific transporter associated with siderophore uptake strategy, commonly present in bacterioplankton, is represented separately (FeSidTr). Other non-specific uptake pathways (endocytosis, direct permeation and an ion channel) are shown. Once inside the microorganism, Fe (Fe_{int}) reacts with intracellular biological ligands (L_{bio}, e.g. Chlorophyll-*a*), is stored (e.g. vacuole, ferritin) or is involved in cellular homeostasis via gene regulation (grey arrow with ± symbol). Release of Fe biological organic ligands (L_{rel}, such as EPS and siderophores) can exert a feedback in the control of both Fe chemistry and bioavailability. Dotted, dashed and full arrows represent aggregation/disaggregation, transfer, and chemical reaction (complexation, redox), respectively. (From Hassler et al, 2011b).

1.5 Organic ligands, siderophores, and humic substances

A considerable amount of work has been undertaken to establish the composition and provenance of natural organic ligands (Gledhill &van den Berg, 1994; Rue & Bruland, 1995, 1997; Wells et al., 1995; Yang & van den Berg, 2009), however, due to the complexity of their structural composition they remain poorly characterised (Hiemstra & van Riemsdijk, 2006; Rue & Bruland, 1995; Vraspir & Butler, 2009). The conditional stability constant of metals, that is the measure of how strongly a ligand coordinates with a metal ion, is currently the method used to distinguish between metal- (in this case Fe) ligand complexes (Vraspir & Butler, 2009). However, even here there are difficulties due to the large range of stability constants that have been measured by titration and CLE-AdCSV (Gledhill & van den Berg 1994; Rue & Bruland, 1995; Croot & Johansson, 2000; Hiemstra & van Riemsdijk, 2006). Dissolved Fe concentrations are highly variable across open oceans and coastal regions; however, determination of natural samples by CLE-AdCSV shows that organic ligands are generally found to be in concentrations in excess of Fe in the water column (Rue and Bruland, 1995; Boye et al., 2001; de Jong et al, 2008). The range of Fe-binding ligand concentrations found in oceanic waters is large at between 0.5–6 nM (Table 1.1), with no apparent regional pattern (Parekh et al., 2004). Like Fe, the ligands exhibit a vertical profile with a nutrient-like distribution and then remain constant at depths > 1000m. (Parekh et al., 2004).

Hunter and Boyd (2007) suggest that seawater likely has a large number of ligand types, but the electrochemical techniques currently used only have the resolution to distinguish one or two discrete ligand classes, known as L_1 and L_2. The limitations of the CLE-AdCSV method mean that ligands that are too weak to be detected within the analytical window of the technique are not measured (Croot & Johansson, 2000), and their contribution to iron biogeochemistry is likely to be underestimated or overlooked (Hassler et al., 2011a). L_1 class ligands are constrained to the upper ocean and characteristically have a high affinity (strong binding capacity, $K_{Fe'L} \geq 10^{12}$) for Fe, whereas L_2 class ligands are found in greater abundance throughout the water column, and have a weaker binding capacity (Rue & Bruland, 1995 &1997; $K_{Fe'L} \geq 10^{8.8}$, lowest stability constant published, Croot & Johansson, 2000). Comparison of conditional stability constants suggests that the composition of L_1 ligands may largely be siderophores, which are low molecular weight chelating compounds with a high binding affinity for Fe (Rue & Bruland, 1995; Wilhelm and Trick, 1994; Witter et al., 2000; Gledhill et al., 2004; Mawji et al., 2008). These compounds are small ligands (< 300 kDa, Neilands, 1981; Chen and Wang 2004) divided

into three classes according to their chemical structure; hydroxamate, catecholate, α-hydroxy-carboxylic acid. Siderophores are produced by heterotrophic bacteria and cyanobacteria only under Fe-limited conditions, as production is energetically very costly (Whitfield, 2001), and are used as a mechanism by which to sequester what little Fe may be present in the water column (Wilhelm & Trick, 1994; Barbeau et al., 2003; Gledhill et al., 2004). Whilst it is known that siderophores are produced as a response to low Fe concentrations, it is not known how depleted the Fe concentration needs to be before production of siderophores is initiated (Gledhill et al., 2004), although this is likely dependent on the specific Fe requirement for growth of a given bacterioplankton species.

Although a number of studies have shown that siderophores produced in cultured marine cyanobacteria and bacteria have stability constants which correspond to L_1 ligands (Witter et al., 2000; Barbeau et al., 2001), Hunter & Boyd (2007) argue that soluble Fe-binding ligands (< 0.02-μm), which includes siderophores, are present in much lower concentrations in surface waters than are measured and defined as L_1 by electrochemical methods. It is suggested that much of the dissolved (< 0.45-μm) ligands are actually present as colloidal (0.02- to 0.45-μm) organic matter which contradicts the idea that all L_1 ligands are siderophores (Boye et al., 2010). In addition, soluble ligands show a lower affinity for binding Fe(III) than colloidal ligands (Boye et al., 2010). Buck et al. (2010) have suggested that upon release the siderophores may become associated with organic colloids. Hiemstra & van Riemsdijk (2006) note that during a phytoplankton bloom Fe complexation is enhanced and the complexing ligands, which have stability constants similar to siderophores or products of cell lysis (i.e. porphyrin complexes), can be found in colloidal organic matter (DOM , size fraction > 0.02- to 0.45-μm).

It is thought that Fe-siderophore complexes mainly enhance the bioavailability of Fe to the bacterial producers (Hutchins et al., 1999). However, previous studies have demonstrated that the bioavailability of Fe bound to siderophores can vary depending on the type of siderophore present. For example, Fe-catecholate are significantly bioavailable to some eukaryotic phytoplankton (Hutchins et al., 1999; Maldonado et al., 2005; Hassler & Schoemann, 2009) whereas, the Fe-hydroxamate is generally poorly available to eukarytotic phytoplankton (Hutchins et al., 1999; Wells, 1999; Hassler and Schoemann, 2009; Buck et al., 2010). Fe bound to the siderophores may be accessed by phytoplankton via reduction by ferrireductases and the uptake of the resulting uncomplexed inorganic Fe (Maldonado & Price, 1999). Work initially carried out by Barbeau and co-workers (Barbeau et al., 2001, 2003) demonstrated that Fe-siderophore containing α-hydroxy-carboxylic acid groups are photosensitive under sunlit conditions which prevail in surface

waters, and may be accessed by eukaryotic phytoplankton following photochemical redox processes. Both biological and photoreduction involve the dissociation of organically bound Fe from the ligand, which may result in higher concentrations of inorganic Fe adjacent to the cell (Maldonado & Price, 2001; Maldonado et al., 2005). It should be noted, however, that siderophores which have undergone photoreduction have similar or slightly weaker chelating properties than the parent siderophore (e.g. Aquachelin has a $K_{Fe'L}$ of $10^{12.2}$ and its photoproduct a $K_{Fe'L}$ of $10^{11.5}$; Barbeau et al., 2001). Only one siderophore, vibrioferrin, exhibits a lower stability constant ($K_{Fe'L}$ of $10^{10.9}$; Amin et al., 2009), comparable with the weaker L_2 class of ligands (Rue & Bruland, 1995). It differs from many other siderophores in that it is highly photoreactive, and the resulting photoproducts have no significant affinity to Fe (Amin et al., 2009). The soluble inorganic Fe resulting for the photochemical transformation of vibrioferrin was bioavailable to a dinoflagellate, enhancing Fe uptake by 20-fold (Amin et al., 2009).

Although siderophores are known to affect Fe chemistry and bioavailability (Hutchins et al, 1999), they are only present in pM concentrations (Gledhill et al, 2004; Mawji et al, 2008) and, therefore, represent a small proportion of the total ligand concentration. The low concentration, coupled with there being little evidence that eukaryotic phytoplankton produce or directly use siderophores, suggests that there must be a number of other ligand sources which control Fe bioavailability (Hassler et al., 2011a). Reports of the excretion of Fe-binding ligands, within the detection limit of the CLE-AdCSV were also reported for several phytoplankton cultures, namely *Emiliania huxleyi* (Boye et al., 2000), a diatom *Thalassiosira* sp. (Rijkenberg et al., 2008), and a toxic *Pseudo-nitzschia* (Rue & Bruland, 2001; Maldonado et al., 2002). This suggests that phytoplankton are able to excrete (or release upon lysis) organic ligands able to strongly bind Fe.

Many marine organisms produce porphyrins which are used intracellularly to bind Fe (Vraspir & Butler, 2009). These can be released into the surrounding waters via the grazing activities of zooplankton and cell lysis, two known pathways for Fe recycling (Strezepek et al, 2005), and passive excretion (Vong et al, 2007; Vraspir & Butler, 2009). Under experimental conditions, Luther et al. (2001) measured an Fe-porphyrin complex with a $K_{Fe'L}$ of $10^{11.9}$ using the commonly found protoporphyrin IX as a model ligand. This value falls within the upper range of the L_2 ligand class and suggests that porphyrins, are contributing to the pool of Fe binding ligands (Rue & Bruland, 1995, 1997; Hutchins et al., 1999; Boye & van den Berg, 2000). Interestingly, siderophores produced by heterotrophs appear not to have the ability to acquire Fe through Fe-porphyrin complexes or inorganic Fe oxides (Hutchins et al., 1999).

The most abundant components of DOM are carbohydrates, with approximately 50% of this being present as polysaccharides (Benner et al., 1992; Benner, 2002). Polysaccharides can account for up to 70% of the total saccharides concentration in surface water, but the concentration decreases with depth where monosaccharides dominate (Pakulski & Benner, 1994). The concentration of monosaccharides varies little with depth, so the behaviour of polysaccharides suggests that they are reactive in surface waters (Pakulski & Benner, 1994). Polysaccharides provide strong binding sites for trace metals, and have been identified as contributing a significant role to the cycling of carbon and trace elements (Quigley et al., 2002; Engel et al., 2004). This suggests that saccharides could potentially be a key player in the cycling of Fe.

A large number of marine bacterio- and phytoplankton release polysaccharides, either as exopolymeric substances (EPS), or from intracellular storage products following cell lysis or grazing. (Decho, 1990; Hoagland et al., 1993; Mancuso Nichols et al., 2005). EPS are produced for a variety of functions including cryoprotection, halotolerance, the formation of chains or colonies, and substrate attachment (Decho, 1990; Hoagland et al., 1993). Due to the many roles, EPS are likely to be present in relatively high concentrations (Hassler et al., 2011a).

EPS are often rich in acid polysaccharides, many of which contain carboxylic groups (Hoagland et al., 1993), such as uronic acids (Janse et al., 1996; Mancuso-Nichols et al., 2005) that are known to bind Fe (Croot & Johansson, 2000; Sreeram et al., 2004). Croot and Johansson (2000) measured a $K_{Fe'L}$ of $10^{8.8}$ from an Fe-gluconic acid complex, which is within the lower range of L_2 ligands. The concentration of uronic acids are variable in both algal and bacterial EPS (Verdugo et al., 2004; Mancuso Nichols et al., 2005), but can account for between 20 and 50% of the polysaccharides produced by some marine bacteria (Kennedy et al., 1987). High concentrations of (poly)saccharides have been shown to enhance reduction of Fe(III) to the more bioavailable Fe(II) through the production of photochemically produced superoxide (O^{-}_{2}) (Öztürk et al., 2004; Morel et al., 2008; Steigenberger et al., 2010). Indeed, laboratory experiments have shown that Fe bound to EPS, uronic acids and other polysaccharides (e.g. dextran) can be highly bioavailable to eukaryotic phytoplankton from the Southern Ocean (Hassler and Schoemann, 2009, Hassler et al., 2011a, b, In press).

Through the production of organic material such as siderophores, EPS, and cell lysis material the microorganisms themselves are clearly exerting a feedback effect on Fe

chemistry (Hutchins et al., 1999; Rijkenberg et al., 2008), although currently the role of these products in Fe biogeochemistry is not fully resolved.

Complexes between natural organic matter (NOM) and metals are common in natural waters, although the stability of these complexes is variable between open ocean and coastal waters (Rose & Waite, 2003a, b). In the open oceans, the solubility of Fe is controlled to a greater degree by the concentration of organic ligands than in coastal waters, due to more stable complexes that are formed (Rose & Waite, 2003). The origins and supply of NOM to coastal waters is much more varied and dynamic, therefore the kinetic properties of the NOM will also vary, giving stability constants in both the L_1 and L_2 classes of ligands (Rose & Waite, 2003a, b).

It has been suggested that a fraction of the unknown weaker ligands found in the deep and coastal ocean could be associated with humic material (Laglera & van den Berg, 2009). Humic substances (HS), often referred to as yellow substances or chromophoric organic matter (COM or CDOM if in the dissolved phase), are ubiquitous in natural organic matter (NOM) present in soil and natural waters (Laglera et al., 2007). HS are divided into high molecular weight (HMW) humic acids (HA), and moderate molecular weight (MMW) fulvic acids (FA) (Malcolm, 1990) by the nature of their solubility, where at pH 1 HAs will precipitate, whilst FAs are soluble (Laglera et al., 2007, 2009). They are refractory in nature, with FAs typically having residence times of centuries, and HAs millennia (Thurman & Malcolm, 1981). The chromophoric group of HS is highly susceptible to photochemical degradation, which can enhance Fe reduction via the production of superoxide (Rose & Waite, 2005). HS can make up a substantial percentage of the DOM pool in aquatic environments, with estimates of between 40 and 80% in freshwater (Thurman, 1985; Obernosterer & Herndl, 2000), and 10 and 50% in estuaries and coastal waters (Laglera et al., 2007). HS are less abundant in marine systems but can account for 5-25% of the DOM pool even in remote ocean regions (Obernosterer & Herndl, 2000).

It was thought that very little terrestrial HS enters the open ocean due to prior precipitation within estuarine systems (Sholkovitz & Copland, 1981), and early work by Mantoura et al. (1978) suggested that the HS present in seawater had a very low metal binding affinity due to competition with Ca and Mg. Consequently, few studies into the interactions between metals and HS in seawater have been made (Yang & van den Berg, 2009). However, more recently it has been found that Fe-binding HS are abundant in coastal waters, and also occur at low concentrations in the deep ocean (Laglera & van den

Berg, 2009). The composition and concentration of HS in aquatic systems varies greatly. In freshwater, estuarine and some coastal regions, HS often occur in relatively high concentrations (mg L^{-1}) and are mostly HAs of allochothonous (terrestrial) origin. In contrast, marine HS is mainly autochthonously produced, consisting predominantly of FAs (~98%), and is present in much lower concentrations (10's to 100's of μg L^{-1}) (Malcolm, 1990; Obernosterer and Herndl, 2000; Laglera *et al*, 2011).

Laboratory experiments have shown that terrestrial HS forms copper (Cu) and Fe complexes with stability constants that are within the L_2 ligand class range (Cu $K_{Cu'-L}$= 20 to 22, Fe $K_{Fe'L}$ ~ 11) (Kogut & Voelker, 2001; Laglera & van den Berg, 2009). In terms of Fe, coastal HS is most similar to HA (Laglera & van den Berg, 2009), indicating that this is likely the more dominant fraction of HS in coastal regions (Yang & van den Berg, 2009), as the proximity to terrestrial sources may suggest.

It is worth noting that shipboard or laboratory electrochemical analysis of ligands, including HS, from deep water profiles has, to the author's knowledge, always been conducted at ambient temperature (i.e. 20 °C). At the low *in situ* temperatures of the deep ocean (~ 2 °C) the kinetics of Fe-ligand association and disassociation are likely to quite different to the kinetics in warmer surface water. This factor is almost always overlooked but consideration should be given to the possibility of this source of uncertainty.

1.6. Summary

It is likely that the organic complexation of Fe to an as yet poorly defined range of ligands exerts the largest influence on iron bioavailability, but our understanding of which sources of Fe are available to which phytoplankton species is unresolved. Fe source determines the origin and the nature of Fe-binding organic ligands, and subsequently the role these ligands play in maintaining Fe solubility and enhancing bioavailability. There are many uncertainties with regard to the nature of natural organic ligands. Currently organic ligands are grouped as to their binding capacities (L_1 and L_2), and whilst laboratory experiments have highlighted a number of Fe-binding compounds (siderophores, EPS, (poly)saccharides, NOM, etc) as contributors to the ligand pool, our knowledge as to their relative importance within marine systems is limited.

1.7. Thesis outline

This thesis investigates the distribution, concentration, and conditional stability constants of naturally occurring Fe-binding organic ligands, including Fe-binding humic substance-like (HS-like) material, present in the Tasman Sea and sub-Antarctic Zone (SAZ). Using a combination of observational and experimental approaches, this thesis also examines how a range of natural organic ligands impact Fe chemistry and the bioavailability of Fe to phytoplankton communities in these regions, and which forms of Fe are most available for algal uptake. Further experimental work focuses on the largely unexplored role of bacterial and algal exopolymeric substances (EPS) in Fe chemistry and how this material affects the solubility of Fe and its bioavailability. Furthermore, as dust-borne Fe may become an increasing important source of Fe to the Tasman Sea and Southern Ocean, the Fe chemistry and bioavailability of dust-borne Fe sourced from the Australian continent are investigated, including the effect of light exposure.

Chapter 2 examines the distribution of HS-like material (detected using cathodic stripping voltammetry (CSV)) in temperate coastal and offshore waters influenced by the East Australian Current (EAC). The seawater samples were collected in spring (October 2010) after significant rainfall, when it was expected that there would be a large cross-shelf gradient in terrestrial to marine origin HS-like material. In addition, perturbation experiments were undertaken to examine the production and consumption of HS-like material and the effect that HS had on phytoplankton growth. The hypotheses tested were that a) contrasting phytoplankton communities from different water masses would have different nutrient status, and that addition of HS-like material could potentially relieve Fe-limitation, and b) the community composition and nutrient status would alter the biological production of HS.

Chapter 3 documents the distribution, concentration and conditional stability constants of organic ligands (detected using competitive ligand exchange-cathodic stripping voltammetry (CLE-AdCSV)) and the distribution and concentration of HS-like material and dissolved Fe from seawater profiles obtained in the northern and southern Tasman Sea. The samples were collected in summer (January 2010) when waters in the northern Tasman Sea were not only potentially Fe limited but also seasonally N and P depleted. Perturbation experiments, again using contrasting northern and southern phytoplankton communities, investigated how the phytoplankton respond to Fe delivered from different sources, i.e. as inorganic or organically bound Fe including inorganic Fe, dust-borne Fe and Fe bound to a siderophore, saccharides and EPS. Quantitative biological response

measurements included growth (biomass) and community structure. Organic ligand concentration and binding affinity of the *in situ* ligands and added ligands were used to assess the degradation/production of organic ligands during the experiment, and to link the biological response to Fe chemistry for each source. This was to test the hypothesis that resident phytoplankton communities would respond in different ways to Fe sources, depending on their nutritional demands and Fe acquisition strategies.

Chapter 4 investigates how four different types of bacterial and algal EPS affect Fe solubility in seawater, the nature of their Fe-binding properties and redox behaviour. In addition, the physico-chemical composition of the EPS was analysed using asymmetrical flow field-flow fractionation (AFIFFF) and further characterisation of functional composition, macronutrient content, elemental composition, and contribution of HS-like material of the four EPS isolates used were examined using colorimetric and electrochemical (CSV) techniques. In addition, laboratory experiments addressed how each EPS might affect the growth and bioavailability of Fe to an Fe-limited Southern Ocean diatom *Chaetoceros simplex.*

Chapter 5 investigates the Fe content and organic ligands associated with dust from an Australian continental source periodically deposited in in the Tasman Sea and Southern Ocean. The association with macronutrients and trace elements was also investigated. The effect of UV exposure on Fe solubility and Fe-binding affinity was explored, together with the growth and bioavailability of the dust-borne Fe to an environmentally and geographically relevant Southern Ocean diatom, *Chaetoceros simplex*.

Finally, the general discussion summarises the key findings and highlights the contributions that this thesis brings to our understanding how organic ligands influence Fe chemistry and bioavailability. The implications to phytoplankton community structure and carbon cycling are addressed, and future research directions are suggested.

CHAPTER 2:

DETERMINATION OF IRON-BINDING HUMIC SUBSTANCE-LIKE MATERIAL IN NATURAL SURFACE SEAWATER AND SHIPBOARD NUTRIENT-ENRICHMENT EXPERIMENTS.

Note and acknowledgements

The data presented in this chapter were obtained from both natural samples and those from two nutrient-enrichment experiments collected during the SS2010-V09 voyage in the Tasman Sea (RV Southern Surveyor, October 2010). I did not participate in the voyage, but was responsible for the analysis of Fe-binding humic substance-like (HS-like) material. Some of the data presented here will contribute to a manuscript 'in preparation' with a working title 'Nutrient limitation of microbial growth and productivity associated with a western boundary current authored by Martina Doblin, Katherina Petrou, Louiza Norman, Christel Hassler, Justin Seymour, Sutinee Sinutok, Mark Brown, Peter Thompson. Martina Doblin is preparing the manuscript and was chief scientist on the voyage. I am grateful to colleagues listed below who provided data and methodologies and to those who participated in the voyage to obtain the samples.

Dr Jason Everett – Providing the location maps (Fig. 2.1).

Dr Andrew Bowie (UTas) – Dissolved Fe data.

Dr Katherina Petrou (UTS) – Shipboard nutrient experiments and sample handling.

Dr Sutinee Sinutok (UTS) – Bacteria and picophytoplankton enumeration (flow cytometry).

Alicia Navidad (CSIRO, Hobart) – Macronutrient analysis.

Ms Lesley Clementson (CSIRO, Hobart) – Pigment analysis.

Dr Nagur Cherukuru (CSIRO, Canberra) – DOC and CDOM data.

2.0 Introduction

Dissolved organic matter (DOM) constitutes the largest potential source of nutrients available to marine ecosystems (Ziegler and Benner, 2000), and is globally one of the major pools of organic carbon (C), being equivalent in magnitude to terrestrially fixed C (Bushaw et al., 1996; Benner, 2002; Kowalezuk et al., 2003).

Heterotrophic microorganisms, primarily bacterioplankton, are major producers and consumers of DOM (Pomeroy, 1974; Benner, 2002), and the production and consumption of DOM are considered the predominant pathways of C cycling in most aquatic environments (Azam 1998; Benner and Ziegler, 1999). DOM is biogeochemically important due to its role in the cycling of nutrients in the form of dissolved organic carbon (DOC), dissolved organic phosphorus (DOP), and dissolved organic nitrogen (DON), but it is ultimately a complex and poorly characterised mixture of dissolved molecules and colloids (Belzile et al., 2006).

In the marine environment, the major sources of DOM are both terrestrial (riverine and aeolian) and marine, derived from the degradation of terrestrial and aquatic plant and algal matter, as well as the exudates of marine organisms (Kirk, 1994; Andrews et al., 2000). Terrestrial DOM has a large refractory component which results in slow degradation by marine microorganisms (Benner, 2002), and it is not found to accumulate in seawater over long time periods. Riverine DOM is largely, if not wholly, terrestrial in signature, and is generally more photoreactive than marine DOM. Riverine DOM entering marine systems is rapidly lost by aggregation and sedimentation due to generally sharp estuarine salinity gradients. In the ocean, photochemical remineralisation or labilisation, and subsequent microbial utilisation are other important removal mechanisms (Sholkovitz, 1976; Miller and Zepp, 1995; Amon and Benner, 1996; Opsahl and Benner 1998). Although globally influential in marine trophodynamics, many of the characteristics of DOM are still poorly defined.

Humic substances (HS) are the chromophoric (coloured), hydrophobic components of DOM, made up predominantly of polyphenols and benzoic/carboxylic acids, which are ubiquitous in both terrestrial and aquatic environments (Buffle, 1990; Laglera et al., 2007 & 2009; van Trump et al., 2013). In marine systems, HS can make up a substantial proportion of the DOM pool, typically accounting for 10 to 50 % in estuaries and coastal waters, and 5 to 25 % in open ocean regions (Obernosterer and Herndl, 2000; Laglera et al., 2007).

In addition to providing nutrients (DOC, DOP, DON or trace elements) for marine organisms (Benner, 2002; Karl and Björkman, 2002; Berman and Bronk, 2003; Bronk et al., 2007), HS perform a variety of functions due to their variable chemical structure, and the complexity of their physical and chemical properties (Amador et al., 1990). Natural organic matter, including HS, has very efficient metal binding properties, which may increase the availability of essential micronutrients, such as Fe and Mn (Sunda, 1988; Kuma et al., 1999; Chen and Wang, 2005), whilst decreasing the toxic effects of other metals such as Cu (Inaba et al., 1996). In addition, the chromophoric nature of these compounds exerts a great deal of control over the light climate of the water column, affecting both the quantity and spectral quality of available light, thereby impacting both primary productivity and ultraviolet radiation (UV) exposure in natural waters (Ziegler and Benner, 2000; Belzile et al., 2006). This chromophoric group of HS are also highly susceptible to photochemical degradation (Vodercek et al., 1997; Nelson et al., 1998; Blough and Del Vecchio, 2002). This process not only alters light transmission through the water column due to photobleaching of the chromophores, but can also enhance the reduction of Fe(III) to Fe(II) via the photoproduction of superoxide and H_2O_2 (Amador et al, 1990; Rose and Waite, 2005; Miller et al., 2009).

Fe-binding HS are abundant in coastal regions (100s µg to mg L^{-1}) and may be an extremely important source of Fe-binding organic ligands in these areas. In the deep ocean, Fe-binding HS occur at low concentrations (Laglera & van den Berg, 2009), and likely comprise part of the poorly characterised 'weak' ligand pool associated with metal complexes (Kogut & Voelker, 2001; Laglera & van den Berg, 2009). The Fe that is bound to both HA and FA appears to be highly bioavailable to phytoplankton (Kuma et al., 1999; Chen and Wang, 2008), possibly as a result of rapid dissociation of the "weak" complexes mediated by living cells, a process that can be enhanced by the photodegradation of the chromophores in HS. However, very high concentrations of HS may result in excessive metal chelation (Price et al., 1988), or enhanced colloid formation and result in nutrient binding (Doblin et al., 1999). Imai et al. (1999), Giesy (1976), and Jackson and Hecky (1980) all suggest the HA and FA can bind Fe so tightly that it becomes unavailable to phytoplankton.

The technique used for the determination of Fe-binding HS-like material is the cathodic stripping voltammetry (CSV) method of Laglera et al. (2007) who demonstrated that Fe-HA complexes adsorb onto the Hg drop, causing a reduction peak for the complexed Fe. The addition of bromate to the sample enhances the catalytic effect of the adsorption and allows for sensitive determination of HS-like material in natural waters. The method is similar to that used by Obata and van den Berg (2001) to measure Fe, however, in this instance the

method measures the Fe reactive organic compounds that adsorb onto the Hg drop, and so it is the Fe reactive organic material that is measured and not the Fe. Although the method is sensitive for use in natural seawater samples, it is not specific to HS and so other Fe-binding components of the dissolved organic matter pool, such as thiol and exopolymeric substances (EPS), may also be detected.

The East Australia Current (EAC) is a strong and highly variable western boundary current (Ridgway and Godfrey, 1997) that travels southwards adjacent to the continental shelf from the Coral Sea to the Tasman Sea, bringing with it warm oligotrophic waters and its resident organisms (Baird et al., 2008; Thompson et al., 2009). A 'separation zone' occurs at ~ 32° S where much of the EAC turns east, away from the coast, whilst the rest of the current continues southwards, resulting in series of mesoscale eddies. The EAC can cause upwelling of nutrient-rich water from the continental slope to the continental shelf through several mechanisms (Ridgway and Godfrey, 1997; Oke and Middleton, 2000; Roughan and Middleton, 2002, 2004). However, coastal upwelling such as this does not always relieve phytoplankton nutrient limitation. Hutchins et al. (1998, 2002) reported that in areas of the Peru upwelling/Humbolt Current system and the Californian coastal upwelling region total Fe concentrations are often very low (< 0.2 nM) and, thus, primary production remains limited by Fe.

Nutrient controls on phytoplankton growth have previously been investigated in the Tasman Sea (Hassler et al., 2011c, 2014; Ellwood et al., 2013), but a significant question remains as to how the increasing southwards transport of subtropical oligotrophic waters in the EAC will affect phytoplankton community composition and primary productivity in waters close to the continental shelf. Changes in nutrient regimes and phytoplankton community structure are also likely to affect the production and consumption of autochthonously produced HS, which may further impact nutrient availability.

The study presented here comprised two components; (1) Collection of natural samples in an area off eastern Australia where HS inputs come from many sources, i.e. riverine inputs of terrestrial HS, mixed terrestrial and marine origin HS at the inner and outer shelf, and open water sites where HS was primarily of marine origin. It was expected that there would be a cross-shelf concentration gradient (high to low from nearshore to offshore), and that the composition signature of the HS would change depending on origin. (2) Two nutrient-enrichment experiments using phytoplankton communities from two contrasted sites which had different phytoplankton community structures, biomass, and nutrient regimes. Here, it was expected that the phytoplankton communities would respond quite differently

to the addition of HS, and that the addition of essential nutrients would result in variable HS production.

The analysis of humic substance-like (HS-like) material was undertaken on both components and aimed to:

a) investigate the distribution of electrochemically detected Fe-binding HS-like material in coastal and offshore regions in eastern Australia;

b) investigate the effect of HS addition on phytoplankton growth;

c) assess whether nutrient enrichment alters biological production of HS-like material.

2.1 Materials and methods

2.1.1 Sampling and physico-chemical measurements of water masses

Sampling took place in the Tasman Sea during the austral spring of 2010 (15th to 31st October) onboard the *RV Southern Surveyor* (voyage SS2010-V09, Fig. 2.1). The voyage was timed to coincide with the seasonal increase in the flow of the East Australian Current (EAC, Ridgway & Godfrey, 1997) and the phytoplankton spring bloom (Thompson et al., 2011). Sampling sites were selected with the assistance of daily Moderate Resolution Imaging Spectroradiometer (MODIS) and Advanced Very High Resolution Radiometer (AVHRR) satellite imagery and targeted the EAC and adjacent water masses, including river plumes, upwelled and continental shelf water, and mesoscale cyclonic (cold core) eddies (locations where HS-like samples were taken are shown in Fig. 2.1).

Physio-chemical properties of the water column (surface (~5 m) to 200 m) were measured at each location using a Seabird SBE911-plus Conductivity-Temperature-Depth (CTD), equipped with an AquaTracker Mk3 fluorometer (Chelsea, UK), Wetlabs C-Star transmissometer (25 cm optical path), Seabird SBE43 dissolved oxygen sensor, and Photosynthetically Active Radiation (PAR; Biospherical Instruments QCP-2300 Log Quantum Cosine Irradiance Sensor) sensor. Seawater samples were collected from the surface (5 m) and the depth of the chlorophyll-*a* maximum (Cmax; as determined by the down-cast fluorescence profile), and four other depths spanning the euphotic zone (nominally surface, 10, 25, 50, 75, 100 m) using 10-L Niskin bottles mounted on an autonomous rosette (M. Doblin, pers comms).

2.1.2 Set-up for nutrient-enrichment experiments

In addition to the sampling of water masses, two shipboard nutrient-enrichment experiments were conducted. The set-up of the experiments was identical except for the location from which seawater was collected; EAC (29 1 °S 145 3 °E), and a cyclonic cold-core eddy (CCE, 32 2 °S 143 8 °E) (Fig. 2.1).

Seawater collected at the chlorophyll maximum (EAC 78m, CCE 40 m) was transferred into acid-cleaned, 20-L LDPE or PC carboys, homogenised, and filtered through an acid-cleaned 200–210 µm mesh to remove mesozooplankton grazers. The water was sampled for initial parameters (i.e. dissolved nutrients, phytoplankton pigments, photo-physiology). Seawater was then transferred, under laminar flow (HEPA filter, MAC 10, Envirco, Sanford, NC, USA), into acid-cleaned 4-L clear polycarbonate bottles.

The experiment was designed to assess which nutrients were limiting growth, so treatments consisted of:

1. Unamended seawater control
2. NO_3 (N; 10 µM)
3. Inorganic Fe (Fe; 1 nM as $FeCl_3$ in 0.5M HCl, ICP grade, Fluka)
4. NO_3 + inorganic Fe (NFe; NO_3 = 10 µM, inorganic Fe = 1 nM)
5. Si (10 µM)
6. Mixed nutrients (Mix; NO_3, 10 µM + Fe, 1 nM + Si, 10 µM + PO_4, 0.625 µM; Redfield ratio).
7. Fulvic acid (FA) in the form of Suwannee River Fulvic Acid (SRFA 200 µg L^{-1}, International Humic Substances Society, Standard I), light incubation (FAL)
8. FA (200 µg L^{-1}) dark incubation (FAD).

Treatments were prepared in triplicate, except for the EAC FAD treatments which were prepared in duplicate due to an insufficient volume of water.

The level of nutrient enrichment for each treatment was determined from dissolved nutrient stocks measured during a previous voyage in these waters (Hassler et al., 2011c), and the biological requirement of key phytoplankton groups likely to be present in the sampled water masses. However, the results gained from the NO_X (nitrate + nitrite) analysis revealed that the NFe and Fe treatments for both the EAC and CCE experiments had been spiked with 10 µM N. This being the case, the Fe treatment was subsequently removed from further analysis.

The SRFA used in the FAL and FAD treatments was not of marine origin, but its composition is representative of what might be found in the open ocean, which is predominantly low molecular mass FA (Obernosterer and Herndl, 2001). The Fe, N and sulphur (S) content of the SRFA used in these experiments were; Fe, = < 2 nmol mg^{-1} SRFA (Laglera et al., 2007), N = 0.72 %, and S = 0.44 % (elemental composition in %(w/w) of a dry, ash-free sample; source, International Humic Substances Society (IHSS).

Once prepared, bottle lids were sealed with parafilm to avoid Fe contamination, and bottles placed in a flow through on-deck incubator at sea surface temperature, and light exposure at 25% of the surface irradiance. During the EAC experiment the bottles received daily enrichment with the appropriate nutrient/s and were sampled for photo-physiological measurements (F_V/F_M) and flow cytometry; they were then resealed and returned to the incubator. During the CCE experiment, daily sampling for F_V/F_M and flow cytometry was carried out, however, only a single initial nutrient addition was given on Day 0 (T0). After 72-h, the experiments were stopped and samples were taken for dissolved macronutrients (NH_4, NO_X, $Si(OH)_4$, PO_4,), HS-like material, dissolved Fe (dFe), chromophoric dissolved organic matter (CDOM), flow cytometry, HPLC pigments, and F_V/F_M. Samples for HS-like material were filtered through 0.2-µm polycarbonate filters (Whatman, 45 mm) and stored at -20 °C prior to analysis on shore (UTS).

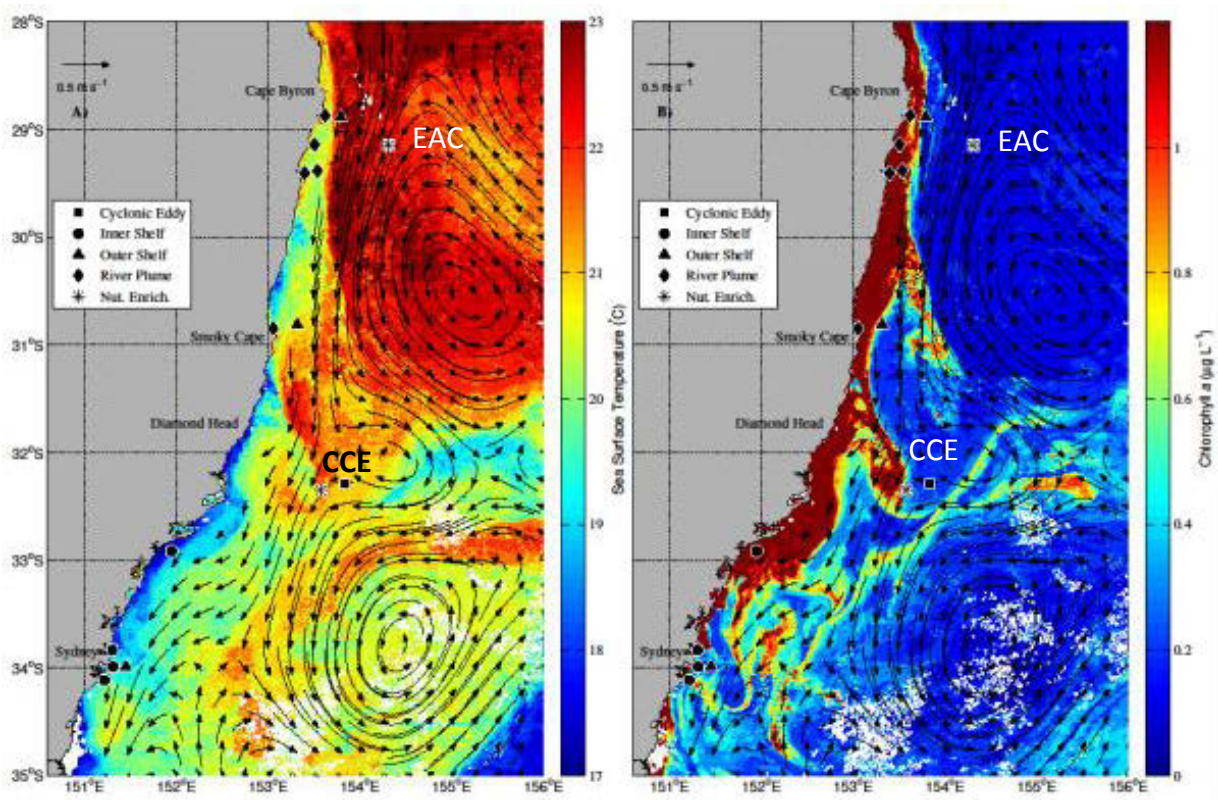

Fig. 2.1 Sea surface temperature (SST) and Chlorophyll-*a* (µg L^{-1}) plots showing the study area and sampling locations for natural humic substance-like material and nutrient-enrichment experiments. Natural samples were collected from at variety of watermass types (river plume, inner shelf, outer shelf, and oceanic (cold-core cyclonic eddy (CCE) and East Australia Current (EAC)), and seawater collected for the nutrient experiments was sampled from the EAC and CCE.

2.1.3 Analysis of humic substance-like (HS-like) material

The concentration of HS-like material was determined using the voltametric method of Laglera et al. (2007). The instruments used were μAutolab II and III potentiostats (Ecochemie, Utrecht, Netherlands) with a hanging mercury (Hg) drop electrode (Hg, Sigma Aldrich, ACS reagent grade, 99.9995% trace metal basis; HMDE drop size 2, 0.4 mm^2 ±10%, VA 663 stand – Metrohm, Herisau, Switzerland), a glassy carbon rod counter electrode, and a double junction, Ag/AgCl, reference electrode with a salt bridge filled with 3M KCl. The instruments were controlled using GPES software, version 4.7. Briefly, 750-μl of a mixed reagent solution of the oxidant $KBrO_3$ (0.4 M sigma), buffer 4-(2-Hydroxyethyl)-1-piperazinepropanesulfonic acid (EPPS; 0.2 M, Sigma), and NH_4OH (0.2 M) was added to 10-mL of sample in the presence of 50 nM Fe (Fe as $FeCl_3$ in 0.5M HCl, ICP grade, Fluka). The final pH of the samples was 8.1. Samples were then left to equilibrate at ambient temperature for 1-h. During analysis, dissolved oxygen was purged from the sample for 250-s using high purity argon (Air Liquide, Beresfield, NSW, Australia), followed by an appropriate deposition time (150- to 300- s) onto a fresh Hg drop. Most samples required 150-s deposition time, however, samples with very low concentrations of HS-like material, i.e., where the sample peak was difficult to distinguish, a longer deposition time was applied to enhance the signal.

Both a standard addition method and a conventional six point calibration were tested to assess which method would be most appropriate to determine the concentration of HS-like substances in the samples. The calibration curve was prepared in synthetic seawater (Table 2.1) and both methods used Suwannee River Fulvic Acid (SRFA; Std 1, International Humic Substances Society, Denver, Colorado, USA) as the model humic substance as per Laglera et al. (2007). Natural seawater samples from both coastal and offshore regions collected during the voyage were used because the natural organic matter (NOM) signature of these regions can be quite different, with coastal samples likely to have a more allochthanous (terrigenous) origin and offshore samples more likely to have an autochthonous (*in situ*/biological) origin. Results indicated that the standard addition method was more appropriate, given the range of samples to be analysed, and that the variations in sensitivity (slope) between samples could provide more information as to the character of the HS-like material measured (Section 2.2.1).

The standard addition analytical protocol for HS used in this study used a deposition time of 150 s, and SRFA increments of 20 μg L^{-1} or 50 μg L^{-1} from a 1575 μg L^{-1} working stock of SRFA (prepared weekly and stored at 4 °C in the dark; reported as SRFA equivalents). The

increments of SRFA addition were determined from the reduction peak of the natural samples, i.e. those with no SRFA added. As a general rule, in samples with reduction peaks < 1 x 10^{-9}, SRFA additions of 20 µg L^{-1} were used, and in those samples with reduction peaks > 1 x 10^{-9} SRFA additions of 50 µg L^{-1} were used. The detection limit of the instruments was 3.63 µg L^{-1} (µAutolab II) and 3.76 µg L^{-1} (µAutolab III) SRFA eq., determined from three times the standard deviation of ten repeated measurements of a Southern Ocean seawater sample using purge and deposition times as per SS2010-V09 voyage and experimental samples. Instrument sensitivity (slope) and the placement of the central point of the reduction peak recorded during analysis were used investigate the nature/origin of the HS-like material.

It should be noted that the model humic substance, SRFA, used as a standard in these analyses was the same material added to the FAL and FAD treatments and is river derived and not from a marine origin. Whilst this is not ideal for the analysis of marine samples, given the different compositions of riverine (allochthonous) and marine (autochthonous) HS, marine HS is not easily recovered from seawater (Yang & van den Berg, 2009) and is currently not commercially available. Compared to freshwater, estuarine, and coastal waters the concentration of HS is very small and so vast quantities of water are required in order to recover very small quantities of HS. For example, Esteves and co-workers (2009) gained just 2.3 g of freeze dried HS from 4,600-L of seawater. A second problem that affects the isolation of HS from all environments, is that regardless of the method used (XAD-8 resin, ultrafiltration, two column array of XAD-8 and XAD-4 resin), recovery of DOM is typically 30 – 35% (Mopper et al., 2007; Esteves et al., 2009; Koprivnak et al., 2009). However, terrestrial FA and marine HS give similar CSV responses and, in the absence of marine HS standards, this has led to the widespread use of terrestrial FA as model compounds (or controls) when determining metal complex stability (Laglera et al., 2007, 2009; Yang & van den Berg, 2009).

Table 2.1 Constituents of synthetic seawater used for humic substance-like analysis. Based on AQUIL media as per Price et al. (1989) using major salt only. Final pH = 8.00

Constituent	Concentration (M)
NaCl	4.20×10^{-1}
Na_2SO_4	2.88×10^{-2}
KCl	9.39×10^{-3}
$NaHCO_3$	7.14×10^{-3}
KBr	8.40×10^{-4}
H_3BO_3	1.46×10^{-3}
NaF	7.14×10^{-5}
$MgCl_2*6H_2O$	5.46×10^{-2}
$CaCl_2*2H_2O$	1.05×10^{-2}
$SrCl_2*6H_2O$	6.38×10^{-5}

2.1.4 Total Dissolved Fe and macronutrient analysis of experimental samples

Dissolved Fe was determined by flow injection analysis (FIA) with chemiluminescence detection following the method of de Jong et al (1998). Accuracy was checked daily using an in-house standard (0.17 ± 0.02 nM).

Macronutrients (nitrate + nitrite (NO_X), silicic acid ($Si(OH)_4$), and phosphate (PO_4)) were determined on board using flow infection analysis according to Cowley et al., (1999). Detection limits were: 0.035 μmol L^{-1} for NO_x, 0.012 μmol L^{-1} for Si and 0.009 μmol L^{-1} for PO_4.

2.1.5 Phytoplankton pigment analysis

Seawater (minimum volume 2.2-L) was filtered under low vacuum (e.g. ≤ 100 mm Hg) through 25-mm GF/F filters in low light (< 10 μmol photons m^{-2} s^{-1}). Filters were folded in half, blotted dry on absorbent paper, placed into screw-capped cryovials and stored in liquid nitrogen until pigment analysis. In the laboratory, pigments were extracted at 4° C in the dark over 15–18-h in 3-mL acetone (100%, diluted to 90% with deionised water for

analysis, Mallinkrodt, HPLC grade) then sonicated on ice for 15-min. Samples were recovered using filtration (GF/F, 0.45-µm, Whatman) and centrifugation (2500 rpm, 5 min at 4° C). Pigment concentrations were measured using High Performance Liquid Chromatography (HPLC). The HPLC instrument comprised a 2695XE separations module with column heater and refrigerated autosampler (Waters-Alliance, Rydalmere, NSW, Australia) using a C_8 column (Zorbax Eclipse XDB-C8, Agilent Technologies, Mulgrave, VIC, Australia) and binary gradient system with an elevated column temperature (55° C) and the analysis followed a modified version of the Van Heukelem and Thomas (2001) method. Pigments were identified by their retention time and absorption spectrum from a photo-diode array detector (Waters-Alliance 2996 PDA). Concentrations of pigments were determined from commercial and international standards (Sigma; DHI, Denmark). The HPLC system was also calibrated using phytoplankton reference cultures (Australian National Algae Culture Collection) whose pigment composition has been documented in the literature (Mantoura and Llewellyn, 1983; Barlow et al., 1993).

2.1.6 Bacterial and picophytoplankton enumeration

Samples for enumeration of bacteria and picophytoplankton were fixed with glutaraldehyde (1% v/v final concentration), cryopreserved in liquid nitrogen and stored at -80° C. Picophytoplankton samples were analysed using a flow cytometer (Becton Dickinson LSR II; BD Biosciences, North Ryde, NSW, Australia). Populations of the cyanobacteria genera *Prochlorococcus* and *Synechococcus* and pico-eukaryotes were discriminated using side scatter (SSC) and red and orange fluorescence (Seymour et al., 2012). Data was analysed using Cell-Quest Pro (BD Biosciences, North Ryde, NSW, Australia).

2.1.7 ^{14}C incubations for determination of carbon fixation rates

Primary productivity was estimated using small volume incubations as described in Doblin et al. (2011). Radiolabeled sodium bicarbonate 6.327 x 10^6 Bq (0.171 mCi) $NaH^{14}CO_3$ was added to 162-mL of sample to produce a working solution of 39.183 x 10^3 Bq per mL (1.1 µC mL^{-1}). Seven mL aliquots of working solution were then added to transparent glass scintillation vials and incubated under ambient temperature for 1-h at 21 light intensities ranging from 0 to 1500 µmol m^{-2} s^{-1}. After 1-h 25-µL of 6 M HCl was added to each vial and they were then agitated for 3-h to ensure that all inorganic carbon was removed. For

radioactive counts, 10-mL Ultima Gold™ (Perkin Elmer) scintillation fluid was added to each vial and shaken. Samples were then counted using a scintillation counter (Packard TriCarb 2900 TR, Perkin Elmer, Glen Waverley, VIC, Australia) with the maximum counting time set at 5-min. In addition, Time 0 counts were taken to determine background radiation and 100% counts were used to determine the specific activity of the working solution. For Time 0 counts, 7-mL aliquots of working solution were subjected to acid addition without any exposure to light, and counted after shaking for 3-h. For 100% samples, 100-µL of working solution from each depth was added to 7-mL NaOH (0.1 M) and immediately counted following the addition of scintillation fluid. Carbon uptake rates were corrected for *in situ* Chlorophyll-*a* (Chl-*a*) concentrations measured using HPLC and for total dissolved inorganic carbon availability analysed using colorimetric procedures (Johnson *et al.*, 1998). Carbon fixation-irradiance relationships were then plotted and the equation of Platt *et al.* (1980) was used to fit curves to data using least squares non-linear regression. Photosynthetic parameters determined included light-saturated photosynthetic rate [P_{max}, mg C (mg Chl-*a*)$^{-1}$ h^{-1}], initial slope of the light-limited section of the carbon fixation-irradiance curve [α, mg C (mg Chl-*a*)$^{-1}$ h^{-1} (µmol photons m^{-2} s^{-1})$^{-1}$], and light intensity at which carbon-uptake became maximal (calculated as P_{max}/ α = E_k, µmol photons m^{-2} s^{-1}).

2.1.8 Experimental and analytical precautions

All plasticware (LDPE and HDPE bottles, pipette tips, forceps, polycarbonate containers, and tubing) to be used during the voyage and for HS-like analysis were cleaned by first soaking in detergent (Citrinox acid detergent, 5% v/v) for 24-h, followed by rinsing five times in deionised water. The items were then soaked for four weeks. in 1 M HCl, save for polycarbonate containers which were soaked for one week. to avoid deterioration. The equipment was then rinsed seven times in ultrapure water (18.2 MΩcm^{-1}, Arium 611UV, Sartorius Stedim, Dandenong, VIC, Australia) and then dried under laminar flow (ISO class 5). For the analysis of HS-like material, all sample manipulations and reagent preparation was carried out in a dedicated 'clean' laboratory area under laminar flow (ISO class 5).

All reagents used in analysis and nutrient solutions were made up in ultrapure water unless otherwise stated, and were passed through Chelex-100 resin (BioRad, conditioned as per Price et al., 1989), except for the silicate solution, prior to use to minimise Fe contamination.

During the voyage, as a general precaution to avoid nutrient, as well as biological cross-contamination, all containers were rinsed three times with Milli-Q™ ultrapure water prior

to being used. In addition, for on-deck incubations, the same bottles were reused for identical experimental treatments.

2.1.9 Data manipulation and statistical analysis

In order to investigate the relationship of HS-like material with physico-chemical (temperature, salinity, turbidity (CTD-derived light transmission)) and biological (Chl-*a* fluorescence) parameters the HS-like concentration data was log-transformed due to the extremely high HS-like concentration in samples taken from the Clarence River plume and the high concentrations of SRFA in the enriched experimental samples. This allowed for clearer graphical representation and assessment of any relationships.

Relationships between measured parameters in the natural and experimental samples were investigated using Pearson correlations and were followed by regression analysis, where relationships were significant ($p < 0.05$). Differences between experimental treatments were analysed using an unpaired t-test.

A range of environmental parameters (TChl-*a*, biomarker pigments, dissolved nutrients, bacterial and picophytoplankton abundance) were used to investigate the origin/nature of the HS-like material present in the experimental incubations using PRIMER 6 (version 6.1.14). Multidimensional scaling (MDS) based on Euclidean distance similarity measure was used to examine the similarities in the experimental treatments. To give insight into which parameters explained most of the variability in HS-like concentration and sensitivity, distance-based redundancy analysis (dbRDA) was used to model the relationship between environmental predictor variables and HS-like material using DISTLM in PERMANOVA+ as described in Anderson et al. (2008). Individual marginal tests were performed to assess the importance of each environmental parameter, and the Akaike information criterion (AIC) was used to identify the combination of environmental variables that best explained the (dis)similarity among the treatments. A maximum cut off of five environmental variables (from a total of 15) was used as the contribution of each subsequent parameter was considered too small to be of any real influence.

As the FAL and FAD treatments represented artificial HS addition, these treatments were excluded from the HS-like concentration analysis, but were included in the analysis investigating HS-like sensitivity as they could provide some insight as to origin and possible biological transformation. So that all the above parameters could be included in multivariate analysis only replicates 1 and 2 of each treatment were used as dFe samples were taken

only from these incubations and not from replicate 3. Likewise, as T0 macronutrient (NO_X, PO_4, $Si(OH)_4$) data was not available for the EAC experiment, T0 samples were removed from the analysis so that data from both experiments could be analysed using identical procedures.

2.2 Results

2.2.1 Validation of standard addition as a method for determination of Fe-binding HS-like material

The standard addition method revealed an order of magnitude difference between the sensitivity (slope of peak height in nA (i_p) versus SRFA concentration; Fig. 2.2) of the surface (5 m) coastal and offshore samples. The samples taken from the Cmax were more similar, but had substantially different sensitivities to the surface samples (Table 2.2). The sensitivity of the six point calibration curve (0.8×10^{-8}) was an order of magnitude lower than all of those determined by standard addition into natural seawater (Fig. 2.2). When the concentration of HS-like material was calculated, values determined from the calibration curve were between 57 and 94% greater than those calculated by standard addition (Table. 2.2). The variability in sensitivity between natural samples, and also between natural seawater and synthetic seawater (calibration curve) suggests that quantification of HS-like material may be sample-matrix dependent.

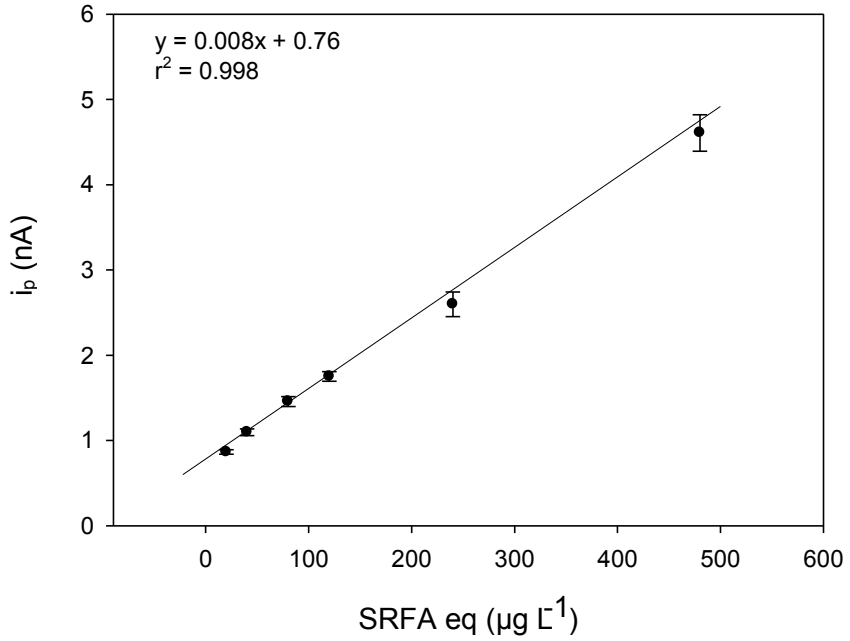

Fig. 2.2 Calibration curve used for the comparison of methods to determine the concentration of electrochemically detected humic substance-like (HS-like) material. Suwannee River Fulvic Acid (SRFA) was used as the HS-like standard in concentrations between 20 and 480 µg L^{-1}. i_p represents the peak height in nA of electrochemically detected Fe′-reactive organic material. Errors = SD of triplicate samples.

Table 2.2 Comparison of concentrations of electrochemically detected humic substance-like (HS-like) determined using a standard addition method into natural seawater and a conventional calibration curve prepared in synthetic seawater. The percentage difference in concentration calculated between methods, sensitivity of natural seawater and position of the reduction peak (E_p, V vs Ag/AgCl electrode) are also presented. Natural seawater samples were taken at 5 m depth and the depth of the chlorophyll maximum (Cmax) from a coastal site and an offshore site in the Tasman Sea. The concentration of HS-like material is expressed as Suwannee River Fulvic Acid (SRFA) equivalents in µg L^{-1}. Sensitivity of the calibration curve = 0.8 x 10^{-8} µg L^{-1}.

Sample	SRFA eq. (µg L^{-1}) Standard addition	SRFA eq. (µg L^{-1}) Calibration curve	% difference	Sensitivity of Std. addition (x 10^{-8})	E_p (V vs Ag/AgCl electrode)
Coastal 5 m	137 ± 7.4	321 ± 17.2	57	1.9	0.522
Offshore 5 m	5 ± 0.2	78 ± 4.4	94	13.2	0.523
Coastal Cmax	41 ± 4.8	249 ± 28.6	84	4.8	0.520
Offshore Cmax	20 ± 1.7	166 ± 14.8	88	6.7	0.524

2.2.2 HS-like material from natural waters

Generally the concentration of HS-like material in the natural samples was low with between 24 and 74 μg L^{-1} measured for the coastal (river plume and shelf) samples, and between 5 and 20 μg L^{-1} measured for the offshore (oceanic) samples (Table 2.3). Only the surface (5 m) and Cmax samples from the Clarence River plume and the Macleay River offshore surface sample contained more HS-like material (8530, 404, 137 μg L^{-1} SRFA eq., respectively; Table 2.3).

Surprisingly, the average concentration of HS-like material measured between river plume and shelf samples (Clarence River plume and Macleay River offshore not included) was the same (32 ± 4 μg L^{-1} versus 40 ± 17 μg L^{-1} SRFA eq., respectively). However, the average concentration of HS-like material measured in the oceanic samples was significantly lower ($p = 0.004$). As noted above, the concentration of HS-like material measured for the Clarence River plume was 400-fold greater (5 m) depth and 22-fold greater (Cmax) than any other sample.

The concentration of HS-like material between sampling depths was variable, showing higher concentrations in the surface (5 m) or subsurface (15 m or Cmax), depending on the station. For example, at some locations, samples taken at 15 m or the depth of the Cmax contained higher concentrations of HS-like material than the 5 m samples (Macleay River Plume, Stockton beach, Port Hacking, and the CCE centre), whereas at other locations the surface samples contained more HS-like material (Clarence River plume, Malabar Ocean outfall, Macleay River – offshore). In the case of the Clarence River plume this was > 20 fold greater at the surface (Table 2.3). At the remaining sites there was very little difference in HS-like concentrations between sampling depths (Clarence River – offshore, Sydney Heads, Richmond River – offshore) (Table 2.3).

Table 2.3 Concentration of electrochemically detected humic substance-like (HS-like) material measured in samples taken during the SS2010-V09 Tasman Sea voyage (*RV Southern Surveyor*, 15th to 31st October 2010, austral spring). Samples were collected at 5 m, 15 m, and the depth of the chlorophyll maximum (Cmax) from water masses comprising river plume, inner and outer shelf, and oceanic waters. Concentration of HS-like material is expressed as Suwannee River Fulvic Acid equivalents (SRFA eq) in µg L^{-1}. Values in **bold** indicate significantly elevated HS-like concentrations. ORS = Ocean reference station. Error = SD pseudo-replicates. NS denotes that no sample was taken. Depth of the Cmax is shown in parenthesis.

Location	CTD No.	Bottom depth (M)	SRFA eq (µg L^{-1}) 5 m	SRFA eq (µg L^{-1}) 15 m	SRFA eq (µg L^{-1}) Cmax
River Plumes					
Macleay River Plume	5	38.4	26 ± 1	NS	39 ± 1.2 (15 m)
Clarence River Plume	13	30.9	**8532 ± 572**	NS	**399 ± 29 (10 m)**
Clarence River - offshore	9	54.0	30 ± 3	31 ± 3	NS
Evans Head	30	40.7	34 ± 5	NS	34 ± 4 (10 m)
Inner shelf					
Stockton Beach	1	64.9	21 ± 2	43 ± 2	NS
Port Hacking	84	104.0	31 ± 3	NS	51 ± 4 (30 m)
Malabar ocean outfall	90	87.0	56 ± 7	24 ± 2	NS
Sydney Heads	91	42.3	74 ± 2	65 ± 6	NS
Outer Shelf					
Macleay River - offshore	8	431.8	**137 ± 7**	NS	41 ± 5 (70 m)
Richmond River - offshore	14	99.0	33 ± 1	35 ± 4	NS
Offshore of ORS	89	136.0	25 ± 1	18 ± 1	NS
Oceanic					
East Australia Current	21	3279	NS	NS	9 ± 0.4 (75 m)
Cyclonic Eddy centre	61	4710	5 ± 0.2	NS	20 ± 2 (45 m)

To investigate overall relationships between HS-like concentration and environmental variables, all stations were included. There was a weak positive relationship between log HS-like concentration and Chl-*a* fluorescence (CTD-derived) ($p < 0.05$; $r^2 = 0.314$), however, the Clarence River plume samples appeared to be driving this relationship. When these samples were removed from the analysis the relationship weakened ($r^2 = 0.144$) suggesting that phytoplankton abundance was not the driver of HS-like distributions (Fig. 2.3). To assess the potential source of HS-like material, relationships with salinity (riverine source) and Chl-*a* (biological) were also examined, but none were evident.

Some grouping of water masses was observed in the sensitivity data, particularly the inner and outer shelf samples which clustered together. A greater spread of sensitivity data was observed in the river plume and oceanic samples, which may reflect changing HS-like composition (Fig. 2.4). However, there were no clear relationships between reduction peak position or sensitivity and any of the environmental parameters (Fig. 2.4). Additionally, there were no relationships between sensitivity and HS-like concentration or sampling depth.

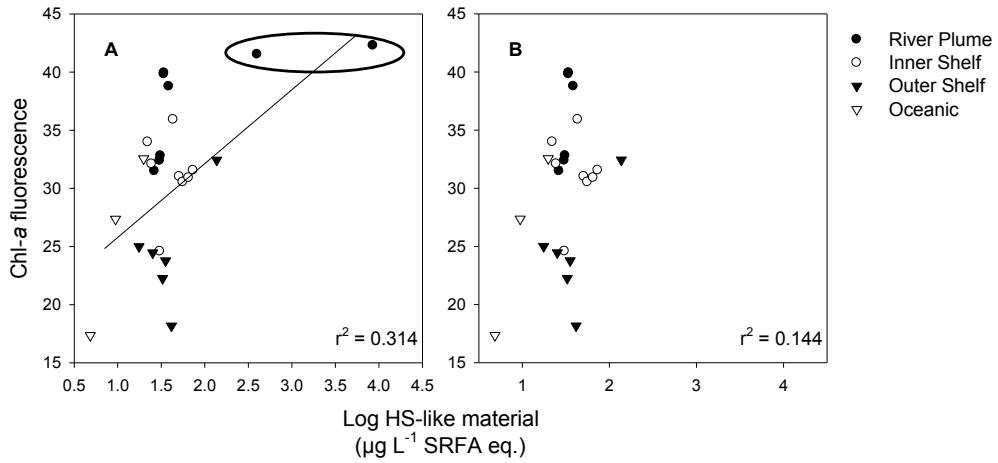

Fig. 2.3 Relationship between the concentration of humic substance-like (HS-like) material (log transformed), and Chl-*a* fluorescence (CTD derived) from samples taken during the SS2010-V09 Tasman Sea voyage (*RV Southern Surveyor*, 15th to 31st October 2010, austral spring). Samples were collected at 5 m, 15 m, and the depth of the chlorophyll maximum from water masses comprising river plume, inner shelf and outer shelf waters, and oceanic waters. Panel A indicates the weak positive relationship with Clarence River plume samples included (circled on the plot), Panel B indicates the relationship with these samples excluded.

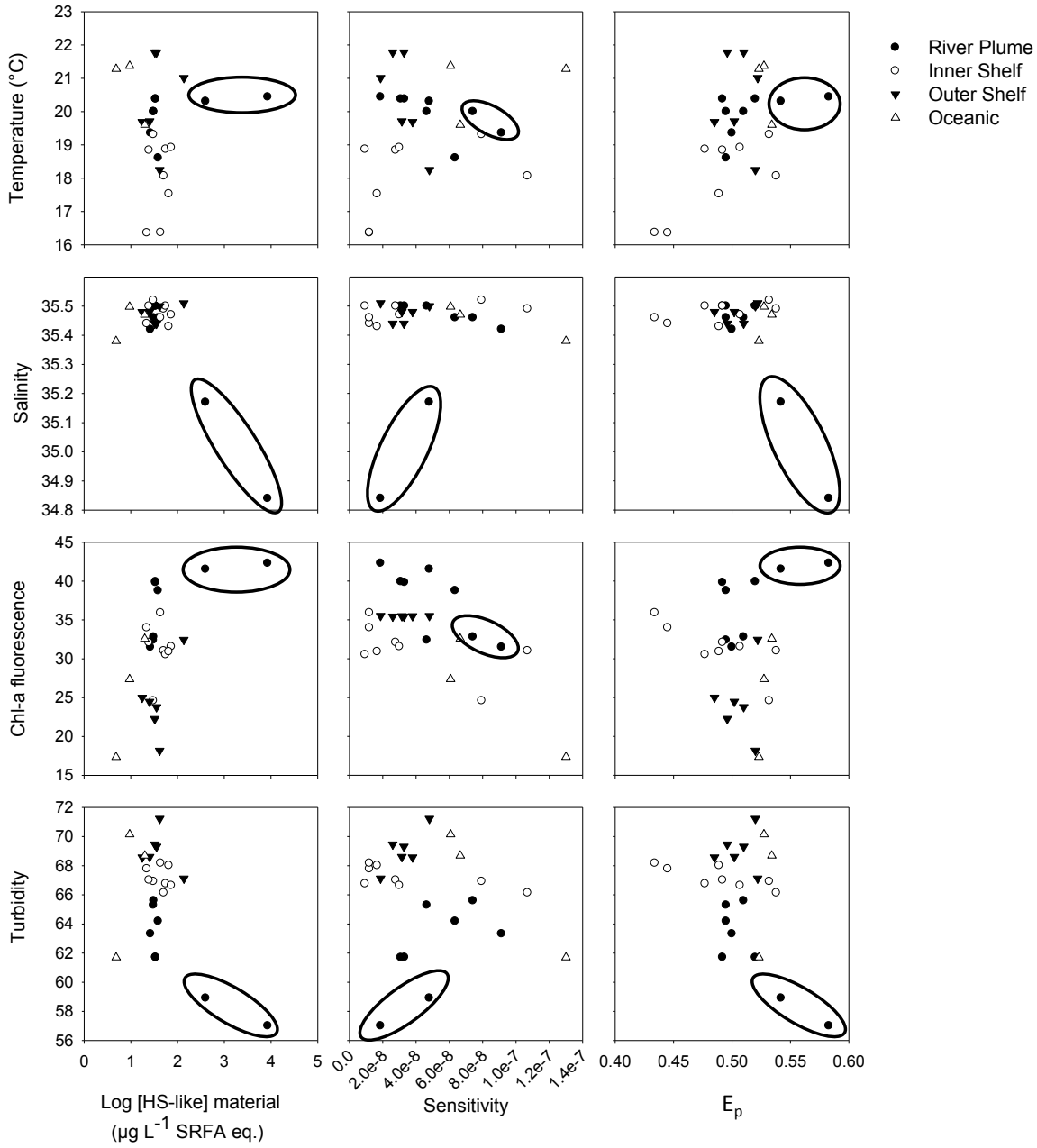

Fig. 2.4 Relationships between the concentration of humic substance-like (HS-like) material, reduction peak position (E_p, V vs Ag/AgCl electrode) or sensitivity with temperature, salinity, Chl-*a* fluorescence (CTD derived), and turbidity (light transmission) from samples taken during the SS2010-V09 Tasman Sea voyage (*RV Southern Surveyor*, 15th to 31st October 2010, austral spring). Samples were collected at 5 m, 15 m, and the depth of the chlorophyll maximum from water masses comprising river plume, inner shelf and outer shelf waters, and oceanic waters. Due to extremely high HS-like concentrations from the Clarence River Plume this data was log transformed to allow for clearer graphical representation. Clarence River Plume samples are circled on the plots.

Only 5 corresponding DOC and CDOM (ay_{440}) data points were available for these samples (3 river plume, 1 inner shelf, and 1 oceanic). A significant negative relationship was apparent between log HS-like concentration and DOC concentration, whilst no relationship was evident with CDOM. However, the DOC relationship was skewed by the single oceanic sample which, when removed, weakened the relationship considerably ($r^2 = 0.37$; Appendix 1). Given the limited data available it was not possible to assess the association of HS-like substances with DOC and CDOM.

2.2.3 Nutrient-enrichment experiments

2.2.3.1 Initial bottle characteristics

All initial dissolved nutrient concentrations for the CCE were low (NO_X = 0.1 ± 0.02 µmol L^{-1}; PO_4 = 0.11 ± 0.01 µmol L^{-1}; $Si(OH)_4$ = 0.52 ± 0.01 µmol L^{-1}; (data unavailable for EAC experiment). The concentration of NH_4 was also low at both sites (EAC = 0.1 ± 0.02; CCE = 0.16 ± 0.01 µmol L^{-1}), although the measured concentration for the CCE was significantly higher than that of the EAC ($p = 0.005$) (Fig. 2.5A-D). No T0 dFe data was available for either experiment.

The initial abundance of bacteria and picophytoplankton groups was quite different between the two sites. The T0 samples revealed that the numbers of small and large eukaryotes were similar between sites, however, bacterial numbers were slightly, but significantly ($p = 0.03$) higher at the CCE site compared to the EAC (Fig. 2.7). The biggest difference in picophytoplankton groups between sites was the abundance of *Synechococcus* and *Prochlorococcus*. *Prochlorococcus* abundance was 13-fold greater compared to the CCE (mean ± 81 x 10^3 ± 3.1 x 10^3 cells ml^{-1} and 6.2 x 10^3 ± 1.0 x 10^3 cells ml^{-1}, respectively, and *Synechococcus* abundance was more than twice that of the CCE site (mean ± SD; 17 x 10^3 ± 2.5 x 10^2 cells ml^{-1} and 7.5 x 10^3 ± 1.8 x 10^2 cells ml^{-1}, respectively; Fig. 2.7).

The concentration of total chlorophyll-*a* (TChl-*a*) in the samples taken from the EAC were three fold lower than that measured in the CCE (0.11 ± 0.01 µg L^{-1} and 0.32 ± 0.04 µg L^{-1}, respectively; Fig. 2.8). Analysis of biomarker pigments suggested that haptophytes (hex-fucoxanthin and but-fucoxanthin) were dominant in the EAC samples, with cyanobacteria (Chl-*b*),diatoms (fucoxanthin) and dinoflagellates (diadinoxanthin) present but less abundant. In the CCE, diatoms and haptophytes were dominant, with a smaller proportion of dinoflagellates (Fig. 2.9).

2.2.3.2 Macronutrients and dFe concentrations at the conclusion of the incubations

After 72-h incubation generally NO_X, PO_4 and $Si(OH)_4$ concentrations were similar or declined during both experiments relative to the unamended control and T0 (CCE only), except where nutrients had been added. The exceptions were the FAL and FAD treatments, where a significant increase in NO_X concentration was measured for both experiments ($p = \leq 0.002$), and in $Si(OH)_4$ concentration in the CCE FAL and FAD experiments ($p = \leq 0.047$) relative to the control. The elevated NO_X may have been, in part, due to the addition of approximately 0.08 μmol L^{-1} (EAC) and 0.02 μmol L^{-1} (CCE) N with the SRFA used as the FA source. However, $Si(OH)_4$ for both the CCE FAD and FAL treatments and NO_X in the CCE FAL treatment were still in lower concentration compared to T0 ($p \leq 0.004$).

The concentration of NH_4 was more variable, where the EAC N, FAL and FAD treatments all had significantly higher NH_4 concentrations compared to the control ($p \leq 0.03$; Fig. 2.5A). In the CCE experiment the control, Mix and FAD treatments contained significantly more NH_4 compared to T0 ($p \leq 0.012$); however, NH_4 was only elevated in the FAD treatment compared to the control ($p = < 0.001$). NH_4 declined in all other treatments.

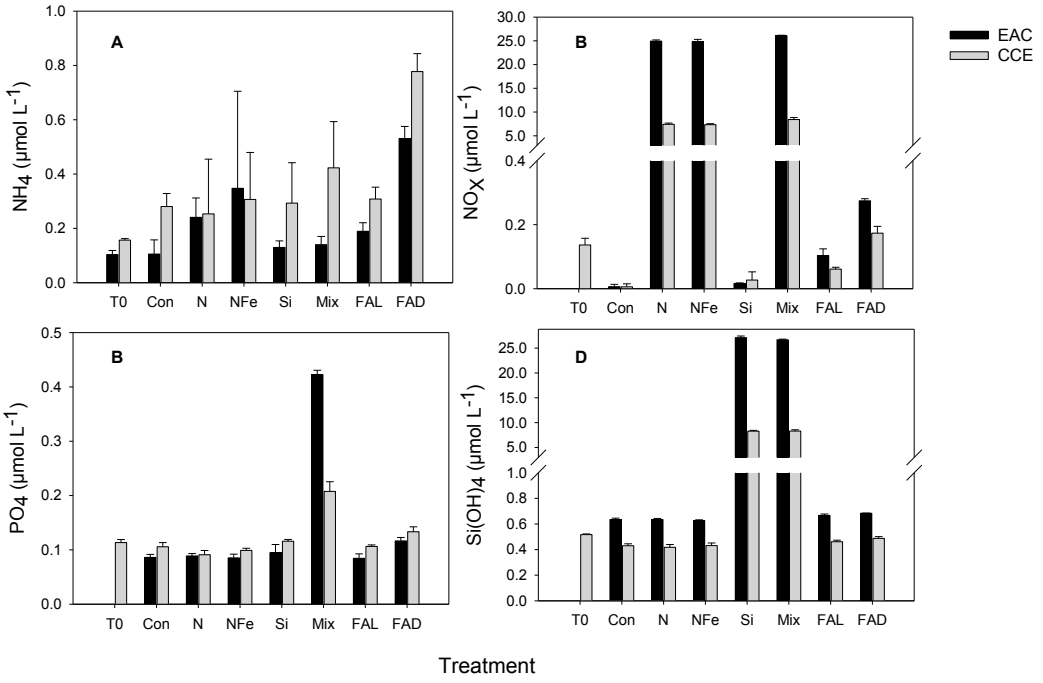

Fig. 2.5 Concentration of macronutrients (ammonia (NH_4), nitrate + nitrite (NO_X), silicic acid ($Si(OH)_4$), and phosphate (PO_4), µmol L^{-1}) in experimental bottles measured at T0 and after 72-h shipboard, nutrient-enrichment experiments undertaken during the SS2010-V09 Tasman Sea voyage (*RV Southern Surveyor*, 15th to 31st October 2010, austral spring). The experiments were conducted in 200–210-µm filtered seawater collected from the depth of the chlorophyll maximum at two sites in the Tasman Sea; East Australia Current (EAC, 29 1 °S 154 3°E), and a cold-core eddy (CCE, 32 2°S 153 8°E). T0 = unamended seawater at the start of the experiment. The treatments were; unamended control (Con), nitrate (N, 10 µM), nitrate + inorganic Fe (NFe, 10 µM + 1 nM), silicate (Si, 10 µM), mixed nutrients (Mix; NO_3 + Fe + Si + P, 10 µM + 1 nM + 10 µM + 0.625 µM), Suwannee River fulvic acid exposed to light (FAL, 200 µg L^{-1}), Suwannee River fulvic acid dark incubation (FAD, 200 µg L^{-1}). Daily additions of nutrients were given to the East Australia Current incubations, and a single initial nutrient addition was given to the cold-core eddy incubations. Errors = SD of triplicate incubations except for EAC FAD where errors represent half interval (range) of duplicates incubations.

Dissolved Fe (dFe) concentration in the EAC controls was less than half that of the CCE samples (EAC 0.43 and 0.33 nM, CCE 1.34 and 1.08 nM; Fig 2.6). In the samples where inorganic Fe had not been added (N, Si, FAL, FAD), dFe was slightly elevated in both EAC and CCE samples in the N and FAD treatments, except for one CCE N sample which contained 5.25 nM dFe, likely due to contamination (Fig. 2.6). However, in the FAL samples dFe was almost double (EAC 0.78 and 0.79 nM, CCE 2.57 and 2.08 nM) the control. The calculated contribution of Fe from the SRFA to the FAL and FAD treatments at the start of the

experiment was ~0.03 nmol L^{-1} and ~ 0.01 nmol L^{-1} in the EAC and CCE incubations, respectively. The concentration of dFe in the Si treatments was comparable to the NFe treatment even though no Fe had been added (Fig. 2.6). Unlike the other nutrient solutions, the Si was not passed through Chelex 100 resin as it was found that this process removed not only Fe but also the Si. The excess of Fe in the Si treatments may, therefore, be due to Fe contamination from the inorganic salts. The Mix treatment contained ~10 µM dFe rather than the 1 µM expected.

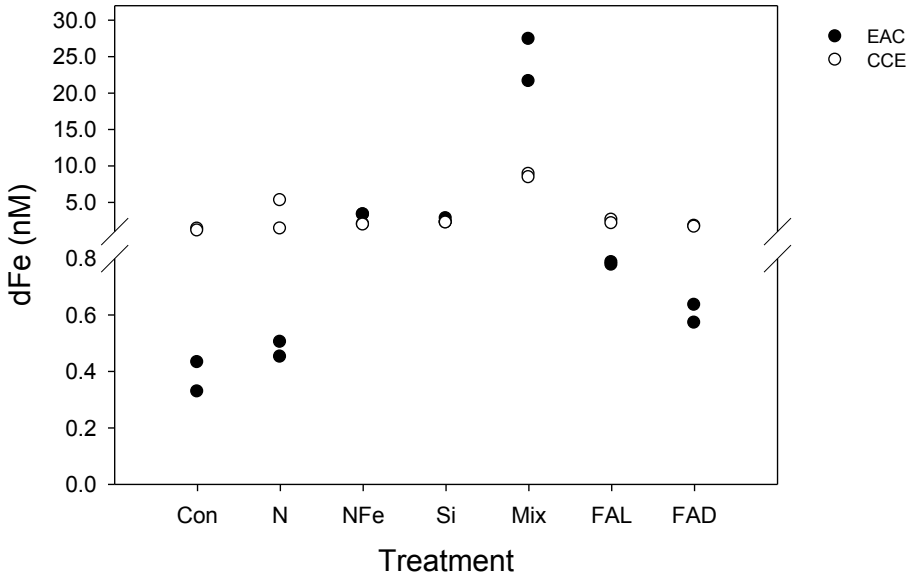

Fig. 2.6 Concentration of dissolved Fe (dFe, nM) measured at the conclusion of two 72-h shipboard nutrient-enrichment experiments undertaken during the SS2010-V09 Tasman Sea voyage (*RV Southern Surveyor*, 15th to 31st October 2010, austral spring). The experiments were conducted in 200–210-µm filtered seawater collected from the depth of the chlorophyll maximum at two sites in the Tasman Sea; East Australia Current (EAC, 29 1 °S 154 3°E), and a cold-core eddy (CCE, 32 2°S 153 8°E). Treatments were as per Fig. 2.5. Samples for the analysis of dFe were taken from replicates 1 and 2 of each treatment, therefore duplicate data points are shown for each treatment and experiment.

The abundance of bacteria, *Prochlorococcus* and small eukaryotes all declined in the EAC control compared to T0 (Fig 2.7A, B, D). This decline was significant for *Prochlorococcus* ($P < 0.001$) where abundance was reduced by > 50% during the 72-h incubation (Fig. 2.7B). In contrast, *Synechococcus* abundance increased by ~ 25%, and a small increase in large eukaryote abundance was also measured (Fig. 2.7C, E). Overall, addition of nutrients did not

appear to benefit either the bacteria or picophytoplankton groups, as cell abundance was either unchanged or declined in the EAC treatments compared to the control (Fig. 2.7A-E).

In the CCE experiments, the abundance of bacteria, *Prochlorococcus* and large eukaryotes did not change in the control from T0 (Fig. 2.7A, B, E). In contrast, the abundance of *Synechococcus*, and small eukaryotes significantly increased ($p \leq 0.010$); for *Synechococcus* this amounted to an increase in cell abundance of ~ 60% (Fig. 2.7C, D). Bacterial abundance was 1.3 and 1.9 fold larger in the CCE Si and Mix treatments ($p \leq 0.002$) respectively, but was unchanged in all other treatments (Fig. 2.7A). *Prochlorococcus* and small eukaryote abundance was either unchanged or declined across all treatments compared to the control, whereas the abundance of large eukaryotes was significantly enhanced in all treatments ($p = \leq 0.046$), except for N, Si and FAD (Fig. 2.7B, D, E).

In both the EAC and CCE experiments the FAD treatment resulted in a much greater decline in cell abundance across all picophytoplankton groups compared to all other treatments (Fig. 2.7B-E).

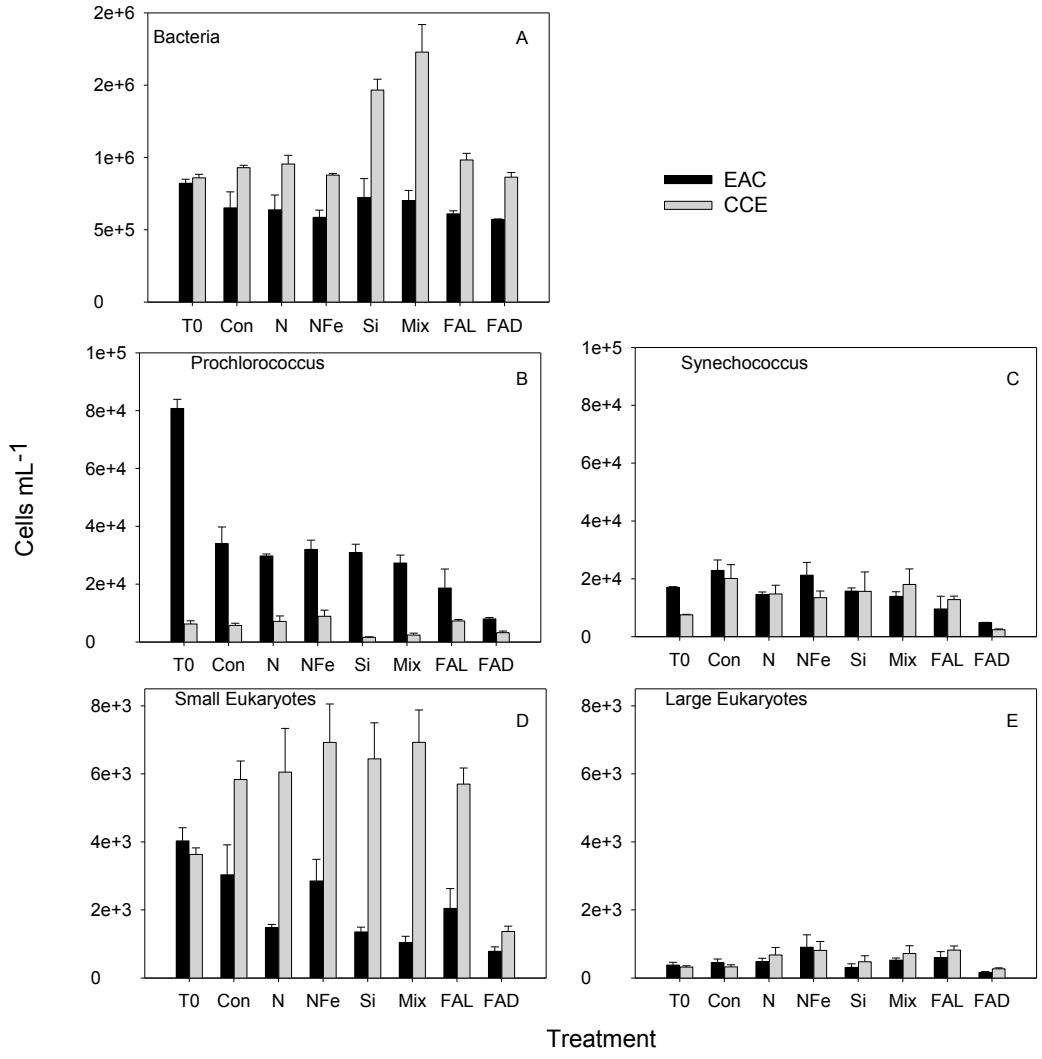

Fig. 2.7 Cell abundance (cells mL^{-1}) of bacteria (A), and picophytoplankton *Prochlorococcus* (B), *Synechococcus* (C), small eukaryotes (D) and large eukaryotes (E) measured by flow cytometry at T0 and at the conclusion of two 72-h shipboard nutrient-enrichment experiments undertaken during the SS2010-V09 Tasman Sea voyage (*RV Southern Surveyor*, 15th to 31st October 2010, austral spring). The experiments were conducted in 200–210-µm seawater collected from the depth of the chlorophyll maximum at two sites East Australia Current (EAC, 29 1 °S 154 3°E), and a cold-core eddy (CCE, 32 2°S 153 8°E). T0 = unamended seawater at the start of the experiment. Treatments were as per Fig. 2.5. Error = SD of triplicate incubations except for EAC FAD where errors represent half interval (range) of duplicate incubations. Note differences in y-axis scale.

TChl-*a* concentration did not change between the EAC T0 and control, however, a significant decrease ($p = 0.006$) of ~ 30% was measured between the T0 and control in the CCE samples (Fig. 2.8).

During the EAC experiment, the measured TChl-*a* concentration in the N, NFe, Mix and FAL treatments were 2 to 2.5-fold higher than those measured in the control samples ($p \leq 0.03$; Fig 2.8), but were not significantly different from each other, however, the Si and FAD treatment did not vary from the control. In the CCE experiments, TChl-*a* in all treatments was significantly enhanced compared to the control by between 1.5 and 3.8-fold ($p < 0.024$; Fig. 2.8) except for FAL, which did not differ from the control, and FAD, where TChl-*a* concentration was significantly lower ($p = 0.006$).

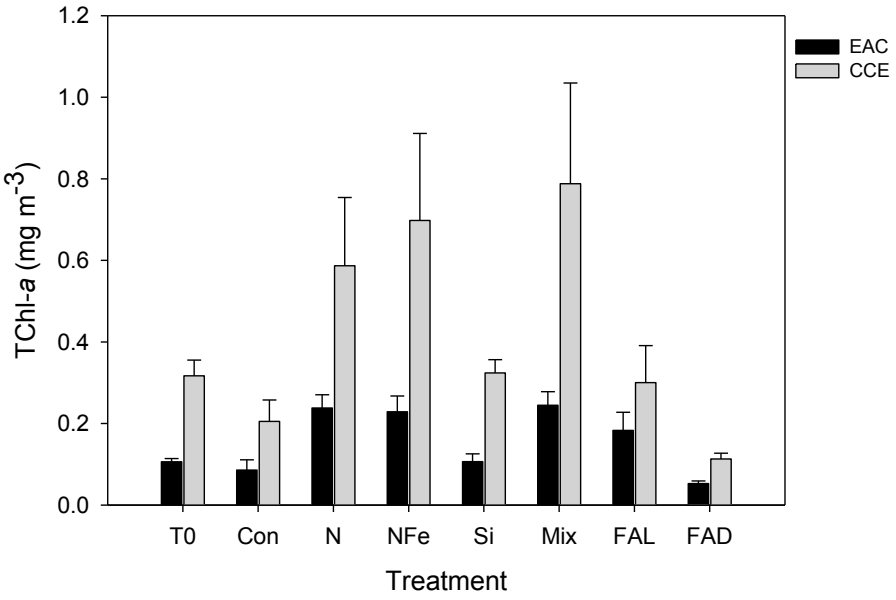

Fig. 2.8 Concentration of total chlorophyll-*a* (TChl-*a*, mg m^{-3}) measured at T0 and at the end of two 72-h shipboard nutrient-enrichment experiments undertaken during the SS2010-V09 Tasman Sea voyage (*RV Southern Surveyor*, 15th to 31st October 2010, austral spring). The experiments were conducted in 200–210-µm filtered seawater collected from the depth of the chlorophyll maximum at two sites East Australia Current (EAC, 29 1 °S 154 3°E), and a cold-core eddy (CCE, 32 2°S 153 8°E). T0 = unamended seawater at the start of the experiment. Treatments were as per Fig. 2.5. Error = SD of triplicate incubations except for EAC FAD where errors represent half interval (range) of duplicates incubations.

Biomarker pigments indicated that all phytoplankton groups declined in the control from T0, and in the FAD treatment in both experiments (Fig. 2.9). In the EAC incubations Chl-*b* and peridinin, present at T0, were absent in the control and did not recover in any incubations regardless of nutrient enrichment, indicating a loss of some cyanobacteria and haptophyte species. However, fucoxanthin, but-fucoxanthin, hex-fucoxanthin and diadinoxanthin remained present in all incubations, and increased in all enrichments where N and Fe were added (including the Mix treatment), as well as in the FAL treatment, although concentrations varied (Fig. 2.9).

In the CCE incubations, the concentration of fucoxanthin increased in all treatments, except for FAD, compared to T0 and the control, suggesting an increase in diatoms (Fig. 2.9). The Si and FAL treatments varied little from T0. The increase in hex-fucoxanthin, diadinoxanthin and peridinin in the N, NFe and Mix treatments compared to the control indicated that haptophytes and dinoflagellates, for the most part, recovered to what was measured at T0 (Fig. 2.9).

Overall, there was some variability in phytoplankton group abundance between treatments; however, community composition changed very little except for a loss of some cyanobacteria and haptophyte species in the EAC incubations.

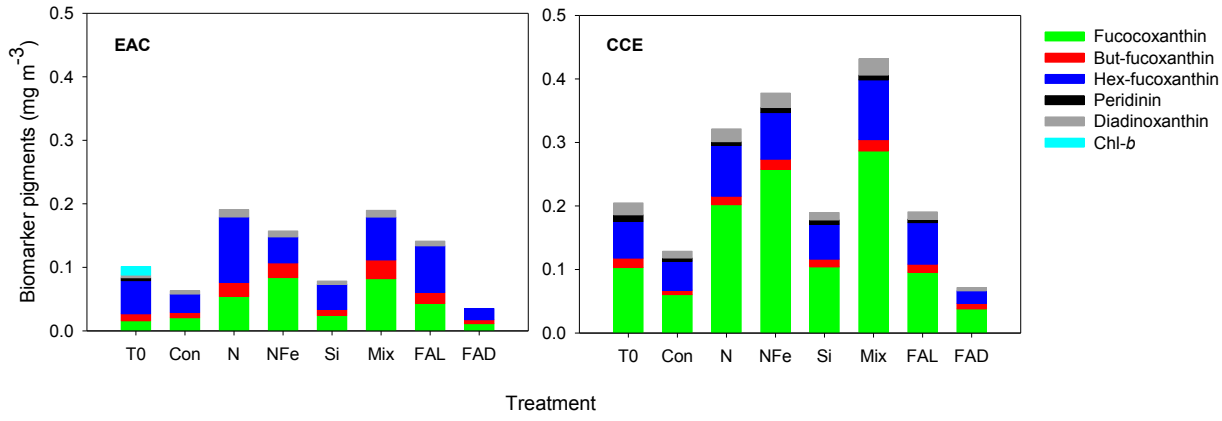

Fig. 2.9 Concentration of biomarker pigments (mg m^{-3}) measured at T0 and at the end of two 72-h shipboard nutrient-enrichment experiments undertaken during the SS2010-V09 Tasman Sea voyage (*RV Southern Surveyor*, 15th to 31st October 2010, austral spring). The experiments were conducted in 200–210-µm filtered seawater collected from the depth of the chlorophyll maximum at two sites East Australia Current (EAC, 29 1 °S 154 3°E), and a cold-core eddy (CCE, 32 2°S 153 8°E). T0 = unamended seawater at the start of the experiment. Treatments were as per Fig. 2.5.

Carbon (C) fixation experiments were conducted using the control, N, NFe, and FAL incubations at 72-h. These experiments revealed that C fixation rate varied depending on the nutrient addition treatment, and that this differed between phytoplankton communities (EAC or CCE). The phytoplankton community in the EAC N incubation had the highest C fixation rate in this experiment, being 1.7-fold higher that the control. Both the NFe and FAL incubations had carbon fixation rates that were lower than the control ($p \leq 0.001$; Fig. 2.10). In contrast, all CCE nutrient-enrichment incubations had C fixation rates that were at least double that of the control (2.3- to 6.3-fold, FAL and NFe, respectively). The N and FAL incubations C fixation rates were similar; however, for the NFe incubations carbon fixation rates were significantly higher ($p < 0.003$: Fig. 2.10).

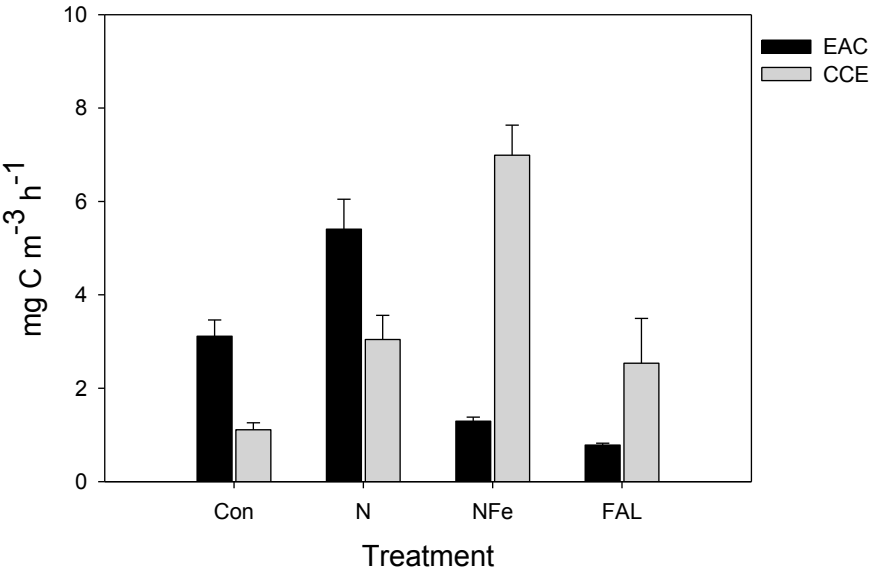

Fig. 2.10 Carbon (C) fixation rates measured from ^{14}C incubations at the end of two 72-h shipboard nutrient-enrichment experiments undertaken during the SS2010-V09 Tasman Sea voyage (*RV Southern Surveyor*, 15th to 31st October 2010, austral spring). The experiments were conducted in 200–210-µm filtered seawater collected from the depth of the chlorophyll maximum at two sites East Australia Current (EAC, 29 1 °S 154 3°E), and a cold-core eddy (CCE, 32 2°S 153 8°E). T0 = unamended seawater at the start of the experiment. Treatments N, NFe, and FAL were as per Fig. 2.5. Error = SD of triplicate incubations.

2.2.3.3 Removal and/or production of HS-like material

The initial (T0) concentration of HS-like material differed between the two experiments, with the EAC water containing 9.43 μg L^{-1} SRFA eq. (± 0.43 μg L^{-1} SD) and the cold core eddy water 14.4 μg L^{-1} SRFA eq. (± 0.84 μg L^{-1} SD), reflecting the different locations and biological characteristics of the two sites.

The final HS-like concentration in the EAC FAD treatment indicated that there had been no significant production or removal of HS during the experiment. In contrast, there was a 62% loss of material in the FAL treatment (Fig. 2.11) from the 600 μg L^{-1} SRFA added during the incubation period. In the other EAC nutrient addition treatments, only the Mix treatment showed any significant change (increase) in the concentration of HS-like material at the end of the 72-h incubation, being significantly higher than the T0, control, N and NFe, treatments ($p = \leq 0.003$; Fig. 2.11).

In contrast to the EAC experiment, in the CCE incubations the FAL treatment contained more HS-like material after 72-h incubation than the FAD treatment, with losses of ~ 60 μg L^{-1} SRFA eq (38%) and ~ 120 μg L^{-1} SRFA eq (59%), respectively (Fig. 2.11). The concentration of HS-like material increased significantly in the NFe treatment compared to both the T0 and control ($p = \leq 0.007$), but decreased in the Si treatment ($p = 0.014$). No other treatment showed a change from the T0 or control concentrations (Fig. 2.11).

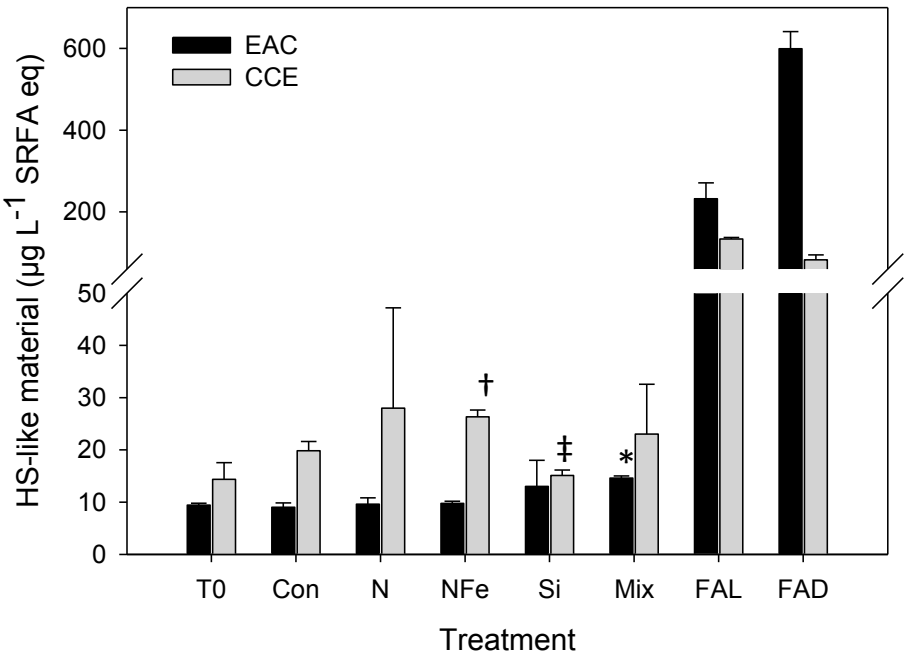

Fig. 2.11 Concentration of electrochemically detected humic substance-like (HS-like) substances measured at the conclusion of two 72-h shipboard nutrient-enrichment experiments undertaken during the SS2010-V09 Tasman Sea voyage (*RV Southern Surveyor*, 15th to 31st October 2010, austral spring). The experiments were conducted in 200–210-µm filtered seawater collected from the depth of the chlorophyll maximum at two sites, East Australia Current (EAC; 29 1 °S 154 3°E), and a cold-core eddy (CCE; 32 2°S 153 8°E). T0 = unamended seawater at the start of the experiment. Treatments were as per Fig. 2.7. The concentration of HS-like material is expressed as Suwannee River Fulvic Acid equivalents (SRFA eq) in µg L^{-1}. Error = SD of triplicate incubations except for EAC FAD where errors represent half interval (range) of duplicates incubations.

***** Significantly higher HS-like concentration compared to all other EAC treatments, except FAL and FAD ($p = 0.003$).

† Significantly higher HS-like concentration compared to CCE T0 and control ($p = 0.007$).

‡ Significantly lower HS-like concentration compared to CCE T0 and control ($p = 0.014$).

Pearson correlations revealed that there were no statistically significant relationships between the concentration of HS-like material and biological parameters (pigments, bacteria, picophytoplankton). However, there were significant relationships between HS-like material and macronutrients, $Si(OH)_4$, PO_4, or dFe, in the EAC experiment, which themselves would not contribute directly to HS-like material. Further investigation using regression analysis suggested that the relationships may have been artificially enhanced by the high concentrations of the nutrients in the enriched samples, particularly between HS-like concentration and $Si(OH)_4$, and revealed two populations of data points, one with high concentrations and another with low concentrations (Fig. 2.12A, D, and F). The concentration of HS-like material and PO_4 was strongly correlated (r^2 = 0.9; Fig. 2.12D). When the Mix treatments were excluded from the regression analysis, the relationship between the concentration HS-like and PO_4 remained (r^2 = 0.707; Fig. 2.12E), suggesting that PO_4 was a significant indirect influence of HS-like concentration. However, this was not the case for $Si(OH)_4$. Regression analysis using the treatments with no Si addition (control, N, NFe; [$Si(OH)_4$] < 0.7 μmol L^{-1}) displayed no relationship with HS-like concentration (Fig. 2.14B), whereas the Si-enriched treatments (Si, Mix; [$Si(OH)_4$] > 26 μmol L^{-1}) displayed a possible negative relationship (Fig. 2.12C). Given the large concentration difference between the non-enriched and enriched samples, and without the benefit of intermediate $Si(OH)_4$ concentrations, the overall relationship was therefore viewed with some caution and excluded from further analysis. In the case of dFe, a strong overall relationship with HS-like concentration was observed (r^2 = 0.871; Fig. 2.12F); however, this relationship weakened considerably when the Mix treatment, which contained < 20 nmol L^{-1} dFe, was removed (r^2 = 0.118; Fig. 2.12G).

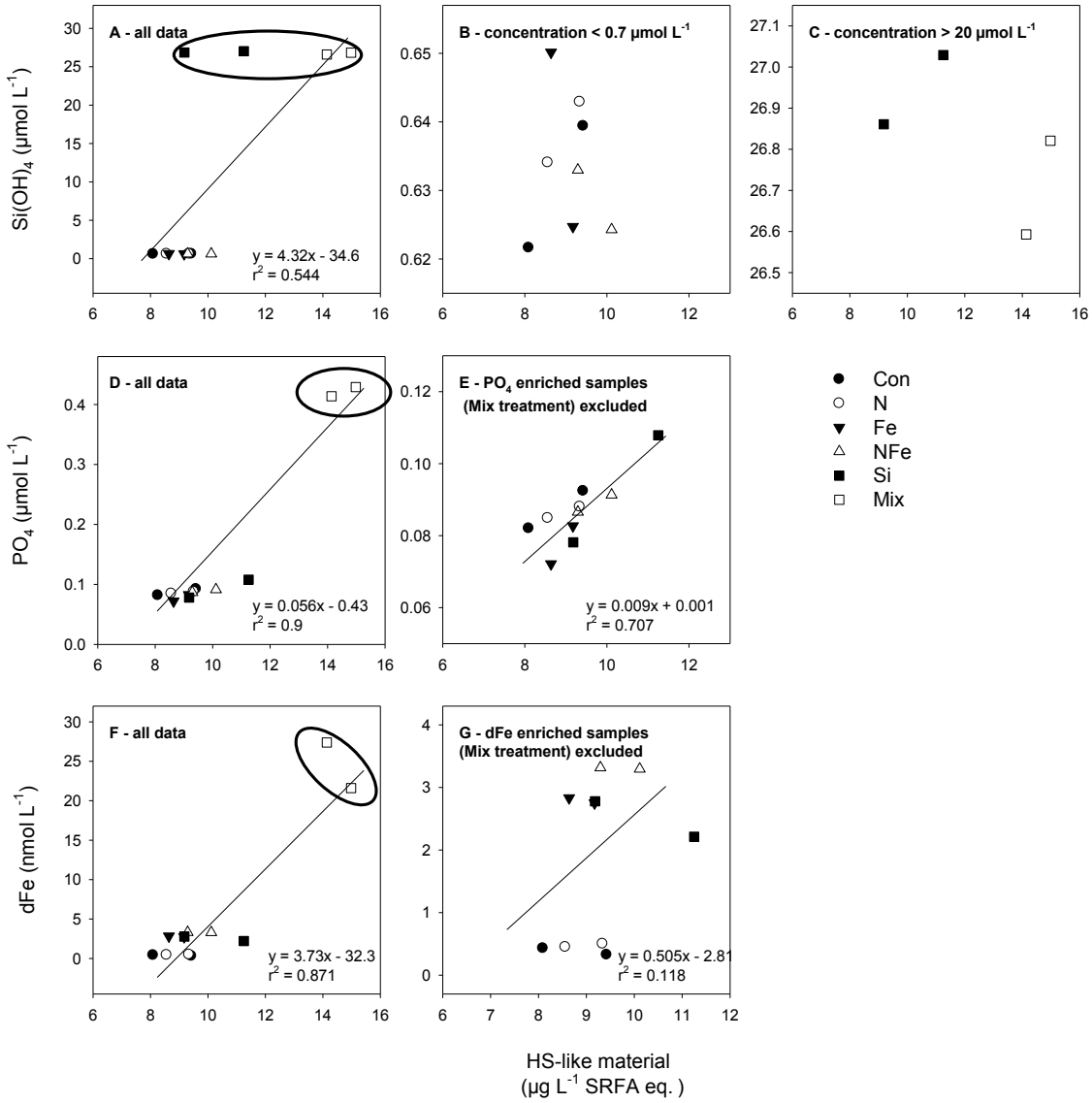

Fig. 2.12 Relationships between the concentration of humic substance-like (HS-like) material and Silicic acid ($Si(OH)_4$), phosphate (PO_4) and dissolved Fe (dFe) at the conclusion of a 72-h shipboard nutrient-experiment undertaken during the SS2010-V09 Tasman Sea voyage (*RV Southern Surveyor*, 15th to 31st October 2010, austral spring). The experiment was conducted in 200–210-µm filtered seawater collected from the depth of the chlorophyll maximum in the East Australia Current (EAC; 29 1 °S 154 3°E). Treatments were as per Fig. 2.5. Panel A = $Si(OH0)_4$ all data; Panel B = treatments where $Si(OH)_4$ < 0.7 µmol L^{-1}; Panel C = treatments where $Si(OH0)_4$ > 20 µmol L^{-1}; Panel D = PO_4 all data; Panel E = PO_4 enrichment treatment (Mix) excluded; Panel F = dFe all data; Panel G = dFe-enrichment > 10 nM (Mix treatment) excluded. High concentrations, subsequently excluded, are circled to highlight (panels A, D, and F).

The multivariate analysis indicated that, considered alone, the concentration of PO_4 explained 86% of the variability in HS-like concentration between treatments, whilst the concentration of dFe alone explained 81% of the variability (for all marginal tests see appendices 2 and 3). Although no other parameters were significantly associated with HS-like concentration, dbRDA indicated in combination with PO_4 and dFe, the concentration of diadinoxanthin and NH_4, and bacterial abundance were 5 parameters that best explained the variability in HS-like concentration ($r^2 = 0.97$). The analysis revealed some redundancy in the explanatory variables, with picocyanobacterial abundance and fucoxanthin concentration showing equivalent explanatory power compared to diadinoxanthin, bacterial abundance, and NH_4 and dFe concentration (Table 2.4).

No individual parameter was significantly correlated with HS-like concentration for the CCE experiments. However, dbRDA indicated that a combination of peridinin, but-fucoxanthin, NH_4, and NO_X concentration, and bacterial abundance best explained the differences in HS-like concentration in these experimental samples ($r^2 = 0.899$). As with the EAC analysis, some redundancy in the explanatory variables was indicated with the concentration of hex-fucoxanthin, TChl-*a* and dFe showing similar explanatory power compared to NO_X and but-fucoxanthin concentration (Table 2.4).

In both the EAC and CCE, the combination of dissolved nutrients, bacteria abundance and a picophytoplankton group were important in explaining the variation in HS-like concentration, implying that phytoplankton composition and bacterial abundance affect nutrient utilisation which, in turn, will affect the quantity and composition of the HS-like material produced.

Table 2.4 Distance based redundancy analysis (dbRDA) of humic substance-like material concentration measured in experimental treatments from two 72-h shipboard nutrient-enrichment experiments undertaken during the SS2010-V09 Tasman Sea voyage (*RV Southern Surveyor*, 15th to 31st October 2010, austral spring) using environmental predictor variables and the AIC selection criterion. Response variables included nutrients (NH_4, NO_X, PO_4, dFe), pigments (TChl-*a*, fucoxanthin (fuco), 19-butanoloxyfucoxanthin (but-fuco), 19-hexanoyloxyfucoxanthin (hex-fuco), peridinin (perid), diadinoxanthin (diadino),) and bacterial and picophytoplankton abundance. The experiments were conducted in 200–210-µm filtered seawater collected from the depth of the chlorophyll maximum at two sites A) East Australia Current (EAC; 29 1 °S 154 3°E), and B) cold-core eddy (CCE; 32 2°S 153 8°E). The treatments included in these analyses were; unamended control, nitrate (NO_3, 10 µM), nitrate + inorganic Fe (NO_3 + Fe, 10 µM + 1 nM), silicate (Si, 10 µM), mixed nutrients (Mix; NO_3 + Fe + PO_4, 10 µM + 1 nM + 0.625 µM).

Best Solutions	**AIC**	**r^2**	**No. of variables**
EAC			
Diandino, NH_4, PO_4, bacteria	70.147	0.957	4
Diandino, NH_4, PO_4, dFe, bacteria	72.563	0.970	5
Fuco, diandino, PO_4, *Synech, Prochloro*	71.904	0.969	5
Hex-fuco, NH_4, PO_4, dFe, bacteria	71.542	0.968	5
Tchl-*a*, fuco, PO_4, *Synech, Prochloro*	71.314	0.967	5
But-fuco, diadino, NH_4, PO_4, bacteria	70.195	0.964	5
CCE			
Perid, but-fuco, NH_4, bacteria	30.11	0.820	4
Perid, but-fuco, NH_4, NOX, bacteria	35.048	0.899	5
Perid, hex-fuco, NH_4, dFe, bacteria	34.647	0.896	5
Perid, but-fuco, NH_4, dFe, bacteria	33.531	0.886	5
Tchl-*a*, perid, NH_4, NO_3, bacteria	33.124	0.882	5

With respect to the electrochemical analysis of the HS-like material, little variability in the position of the reduction peak from the electrochemical analysis was observed. As predicted by electrochemistry theory, the small variations in position (E_p) appeared to reflect changes HS-like concentration rather than composition of material, as predicted by electrochemistry theory (Table 2.5). However, sensitivity varied both between sites and treatments. The sensitivity (or slope) derived from the analysis of the CCE T0 was an order of magnitude higher than that of the EAC. However, whereas there was no significant change between the CCE T0 and the control, the EAC control displayed a higher sensitivity than the T0 (Table 2.5). Most treatments differed from the controls except for the EAC Si treatment and CCE

FAD and NFe treatments. However, in all cases the sensitivities of treatments with nutrient enrichment were lower than the control, with the EAC treatments being higher than T0 and the CCE treatments lower than T0 (Table 2.5). The EAC FAD sensitivity was much lower than all other treatments; however, the N, NFe and FAL treatments were all very similar. The CCE samples displayed a different pattern with N treatment having the lowest sensitivities, whereas the NFe, FAD and Mix treatments were almost double that of the other treatments. When comparing the sites, the EAC Si, and N sensitivities were higher than those of the CCE, whereas the NFe, FAD and Mix treatments were lower. Only the FAL treatment sensitivities were similar between sites (Table 2.5).

Table 2.5 Instrument sensitivity and position of the reduction peak position (E_p, V vs Ag/AgCl electrode) derived from the determination of humic substance-like (HS-like) material. Samples analysed were from nutrient-enrichment experiments at T0 (unamended seawater) and after 4 d incubation in samples with and without the addition of nutrients. The experiments were conducted in 200–210-µm filtered seawater collected from the depth of the chlorophyll maximum at two sites A) East Australia Current (EAC, 29 1 °S 154 3°E), and B) a cold-core eddy (CCE, 32 2°S 153 8°E). Treatments were as per table 2.4.

	Sensitivity (x 10^{-8} µg L^{-1})		**E_p (V vs Ag/AgCl electrode)**	
Treatment	**EAC**	**CCE**	**EAC**	**CCE**
T0	6.07	16.4	0.528 ± 0.01	0.543 ± 0.01
Con	9.08	14.5 ± 2.71	0.527 ± 0.01	0.538 ± 0.004
N	7.76 ± 0.72	5.23 ± 1.44	0.525 ± 0.01	0.534 ± 0.02
NFe	7.69	15.8	0.525 ± 0.01	0.539 ± 0.003
Si	9.97 ± 2.86	7.99	0.532 ± 0.01	0.537 ± 0.01
Mix	8.74 ± 0.09	13.7 ± 1.96	0.527 ±0.01	0.534 ± 0.003
FAL	7.52 ± 0.43	7.65	0.549 ± 0.005	0.543 ± 0.004
FAD	4.57	15.7	0.545 ± 0.01	0.545 ± 0.01

2.3 Discussion

Humic substances, such as those measured in this study, represent a pool of dynamic and reactive organic compounds that can regulate nutrients available for phytoplankton growth. In coastal regions the input of HS can be considerable, and it has been suggested that the Fe-binding ligands present in coastal waters are mostly HS, which have been shown to make up an important component of the Fe-binding ligand pool (Laglera et al., 2007; Laglera and van den Berg, 2009). In this study, compared to the HS-like material measured by Laglera et al (2007) and Laglera and van den Berg (2009), we observed relatively low concentrations of HS-like material in coastal waters along a limited salinity gradient (Table 2.6). However, when nutrients or FA were added to natural phytoplankton communities in off-shore waters of the EAC and CCE, we saw two patterns: (i) significant utilisation of HS-like material and little or no production in the EAC; and (ii) less utilisation but a greater production of HS-like material in the CCE community, which likely reflect the biological activities and nutritional requirements of the different phytoplankton communities present.

2.3.1 Validation of the standard addition method for the determination of Fe-binding HS-like material

The challenge of any analytical measurement is to span an appropriately large concentration range whilst also accounting for a variable sample matrix. The HS-like analysis for the natural seawater and perturbation experiments from this study posed this type of problem, as both the concentration and origin/nature of the samples were likely to be quite different depending on the location or experimental treatment from which the sample came. The large range of sensitivities measured from the standard addition of SRFA during the method validation process suggested that different sensitivities may be linked to different HS matrices. The difference in sensitivity was most apparent between the nearshore and offshore samples which would likely represent more allochthanous input closer to shore and greater autochthonous input/production in open water. This study showed that a conventional calibration curve derived from SRFA in a synthetic seawater matrix, or UV treated seawater (to remove organic material) matrix, did not account for this variability and may have led an overestimation of HS-like concentration. Given that the samples from this voyage were composed of river plume, inner and outer shelf, offshore and experimental samples, likely with varying DOM and humic/fulvic signatures, it was

considered more appropriate to employ the standard addition method to account for this variability.

While the standard addition method reduced the uncertainty in HS-like material concentration estimates and suggested that sensitivity (i.e. slope) may be indicative of changes to the HS matrix, the variability of samples measured in this study was not consistent with water mass or treatment. It is not possible to make a definite statement as to the sources of the HS-like material in natural or experimental samples; however, the sensitivity variations observed in perturbation experiments possibly indicate that the HS-like material produced *in situ* does vary its composition depending on the phytoplankton species present. Further studies that focus on the physico-chemical composition of HS-like material would be required to confirm this.

2.3.2 The distribution of Fe-binding HS-like material in coastal and offshore regions of eastern Australia

This study has provided the first measurements of Fe-binding HS-like material along a cross-shelf gradient in the western Tasman Sea. HS-like concentrations, particularly the river plume and shelf samples, were lower than those measured in the Irish Sea and Pacific Ocean (Laglera et al., 2007; Laglera and van den Berg, 2009; Table 2.6), however the waters sampled by Laglera and van den Berg (2009) were subject to a much larger riverine input than was encountered during this study. Due to the riverine delivery of terrestrial HS into coastal waters, higher HS-like concentrations were expected in samples collected from the river plumes, but there was only one sample (Clarence River plume) where this was the case. Whilst this is not easily explained, it could be due to the ship not sampling in the core of the plume (M. Doblin, pers. comm.), but might also be a result of limited dispersion of HS-like substances. However, the sample taken offshore of the Macleay River contained a more than three-fold greater concentration of HS-like material than any other coastal sample, except for the Clarence River. This high value may be due to complex physical circulation in shelf waters involving mixing, entrainment of coastal water off the shelf and uplift/upwelling of offshore waters onto the shelf (Roughan and Middleton, 2002, 2004).

As is often observed with other components of the DOM pool, i.e., CDOM, the distribution of HS in natural waters can be correlated with salinity, where a low-to-high salinity gradient corresponds to a high-to-low HS-concentration gradient (Blough and Del Vecchio, 2002; Laglera and van den Berg, 2009). Measurements of HS-like material made by Laglera and

van den Berg (2009), determined by the same CSV technique used here, showed such a relationship with a decrease in Fe-binding HS concentration with increasing salinity (HS concentration up to 400 μg L^{-1} at salinity 30, and 70 μg L^{-1} at salinity 34). Although the highest HS-like concentration in this study was associated with the lowest salinities (Clarence River plume, salinity 34.84 at 5 m and 35.17 at 15 m) there was otherwise no relationship with HS-like material observed, likely due to the narrow salinity gradient encountered during this voyage.

Table 2.6 Concentration range of humic-substance like (HS-like) material measured using cathodic stripping voltammetry by Laglera et al. (2007) and Laglera and van den Berg (2009).

Location/Station	HS-like (μg L^{-1})	Salinity	Reference
Liverpool Bay			
Station 1	149 ± 0.004	32.5	Laglera et al., 2007
Station 10	210 ± 0.014	31.8	Laglera et al., 2007
Station 19	120 ± 0.004	32.9	Laglera et al., 2007
Station 20	73 ± 0.006	32.8	Laglera et al., 2007
Station 28	131 ± 0.015	33.2	Laglera et al., 2007
Station 35	583 ± 0.048	31.8	Laglera et al., 2007
Irish Sea			
Near River Mersey outflow	370	30.5	Laglera and van den Berg, 2009
Station 10 (Coastal)	204 ± 14	Not given	Laglera and van den Berg, 2009
Station 35 (Coastal)	366 ± 51	Not given	
Open Irish Sea	70	33.5	Laglera and van den Berg, 2009
Pacific Ocean			
Coastal Pacific (600 m)	178 ± 34		Laglera and van den Berg, 2009
Open Pacific (1000 m)	36 ± 2		Laglera and van den Berg, 2009

In offshore regions, and at the chlorophyll maximum, the majority of HS-like material is produced *in situ* and so a correlation between HS-like concentration and Chl-*a* fluorescence, which is used as a proxy for phytoplankton biomass, might be expected. No relationship between HS-like material and Chl-*a* fluorescence was seen here, in either the whole dataset or in just those samples collected at the Cmax, indicating that the amount of HS-like material in the water was not directly correlated with primary producers. The absence of a relationship between Chl-*a* fluorescence and HS has previously been observed in the Ross Sea (Calace *et al*., 2010), a region where *in situ* HS production would be expected to dominate. Calace and co-workers (2010) found good correlation between particulate FA and Chl-*a* fluorescence, but not with dissolved FA. The authors concluded that there was a

dependency on primary productivity in the case of particulate FA, but not for dissolved FA. The samples analysed from this study were all 0.2-µm filtered and so the HS-like material present were operationally defined as dissolved, which may explain the lack of relationship with fluorescence. In addition, marine HS, being composed mainly of degraded algal matter and exudates (Andrews et al, 2000), is essentially a by-product of photosynthesis reflecting past rather than present biomass, and may have resulted in a poor relationship with 'new' biomass. Alternatively, the fluorescence signal may have been confounded by the presence of CDOM, particularly in the nearshore samples where allochthonous HS may have dominated.

2.3.3 Nutrient-enrichment experiments

2.3.3.1 The effect of HS and other nutrient addition on phytoplankton growth in the EAC and CCE

Growth was stimulated in both phytoplankton communities by the NO_3 and Fe, delivered singularly (N treatment) or combined (NFe treatment) , but there were a number of factors that suggest that the communities were inhabiting different nutrient regimes and experiencing different nutrient limitation. [Note, however, that the two experiments were not directly comparable due to the different nutrient addition regimes, but provide insight into the nutritional status of the phytoplankton resident in each water mass.] The initial concentration of TChl-*a* was approximately three-fold higher for the CCE community than that measured for the EAC. Furthermore, during the three day experiment there was a significant decline in TChl-*a* between the CCE T0 and the control, whereas, for the EAC this was not the case. These observations suggest a greater degree of nutrient limitation for the CCE community, and/or a higher degree of grazing from microzooplankton that were not excluded by the 200-210 µm pre-filtration. The concentration of dFe in the CCE control was more than double that measured in the EAC samples, but despite this the community appeared to be Fe limited. This is supported by the increased TChl-*a* and the enhanced abundance of smaller eukaryotes in the treatments where Fe was added. In addition, TChl-*a* concentration in the CCE Si treatment, whilst not differing from the T0, was enhanced compared to the control and again this was not the case in the EAC Si treatment. The enhanced TChl-*a* concentration, together with Si depletion in the other treatments and a greater proportion of fucoxanthin, suggests a greater population of diatoms in the CCE compared to the EAC, likely in the larger group of cells that were not enumerated by flow cytometry. It has previously been shown that larger cells, like many coastal species, often

have a greater biological Fe demand than smaller cells (Sunda et al., 1991, Sunda & Huntsman, 1995; Gerringa et al., 2000, Sarthou et al., 2005). However, it has also recently been demonstrated that many diatom species, in fact, have relatively low intracellular Fe requirements compared to smaller cells, but are limited by their uptake rates. It is suggested that the inability of diatoms to outcompete the smaller cells (i.e. cyanobacteria) or access sufficient recycled Fe suggests that they may require the presence of higher ambient dFe concentrations in order to bloom (Boyd et al., 2012). Thus, the concentration of Fe at the CCE site, although elevated compared to the EAC, may not have been enough to sustain growth in the bottles during the experiment. The enhanced carbon fixation rates in the EAC NFe incubations also support greater Fe limitation at the CCE site compared to the EAC site, whilst both sites appeared to be N limited.

Interestingly, an increase in bacterial abundance was measured in the CCE Si and Mix treatments. The reason for this increase is not clear as the addition of Si on its own would only have stimulated growth of silicoflagellates and diatoms. The increase in bacteria in the Si treatment may be an indirect effect of larger cells dying in the bottles and the bacteria consuming the organic material liberated. In the Mix treatment, which contained Si as well as NO_3, PO_4 and Fe, bacterial abundance may have been elevated because of the general increase in phytoplankton biomass (in larger size fractions that were not enumerated by the flow cytometer) and consequently more DOC being released from living cells compared to other treatments.

It is worth noting that, although both the EAC and CCE incubations were set up to receive just 25 % of the surface irradiance, the median light levels received by the incubations during the 72-h experimental period were 20-fold (EAC) and 2-fold (CCE) higher than that measured *in situ* at the depths at which the water was collected. Whilst light inhibition and/or photo damage does not appear to have greatly affected the communities as a whole with maximum quantum yield remaining constant), particularly in the EAC incubations, it may, in part, account for the measured decline in cell numbers of some phytoplankton species, most notably *Prochlorococcus* sp.

In light of the differences in the phytoplankton communities in different water masses, it was expected that they would have divergent responses to addition of FA. Under dark incubation in both experiments, FA did not stimulate phytoplankton growth and a decline in both the TChl-*a* concentration and the abundance of picophytoplankton groups was observed. Bacterial abundance was also not stimulated by the presence of degrading autotrophic cells in FAD treatments in either experiment. However, under light exposed

conditions, the EAC community responded positively to FA addition, as inferred from the elevated TChl-*a* results, whereas the CCE community showed no change in TChl-*a*. Moreover, biomarker pigments indicated that diatoms and haptophytes were the main beneficiaries from the addition of FA in both experiments, suggesting that these groups were able to utilise nutrients, specifically N and Fe, either bound to or labilised by FA. In addition to a potential direct uptake of FA, they may also have indirectly affected growth. HS can enhance the concentration of bacterially produced N (Carlsson and Granéli, 1993), whilst Fe can also be remineralised through both bacterial activity and HS-mediated photochemical processing (Rose and Waite, 2005; Strzepek et al., 2005; Miller et al., 2009). In the FAL treatments, the concentrations of NH_4, NO_X, and dFe were all enhanced compared to the control. For the N components this may be partly due to the addition of N with the SRFA, however this does not amount to all of the N (as NH_4 and NO_X) present. Given the likelihood of N and Fe limitation at both sites, remineralised constituents may have contributed to the increased biomass observed in some phytoplankton groups.

Past studies investigating the response of phytoplankton to the presence of HS have also yielded varied results. The dinoflagellate *Alexandrium tamarense* (Gagnon et al., 2005, humic and fulvic acids) and the green alga *Pseudokirchneriella subcapitata* (Lee et al., 2009, hydrophobic fraction of DOM) have all shown enhanced growth and biomass in the presence of HS, as has *Gymnodinium catenatum* (dinoflagellate; Doblin et al., 1999, humic acid). However, Doblin et al. (1999) found that this response was concentration dependent whereby at high concentrations of HA (3.23 mg L^{-1}) growth decreased, but at lower concentrations (0.33 and 1.64 mg L^{-1}) growth was similar to that of seawater with no added HA. Devol et al. (1984) found no response on addition of humic and fulvic acids (10 mg L^{-1}) from a natural lake community compared to inorganic nutrients. Furthermore, the growth of the cyanobacterium *Microcystis aeruginosa* has shown to be both inhibited by FA (2 mg L^{-1}, Imai et al., 1999), and enhanced by HS (4 mg L^{-1} Kosakowska et al., 2007), although it should be noted that Fe was also added in the experiments by Kosakowska et al. (2007). In this study, the concentration of FA added to the incubations was high compared to natural concentrations generally measured in open water (Laglera et al., 2007; Laglera and van den Berg, 2009). However, it is unlikely that growth inhibition due to a concentration effect is the sole reason for the different responses of the phytoplankton communities, as the positive response was measured in EAC incubations which had three-fold greater FA addition (600 μg L^{-1}).

Metal complexation by HS is commonly accepted as a mechanism accounting for concentration-dependent changes in phytoplankton growth, although Fe bound to HS can be highly bioavailable to phytoplankton (Kuma et al., 1999; Chen and Wang, 2008). The Fe-binding capacity of HA has been shown to be approximately twice that of FA at 31.9 nM Fe (mg HA)$^{-1}$ and 16.7 nM Fe (mg FA)$^{-1}$, respectively (Laglera and van den Berg, 2009), and with a higher conditional stability constant (log $K_{Fe'L}$), 11.1 and 10.6, respectively. Furthermore, photochemical reduction of HS and organically bound Fe(III) may enhance the concentration of bioavailable forms of Fe (Waite and Morel, 1984; Barbeau et al., 2001; Rose and Waite, 2005, 2006). These factors suggest that the FA used in these incubations was relatively labile. As there was a removal of HS observed in the FA treatments in both experiments, it is reasonable to expect that the removal and transformation dynamics would have labilised nutrients (mainly N and Fe) for biological uptake.

The addition of FA enhanced C fixation in the CCE community relative to the control, whereas, in the EAC community the carbon fixation rate declined. The reasons for the different responses observed between the EAC and CCE FAL incubations may be two-sided. Firstly it could reflect the varying abilities of the bacterial and phytoplankton communities present to access and utilise the nutrients bound to, or labilised by, the FA. Secondly, it suggests a greater dependence on humic-bound Fe when the community is Fe limited, as was the case for the CCE community where there was N and Fe co-limitation.

2.3.3.2 HS production and consumption and the effect of nutrient enrichment on these processes

The decline in HS-like concentration observed in the FAL and FAD incubations is likely due to processes such as photochemical degradation (FAL treatments only; Vodercek et al., 1997; Nelson et al., 1998; Blough and Del Vecchio, 2002) and bacterial utilisation (Amon and Benner, 1994, 1996; Benner, 2002; Obernosterer et al., 2008), the latter of which can increase under sunlit conditions (Kieber, 2004). As both processes can mediate the release or remineralisation of biologically labile products that may be available to phytoplankton (Kieber et al., 1989; Amon and Benner, 1994), biological utilisation in the FAL treatments probably also, indirectly, includes phytoplankton not just heterotrophic bacteria. In the absence of light, heterotrophic bacterial utilisation would likely have been the dominant removal mechanism in FAD incubations (Carlsson and Granéli, 1993). This assumption is supported by the higher concentrations of NH_4 and NO_X measured in the FAD treatments, compared to the FAL, as this is often a result of the bacterial reduction of N. It is, however,

acknowledged that some of the increase in NH_4 and NO_X measured in the FAD treatment may be due to the release of these products following the death of autotrophic cells kept under dark conditions.

The rate at which HS-like material (predominantly added FA) was removed, either photochemically or biologically, in the EAC FAL incubations was ~ 122 μg d^{-1} (~ 5 μg h^{-1}) which was 5.5-fold greater than the CCE FAL incubation (~22 μg d^{-1} or 0.92 μg h^{-1}). Given that the two experiments received the similar light intensities, and that the initial bacterial abundance was higher in the CCE FAL incubation compared to the EAC FAL incubation, the reason for the enhanced removal of HS-like material in the EAC is unclear. It is possible that, despite the lower cell abundance in the EAC, bacterial activity was higher although the comparatively low rate of HS removal in the FAD incubation does not appear to support this. Alternatively, other DOM consumers (i.e. small zooplankton not excluded in the pre-filtration, or protists) also contributed to HS removal; however, the abundance or activity of these organisms were not measured so this cannot be confirmed.

Two replicates were prepared for the EAC FAD incubations which contained 557 μg L^{-1} and 641 μg L^{-1} SRFA eq., respectively, at the end of the incubation. This represents a loss/gain of ~ 14 μg d^{-1}, whereas the average HS-like removal rate in the CCE FAD incubations was higher at ~ 39 μg d^{-1}. The higher rate of removal calculated for the CCE FAD incubations is likely due to the significantly higher bacterial abundance measured in comparison to the EAC incubations. Although the effect of HS on bacterial productivity has been previously studied (Amon and Benner, 1994, 1996; Moran and Hodson 1989, 1990, 1994; Anesio et al., 2005), few have focused on the bacterial utilisation rates of HS, but rather consider the whole DOM or DOC pool. However, work by Moran and Hodson (1989, 1990) indicates that there is significant heterogeneity in the rate at which bacteria utilise HS, which is largely dependent on the origin, and therefore composition, of the material.

Significant increases in HS-like concentration were only measured in the EAC Mix and CCE NFe treatments which corresponded with increases in biomass, although biomass also increased in many other treatments. However, C fixation was stimulated to the greatest degree in the NFe treatment in the CCE suggesting N+Fe limitation, and in the N treatment in the EAC. Furthermore, the dbRDA analysis showed that the concentration of N and Fe in the CCE and PO_4 and Fe in the EAC were influential in the variability of HS-like material measured. When considered with the TChl-a measurements, the results of the dbRDA indicate that the more N and Fe (CCE) or $P0_4$ and Fe (EAC) present (both added as part of the Mix treatment) the greater the concentration of HS-like material.

As the electrochemical technique (CSV) used in these analyses is not specific to HS, the increase in HS-like material could be a result of the detection of additional biological exudates, measured as part of the HS-like pool, that were released in response to specific nutrient enrichment. The release of bacterially produced siderophores is certainly a response to Fe enrichment (Gledhill and Buck, 2012 and refs therein), although siderophores (i.e. DFB) do not appear to be detected within the HS-like pool by CSV (C. Hassler, pers comm.). However, CSV can detect exopolymeric substances (EPS) (C. Hassler, pers comm.) and these substances, produced by bacteria and phytoplankton, can be significant contributors to Fe biogeochemical cycling and bioavailability (Hassler, Norman et al., in press; Norman et al., in press; Chapter 4). Furthermore, EPS are associated with other macronutrients and trace elements (N, P, Zn etc.) suggesting that they may also contribute to the bioavailability of these constituents (Norman et al., in press; Chapter 4). Whilst the EAC community was clearly N limited, the relevance of PO_4 and dFe in the statistical analysis may suggest a degree of co-limitation for the EAC and a release of substances that may help to sequester nutrients and relieve nutrient stress.

In addition to N, P and dFe, the dbRDA also highlighted various pigments and picophytoplankton groups as important factors relating to variations in HS-like concentration. This may purely be a reflection of the different community structure at each site, but changes in nutrient regime can alter community composition (Boyd et al., 2000; de Baar et al., 2005, Chapter 3). However, as indicated above, the phytoplankton themselves clearly contribute to the pool of HS-like material, although the degree of contribution may differ from species to species. In addition, bacterial abundance and NH_4 also featured significantly in the dbRDA, particularly for the CCE site. This is interesting not only as it reinforces the important role that bacteria play in DOM cycling, but also because both are related to the remineralisation of macronutrients and trace elements. The concentration of HS-like material produced *in situ* is, therefore, likely to vary depending on the nutrient status, and resident phytoplankton species composition and abundance, as well as the degree of microbial activity.

2.4 Implications

This study showed the average concentration of HS-like substances in the western Tasman Sea was relatively low, with some occasional high concentrations appearing in samples on the shelf. The oceanographic voyage was undertaken in the spring and the timing was such that it followed at least a week of significant rainfall in the northern part of the study

domain. Thus, river discharges and terrestrially-derived humic materials were probably at a seasonal high. The biological response to these HS-like substances was dependent on water mass, with the TChl-*a* increasing but the rate of carbon fixation declining in EAC incubations where *Prochlorococcus* was abundant, and increasing TChl-*a* and carbon fixation in the CCE where larger-celled phytoplankton were dominant. Whilst this may be due to EAC phytoplankton receiving three-fold more FA, it may also reflect the ability of different phytoplankton groups to access nutrients (N, P and Fe) bound to HS, or competition between phototrophs and heterotrophs for these resources. The EAC represents an oligotrophic water mass whose resident phytoplankton communities are likely to be highly dependent on regenerated nutrients in surface waters, particularly N, P and Fe, rather than inorganic forms. Collectively, these observations suggest that allochthonous HS could supplement microbial communities in the EAC if they were transported onto the shelf, potentially stimulating productivity in this region and also in mesoscale eddies created by the southward flow of the EAC. How this plays out in the future with the intensification of the EAC (Wu et al. 2012) and potential changes in rainfall in northern NSW, remains a major research challenge.

CHAPTER 3:

IRON CHEMICAL SPECIATION OF SEAWATER PROFILES FROM THE TASMAN SEA AND THE RESPONSE OF NATURAL PHYTOPLANKTON COMMUNITIES TO IRON FROM DIFFERENT SOURCES.

Note and acknowledgements

The data presented in this chapter were obtained from three seawater depth profiles and two 4-day shipboard Fe enrichment experiments undertaken during the PINTS voyage (RV *Southern Surveyor*, 23rd January to 15th February 2010, Prof. Christel Hassler, Chief Scientist). I did not participate in the voyage, but was responsible for the analysis of Fe chemical speciation and humic substance-like (HS-like) material. Here, the results of the Fe speciation and HS-like material analysis are presented, together with chlorophyll-*a* and pigment data, which have been kindly provided by Prof. Christel Hassler, who also collected the clean water samples and conducted the incubation experiments at sea. The biological responses observed from these experiments in the treatments where Fe enrichment had come from atmospheric dust or Fe bound to bacterial EPS led to further experiments that are detailed in chapters 4 and 5 of this thesis.

I am grateful to the following people for providing methodologies, analysis, and data for this chapter.

Dr Carol Mancuso Nichols (CSIRO, Hobart) – Isolation of EPS

Prof. Grant McTainsh - (Griffith University) – Provision of processed atmospheric dust

Dr. Veronique Schoemann (University of Brussels) – Dissolved Fe analysis.

Roslyn Watson and Lesley Clementson (CSIRO, Hobart) – Chlorophyll *a* and pigment analysis.

Alicia Navidad (CSIRO, Hobart) – macronutrient analysis (site characteristics only used here).

Dr Edward Butler (AIMS, NT) – Experimental and sampling assistance.

Claire Thompson (Australian National University, Canberra) - Experimental and sampling assistance.

3.0 Introduction

Iron (Fe) bioavailability is highly influenced by the different uptake strategies of resident bacterio- and phytoplankton (Barbeau et al., 1996; Hutchins et al., 1999; Strzepek et al., 2005), and also by the chemical forms of Fe in seawater (speciation, redox; Kuma et al., 1996; Barbeau et al., 2001; Rose and Waite, 2002, 2003), which are in turn influenced by Fe source. In addition, the association of Fe with a variety of organic ligands, the majority of which are biologically produced, can further impact Fe chemistry and thus, Fe bioavailability (Hassler et al., 2011a, b). Identification of the Fe sources which are available for phytoplankton uptake is therefore critical to understanding the relationship of Fe with bioavailability, as this affects the retention time and chemical reactivity of Fe in the euphotic zone.

Fe is supplied to the upper ocean from a variety of different sources, i.e. atmospheric aerosols (dust, ash etc), upwelling, and biological recycling (Barbeau et al., 1996; Johnson et al., 1999, 2003; Jickells & Spokes, 2001; Jickells et al., 2005; Strzepek et al., 2005; Nicol et al., 2010). The Fe from each source is likely to vary in size fraction (particulate and dissolved, as soluble and colloidal Fe; Gledhill and Buck, 2012), and in the relative the proportions of these size fractions. Source will also determine the form or species (inorganic or organically complexed Fe(II) and Fe(III)), and reactivity. For example, Fe from crustal material will have different proportions of reactive and refractory Fe depending on the source geology (McTainsh et al., 1990; Mackie et al., 2008), and the species of Fe will depend on the physical and chemical processing that the dust particles undergo before entering the ocean (Duce and Tindall, 1991; Pehkonen et al., 1993; Jickells and Spokes, 2001; Willey et al., 2008). The characteristics of biologically recycled Fe however, will be highly dependent on the prey (i.e. phyto- or bacterioplankton and species) and the mode and efficiency of regeneration (Hassler et al., 2012). Therefore, the Fe delivered to the surface waters from these diverse sources is likely to differ in its potential bioavailability.

As with Fe sources, the source of Fe-binding organic ligands are extremely diverse, i.e. bacterially produced siderophores (Rue and Bruland, 1995; Gledhill et al., 2004; Mawji et al., 2008), algal and bacterial exopolymeric substances (EPS), (poly)saccharides (Hassler and Schoemann 2009; Hassler et al., 2011a, b; Hassler, Norman et al., in press, Norman et al, in press), natural organic matter (NOM; Rose and Waite, 2003), humic and fulvic acids (Laglera et al., 2007, 2009). This association with organic ligands can determine the chemical speciation of Fe, as each ligand has its own Fe-binding strength and stability, and therefore reactivity, which are highly influenced by redox and photochemical processes

(Rose and Waite, 2005, 2006; Garg et al, 2007, Hassler et al., 2011a; Gledhill and Buck, 2012). Thus, Fe-ligand complexation can have differing effects on Fe bioavailability. On the one hand, some organic ligands may reduce bioavailability of Fe to phytoplankton (Boye et al., 2001; Hassler and Schoemann, 2009), but on the other, organic complexation has been shown to increase and maintain the solubility of Fe in seawater (Kuma et al., 1996; Lui and Millero, 2003., Chen et al., 2004; Norman et al., submitted; chapter 5 this thesis), and also increase the bioavailability of Fe above that of inorganic Fe (Hassler, Norman et al., in press; Chapter 5).

The Tasman Sea is likely to be one of the most affected areas of the ocean under climate change scenarios (Hobday et al., 2008). In addition, it is an area that is subject to nutrient limitation (mainly N and/or Fe) both of which are likely to severely impact primary productivity. The north and south Tasman Sea represent two quite different regimes in terms of macro- and micronutrient concentration, (Law et al., 2011; Ellwood et al., 2013; Hassler et al., 2014), and phytoplankton community structure (Hassler et al., 2014). Although both regions are reported or predicted to be limited by nutrients, the northern Tasman Sea is predominantly limited by N and Fe, whereas the southern Tasman Sea, close to the sub-Antarctic Zone (SAZ), is limited by light, Si and trace elements, including Fe (Moore et al., 2001; Law et al., 2011, Hassler et al., 2014).

The natural seawater profiles and Fe enrichment experiments reported in this study were collected/conducted during the PINTS voyage ('Primary productivity induced by Iron and Nitrogen in the Tasman Sea'; see Hassler et al., 2014 for details of the study region). The experiments aimed to investigate how *in situ* phytoplankton communities from two contrasting regions respond to Fe delivered from different sources in terms of their growth (biomass) and community structure. The phytoplankton were exposed to dust sourced from the Australian continent, which is periodically deposited into the surface ocean at both northern and southern Tasman Sea locations (Mackie et al., 2008), and inorganic Fe bound to a variety of organic ligands of the type that would be found in this area, i.e. biologically produced exudates (EPS, siderophores etc) and natural organic matter (NOM), which have varying binding affinities for Fe. In addition to characterising changes in the phytoplankton community (e.g., photosynthetic efficiency of PSII (F_V/F_M), total chlorophyll-*a* (TChl-*a,* a proxy for biomass), and biomarker pigments), electrochemical measurements were also made to determine the concentration and binding affinity of the *in situ* ligands and added ligands. These measurements were used to assess the degradation/production of organic ligands during the experiment, and to link the biological response to Fe chemistry for each source.

As the nutrient regimes and phytoplankton community structure at the two sites differed (Hassler et al., 2014), it was expected that the two communities would respond differently to the various Fe additions. It was hypothesised that inorganic Fe would be highly bioavailable and initiate a positive response in both communities, as has been demonstrated in numerous field and laboratory experiments (see reviews from Boyd et al., 2007; Boyd & Ellwood 2010). Whereas, the bioavailability of organically bound Fe may be dependent on their Fe-binding affinities and the phytoplankton nutritive status and ability to acquire these organic forms. For example, for a given phytoplankton community, where Fe was bound to ligands with a strong binding affinity (i.e. siderophores) it would be less accessible than Fe bound to weaker ligands (i.e. saccharides) or those that are highly reactive (i.e. photodegraded NOM). In addition, it was anticipated that the phytoplankton and microbial communities would produce organic ligands (e.g. siderophores, EPS and humic substance-like (HS-like) material) in response to Fe enrichment and further contribute to the organic ligand pool.

3.1 Materials and methods

3.1.1 Experimental precautions

Water acquisition and sample handling was carried out as per GEOTRACES recommendations (Cutter et al., 2010). During the voyage, sampling and experimental set up were conducted in a dedicated trace metal clean van under a HEPA filter (ISO class 5 conditions), and in the land-based laboratory all sample manipulations and reagent preparation was carried out in a dedicated clean laboratory area in an ISO Class 5 laminar flow hood. All materials used (e.g. polycarbonate bottles, HDPE bottles, colourless pipette tips) were acid cleaned using GEOTRACES procedures as detailed in Bowie and Lohan (2009). Reagents were made up in ultra-pure water (UPW: 18.2 $M\Omega cm^{-1}$, Arium 611UV, Sartorius Stedim) unless otherwise stated, and were passed through Chelex-100 resin (BioRad, conditioned as per Price et al., 1989) prior to use to minimise Fe contamination.

3.1.2 Sampling and experimental set-up

Seawater sampling was conducted using non-contaminating procedures as per GEOTRACES recommendations using Teflon coated X-1010 Niskin bottles (General Oceanics, Miami, FL, USA) mounted on an autonomous rosette (Model 1018, General Oceanics, Miami, FL, USA), deployed via a Dynex hydroline (*Dynex Dyneema* 75, Hampidjan Ltd, New Zealand). The

firing of the Niskin bottles was controlled electronically from the vessel. Upon retrieval, the bottles were transferred to the on-deck clean room container as quickly as possible for sub-sampling and then collected unfiltered or filtered (0.2-µm pre-cleaned Acropak filters< PALL, Sydney, Australia), depending on the analysis to be performed. Samples for Fe speciation and HS-like material were stored at -20 °C until analysis; whilst samples for dissolved Fe (dFe) were acidified with ultra-pure HCl (1 mL L^{-1}) and stored at ambient temperature until analysis. Sampling for chlorophyll-*a* (Chl-*a*) was conducted as detailed below (3.1.5, 3.1.6).

The seawater profiles presented here were taken at from three sites in the Tasman Sea, a northern site (P1, 30.0 °S, 156.0 °E), and two southern sites, one in the SAZ (P3, 46.2 °S, 159.5 °E), and the other close to Tasmania (Stn 14, 44.6 °S, 149.4 °E; PINTS voyage, SS01-2010, RV *Southern Surveyor*, Jan-Feb 2010; Fig. 3.1). Stn 14 is a reoccupation of the SAZ-Sense voyage (Feb 2007: see publications in Deep-Sea Res. II. 58; Hassler et al., 2014).

Water to be used for the Fe-enrichment experiments was obtained from the depth of the fluorescence maximum at process stations P1 and P3. After sampling, the seawater was homogenised and filtered through a 200–210-µm mesh to remove mesozooplankton grazers but maintain the *in situ* phytoplankton community. In order to investigate the effect of photochemistry and viruses on Fe cycling and organic ligand production/consumption, 0.2-µm filtered (pre-cleaned Acropak cartridges, PALL, Sydney Australia) seawater was also collected. The resulting filtrates were collected separately in acid cleaned, 20-L polycarbonate carboys and homogenised, after which the two size fractions were dispensed into acid cleaned, 4-L polycarbonate bottles.

In addition to unamended controls, seven further treatments were prepared to provide a 2 nM Fe enrichment in the presence or absence of Fe-binding organic ligands. Into five treatments inorganic Fe (Fe′; Fe as $FeCl_3$ in 0.5M HCl, ICP grade, Fluka) was added to complement the background dFe present in the added organic ligands. One treatment was left as Fe′ only, whilst an excess of Fe'-binding organic ligand was added to the other four. The ligands used were: (A) a bacterial siderophore, desferrioxamine B (DFB, [15 nM], Sigma Aldrich); (B) glucuronic acid, (GLU, [15 nM], Sigma Aldrich); (C) natural exopolymeric substances (EPS, [0.8 nM]) isolated from a pelagic Southern Ocean bacteria (Mancuso Nichols et al., 2005), all representative of autochthonous biological sources; (D) fulvic acid (FA, [100 µg L^{-1}], as Suwannee River Fulvic Acid, International Humic Substances Society, standard I). The remaining two treatments contained atmospheric dust, one collected from the 2009 Brisbane dust storm (D1) and a red composite (D2) ([0.5 mg L^{-1}]), representing

continental input via atmospheric deposition. Both dust samples originated from the Buronga region, NSW. Total acid-leachable Fe concentration of the dust was determined by ICP-MS using a dust concentration of 0.5 mg L^{-1} resuspended in 0.2-µm filtered Tasman Sea surface water and acidified for 9 months prior to analysis (2 mL L^{-1} qHCL, Seastar, V. Schoemann, pers. comm.). The total amount of leachable Fe contained in the dust samples was 372 nM for D1 and 326 nM for D2. Due to the insoluble nature of particulate Fe, the dissolved fraction of the two dusts were measured as 1.84 nM (D1) and 1.83 nM (D2). This was comparable to the concentration of inorganic Fe added to the other ligand treatments and so no extra inorganic Fe was added to the dust enrichments. The incubations where phytoplankton were present (passed through 200–210-µm mesh to remove mesozooplankton grazers but hereafter referred to as unfiltered) were prepared in duplicate, whilst a single incubation per treatment was prepared for the sample set where phytoplankton were excluded by filtration through using 0.2-µm filtered seawater (passed through pre-cleaned Acropak cartridges, PALL, Sydney, Australia; hereafter referred to as filtered). The bottle lids were then sealed with parafilm and triple bagged (clear plastic) to minimise the risk of contamination. The mesocosm experiments were then run over a 4-d period, at the *in situ* temperature and light intensity measured at the chlorophyll maximum (Cmax; P1 = 25 µmol photons m^{-2} s^{-1}, P3 = 13 µmol photons m^{-2} s^{-1}) in an on-deck incubator.

At the conclusion of the experiments, the bottles were gently inverted to homogenise, thereby minimising the risk of cell damage in the incubations where phytoplankton were present. Samples for total dissolved Fe (dFe), Fe chemical speciation and HS-like material were filtered on acid washed Sterivex units (Durapore, Millipore, 0.2-µm, Merck Millipore, Bayswater, VIC, Australia) using a multi-channel Gilson pump with Teflon capillaries at a flow rate of 3–5 mL min^{-1}. Samples for phytoplankton size fractionation and pigment analysis were collected using gentle vacuum filtration as detailed below (3.1.7, 3.1.8).

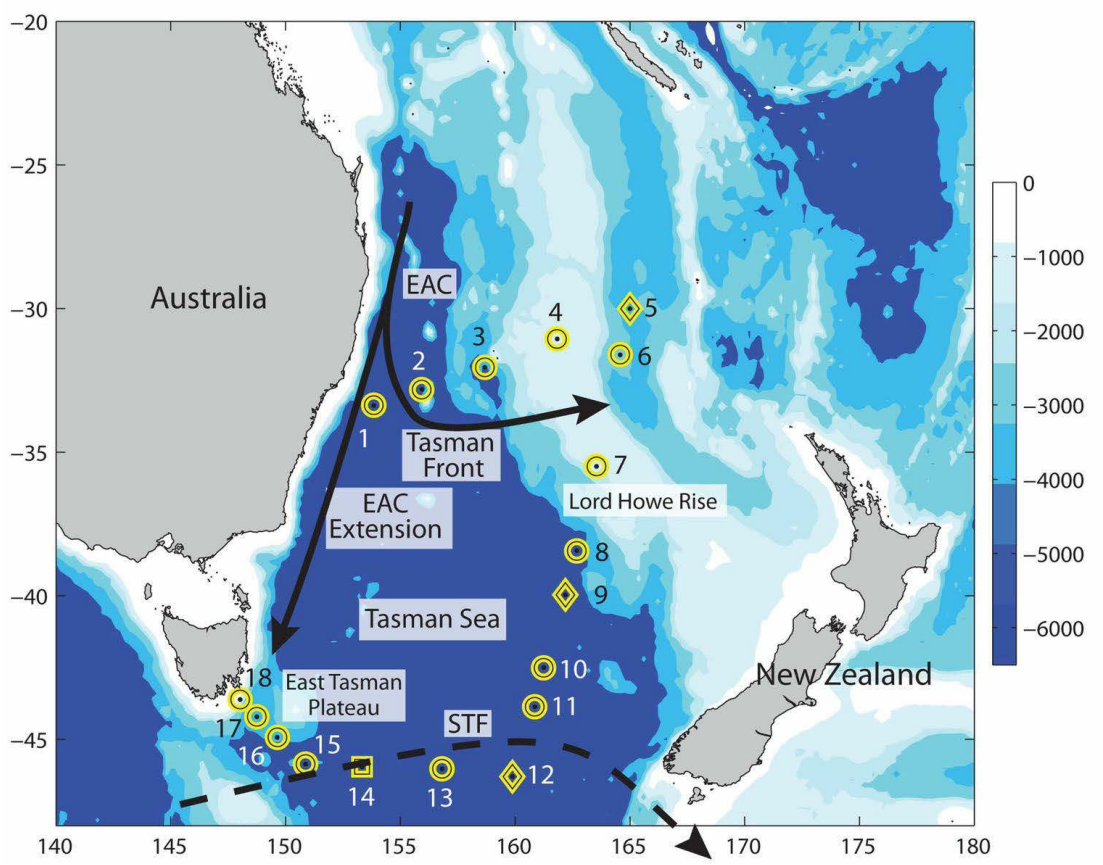

Fig. 3.1 Cruise track from the Primary productivity induced by Iron and Nitrogen in the Tasman Sea (PINTS) voyage (RV *Southern Surveyor*, Jan-Feb 2010). Transect stations are shown as circles and process stations as diamonds. Profiles presented in this chapter were from two process stations P1 (30.0 °S, 156.0 °E, also Stn 5) and P3 (46.2 °S, 159.5 °E, also Stn 12) and from Stn 14, 44.6 °S, 149.4 °E. Stn 14 was a reoccupation of process station 3 from the SAZ-Sense expedition (*Aurora Australis*, January–February 2007). Water for the Fe-enrichment experiments was collected stations P1 and P3. Thicker solid lines indicate the East Australian Current (EAC), Tasman Front (TF), and EAC Extension. The dashed line represents the path of the subtropical front (STF) (From Hassler et al., 2014).

3.1.3 Dissolved Fe determination

Dissolved Fe (dFe) concentrations in the depth profiles (Stn 14 and process stations P1, and P3) was determined by flow injection analysis (FIA) with chemiluminescence detection using methods adapted from Obata et al. (1993) and de Jong et al. (1998) as described in Hassler et al. (2014).

Determination of dFe in the perturbation experiment samples was conducted by isotope dilution multiple collector inductively coupled plasma mass spectrometry (ID-MC-ICP-MS) using a ^{54}Fe spike as described by de Jong et al. (2008). 50-mL samples, acidified at pH 1.9, underwent a pre-concentration step on micro-columns filled with NTA Superflow resin (Qiagen, Chardstone, VIC, Australia). The Nu Plasma MC-ICP-MS (Nu Instruments, Wrexham, UK) was operated at low resolution in dry plasma mode using an Aridus II desolvating sample inlet system (Cetac Technologies, Omaha, NE, USA). The detection limit for the session during which the samples were extracted was 0.029 nmol L^{-1}, determined from 3 x the standard deviation of the procedural blanks. SAFe reference seawater (Johnson et al., 2007) were analysed simultaneously as a quality control and were in good agreement with consensus values (Surface-1, 0.094 ± 0.008 nmol L^{-1}, 1 SD; Deep-2, 0.923 ± 0.029 nmol L^{-1}, 1 SD).

3.1.4 Fe chemical speciation

Fe chemical speciation was measured by Competitive Ligand Exchange Adsorptive Cathodic Stripping Voltammetry (CLE-AdCSV) following the method of Croot and Johannson (2000). The instruments used were μAutolab II and III potentiostat (Ecochemie, Utrecht, Netherlands) with a hanging mercury (Hg) drop electrode (Hg, Sigma Aldrich, ACS reagent grade, 99.9995% trace metal basis; HMDE drop size 2, 0.4 mm^2 ±10%, VA 663 stand – Metrohm, Herisau, Switzerland), a glassy carbon rod counter electrode, and a double junction, Ag/AgCl, reference electrode with a salt bridge filled with 3M KCl. The instruments were controlled using GPES software, version 4.7.

Samples were prepared for analysis by dispensing 10-mL of sample into polypropylene tubes to which increasing concentrations of inorganic Fe was added from a 1 μM standard (prepared daily; Fe as $FeCl_3$ in 0.5M HCl, ICP grade, Fluka). The number of subsamples prepared for titration was determined by considering the known or estimated binding capacity of the ligand used in each treatment (i.e. a weak or strong ligand), but at least 12

increments were prepared per sample. For the control, Fe, GLU, D1 and D2 treatments Fe addition between 0 and 10 nM Fe were prepared, and for the DFB treatment between 0 and 20 nM Fe was prepared. As there was little data available regarding the Fe'-binding capacity of EPS, a larger concentration range and number of samples was prepared (0 and 32 nM Fe) so as to include known functional groups with low binding affinities (i.e. uronic acid) and any uncharacterised components that may have higher binding affinities . The samples were buffered to a pH of 8.1 using 50-µL of 1 M EPPS (SigmaUltra) in 0.3M NH_4OH (Seastar, Baseline ®). Samples were left to equilibrate at ambient temperature for 2-h after which 10-µL of the exchange ligand 2-(2-Thiazolylazo)-p-cresol, TAC, (Sigma; 0.01 M dissolved in triple quartz distilled methanol, Mallinkrodt HPLC grade, prepared fortnightly) was added, and the samples left to equilibrate for a further 18- to 20-h at ambient temperature in the dark. Samples were analysed in polycarbonate titration cells and stirred continually (save for a period of quiescence when measuring) with an inbuilt PTFE rod (1500 rpm). Dissolved oxygen was purged from the sample for 240-s using high purity argon (Air Liquide, Air Liquide, Beresfield, NSW, Australia), followed by 120-s deposition time onto the Hg drop.

The sensitivity of the instrument(s) was determined by the slope of the peak height of the reduction current to the increase of Fe addition when all organic ligands are saturated (at least five points required, $r^2 > 0.993$ in all cases). Labile Fe concentrations (Fe_{Labile}, i.e. $[Fe(TAC)_2]$ detected) could then be determined by dividing the peak height of the reduction current of the sample without Fe addition by the sensitivity of the instrument(s). The detection limit of both instruments was 0.05 nmol determined from three times the standard deviation of eight repeated measurements of a UV treated Southern Ocean seawater sample using purge and deposition times as per samples. The concentrations and conditional stability constants ($\log K_{Fe'L}$) of the Fe-binding ligands present were determined from the speciation data using the non-linear fit method of Gerringa et al. (1995), and compared to the linear fit method of van den Berg (1995). As a quality control of the data presented, the non-linear fit method was checked to be within 10 % of the data using a linear curve-fit method (Harris, 1998). A conditional side reaction coefficient ($\alpha_{Fe'(TAC)2}$) of 636 ± 48 (10 µM TAC) was used for calculations (appendix 4). This coefficient was determined using UV-oxidised, 0.2-µm filtered, Southern Ocean water in the presence of 10 nM inorganic iron and DTPA (Diethylenetriaminepentaacetic acid, Sigma) using non-linear fit as per Croot and Johannson (2000) and Hassler et al. (2013).

3.1.5 Analysis of humic-substance like (HS-like) material

The concentration of HS-like material was determined using the voltametric method of Laglera et al (2007) as per Chapter 2 (p 36). Samples were analysed using 250-s purge time and 300-s deposition time, and standard additions of Suwannee River Fulvic Acid (SRFA; Std 1, International Humic Substances Society, Denver, Colorado, USA) in increments of 0.02 mg L^{-1} or 0.05 mg L^{-1} from a 15.75 mg L^{-1} working stock (prepared weekly and stored at 4 °C in the dark). The detection limit of the instruments was 1.49 µg L^{-1} determined from three times the standard deviation of ten repeated measurements of a Southern Ocean seawater sample using purge and deposition times as per samples. The position of the reduction peak and the sensitivity were used to investigate differences in the nature of the HS-like matrix in the experimental samples.

3.1.6 Macronutrient analysis

Macronutrient determination (reactive phosphorus (PO_4), silicic acid ($Si(OH)_4$), nitrate + nitrite (NO_X) was performed on-board using flow injection analysis and colorimetric techniques (Reynolds and Navidad, 2012), as detailed in Hassler et al. (2014).

3.1.7 Phytoplankton size fractionation

Three phytoplankton size fractions (0.7–2-µm, 2–10-µm, and ≥ 10-µm) were collected using gentle sequential filtration (< 5mm Hg) of 1-L of the final experimental solutions through 10-µm, 2-µm polycarbonate filters (Whatman) and 0.7-µm GF/F filters (Whatman). Filters were then cryopreserved and stored in liquid nitrogen at -80 °C prior to pigment analysis.

3.1.8 Phytoplankton pigment analysis

In addition to using total chlorophyll-*a* (TChl-*a*) to assess the biomass and growth of the phytoplankton communities, a range of other phytoplankton pigments were used as biomarkers to provide information as to the composition of the microalgal phototrophs in each treatment. Chl-*a*, and biomarkers pigments chlorophyll-*b* (Chl-*b*), divinyl chlorophyll-*a* (DVChl-*a*), fucoxanthin (fuco), 19 butanoloxyfucoxanthin (but-fuco), 19 hexanoyloxyfucoxanthin (hex-fuco), zeaxanthin , and peridinin were extracted in 100% methanol at 4 °C in the dark prior to HPLC analysis (Waters – Alliance high performance

liquid chromatography system; Waters-Alliance, Rydalmere, NSW, Australia) using a modified version of Van Heukelem and Thomas (2001) as detailed in Hassler et al. (2012 and 2014).

3.1.9 Photophysiology measurements

Estimates of the maximum quantum yield of photosystem II (F_V/F_M) were made on phytoplankton samples using a Pulse Amplitude Modulated fluorometer (Water-PAM; Walz GMBH, Germany). A 3-mL sample was placed into a cylindrical quartz cuvette and dark-adapted for 15-min. Once the fluorescence signal was stable, a saturating pulse was applied to give the dark-adapted maximum fluorescence (F_M). F_V/F_M was calculated as (F_M-Fo)/F_M (Schreiber, 2004).

3.1.10 Data presentation, manipulation and statistical analysis

Fe chemical speciation and HS-like material samples for the natural samples were obtained at depths between 15 m and 1000 m, and for consistency macronutrient and dFe profiles are presented for depths corresponding to these samples. Full-depth profiles for macronutrients and trace elements are presented in Hassler et al. (2014). TChl-*a* data presented here were obtained at depths between 15–50 m for Stn 14; 15–125 m for P1; 15–80 m for P3.

Relationships between Fe speciation parameters and HS-like with TChl-*a,* and dFe and macronutrients (NO_X, PO_4, $Si(OH)_4$) were investigated initially using Pearson correlations, followed by regression analysis where relationships were significant ($p < 0.05$). Both individual profiles and pooled data were tested. Relationships with macronutrients (NO_X, PO_4 and $Si(OH)_4$) were considered using data between 15 and 300 m to avoid 'skewing' of the data from the much higher 1000 m concentrations.

Statistical analysis was performed, where possible, to investigate differences in the experimental treatments. Where only one sample was available for analysis (some Fe chemical speciation data and all filtered sample sets), the differences between enrichments are described in terms of proportions. Where replicates were available (HS-like analysis and TChl-*a* data) statistical differences were explored using an unpaired t-test at a significance level of < 0.05.

3.2 Results

3.2.1 Natural samples

The concentration of macronutrients (NO_X, PO_4, and $Si(OH)_4$) showed typical nutrient profiles of depletion in the euphotic zone and increasing with depth (Fig. 3.2A, B, and C). NO_X and PO_4 were much more depleted at P1 compared to P3 and Stn 14, with concentrations of < 0.1 µmol L^{-1} present in the top 90 m of the water column for both constituents. NO_X at P1 was below detection in the top 50 m (Fig. 3.2A and B). P3 and Stn 14 were extremely similar in NO_X concentration throughout the water column except at 15 m where Stn 14 was much more depleted in NO_X (by 8-fold; Fig. 3.2A). PO_4 was a little more variable, with P3 generally being between 0.1 and 0.5 µmol L^{-1} higher in concentration than Stn 14 in the top 125 m of the water column (Fig. 3.2B).

$Si(OH)_4$ was extremely depleted at all stations in the top 50 m of the water column (≤ 1.3 µmol L^{-1}) but was elevated at Stn 14 by ~ 0.3 µmol L^{-1} compared to both P1 and P3. $Si(OH)_4$ remained very low at P1 until 1000 m, whereas concentration increased at P3 and Stn 14 to between 3 and 5 µmol L^{-1} from 90 to 300 m (Fig. 3.2C). All macronutrients were enriched at 1000 m (Fig. 3.2A, B, C; refer to Hassler et al. (2014) for full profile descriptions).

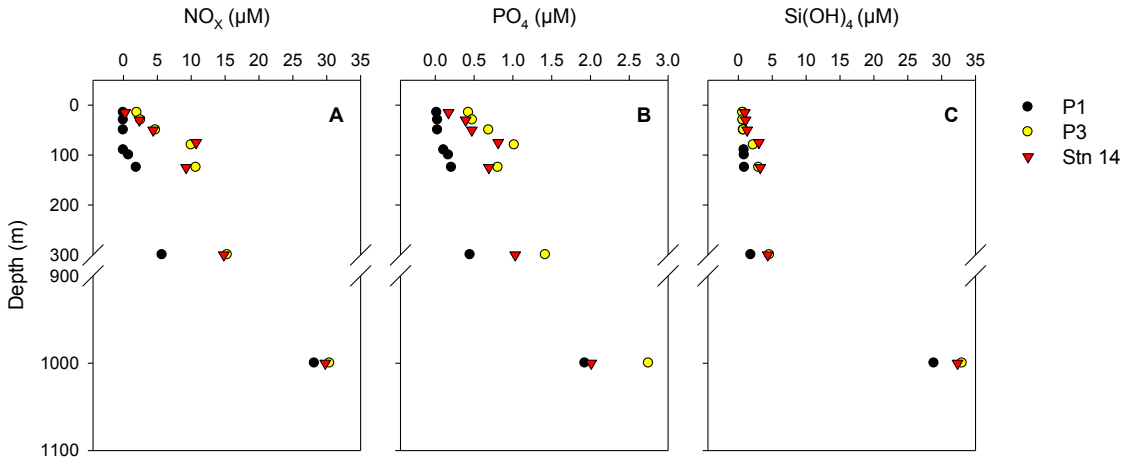

Fig. 3.2 Seawater depth profiles of dissolved nutrients nitrate + nitrite (NO_X; panel A), reactive phosphorus (PO_4; panel B), and silicic acid ($Si(OH)_4$; panel C), measured at stations P1 (30.0 °S, 156.0 °E,), P3 (46.2 °S, 159.5 °E,) and Stn 14 (44.6 °S, 149.4 °E) collected during the PINTS voyage (RV *Southern Surveyor*, Jan-Feb 2010).

3.2.1.1 Total chlorophyll-a profiles

Depth profiles of total chlorophyll-*a* (TChl-*a*) revealed that the vertical distribution of phytoplankton differed considerably between the northern (P1) and southern (P3 and Stn 16) sites. A deep Cmax was present at P1 (~120m), whereas at P3 and Stn 14 the highest TChl-*a* concentrations were measured in the top 30 m (Fig. 3.3; Hassler et al., 2014).

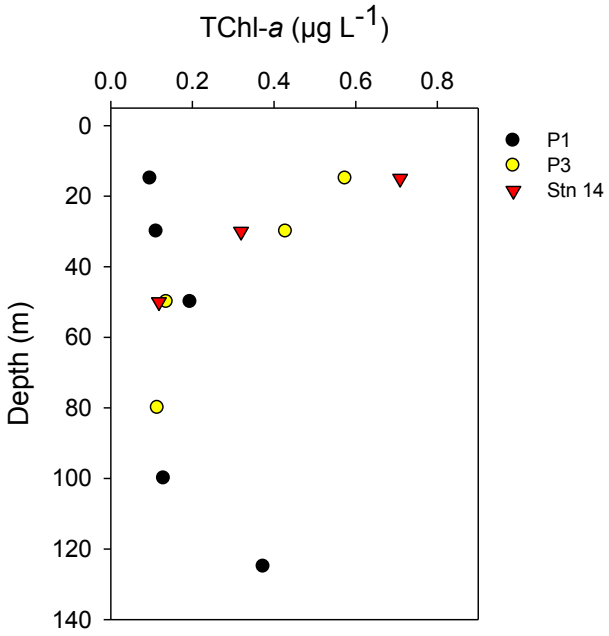

Fig. 3.3 Seawater depth profiles of total chlorophyll-*a* (TChl-*a* µg L^{-1}) measured at stations P1 (30.0 °S, 156.0 °E, depths 15 to 125 m), P3 (46.2 °S, 159.5 °E, depths 15 to 80 m) and Stn 14 (44.6 °S, 149.4 °E, depths 15 to 50 m) collected during the PINTS voyage (RV *Southern Surveyor*, Jan-Feb 2010).

3.2.1.2 Dissolved Fe, Fe-binding organic ligands, conditional stability constants, and HS-like material

Dissolved Fe was < 1 nM, throughout the water column (to 1000 m) at all sites, and was particularly depleted for the P1 profile where concentrations were < 0.2 nM between 30 and 125 m. Slightly elevated sub-surface (15 m) dFe concentrations were measured at P1 and P3, although the concentration at P1 was almost double that of P3 (0.39 nM and 0.24 nM, respectively; Fig 3.4A). At Stn 14, a maximum concentration of 0.87 nM was measured at 30 m (Fig. 3.4A). From 30 m depth, the overall trend at P3 and Stn 14 was an increase in concentration with depth, whereas this increase in dFe concentration did not occur at P1 until ~300 m. (Fig. 3.4A).

The average sum of all ligands (ΣL) and log $K_{Fe'L}$ of each profile were not significantly different from each other, and gave an overall average of 4.23 ± 1.37 nM ΣL and a log $K_{Fe'L}$ of 11.52 ± 0.26. Most of the highest ligand concentrations (4 to 5 nM) were measured in samples within, or adjacent to, the Cmax at all stations, although a high concentration of weaker ligands were detected at depths below 125 m (4.3 to 6.6 nM; Fig. 3.4B and C). Throughout the water column, all ligands were present in excess of dFe (ExL), with the greatest excess occurring close to the Cmax. At P1 the concentration of ExL at 15 and 1000 m was ~ 8-fold greater than dFe, but was in greater excess between 50 and 125 m (~40-to 50-fold > dFe). At P3 the trend was more varied throughout the water column, although the greatest excess (~14 to 21-fold > dFe) was in the top 50 m, concomitant with the highest biomass. At Stn 14, the concentration of ExL was generally lower than P1 and P3, reflecting both the slightly higher dFe levels, and lower concentrations of Fe-binding organic ligands measured in the top 200 m of the water column, with greatest excess occurring at 75 m (15-fold > dFe). At all sites, log $K_{Fe'L}$ was mostly in a range of 11.3 to 11.65, however stronger L_1 ligands (log $K_{Fe'L}$ 12.15) were measured in the 50 m sample at Stn 14, and weaker ligands ($K_{Fe'L}$ < 11.2) were measured at depth (Fig. 3.4C). Generally, the highest conditional stability constants (log $K_{Fe'L}$), and thus, the stronger ligands, were present in the upper water column (above 80 m; Fig. 3.4C).

HS-like concentrations were generally very low (< 6 μg L^{-1} SRFA eq.) across all sites, although elevated concentrations occurred at or adjacent to the Cmax at P1 and P3 (P1, 50m 12.9 μg L^{-1} SRFA eq.; P3, 30 m 20.2 μg L^{-1} SRFA eq.). However, at Stn 14 concentrations were elevated throughout the top 50 m of the water column (19.6 to 57.3 μg L^{-1} SRFA eq.) particularly at 15 m (Fig. 3.4D).

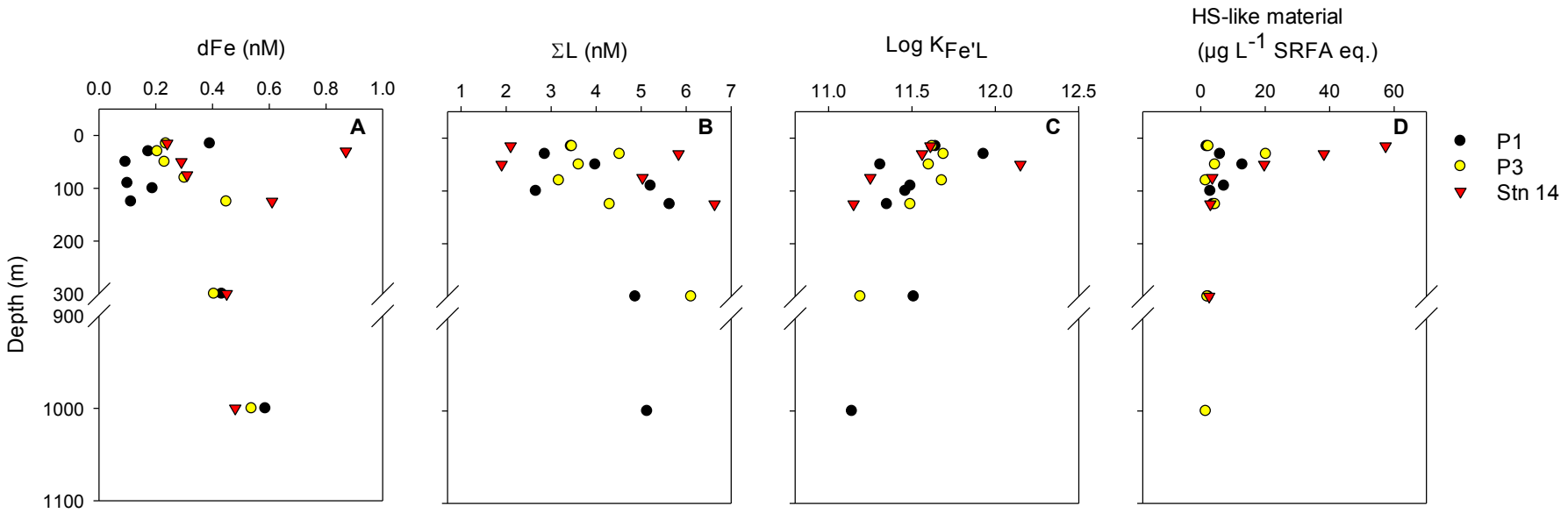

Fig. 3.4 Seawater depth profiles (15 to 1000m) from process stations P1 (30.0 °S, 156.0 °E), and P3 (46.2 °S, 159.5 °E) and Stn 14 (44.6 °S, 149.4 °E) collected during the PINTS voyage (RV *Southern Surveyor*, Jan-Feb 2010). Concentration of dissolved Fe (dFe, nM) and the concentration of electrochemically detected Fe′-binding organic ligands (ΣL, nM) and their calculated conditional stability constant (Log $K_{Fe'L}$) are presented together with the concentration of humic substance-like (HS-like) material. HS-like material is expressed as Suwannee River Fulvic Acid (SRFA) equivalent µg L^{-1}.

Examination of relationships between ΣL, Log $K_{Fe'L}$, HS-like concentration and TChl-*a* revealed that a negative relationship between ΣL and log $K_{Fe'L}$ occurred at all stations (r^2 = P1, 0.34; P3 0.74; Stn 14, 0.63; data not shown) and also in the pooled data (r^2 = 0.54; Fig 3.5), reflecting the expected pattern of higher concentrations being associated with weaker ligands. Relationships were also calculated between log $K_{Fe'L}$ and TChl-*a* (r^2 = 0.35, negative relationship) and ΣL and TChl-*a* (r^2 = 0.88, positive relationship) at P1, and HS-like and ΣL at Stn 14 (r^2 = 0.27, negative relationship; Fig 3.6. A final strong positive relationship was observed between HS-like concentration and TChl-*a* at Stn 14, however this relationship was based on just three points (r^2 = 0.97, data not shown). No other relationships were evident when the data was pooled. In addition, relationships between dFe and ΣL, log $K_{Fe'L}$ and HS-like substances were tested, but none were found.

Relationships between dFe concentrations and macronutrients were also explored. No relationships were evident at P1 and Stn 14, however positive relationships with all macronutrients were observed for P3 (NO_X, r^2 = 0.75; PO_4, r^2 = 0.47; $Si(OH)_4$, r^2 = 0.79; Fig. 3.7).

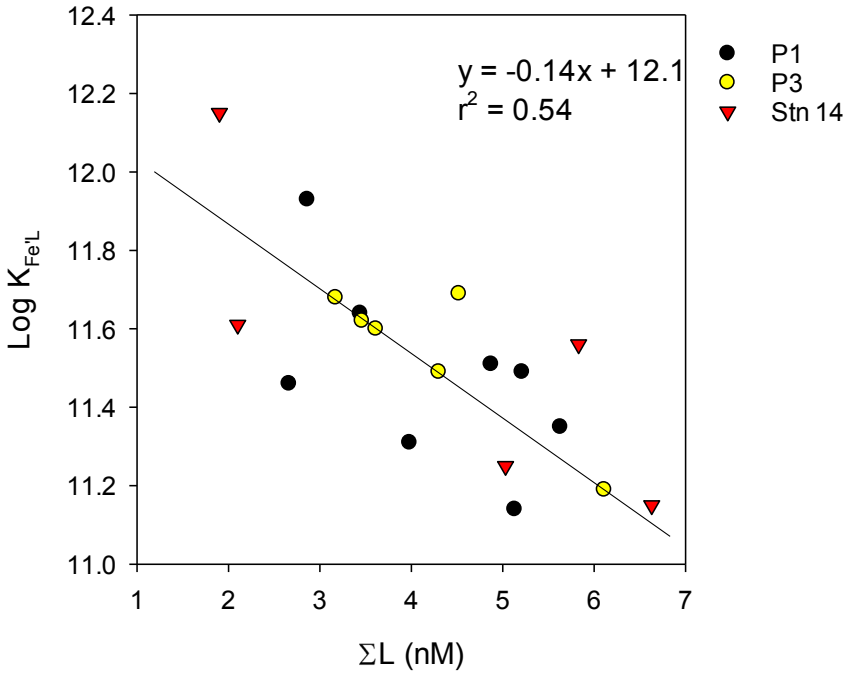

Fig. 3.5 Relationship between the concentration of Fe-binding organic ligands (ΣL) and the conditional stability constant (Log $K_{Fe'L}$) for process station P1 (30.0 °S, 156.0 °E), process station P3 (46.2 °S, 159.5 °E) and Stn 14 (44.6 °S, 149.4 °E). Samples were collected during the PINTS voyage (RV *Southern Surveyor*, Jan-Feb 2010; Hassler et al., 2014).

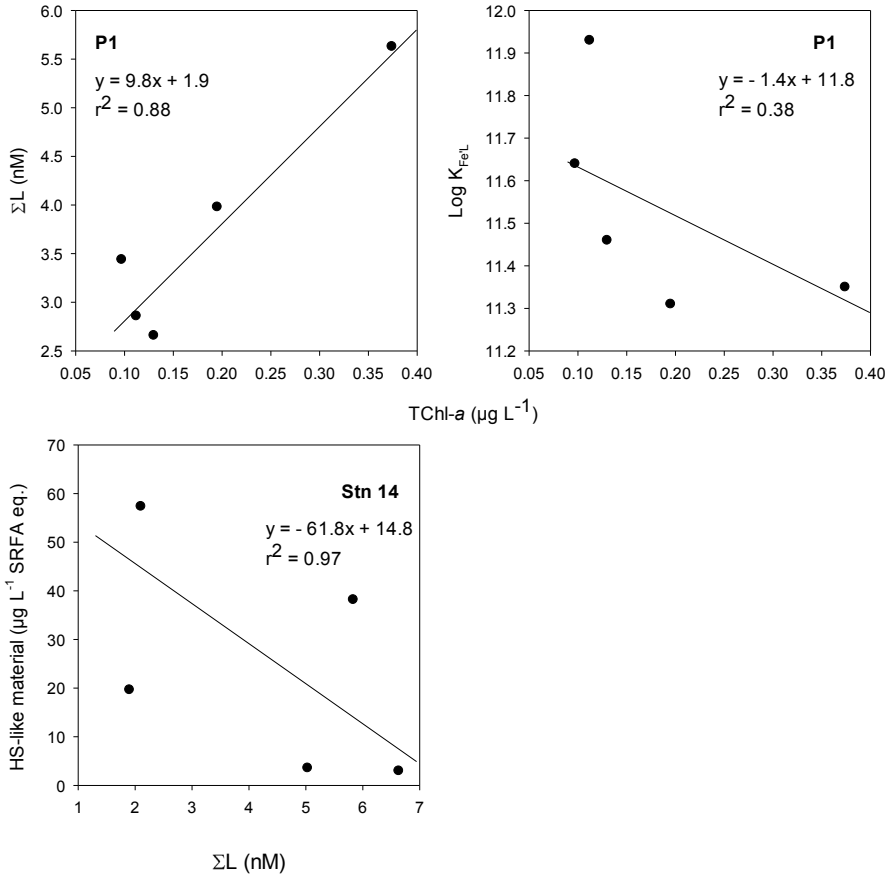

Fig. 3.6 Relationships between the concentration of total chlorophyll-*a* (TChl-*a*) and the sum of Fe-binding organic ligands (ΣL), TChl-*a* and ligand conditional stability constant (log $K_{Fe'L}$) at depths between 15 and 125 m at process station P1 (30.0 °S, 156.0 °E), and TChl-*a* and ΣL at depths between 15 and 50 m, humic substance-like (HS-like) material and ΣL at depths between 15 and 300 m and at Stn 14 (44.6 °S, 149.4 °E). Samples were collected during the PINTS voyage (RV *Southern Surveyor*, Jan-Feb 2010; Hassler et al., 2014). HS-like material is expressed as Suwannee River Fulvic Acid (SRFA) equivalent in µg L^{-1}.

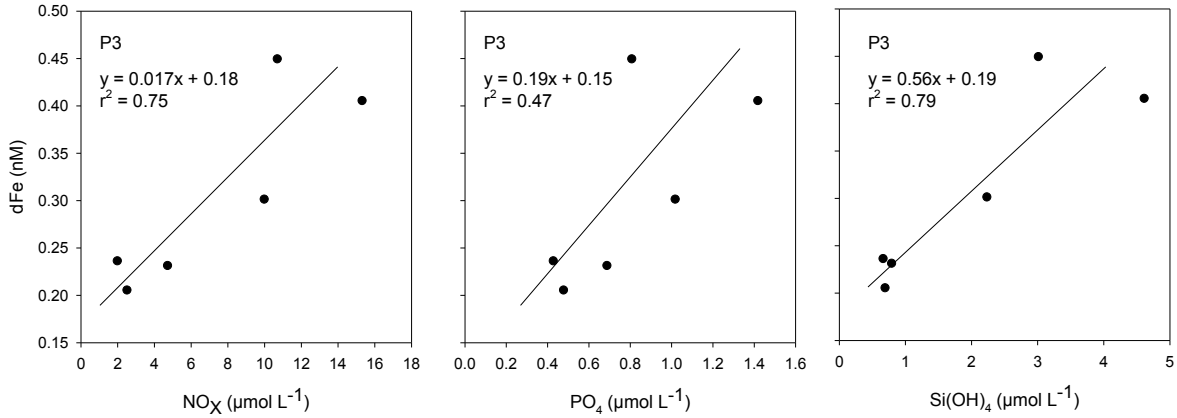

Fig. 3.7 Relationships between dissolved Fe (dFe) concentration (nM) and macronutrients nitrate + nitrite (NO_X), phosphate (PO_4) and silicic acid ($Si(OH)_4$) (µmol L^{-1}) at process station P3 (46.2 °S, 159.5 °E) at depths between 15 and 300 m. Samples were collected during the PINTS voyage (RV *Southern Surveyor*, Jan-Feb 2010; Hassler et al., 2014).

3.2.2 Fe-enrichment experiments

3.2.2.1 Overview of site characteristics

The two stations (P3 and P1) exhibited very different characteristics. P1 had a much deeper Cmax, and lower TChl-*a* (proxy for phytoplankton biomass), but higher F_V/F_M than measured at P3 (Table 3.1; full details in Hassler et al, 2014). The concentrations of macronutrients at the depth of the Cmax were similar at both stations, except for silicate (Si) which was greater at P1 (Table 3.1; Hassler at al., 2014). Dissolved Fe (dFe) at P1 was more than double that measured in the P3 (Table 3.1; Hassler et al., 2014).

Table 3.1. Depth of chlorophyll maximum (Cmax), and in situ concentration of total chlorophyll *a* (TChl-*a*), nutrients (silicate (Si), nitrate + nitrite (NO_x), phosphate (PO_4)), and F_V/F_M from process stations P1 (30.0 °S, 156.0 °E), and P3 (46.2 °S, 159.5 °E). Water was collected at the depth of the fluorescence/chlorophyll-*a* max (Cmax) from these two stations to conduct Fe-enrichment experiments during the PINTS voyage (RV *Southern Surveyor*, Jan-Feb 2010).

Station	Depth of Cmax (m)	TChl *a* (µg L^{-1})	dFe (nM)	Nutrients (µM)	F_V/F_M
P1	90 - 110	0.37	0.67	Si: 1.06 NO_X: 1.18 PO_4: 0.18	0.70
P3	15 – 30	1.33	0.21	Si: 0.68 NO_X: 1.1 PO_4: 0.26	0.54

3.2.2.2 Fe biogeochemistry

3.2.2.2.1 Total dissolved Fe (dFe) and labile Fe (Fe_{Labile})

Initial (T0) dFe samples were not taken for the enrichments, but taking into account the *in situ* dFe measured (Table 3.1) and the added inorganic Fe (2 nM), the total dFe concentrations were 2.67 nM and 2.29 nM dFe for P1 and P3, respectively, at T0. As the dFe in D1 and D2 was 1.84 nM and 1.83 nM, respectively, T0 for D1 was ~2.53 nM and 2.13 nM, and D2 ~2.52 nM and 2.12 nM for P1 and P3, respectively in both cases.

At the conclusion of the 4-d incubation, the concentration of dFe in the P1 unamended control had diminished considerably to about half that measured in the T0 sample; whereas in the control-F (filtered control) the concentration of dFe had increased to 0.90 nM (Fig. 3.8A). In the unfiltered incubations, dFe concentration in all enrichments was lower than the nominal T0. Larger decreases were measured in the dust enrichments (D1, D1-F, D2, D2-F) where ~ 2 nM dFe had been removed from that initially present (Fig. 3.8A). The concentration of dFe had also substantially decreased in the EPS and EPS-F enrichments to < 50 % of the nominal T0 (Fig. 3.8A). The reduction in dFe was less marked in the other enrichments (Fe, DFB, GLU, and FA), where between 63% and 94% remained.

For P3, the concentration of dFe in the control (unfiltered) compared to the T0 (0.21 nM) differed between the duplicates, with a decrease measured in one sample (0.15 nM), but an increase in the other (0.40 nM) (Fig. 3.8B). Control-F was also slightly elevated at 0.36 nM

(Fig. 3.8B). D1, D2, and EPS all contained substantially less dFe than the nominal T0 for these enrichments (all < 0.55 nM; Fig. 3.8B). In contrast to P1, dFe in the P3 GLU enrichment had decreased by half from the nominal T0 (Fig. 3.8B). Again, a smaller reduction in dFe concentration was measured in the Fe, DFB and FA enrichments where between 74 % and 87 % remained (Fig. 3.8B).

Except for P1 D2 and P3 DFB, dFe was elevated in the filtered incubations compared to the corresponding unfiltered incubations for both the P1 and P3. In the control-F, Fe-F, GLU-F, and FA-F P1 and P3 incubations dFe was measured in excess of the T0 (or nominal T0; Fig. 3.8A, B; Table 3.2). At P1, the enhanced dFe concentration in the filtered samples compared to the unfiltered samples amounted to between 2 and 15 % for the D1-F, EPS-F and DFB-F, and ~ 30 % for the Fe-F, GLU-F and FA-F incubations. At P3, the enhanced dFe in the filtered samples was greater than at P1 at 30 % to 40 % in the Fe-F, EPS-F and FA-F and 70 % to 85 % for D1, D2 and GLU (Fig. 3.8A, B).

The daily uptake of dFe was calculated for each incubation based on the T0 or nominal T0. This revealed that in the P1 unfiltered and filtered incubations the greatest uptake, by far, was in the D2 enrichment, followed by the EPS and the D1 enrichments, and that uptake was similar between the unfiltered and filtered samples. dFe uptake in the GLU and FA unfiltered incubations were similar to the control despite the increased concentration of dFe in these incubations at T0 (Table 3.2). The DFB unfiltered and filtered dFe uptake were low compared to D2, EPS and D1 (< half) (Table 3.2).

Similarly, the P3 EPS, D2 and D1 unfiltered incubations also had the greatest dFe daily uptake; however, at this site the GLU incubation was comparable to the D1 incubation. Uptake of dFe was lowest in the DFB incubation. The P3 control and FA replicates gave contrasting results with uptake in one replicate and apparent remineralisation in the other (Table 3.2). Uptake in the filtered P3 EPS incubation was again quite similar to the unfiltered sample; however uptake was 2.5- and 4.1-fold lower in the D1-F and D2-F samples compared to the unfiltered. (Table 3.2)

Table 3.2 Daily uptake of dissolved Fe (dFe, nM) from Fe enrichment experiments at the conclusion of a 4-day incubation in samples with and without the addition of organic ligands. Water for the experiments was collected from two sites in the Tasman Sea, P1 (30.0 °S, 156.0 °E) and P3 (46.2 °S, 159.5 °E) during the PINTS voyage (RV *Southern Surveyor*, Jan-Feb 2010). Treatments measured after 4-d incubations comprised an unamended control (Con), two treatments containing Australian desert dust (D1, 2009 Brisbane dust storm, and D2, red composite from the Buronga region) which were predicted to release ~2 nM Fe, inorganic Fe only (2 nM), and organic ligands desferrioxamine B (DFB [15 nM]) natural pelagic bacterial exopolymeric substances (EPS, [0.8 nM]), glucuronic acid (GLU [15 nM]), and fulvic acid (FA, [100 µg L^{-1}], as Suwannee River Fulvic Acid). DFB, EPS, GLU and FA treatments also contained 2 nM inorganic Fe. Unfiltered = incubations where phytoplankton were present, filtered = incubations where phytoplankton was absent (0.2-µm filtered). Errors are the half interval of duplicate samples. Where no errors are stated the values are from a single sample.

Treatment	P1 unfiltered dFe uptake nM d^{-1}	P1 filtered dFe uptake nM d^{-1}	P3 unfiltered dFe uptake nM d^{-1}	P3 filtered dFe uptake nM d^{-1}
Con	0.09 ± 0.016	0.06 †	0.04 (0.03†)	0.02 †
Fe	0.19 ± 0.003	0.08 †	0.15± 0.278	0.11 †
DFB	0.15 ± 0.104	0.13	0.08 ± 0.286	0.13
GLU	0.05 ± 0.002	0.19 †	0.33 ± 0.073	0.12 †
EPS	0.42	0.37	0.51	0.47
FA	0.06 ± 0.004	0.23 †	0.18 (0.04†)	0.16 †
D1	0.35 ± 0.022	0.34	0.36 ± 0.142	0.14
D2	0.48 ± 0.008	0.49	0.47 ± 0.010	0.11

† indicates an increase in dFe rather than uptake.

The P1 T0 sample contained a slightly higher proportion of labile Fe (Fe_{Labile}) than the P3 T0 (58% and 53%, respectively). After 4-d incubation, Fe_{Labile} concentrations in the P1 controls had increased by ~25% (Fig. 3.7B and G). Whereas, the two P3 controls showed different responses, with no substantial change in one (51%) and an increase of ~25% in the other. The lowest Fe_{Labile} was measured in the DFB and DFB-F enrichments (< 20 % Fe_{Labile} both P1 and P3), and the highest Fe_{Labile} was measured in the EPS and EPS-F enrichments (>80%, Fig. 3.8B and G). The two dust samples (D1 and D2) gave quite different proportions of Fe_{Labile}. D1 and D1-F enrichments for both P1 and P3 ranged from 61 to 82% (Fig 3.8B and G), whereas D2 and D2-F were highly variable, particularly in the P3 incubations (P1- D2 ~ 50%, D2-F ~ 60%; P3 – D2 > 90 %, D2-F < 20 %; Fig. 3.8B and G). Fe_{Labile} was below 55 % in all other enrichments and this was similar between P1 and P3 (Fig. 3.8C and D).

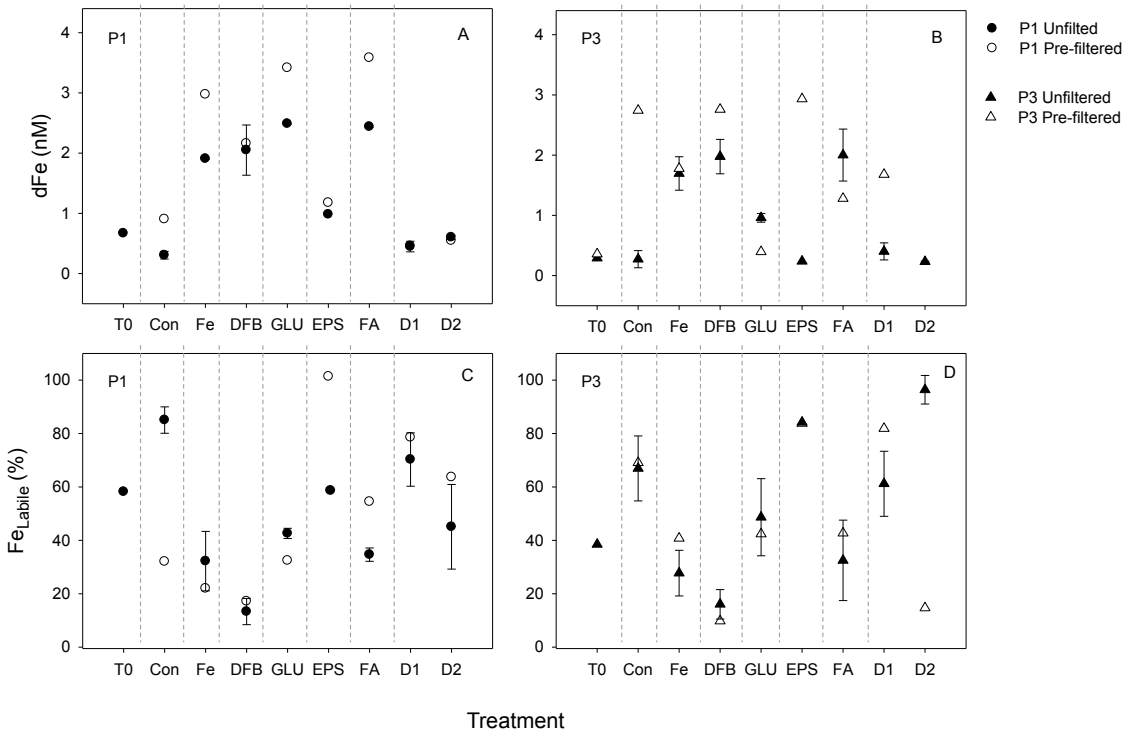

Figure 3.8 Concentrations of dissolved Fe (dFe, nM) and relative concentration (%) of labile Fe (Fe_{Labile}) associated with Fe enrichment experiments using phytoplankton communities collected from two sites in the Tasman Sea, P1 (30.0 °S, 156.0 °E, panels A and C) and P3 (46.2 °S, 159.5 °E, panels B and D) during the PINTS voyage (RV *Southern Surveyor*, Jan-Feb 2010). The data presented comes from unamended seawater (T0) and after 4-d incubation in samples with and without the addition of Fe and organic ligands. Treatments measured after 4-d incubation comprised an unamended control (Con), inorganic Fe only (2 nM, Fe), desferrioxamine B ([15 nM], DFB), glucuronic acid ([15 nM], GLU), natural pelagic bacterial exopolymeric substances ([0.8 nM], EPS), fulvic acid ([100 μg L^{-1}], as Suwannee River Fulvic Acid, FA), and two treatments containing Australian desert dust (D1, 2009 Brisbane dust storm, and D2, red composite, both from the Buronga region, NSW) which were predicted to release ~2 nM Fe. DFB, EPS, GLU and FA treatments were all enriched with 2 nM inorganic Fe. Closed symbols indicate samples with phytoplankton present, open symbols indicate samples where phytoplankton were absent (0.2-μm filtered, single incubations). Error bars represent half-interval of duplicate samples; where no error bars are present the data presented is from a single sample.

3.2.2.2.2. Ligand concentration and conditional stability constants associated with natural and added ligands

The initial (T0) P1 and P3 samples displayed similar characteristics in both ligand concentration (ΣL; P1 2.24 nM; P3 2.60 nM) and conditional stability constant (log $K_{Fe'\Sigma L}$; P1 11.62; P3 11.61). After 4-d incubation the ΣL had increased and log $K_{Fe'\Sigma L}$ had decreased in both controls (P1 and P3; Fig 3.9).

In the unfiltered samples, ΣL was elevated in all P1 enrichments compared to the control (1.2 to 10 fold), except for D2, and was particularly high in the EPS enrichment (Fig. 3.9A). Log $K_{Fe'sumL}$ in the P1 unfiltered GLU, FA and D2 incubations was similar to the control, however stronger ligands (log $K_{Fe'sumL}$ > 11.85) were measured in both Fe and DFB incubations (Fig. 3.9C). The lowest log $K_{Fe'\Sigma L}$ (10.43) was measured in the EPS enrichment. An increase in ΣL was also measured in the filtered samples (1.2- to 2-fold; Fig. 3.9A) compared to control-F, except for EPS-F where no ligands were detected. Log $K_{Fe'\Sigma L}$ decreased from the control-F in all incubations, except for Fe-F and DFB-F (11.88 and 11.91, respectively; Fig. 3.9C).

In the P3 incubations ΣL was elevated in both the control and control-F and log $K_{Fe'\Sigma L}$ was similar compared to the T0 (Fig. 3.9B). ΣL was elevated in all P3 enrichments (up to 2.8 fold) compared to the control, with the highest concentration measured in the EPS enrichment (11.85 nM; Fig. 3.9D). Log $K_{Fe'\Sigma L}$ measured in the P3 GLU, FA, and D1 enrichments were similar to the control values, whereas the Fe and DFB had a stronger log $K_{Fe'\Sigma L}$ (≥ 11.8). D2 and EPS enrichments had the lowest log $K_{Fe'\Sigma L}$ of the P3 unfiltered incubations (≤ 11.15; Fig. 3.9D). ΣL was also elevated in all P3 filtered incubations (between 1.3 and 3.4 fold), with the highest occurring in the D1-F and DFB-F enrichments (Fig. 3.9B). Higher log $K_{Fe'\Sigma L}$ (≥ 11.8) were measured in the D2-F and DFB-F incubations, whereas D1-F, EPS-F, GLU-F and FA-F all had log $K_{Fe'\Sigma L}$ ≤ 11.5 (Fig. 3.9D).

The D1 enrichments for P1 and P3, and the P3 Fe enrichment were the only incubations where two ligands were measured. At P1 the first (L_1) had a ligand concentration of 1.89 ± 0.52 nM and a conditional stability constant (log $K_{Fe'L1}$) of 11.95 ± 0.03, close to the log $K_{Fe'SumL}$ of the DFB incubation, whereas the second (L_2) had a much higher concentration of 7.21 ± 1.65 nM, but a lower log $K_{Fe'L}$ (log $K_{Fe'L2}$ = 11.19 ± 0.10; Fig. 3.9A, C). At P3, the concentration of L_1 was about half that of L_2 in both D1 and Fe enrichments and again, log $K_{Fe'L1}$ was higher than log $K_{Fe'L2}$ (both >12, and ~11.55, respectively; Fig. 3.9B, D).

A comparison between the unfiltered and filtered samples for both P1 and P3 showed that ΣL was higher in all filtered treatments, except for P1 DFB-F and EPS-F, compared to the corresponding unfiltered samples (Fig. 3.9A, B). Generally, $K_{Fe'\Sigma L}$ was similar or lower in the filtered samples for both P1 and P3, except for the control-Fs which were slightly elevated compared to the control (Fig. 3.9C, D).

Overall, the expected inverse relationship between Fe_{Labile} and log $K_{Fe'L}$ (i.e. high Fe lability and lower log $K_{Fe'L}$ and vice versa) was observed in both the P1 and P3 experiments. Those samples that contained < 30% Fe_{Labile} (Fe, DFB, Fe-F and DFB-F) all had a stronger class of ligand associated with them ($\log K_{Fe'\Sigma L} \geq 11.8$), whereas those with Fe_{Labile} > 80% (EPS, P1 control and P3 D2) were associated with measurably weaker ligands (Log $K_{Fe'\Sigma L}$ – ≤ 11.4). Finally, the DFB/DFB-F and GLU/GLU-F samples had lower concentrations of ligands present at the end of the 4-d incubation than the 15 nM originally added for both P1 and P3.

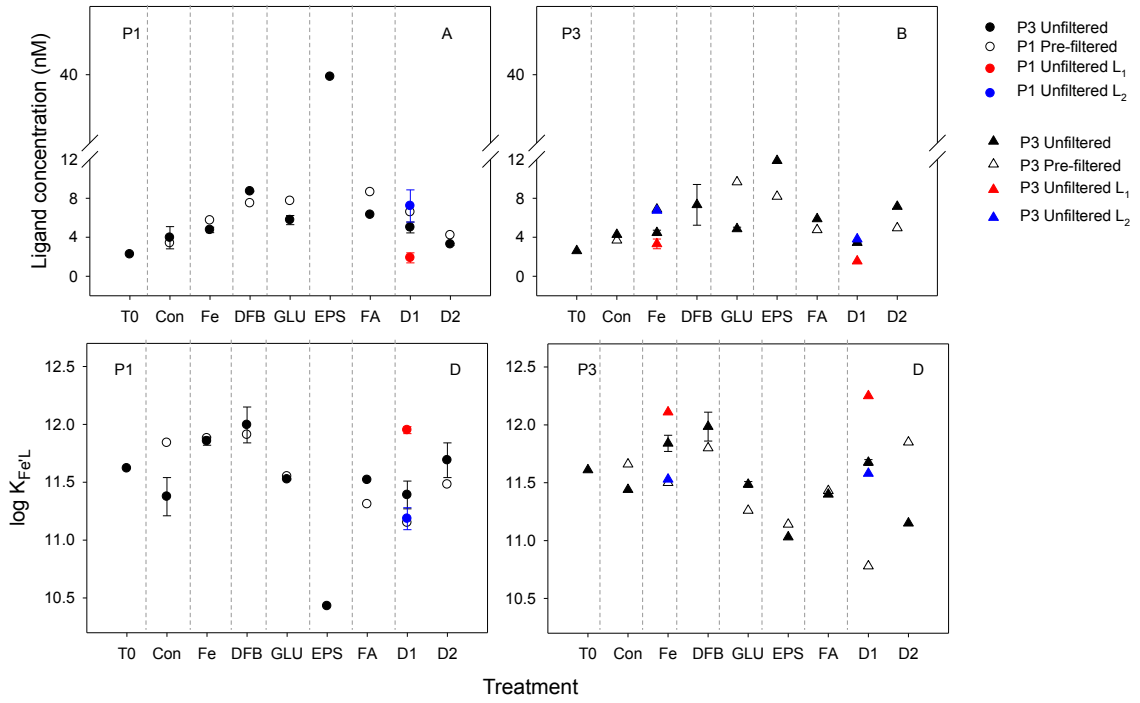

Figure 3.9 Concentration of organic ligands and calculated conditional stability constants (log $K_{Fe'L}$) associated with Fe-enrichment experiments using phytoplankton communities collected from two sites in the Tasman Sea, P1 (30.0 °S, 156.0 °E, panels A and C) and P3 (46.2 °S, 159.5 °E, panels B and D) during the PINTS voyage (RV *Southern Surveyor*, Jan-Feb 2010). The data presented comes from unamended seawater (T0) and after 4-d incubation for samples with and without the addition of Fe and organic ligands. Treatments were as per Fig. 3.8. Closed symbols indicate samples with phytoplankton present, open symbols indicate samples where phytoplankton were absent (0.2-µm filtered, single incubations). Where two ligand classes were detected, stronger ligands are indicated by a red symbol and weaker ligands by a blue. Error bars represent half-interval of duplicate samples; where no error bars are present the data presented is from a single sample.

3.2.2.3 Changes in the concentration of HS-like material

The concentrations of HS-like material in T0 samples from P1 were below half that of site P3 (13.9 ± 1.31 and 38.9 ± 5.79 µg L^{-1} SRFA eq., respectively). After 4-d incubation, the concentration had decreased in the control and control-F samples from both sites, although this change was almost negligible in the P1 control (Fig. 3.10). The FA enrichments from both P1 and P3 contained significantly more HS-like material ($p \leq 0.03$) due to the initial addition of 100 µg L^{-1} SRFA. A loss of HS-like material was measured in both P1 FA and FA-F, however, this was variable between the two unfiltered samples with a loss of > 50% in replicate A, and ~ 10% in replicate B. The concentration of HS-like material did not increase

in any unfiltered enrichment compared to either T0 or control at P1, but all filtered treatments, except for Fe-F were elevated by between 2- and 6-fold from the control-F (Fig. 3.10).

In contrast, at P3, assuming a total concentration of ~ 140 L^{-1} SRFA eq. was present at T0 (unamended T0 + 100 µg addition) in the FA and FA-F incubations, an increase of ~ 20 µg L^{-1} was measured in the FA incubations, whereas a loss of ~ 20 µg L^{-1} was measured in the FA-F incubation (Fig. 3.10). In the unfiltered incubations, only the D1 and EPS differed from the control, both being significantly higher in concentration ($p \leq 0.041$; Fig. 3.10). Similarly to P1, all filtered enrichments, except for Fe-F, had higher concentrations of HS-like material than the control-F, and this was most apparent in the DFB-F, EPS-F, and D2-F incubations (two to three-fold increase; Fig. 3.10).

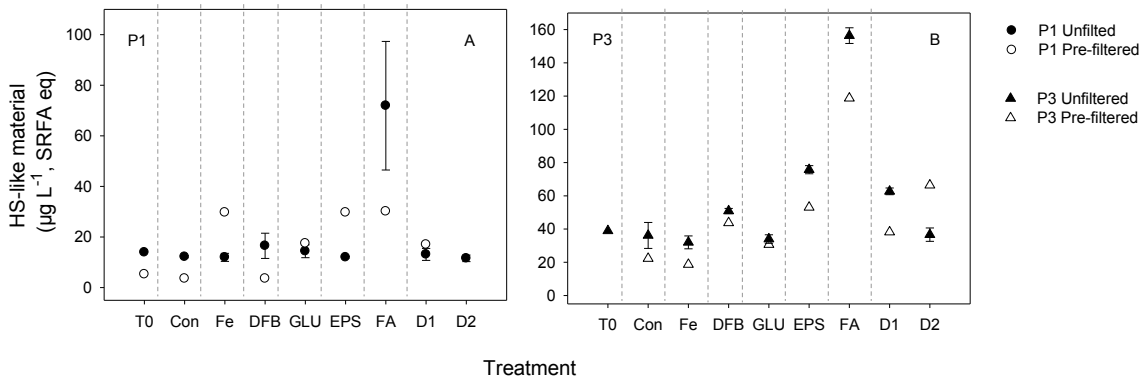

Figure 3.10 Concentration of humic substance-like material (HS-like), expressed as Suwannee River Fulvic Acid equivalents (SRFA eq) in µg L^{-1}, associated with Fe enrichment experiments using phytoplankton communities collected from two sites in the Tasman Sea, P1 (30.0 °S, 156.0 °E, panel A) and P3 (46.2 °S, 159.5 °E, panels B) during the PINTS voyage (RV *Southern Surveyor*, Jan-Feb 2010). The data presented comes from unamended seawater (T0) and after 4-d incubation for samples with and without the addition of Fe and organic ligands. Treatments were as per Fig. 3.8. Closed symbols indicate samples with phytoplankton present, open symbols indicate samples where phytoplankton were absent (0.2-µm filtered, single incubations). Error bars represent half-interval of duplicate samples; where no error bars are present the data presented is from a single sample. Note difference in y-axis scale.

3.2.2.4 Changes in the nature of HS-like material

The peak in the reduction potential (E_p) from the HS-like analysis varied little in both the P1 and P3 samples, except for P1 D1, (lower than control, EPS and GLU, $p \leq 0.048$; Table 3.3), P1 FA (lower than EPS, $p = 0.048$) and P3 DFB (higher than control and D1, $p \leq 0.048$; Table 3.3). Overall, the P1 and P3 peaks in reduction potentials of the unfiltered samples were similar, however, the filtered samples were significantly different from each other ($p = 0.04$; Table 3.3).

The sensitivity (slope) of the HS-like analysis was used to investigate any differences in the nature of the HS-like material in incubations. The T0 sensitivities were quite different at 3.41×10^{-8} and 5.17×10^{-8} μg L^{-1} for P1 and P3, respectively, and these sensitivities increased in both the P1 and P3 control over the incubation period. However, sensitivity decreased in control-F samples for both sites (Table 3.3). In the P1 unfiltered samples, only the EPS and FA incubations varied significantly from the control, with the EPS having a higher sensitivity ($p = 0.031$) and the FA having a lower sensitivity ($p = 0.016$). The FA treatment also had a significantly lower sensitivity than all other enrichments, except for DFB and GLU ($p = \leq 0.047$; Table 3.3). Little variation in sensitivity was found between the filtered samples, except for the Fe-F enrichment which was considerably higher than all other enrichments (Table 3.3). All unfiltered samples had a higher sensitivity than the filtered samples, except for control/control-F, and Fe/Fe-F where the opposite was noted.

Sensitivity in the P3 enrichments did not vary from the control in the P3 samples, but there were some significant differences between enrichments (Table 3.4). Given the similarity in source region of the two dust samples (D1 and D2), variability in both HS-like concentration and sensitivity in the P3 incubations was interesting, particularly as both parameters were similar in the P1 incubations. All sensitivities in the filtered P3 incubations were lower than control-F by between 1.1-fold (Fe-F) and 2.3-fold (EPS-F). There was greater variation between the unfiltered and filtered P3 incubations than was seen in the P1 incubations; with Fe and Fe-F being very similar; control, D1, DFB, and FA all having lower sensitivity than the corresponding filtered sample; and D2, EPS, and GLU all having higher sensitivity than the corresponding filtered sample (table 3.3).

Relationships between HS-like concentration, reduction peak potential, sensitivity, ΣL, Log $K_{Fe'\Sigma L}$, and TChl-*a* concentration were investigated, but only one weak relationship was evident in the filtered P3 samples between reduction peak potential and log $K_{Fe'\Sigma L}$ ($r^2 = 0.37$).

Table 3.3 Instrument sensitivity (expressed as Suwannee River Fulvic Acid equivalents (SRFA eq) in μg L^{-1}) and the reduction peak potential (E_p, V vs Ag/AgCl electrode) from the determination of humic substance-like (HS-like) material from Fe enrichment experiments at T0 (unamended seawater) and after 4-d incubation in samples with and without the addition of organic ligands. Water for the experiments was collected from two sites in the Tasman Sea, P1 (30.0 °S, 156.0 °E) and P3 (46.2 °S, 159.5 °E) during the PINTS voyage (RV *Southern Surveyor*, Jan-Feb 2010). Treatments were as per Table 3.2. Unfiltered = incubations where phytoplankton were present, filtered = incubations where phytoplankton absent (0.2-μm filtered). Errors are the half interval of duplicate samples. Where no errors are stated the values are from a single sample.

	Sensitivity (x 10^{-8} μg L^{-1} SFRA eq.)		**E_p (V vs Ag/AgCl electrode)**	
Treatment	**P1 - Unfiltered**	**P1 - 0.2-μm**	**P1 - Unfiltered**	**P1 - 0.2-μm**
T0	3.41		0.515	
Con	4.23 ± 0.41	5.71	0.523 ± 0.003	0.510
Fe	5.02 ± 0.99	6.65	0.518 ± 0.008	0.505
DFB	4.57 ± 0.10	2.41	0.528 ± 0.008	0.505
GLU	4.19 ± 0.11	3.07	0.523 ± 0.003	0.500
EPS	5.93 ± 0.11	4.80	0.528 ± 0.003	0.505
FA	2.00 ± 0.05	3.22	0.520 ± 0	0.505
D1	5.75 ± 0.48	3.09	0.515 ± 0	0.515
D2	5.89 ± 0.45	3.99	0.523 ± 0.003	0.505
Treatment	**P3 - Unfiltered**	**P3 - 0.2-μm**	**P3 - Unfiltered**	**P3 - 0.2-μm**
T0	4.98		0.510	
Con	6.47 ± 1.12	8.86	0.523 ± 0.003	0.520
Fe	8.32 ± 0.26	8.22	0.525 ± 0.005	0.515
DFB	4.57 ± 1.45	5.79	0.530 ± 0	0.525
GLU	8.84 ± 0.06	4.19	0.523 ± 0.008	0.505
EPS	5.85 ± 0.15	3.79	0.528 ± 0.008	0.510
FA	5.20 ± 0.30	6.37	0.532 ± 0.007	0.525
D1	4.36 ± 0.33	8.01	0.518 ± 0.003	0.510
D2	7.48 ± 0.19	5.02	0.528 ± 0.003	0.515

Table 3.4 Variability in instrument sensitivity between experimental treatments after 4-d incubations in samples with and without the addition of organic ligands. Water for the experiments was collected at process station P3 (46.2 °S, 159.5 °E) in the Tasman Sea during the PINTS voyage (RV *Southern Surveyor*, Jan-Feb 2010). Treatments were as per Table 3.2. Statistically significant differences ($p \leq 0.05$) are highlighted in bold type.

	Con	**Fe**	**DFB**	**GLU**	**EPS**	**FA**	**D1**
Fe	0.125						
DFB	0.203	0.063					
GLU	0.085	0.093	**0.049**				
EPS	0.319	**0.007**	0.235	**0.001**			
FA	0.194	**0.008**	0.354	**0.004**	0.096		
D1	0.106	**0.005**	0.450	**0.003**	**0.026**	0.098	
D2	0.235	0.060	0.092	**0.011**	**0.011**	**0.012**	**0.007**

3.2.2.5 Biological response – TChl-a, F_V/F_M, and biomarker pigments

TChl-*a* decreased in both the P1 and P3 controls compared to T0, by ~60% and ~20%, respectively. F_V/F_M decreased by ~ 10% in the P1 control compared to T0, but did not change in the P3 control (Fig. 3.11A, B and Table 3.1).

A significant increase in TChl-*a* concentration was measured in all P1 enrichments ($P \leq 0.032$), except for FA and D1. However, compared to the addition of inorganic Fe only, DFB, FA and D2 enrichments (Fe + ligand) had significantly lower TChl-*a* concentrations ($p \leq 0.047$; Fig. 3.11A). F_V/F_M significantly decreased in the DFB, GLU, EPS, D1, and D2 enrichments compared to the control ($p \leq 0.020$); whereas, no difference was measured between the control, and the Fe and FA enrichments. No Fe-ligand enrichments showed any significant variation in F_V/F_M from inorganic Fe only (Fig. 3.11B).

For P3, TChl-*a* concentration significantly increased in all enrichments ($p \leq 0.027$), except for DFB. However, when compared to inorganic Fe, the EPS enrichment was the only enrichment with a significantly higher concentration of TChl-*a* ($p = 0.025$; Fig. 3.11A). In contrast to P1, all P3 enrichments, except for DFB, had significantly higher F_V/F_M compared to T0 ($p \leq 0.020$; Fig 3.11B). Only the dust enrichments varied from inorganic Fe, in terms of F_V/F_M, with D1 having a significantly lower F_V/F_M, and D2 a significantly higher F_V/F_M ($p = < 0.001$ and 0.014, respectively; Fig. 3.11B).

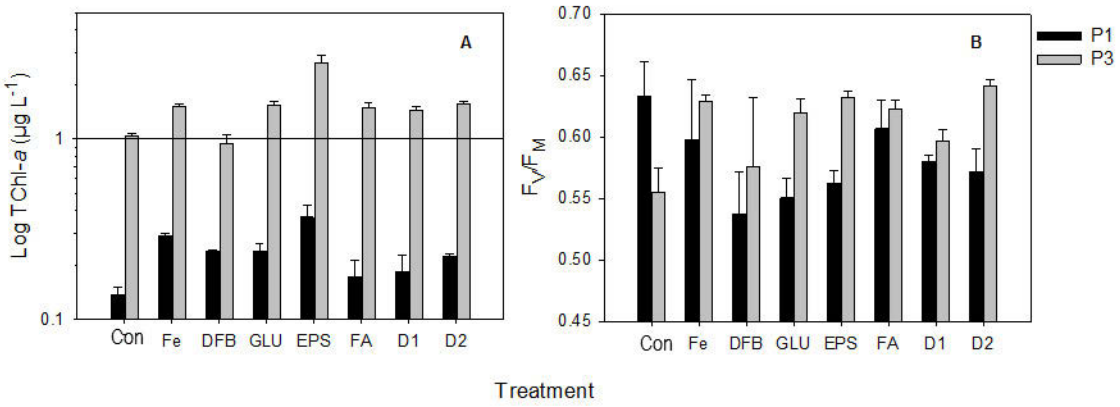

Figure 3.11. Changes in total chlorophyll-*a*, (TChl-*a*) (A) and F_V/F_M (B) from Fe-enrichment experiments after 4-d incubation with and without the addition of organic ligands. Water for the experiments was collected from two sites in the Tasman Sea, P1 (30.0 °S, 156.0 °E) and P3 (46.2 °S, 159.5 °E) during the PINTS voyage (RV *Southern Surveyor*, Jan.-Feb. 2010). Treatments were as per Fig. 3.8 Error bars represent the half interval of duplicate samples. T0 values not shown; see Table 3.1.

TChl-*a* concentrations of size fractionated phytoplankton communities revealed that for P1, although microphytoplankton (> 10 µm) were not detected in the control, all Fe-ligand complexes, except for DFB, significantly enhanced the TChl-*a* in this size fraction ($p \leq 0.032$), particularly in the Fe and EPS enrichments (Fig. 3.12). All enrichments, except for FA and D1, significantly enhanced TChl-*a* in the nanophytoplankton (2–10 µm; $p \leq 0.046$: Fig. 3.12), but TChl-*a* in the picophytoplankton (0.7–2 µm) was enhanced only in the Fe, DFB, EPS and D2 enrichments ($p \leq 0.047$; Fig. 3.12).

For P3, TChl-*a* concentrations were significantly enhanced from the control in nano- and microphytoplankton size fractions in all enrichments ($p \leq 0.036$), except for DFB (Fig. 3.12). The picophytoplankton were significantly enhanced only in the EPS enrichment ($p = 0.017$) compared to the control, and were suppressed by the DFB enrichment ($p = 0.047$).

Compared to the addition of inorganic Fe only, no Fe-ligand complexes significantly enhanced TChl-*a* in any size fraction in the P1 incubations above that of inorganic Fe. At P3, only the EPS enrichment enhanced TChl-*a* in the pico- and microphytoplankton size classes ($p \leq 0.024$), whereas DFB significantly decreased TChl-*a* concentration in the pico- and nanophytoplankton size classes ($p \leq 0.030$; Fig. 3.12).

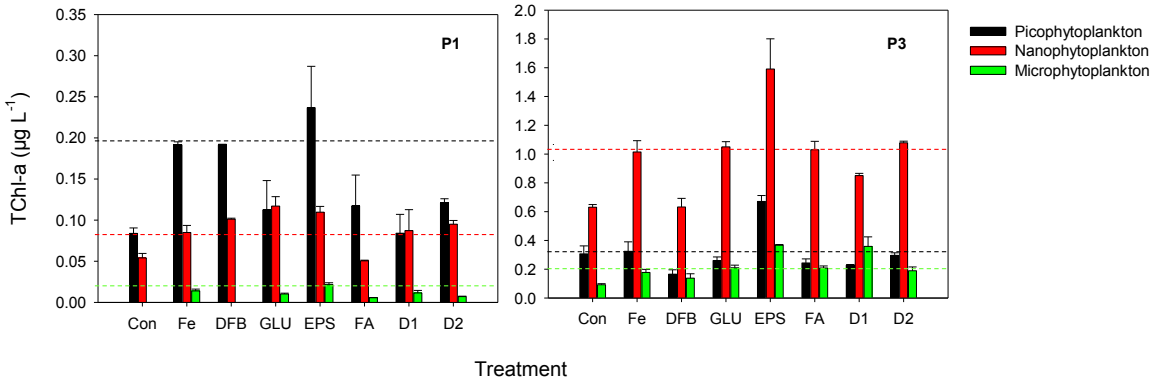

Figure 3.12 Total Chl-*a* concentrations (TChl-*a*) of size fractionated phytoplankton communities from Fe-enrichment experiments after 4-d incubation with and without the addition of organic ligands. Pico-, nano-, microphytoplankton were defined by sequential filtration as > 0.7–2 µm, 2–10 µm, ≥10 µm, respectively. Water for the experiments was collected from two sites in the Tasman Sea, P1 (30.0 °S, 156.0 °E) and P3 (46.2 °S, 159.5 °E) during the PINTS voyage (RV *Southern Surveyor*, Jan-Feb 2010). Treatments were as per Fig. 3.8 Error bars represent the half interval of duplicate samples. Dashed lines represent a comparison of the Fe-ligand complexes with Fe addition only.

Biomarker pigments (normalised to TChl-*a*) were used to identify the dominant phytoplankton groups in each experimental treatment, and to identify any changes in community structure from the original *in situ* phytoplankton communities. The controls indicated quite different initial community structures between the sites P1 and P3. At P1 the community appeared to be dominated by cyanobacteria (Chl-*b* and zeaxanthin), particularly in the picophytoplankton size fraction, with a smaller contribution from haptophytes (hex-fucoxanthin) and diatoms in the nanophytoplankton size fraction (Fig. 3.13). In the P3 control sample, hex-fucoxanthin was the dominant pigment in both the pico- and nanophytoplankton size classes, indicating a proliferation of haptophytes, with a smaller contribution from cyanobacteria (Chl-*b*). Chl-*b* was also measured in the microphytoplankton size fraction; however, this may be an artefact of filtration. Diatoms (fucoxanthin) in both the nanophytoplankton and microphytoplankton size fractions were in greater abundance at P3 compared to P1. Fucoxanthin was also present in the picophytoplankton size fraction, however, diatoms are not expected in this size fraction. Whilst the occurrence of fucoxanthin may be an artefact of filtration, it is also possible that other small fucoxanthin containing eukaryotes (i.e. chrysophytes or some species of prymnesiophyte), were present in the picophytoplankton size class. Dinoflagellates

(peridinin) were also present in the P3 control, mostly in the microphytoplankton size fraction, but were absent in the P1 control (Fig. 3.13).

The main community changes seen for P1 treatments were a suppression of cyanobacteria and prochlorophytes in the picophytoplankton and nanophytoplankton size fraction in D1, indicated by the absence of Chl-*b* and reduced/absent zeaxanthin, but an increase in diatoms in D1(enhanced fucoxanthin), and haptophytes (enhanced hex-fucoxanthin) in D1, D2 and EPS in the nanophytoplankton size fraction. An increase of diatoms in the microphytoplankton size fraction was observed in all enrichments (Fig. 3.13).

For P3, the biggest changes were again observed in the D1 enrichment, with a suppression of cyanobacteria in the picophytoplankton size fraction, and an increase in prasinophytes (enhanced prasinoxanthin) in the nano- and microphytoplankton size fraction (Fig. 3.13). Except for a small number of prasinophytes in the D2 nanoplankton, no other major changes were observed. The biomarker data also indicated that the presence of FA, DFB, and GLU did not change the original community structure for P1 or P3 (data not shown).

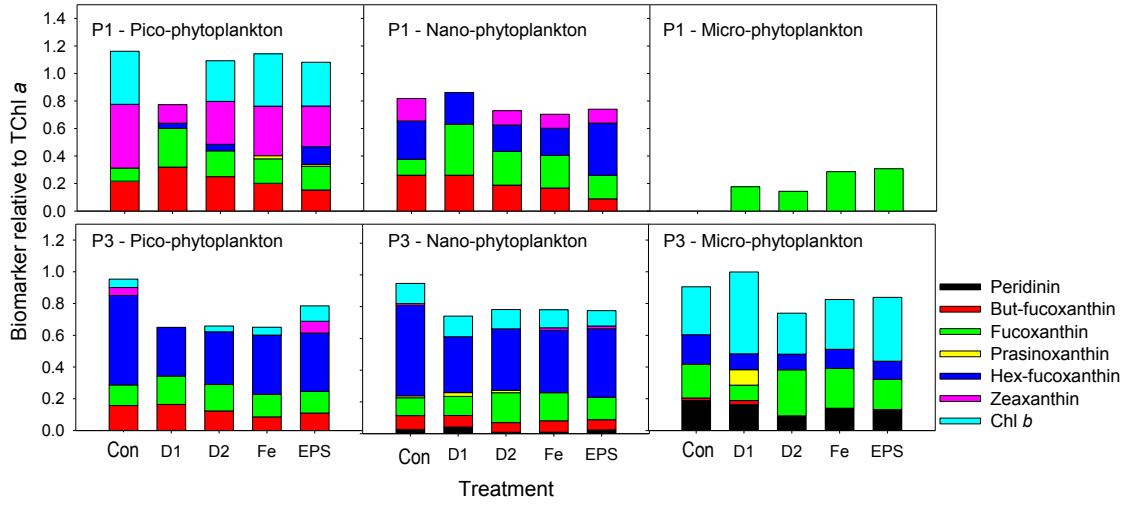

Figure 3.13 Size-fractionated biomarker pigment data (measured by HPLC) from Fe enrichment experiments after 4 d incubation with and without the addition of organic ligands. Pico-, nano-, microphytoplankton were defined by sequential filtration as > 0.7–2 µm, 2–10 µm, ≥10 µm, respectively. Water for the experiments was collected from the depth of the fluorescence maximum at two sites in the Tasman Sea, P1 (30.0 °S, 156.0 °E) and P3 (46.2 °S, 159.5 °E) during the PINTS voyage (RV *Southern Surveyor*, Jan.-Feb. 2010). Treatments were as per Fig. 3.8.

3.3 Discussion

3.3.1 Depth profiles of process stations P1, P3 and Stn 14

The patterns of macronutrient depletion and enrichment throughout the water column at P3 and Stn 14 were generally concomitant with high productivity. At P1, nutrient depletion was not just restricted to the deeper Cmax but also to the surface waters. The extreme depletion of N at P1, together with a high C:N ratio (9:6, as determined in Hassler et al., 2014) indicate that N was the key limiting nutrient at P1. In contrast, the correlation of dFe with all macronutrients (NO_X, PO_4, $Si(OH)_4$) at P3 suggests a more important role of Fe at this site. However, calculations of Fe* (a comparison of dFe and PO_4 concentrations with respect to Fe and P phytoplankton cellular quota) suggest that Fe may have been co-limiting at P1 (Hassler et al., 2014).

Whilst dFe concentration was low across all sites, it was consistent with what has been previously reported in this region (Bowie et al., 2009, 2011; Ellwood et al., 2011; Ibisanmi et al., 2011; Hassler et al., 2012). Generally, the dFe profiles displayed a nutrient-like profile indicative of biological utilisation in the surface waters and regeneration of sinking biogenic particles in deeper waters (Johnson et al., 1997; Vraspir & Butler, 2009; Ibisanmi et.al., 2011).

As previously reported (Rue and Bruland, 1995; Boye et al., 2001, 2005; Frew et al., 2006; Ibisanmi et al., 2011), Fe-binding organic ligands (ΣL) were in excess of dFe throughout the water column, however no relationships between ligand concentration and dFe were apparent, an observation also noted by Ibisanmi et al. (2011). The excess of ligands reported in this study are greater than those previously reported. However, this is likely a result of considering the sum of all ligands present (ΣL) rather than L_1 and L_2 classes separately, because the detection of ΣL, using CLE-AdCSV, is influenced by the L_1 and L_2 ligands detected and also those ligands that are outside of the detection window of the method. There was little variation in the concentration of ΣL throughout the water column, although slightly higher concentrations were measured at, or adjacent to, the Cmax, again as previously reported by Boye et al. (2001) and Ibisanmi et al (2011). Although the ΣL measured in the profiles were higher than those previously measured in the SAZ (Boye et al., 2001; Ibisanmi et al., 2011) they were within the range of reported values measured in open water (See Table 1.1, Chapter 1).

Conditional stability constants (log $K_{Fe'L}$) were also representative of those measured by other groups (log $K_{Fe'L}$ = 11 to 13.5; Rue & Bruland, 1995, 1997; Boye et al., 2001, 2005;

Cullen et al., 2006; Frew et al., 2006; Kondo et al., 2008; Ibisanmi et all, 2011, see also review by Hassler et al., 2012). Unlike Ibisanmi et al. (2011) who measured strong ligands in a number of profiles down to a depth of 200 m, only one profile (Stn 14) contained strong ligands (L_1, $K_{Fe'L} \geq 12$), which were measured close to the Cmax. The occurrence of L_1 ligands is generally attributed to the production of siderophores by the bacterial community, as the $K_{Fe'L}$ of siderophores is generally in the L_1 class, and also because the distribution of L_1 ligands is often consistent with bacterial abundance (Ibisanmi et al., 2011). Bacterial abundance at this site was not known, but the highest TChl-*a* concentrations were measured at Stn 14 and it has been shown that increased bacterial production can be measured in association with high TChl-*a* (i.e. bloom periods; Obernosterer et al., 2008). However, the strong ligands measured might not all have been siderophores, as algal and bacterial exopolymeric substances have been shown to be associated with both L_1 and L_2 ligand classes (Norman et al., in press; Chapter 4 this thesis).

The low concentrations of HS-like material are what might be expected from regions that have little or no terrestrial input. However, the high concentrations measured in the top 50 m of the water column at Stn 14 were considerably elevated compared to P1 and P3. Inputs of atmospheric dust are known to periodically be deposited into this area (Bowie et al., 2009; Mongin et al., 2011; Cropp et al., 2012); however, except for one elevated dFe measurement at 30 m, there appeared to be no suggestion of additional atmospheric Fe at this site. Had this region received atmospheric dust input around the time of sampling it would likely have resulted in elevated dFe concentrations throughout the upper water column (Bowie et al., 2009). Furthermore, depending on the type (mineraliferous or soil-derived) and intensity of the dust supplied to the upper ocean, dust inputs may not contribute significantly to the concentration of HS-like material. Analysis of HS-like material associated with atmospheric dust (Chapter 5 this thesis) demonstrated that at a concentration of 0.5 mg L^{-1} the dust used (D1 from this study) contained < 6 µg L^{-1} SRFA eq. (unfiltered sample). However, HS-like concentration was correlated with TChl-*a* at Stn 14, whereas no correlations were present at P1, P3 or when the data was pooled. This correlation with TChl-*a* is unusual as generally HS-like material in the dissolved phase appears not to be correlated with TChl-*a* (Calace *et al*., 2010; Chapter 2 this thesis). This reported lack of correlation is likely due to the composition of marine humic material which is predominantly degraded organic material rather than fresh production (Andrews et al., 2000). Given that an L_1 class ligand was also measured here, it is possible that the correlation with TChl-*a* was an indirect relationship, and that the degradation of organic material by the microbial community, which can result in an accumulation of refractory

organic material (Hansell et al., 2012), or the effects of photochemical degradation contributed to this relationship.

Overall, few relationships between organic parameters (ΣL, Log $K_{Fe'L}$ and HS-like material) and TChl-*a* existed, and those relationships that were present were not consistent between sites. Organic ligands (excluding HS-like material) were correlated with TChl-*a* at P1 but not at P3 or Stn 14, and HS-like material and ΣL were weakly correlated at Stn 14 only. These inconsistences may be due to a difference in the nature/composition of the ligands present as different phytoplankton and microbial communities were resident at each site and the contribution that each community makes to the ligand or HS pool will vary.

3.3.2 Fe-enrichment experiments

3.3.2.1 Fe biogeochemistry

The higher concentration of dFe in the filtered samples (compared to the unfiltered samples at both P1 and P3) would be primarily due to a reduction in biological consumption, due to the absence of phytoplankton. However, recycling of Fe by small bacteria and protists, which might have been present, may also have made a small contribution to dFe uptake/dynamics. It is also acknowledged that the increased dFe measured in some of the filtered samples, compared to the T0 may be the result of a small amount of contamination.

The greatest uptake of dFe in the unfiltered incubations was seen D1, D2 and EPS enrichments for both P1 and P3 and also the P3 GLU enrichment. This uptake was reflected in the biomass (enhanced TChl-*a*) of D2 and EPS for P1 and all four enrichments for P3. However, a positive TChl-*a* response was also measured in the DFB enrichments at P1, which exhibited a much lower uptake of dFe than the D1, D2 and EPS enrichments. The same significant decrease in dFe was measured in the D1, D2 and EPS filtered samples and so some loss of dFe through adsorptive or aggregation processes cannot be ruled out in the dust and EPS incubations.

Overall, the concentration of ligands (ΣL) increased in all incubations for both the P1 and P3 experiments. The increase in organic ligands in the controls and Fe/Fe-F incubations is evidence that the phytoplankton and microbial communities were producing Fe-binding ligands during the course of the experiments, as previously reported (Rue and Bruland, 1997; Boye et al., 2005; Kondo et al., 2008). Therefore, the increased concentrations measured in the Fe-ligand enrichments would have been a combination of the added ligand and *in situ* production. However, during the 4-d incubation, consumption and destruction

of both the added ligands and those newly produced would also have taken place through processes such as microbial activity and UV photodegradation. It is, therefore, not possible to calculate with certainty the proportion of new, biologically produced ligands present at the conclusion of the experiment in those incubations where organic ligands were added.

The substantial reduction in ligand concentration in the DFB incubations from 15 nM added maybe partially a result of microbial consumption, however DFB not only strongly binds Fe but other metals as well (i.e. Cu). It is, therefore, also likely that not all ligands were measured due to an association with other trace elements. Furthermore, DFB is a hydroxamate siderophore that is photochemically stable when both bound to Fe and free (Barbeau et al., 2003). The measured $K_{Fe'L}$ of 11.8 to 12 is comparable to previous measurements ($K_{Fe''L}$ = 11.8 in UV photo-oxidised seawater, Maldonado et al., 2005; 12.28 in synthetic seawater, Hassler et al., 2013) indicating that photodegradation did not contribute to the loss of DFB.

The dust enrichments were selected as an Fe source rather than an Fe-ligand complex for these experiments. However, whilst one cannot be sure of the origin of the ligands measured, weak ligands associated with D1 have been measured with log $K_{Fe'L}$ of between 10.7 and 11.6 (measured in ligand free synthetic seawater; Chapter 5 this thesis) and are likely to have contributed to the ligands measured.

In natural samples the CLE-AdCSV method does not allow us to distinguish between individual ligands, only between stronger (L_1 = log $K_{Fe'L} \geq 12$; Rue and Bruland, 1995) and weaker (L_2 = log $K_{Fe'L} < 12$) ligands. As with the profiles, the conditional stability constants of the T0 and controls for both P1 and P3 were representative of those found in an open-ocean environment, as were the majority of the enrichment samples for both P1 and P3. The organic ligands used in these experiments, and those produced during the experimental period, clearly reflect the types of compounds that make up the complex matrix of the natural organic ligand pool in seawater (e.g. biological exudates, saccharides, porphyrins).

The stronger ligand classes measured in D1 enrichments for both experiments, and the P3 Fe enrichments had similar conditional stability constants to some bacterial siderophores and porphyrin (cell-lysis products) complexes (log $K_{Fe'L}$ 11.6 to 12.4: Rue and Bruland, 1995; Witter et al., 2000) and also the strong ligands measured in association with algal and bacterial EPS (log $K_{Fe'L}$ 11.87 to 12.12, Chapter 5 this thesis). Interestingly, these stronger ligands were not measured in the D2 incubations in either P1 or P3. The decrease in dFe associated with D2 was higher than that of D1 for both P1 and P3, and so the variation in organic ligands may reflect a different biological response, or ease of acquisition, of the Fe

associated with D2 compared to D1, or a greater loss through adsorption. Furthermore, despite the similar source region of D1 and D2 they may have differed in mineralogy which can vary in Fe content and reactivity, and thus solubility and potentially bioavailability (McTainsh et al., 1990; Duce et al., 1991; Visser et al., 2003; Mackie et al., 2008). Unfortunately mineralogy data was not available for the two dusts and so it is not possible to comment on any differences between them.

3.3.2.2 HS-like material

HS-like material and the organic ligands used in these experiments, like much of the DOM pool, can be a vital source of organic C that can support considerable heterotrophic production (Amon and Benner, 1994, 1996; Moran and Hodson, 1994; Obernosterer et al., 2008). The low light levels and reduced or absent UV irradiation, due to the use of polycarbonate bottles, indicates that the removal of HS-like material from the P1 and P3 control, control-F, FA-F, and P1 FA, was predominantly due to microbial consumption. Whilst the filtered samples would have contained viruses and small bacteria, a large proportion of the microbial community would have been removed via 0.2-µm filtration. Thus, the accumulation of HS-like material in most filtered samples supports the notion of dominant microbial removal in the unfiltered samples.

The elevated HS-like concentrations in the P3 D1 may, in part, be due to increased terrestrially derived HS from the dust. However, HS-like concentrations were also elevated in the P3 EPS samples. It is possible that the EPS was detected as part of the HS-like pool as the analytical technique used is not specific to HS but may also detect other Fe-binding components of the dissolved organic matter pool. For instance, EPS and lignin have been found to contribute to the HS-like signature, whereas DFB, GLU, dextran, protoporphyrin IX, cytochrome C and amino acids cysteine and alanine do not (C. Hassler, pers. comm.).

As described in Chapter 2, the sensitivity (slope of the standard addition) may give some insight as to the nature/origin of the HS-like material. In this study no significant relationships between sensitivity, TChl-*a*, ΣL or log $K_{Fe'sumL}$ were found. Whilst the variability observed may indicate that the origin of the HS-like material affects sensitivity, it is not clearly defined in these experiments. This is possibly due to the complex matrix of added ligands, together with the *in situ* production and consumption of HS-like material by the phytoplankton and microbial communities that occurred during the 4-d incubation. A further laboratory study that measures HS-like material in a range of organic Fe-binding

ligands, using synthetic seawater devoid of organic material rather than natural seawater, may help to establish if sensitivity is a useful tools to determine HS-like origin.

Although HS-like substances, ligand concentration, and log $K_{Fe'L}$ are clearly associated with biological activity no relationships between these parameters and TChl-*a* were evident. As mentioned above, this disconnection between producers (as measured by the biomass proxy of TChl-*a*) and HS-like material is to be expected, as HS-like material is an evolved product which has been subjected to degradation/maturation (Andrews *et al*, 2000). Additionally, the input of organic ligands from the microbial community (e.g. siderophores) together with the additional ligands from the enrichments may also weaken any relationship between the ligand pool and TChl-*a*.

3.3.2.3 Effect of Fe-ligand enrichment on phytoplankton growth

The decrease in TChl-*a* and F_V/F_M in the P1 control from the T0 suggests that nutrient consumption during the 4-d incubation induced nutrient limitation at this site. The addition of Fe, regardless of source, did not increase the F_V/F_M in the P1 experimental samples indicating that, as inferred from the profiles and suggested by Hassler et al (2014), Fe was not the main factor limiting factor affecting phytoplankton growth at this site and that N limitation was a major contributor. In contrast, the enhanced TChl-*a* and F_V/F_M in all P3 enrichments, except for DFB, suggest that the phytoplankton community here could have been mildly Fe-limited (Hassler et al., 2014). In addition, results from C fixation experiments, (Hassler et al., 2014) demonstrated that, despite the shallower Chl-*a* maximum at P3, *in situ* C fixation was limited by low light intensity (13 μmol photons m^{-2} s^{-1} at 25 m). It is worth noting that the use of F_V/F_M as a measure of cell health should be treated with some caution as a) cyanobacteria can decrease the F_V/F_M signal in the instrument used during these experiments (water PAM) due to their different light absorption properties compared to eukaryotes, and b) whilst F_V/F_M is a reasonable indicator for Fe-limitation it is not sensitive to the co-limitation of N and Fe (Behrenfeld and Milligan, 2013; Hassler et al., 2014).

Different phytoplankton species have varying Fe requirements for growth, and often different size classes do not respond in the same way to Fe addition (Sunda and Huntsman, 1995; Wilhelm, 1995; Hassler et al, 2011a). When the TChl-*a* from these experiments was split into the three phytoplankton size fractions, such variable responses were evident. Only Fe delivered with the bacterial EPS, for all phytoplankton classes, enhanced TChl-*a* above the control and inorganic Fe. However, here too, the size fraction that benefited most from

the Fe bound to EPS was different for P1 (picophytoplankton) compared to P3 (nanophytoplankton). This is interesting, as it has been shown that many phytoplankton are unable to utilise Fe bound to bacterial siderophores (Hassler and Schoemann, 2009; Buck et al., 2010); whereas, this study indicates that Fe bound to bacterial EPS is accessible to a wide range of phytoplankton species. In addition, EPS has been shown to be associated with a range of macronutrients and trace elements, including N, P, Zn and Co (Norman et al, in press; Chapter 4 this thesis), which are essential for phytoplankton growth. The elevated growth observed in these experiments may therefore not only be due to Fe enrichment, but also the enrichment of co-limiting nutrients (Hassler, Norman et al., in press).

The addition of Fe, in both mesocosm and large-scale Fe fertilisation experiments, has previously been shown to stimulate phytoplankton blooms and initiate community shifts (Buma et al., 1991, Price et al., 1994; Coale et al., 1996; Boyd et al., 2000; de Baar et al., 2005). However, during the PINTS experiments whilst all Fe-ligand complexes, except for P3 DFB, enhanced phytoplankton growth in terms of TChl-*a* (relative to the controls), not all Fe-ligand complexes affected community structure. Whilst diatoms benefited from the Fe, D2 and EPS enrichments, Fe associated with the dust from the Brisbane dust storm (D1) initiated the largest community shift. Not only was diatom growth enhanced, but cyanobacteria were suppressed at both P1 and P3.

This group or species-specific response has been previously reported. Diatoms, for example, are often seen to benefit from Fe addition (Buma et al., 1991, Price et al., 1994; Boyd et al., 2000, 2007), but there is evidence that not all organically bound Fe is available to all species of bacterio- and phytoplankton. Studies of laboratory cultured and natural assemblages indicate that prokaryotic and eukaryotic phytoplankton use different organically complexed Fe sources (Hutchins et al. 1999). Hutchins et al (1999) demonstrated that Fe complexed by porphyrin was poorly available to prokaryotes (cyanobacteria); whereas, this type of Fe was accessed much more efficiently by eukaryotes. In contrast, siderophore-(DFB)-bound Fe was more available to prokaryotes than eukaryotes (Hutchins et al., 1999), and in some cases, as was observed for the P3 incubations here, suppressed the growth of eukaryotic phytoplankton (diatoms in natural bloom, Wells et al., 2009; *Phaeocystis* sp., *Chaetoceros* sp., *Thalassiosira antarctica, Fragilariopsis kerguelensis*, Hassler and Schoemann, 2009; natural community, Hassler et al., 2011b).

However, this is not by any means the rule, because some eukaryotes have been shown to utilise Fe-DFB complexes relatively efficiently (*Phaeodactylum tricornutum*, Soria-Dengg and Horstmann, 1995; *Thalassiosira oceanica*, Soria-Dengg et al., 2001; Maldonado and

Price, 1999, 2001; Maldonado et al., 2005), and catecholate siderophores may be more bioavailable to eukaryotes than hydroxamate siderophores, such as DFB (Hutchins et al., 1999; Maldonado et al., 2005, Hassler and Schoemann, 2009). There is also a suggestion that Fe bound to DFB may vary in its bioavailability depending on the physiological state of the phytoplankton i.e. bloom-forming or bloom decline (Soria-Dengg and Horstmann, 1995; Kondo et al., 2013). This variable bioavailability of Fe complexes has also been reported for Fe bound to humic material. Kuma et al. (1999) reported enhanced bioavailability of Fe bound to FA to the diatom *Chaetoceros sociale,* which they suggest was due to rapid dissociation of 'weak' complexes. However, Imai et al (1999) reported that the growth of the cyanobacterium *Microcystis aeruginosa* was limited by Fe complexed with FA, despite the production of hydroxamate siderophores.

Clearly the bioavailability of Fe is complex and cannot be attributed to a single factor. Cell size, Fe biological requirement, bacterio- and phytoplankton uptake strategies, Fe speciation and the mode of supply all play interconnected roles.

3.4 Conclusion

The result from the natural profiles shows that organic Fe-binding ligands are present in excess of dFe throughout the water column. The presence of these ligands increases the solubility of dFe (Kuma et al., 1996; Lui and Millero, 2003., Chen et al., 2004; Norman et al., in press); not only potentially making it more available for biological uptake in the euphotic zone, but also increasing Fe availability in areas of upwelling (Ibisanmi et al., 2011). Although little correlation between ligand concentration and TChl-*a* exists, higher concentrations of ligands are measured close to the Cmax, where dFe concentrations are often at their lowest. Thus, the higher concentrations are likely evidence of the production of organic ligands by bacterio- and phytoplankton in response to low Fe concentrations, as reported for siderophore production (Whitfield, 2001; Barbeau et al., 2003; Gledhill et al., 2004).

The experiments from this study demonstrate not only the differing Fe requirements of phytoplankton, but also reinforce the fact that the bioavailability of the various Fe species and sources differ between size fractions and from one bacterio- or phytoplankton species to another. The range of organic ligands selected (biologically produced/excreted saccharides, siderophores (DFB), NOM) represent significant sources of ligands to the Tasman Sea. However, the Fe bound to the bacterial EPS or Fe delivered with dust from the

Brisbane dust storm (D1) made the biggest impact on both phytoplankton communities, in terms of ligand production, biological growth and community structure. The Tasman Sea and SAZ receive periodic inputs of dust-borne Fe (Hesse, 1994; Hesse and McTainsh, 2003; Mackie et al., 2008; Gabric et al., 2010; Cropp et al, 2013), the frequency and intensity of which may be increasing (Hobday et al., 2008; Mitchell et al., 2010). Under these conditions, changes in phytoplankton community structure may become longer lasting or permanent, which may have implications for nutrient and C cycling depending on the species or group that dominate (Boyd and Newton, 1999; DiTullio et al., 2000; Moore et al., 2002; Veldhuis and De Baar, 2005; Hassler et al., 2014).

The original *in situ* community, chemical species of Fe (inorganic or organically bound FeIII), and Fe source are important factors to consider for the prediction of the impact of Fe. Identification of which of the many species and forms of Fe can be utilised by phytoplankton is, therefore, of great importance to our understanding of how Fe controls phytoplankton, and in turn ecosystem functioning.

CHAPTER 4:

THE ROLE OF BACTERIAL AND ALGAL EXOPOLYMERIC SUBSTANCES IN IRON CHEMISTRY AND BIOAVAILABILITY

Note and acknowledgements

The Fe chemistry data presented in this chapter has been accepted (in press) for publication to Marine Chemistry. The manuscript is titled 'The role of bacterial and algal exopolymeric substances in iron chemistry, and authors are; Louiza Norman, Isabelle A. M. Worms, Emilie Angles, Andrew R. Bowie, Carol Mancuso Nichols, A. Ninh Pham, Vera I. Slaveykova, Ashley T. Townsend, T. David Waite, and Christel S. Hassler .

A companion manuscript presenting the bioavailability aspect of this work has been accepted (in press) for publication in Marine Chemistry. The manuscript is titled 'Exopolymeric substances can relieve iron limitation in oceanic phytoplankton' and authors are; Christel S. Hassler, Louiza Norman, Carol A. Mancuso Nichols, Lesley A. Clementson, Charlotte Robinson, Véronique Schoemann, Roslyn J. Watson, Martina A. Doblin.

All Fe chemical and biological data is presented in this chapter. Analyses that I carried out myself were Fe chemical speciation, Fe-binding humic substance-like (HS-like) material, macronutrients, and total hydrolysable saccharides, conducted at UTS, and Fe redox work carried out at UNSW in the laboratory of Prof. T. David Waite under the supervision of Dr An Ninh Pham. I also assisted Prof. Christel Hassler with the analysis of Fe size fractionation, Fe solubility, bioavailability and phytoplankton growth experiments. I am grateful to the following colleagues for analysis, data, and methodologies as detailed below.

Dr Carol Mancuso Nichols (CSIRO, Hobart) and Emilie Angles – Isolation and characterisation of EPS

Prof Vera Slaveykova and Dr Isabelle Worms (Uni. Of Geneva) – Size and molar mass distribution.

Dr Andrew Bowie and Dr Ashley Townsend (Uni. of Tasmania) – Trace element analysis

Charlotte Robinson (UTS) – F_V/F_M

4.0 Introduction

The parameters that control Fe bioavailability to phytoplankton (i.e. the fraction of Fe that is accessible and can be utilised for growth) is not well understood, but is strongly influenced by the physical and chemical forms of Fe, its biogeochemical cycling, and the various Fe requirements and uptake strategies of bacterio- and phytoplankton communities (Wells et al., 1995; Sunda & Huntsman, 1998; Hutchins et al., 1999; Barbeau et al., 2001; Maldonado et al., 2005; Strzepek et al., 2005; Worms et al., 2006).

The chemistry of Fe in seawater and its relationship with the biology of surface water is extremely complex and dynamic. Inorganic Fe(III) is highly insoluble in seawater (Sunda & Huntsman, 1998) and rapidly hydrolyses to form colloidal and particulate Fe oxyhydroxides (Kuma et al., 1998; Liu & Millero, 2002). In large areas of the oceans, dissolved Fe concentrations (dFe <0.2-µm; present as soluble, < 0.02-µm, and colloidal, 0.02 to 0.2-µm, fractions; Gledhill and Buck, 2012) in surface waters are extremely low, often < 1 nM (de Baar & de Jong, 2001), and in regions such as the Southern Ocean dFe concentrations at sub-nanomolar levels are often measured (Boye et al, 2001, de Jong et al, 2008; Lannuzel et al., 2008). However, the reported concentrations, although very low, are often higher than the solubility of Fe in surface waters (which is as low as 0.01 nM, at pH 8.1, 25 °C; Liu and Millero, 2002). It is now well accepted that the reason for this disparity is that almost all of the dFe (> 99%) present in the oceans is bound to organic ligands (Gledhill & van den Berg, 1994; Rue & Bruland, 1995; Hunter and Boyd, 2007), which increases Fe solubility and retards hydrolysis and precipitation (Kuma et al., 1996, 1998; Liu and Millero, 2002; Chen et al., 2004; Hunter and Boyd, 2007; Boyd and Ellwood, 2010) potentially enhancing retention time in surface waters (Tagliabue et al., 2009). Organic complexation also influences the redox speciation of Fe in seawater (Rijkenberg et al., 2006). Not only can organic complexation slow oxidation kinetics (Millero et al., 1987; Santana-Casiano et al., 2000; Croot et al., 2001; Roy et al., 2008), but it can also mediate direct photoreduction of Fe(III)-organic ligand complexes (Barbeau et al., 2001, 2003), or the photoreductive dissolution of colloidal Fe (Waite & Morel, 1984, Waite et al., 1986). There are a great variety of Fe-binding organic ligands (Hunter and Boyd, 2010), each potentially possessing varying chemical labilities and susceptibility to photochemical transformation (Amin et al, 2009; Gledhill and Buck, 2012 and refs therein).

The fact that most of the dFe is complexed with organic ligands suggests that this could be the main factor regulating oceanic Fe reactivity and bioavailability (Hassler et al., 2011a). Currently, the organic ligand pool is poorly characterised. Detection using electrochemical

methods (competitive ligand exchange- adsorptive cathodic stripping voltammetry, CLE-AdCSV) allows us only to distinguish two discrete organic ligand classes, defined as L_1 and L_2, based on their relative binding affinities with Fe (Hunter and Boyd, 2007). L_1 class ligands characteristically have a high affinity (strong binding capacity, $K_{Fe'L} \geq 10^{12}$) for Fe, whereas L_2 class ligands have a weaker binding capacity (Rue & Bruland, 1995 &1997; $K_{Fe'L} \geq 10^{8.8}$, Croot & Johansson, 2000). The CLE-AdCSV method has its limitations; ligands that are too weak to be detected are not measured (Croot & Johansson, 2000), and their contribution to iron biogeochemistry is likely to be underestimated or overlooked (Hassler et al., 2011a).

In open-ocean systems, organic ligands are generally found to be present at concentrations in excess of that of dFe in the water column (Gledhill and Buck, 2012), both as soluble and colloidal forms (Boye et al., 2010). Most are biologically produced, by bacteria and phytoplankton, *in situ* (Hassler and Schoemann, 2009); for example, bacterially produced siderophores which have been widely studied for Fe binding (Hutchins et al., 1999; Maldonado and Price, 1999; Barbeau et al., 2001, 2003; Maldonado et al., 2005; Mawji et al., 2008, 2011; Amin et al., 2009; Hassler & Schoemann, 2009). A comparison of conditional stability constants suggests that siderophores form part of the L_1 class of ligands (Wilhelm and Trick, 1994; Gledhill et al., 2004; Mawji et al., 2008, 2011). Other types of ligands such as intracellular compounds present in phytoplankton (for example, heme (Gledhill and Buck, 2012) and ferritin (Marchetti et al., 2009)) are also considered to be part of the L_2 class of ligands.

More recently, interest has been growing in the role of saccharides in Fe complexation (Steigenberger et al., 2010; Hassler et al, 2011a, b). In surface waters, biologically produced saccharides make up a significant bioreactive component of the marine dissolved and colloidal organic matter pool (Benner et al., 1992; Benner and Pakulski, 1994; Benner, 2011) and are present in nanomolar to micromolar concentrations (Panagiotopoulos and Sempéré, 2005), unlike siderophores which are reported in picomolar concentrations (Gledhill et al, 2004; Mawji et al, 2008, Velasquez et al., 2011). Although the measured conditional stability constant of saccharides is weaker than that of siderophores, their abundance suggests that they have the potential to outcompete the L_1 ligands for iron binding, which is an important consideration with regard to Fe bioavailability (Rue and Bruland, 2001; Hassler at al., 2011a).

Another group of as yet poorly studied organic ligands are exopolymeric substances (EPS) which are non-uniform, polyfunctional macromolecules containing functional groups, such

as uronic acids, neutral sugars, mono- and polysaccharides, amino acids, and proteins (Verdugo et al., 2004, Mancuso Nichols et al., 2005, Hassler et al., 2011a, b). EPS are produced by both bacteria and algae for a variety of functions, including cryoprotection, halotolerance, chains or colony formation, and substrate attachment (Decho, 1990; Hoagland et al., 1993; Aluwihare and Repeta, 1999). The many ecological roles fulfilled by EPS suggest that these substances are likely to be present in surface waters in high concentrations (Hassler et al 2011a). Aggregated EPS also forms a substantial part of both marine transparent exoploymeric substances and marine snow, and occur mainly as colloidal organic matter (Verdungo et al., 2004; Hassler et al., 2011a). Laboratory experiments have shown that Fe bound to bacterial EPS, uronic acids and other polysaccharides (e.g. dextran) can be highly bioavailable to eukaryotic phytoplankton from the Southern Ocean (Hassler and Schoemann, 2009, Hassler et al., 2011a, b). To date, little work has investigated the role of algal EPS. In addition, EPS remain poorly characterised in terms of their effect on Fe chemistry. While several studies have gone some way to chemically analyse bacterial and algal exudates (Nanninga et al., 1996; Aluwihare et al 1999; Mancuso Nichols et al., 2004, 2005) and investigate their role in Fe bioavailability (Steigenberger et al., 2010; Hassler et al., 2011b), few have examined the effect of natural bacterio- and phytoplankton EPS on Fe chemistry.

The aim of this study was to investigate how bacterial and algal EPS affect Fe chemistry, in terms of Fe solubility, the nature of their Fe-binding properties and redox chemistry. Characterisation of the isolated EPS was also identified in terms of functional composition, macronutrient concentration, elemental composition, and contribution of electrochemically detected humic substance-like (HS-like) material. In addition, laboratory experiments were also carried out to investigate how each EPS might affect the bioavailability of Fe to an Fe-limited Southern Ocean diatom *Chaetoceros simplex.* For this study, we used four EPS isolates purified from; 1) sea ice bacteria of the genus *Pseudoalteromonas* (Mancuso Nichols et al., 2004); 2) a mixed bacterial and phytoplanktonic community from surface waters of the Sub-Antarctic Zone (SAZ bloom); 3) an axenic laboratory culture of the haptophyte *Phaeocystis antarctica*; and 4) an axenic laboratory culture of the cocolithophorid *Emiliania huxleyi*. *P. antarctica* and *E. huxleyi* were selected as both are major bloom forming species in the Southern Ocean which contribute to oceanic carbon export (Di Tullio et al., 2000). Both species have also been shown to produce exudates in response to Fe addition that are rich in polysaccharides (Aluwihare et al., 1999, Boye et al., 2000).

4.1 Materials and methods

4.1.1 Isolation and characterisation of bacterial and algal EPS

4.1.1.1 Growth of bacterial culture and EPS Isolation

The bacterium *Pseudoalteromonas sp.* (strain CAM025) was isolated from Antarctic sea ice and phenotypically characterised as described in Mancuso Nichols et al. (2005). Growth of the isolated bacterium and subsequent isolation of the EPS was conducted as described in Hassler at al. (2011b).

4.1.1.2 Growth of phytoplankton cultures

For the isolation of phytoplanktonic EPS, *Phaeocystis antarctica* (CS 243, Prydz Bay, Antarctica) and *Emiliania huxleyi* (CS 812, Mercury Passage, Tasmania, Australia) were obtained from the Australian National Algal Culture Collection. Cultures were maintained in 0.2-µm filtered seawater collected in the Sub-Antarctic Zone (SAZ-Sense voyage, RV Aurora Australis, 153 01 °E 45 03 °S, 11th Feb. 2007) to which micronutrients (Fe, Zn, Co = 5 nM, Cu and Ni = 2 nM, Se = 1nM), macronutrients (NOx = 30 µM, PO_4 = 2 µM, Si = 30 µM; stripped of trace metals by Chelex 100 extraction) and vitamins (as per media F/20) were added. The cultures were then maintained under appropriate light and temperature conditions for the species selected (*P. antarctica* 2.5 °C under 55 µmoles photons m^{-2} s^{-1}; *E. huxleyi* 20 °C under 150 µmoles photons m^{-2} s^{-1}), and both cultures were exposed to a 12 h: 12 h light: dark cycle. The cultures were grown for ten days until the cells reached stationary growth phase, after which they were filtered under laminar flow using GF/C or precombusted GF/934-AH glass fibre filters (Whatman, 1.2 to 1.5-µm) pre-rinsed with 0.5 M quartz-distilled HCl (Seastar) and Milli-Q™ water. The use of glass fiber filters assisted with the breaking up of *P. antarctica* colonies, whilst leaving the cells intact, and allowed for a greater quantity of EPS to be collected. As such, the isolated EPS contained both exuded EPS and that associated with the mucus from the colony. Filters were stored at – 20°C for further fatty acid analysis to check for bacterial contamination and POC analysis.The filtrate was collected into an acid-cleaned carboy and stored at 4 °C in the dark until ultrafiltration. Sodium azide (4 g, Sigma) was added to the filtrate to prevent bacterial growth.

The natural phytoplankton community (SAZ bloom) was sampled at the depth of the fluorescence maximum in the sub-Antarctic Zone (46.2 °S, 159.5 °E, PINTS voyage, SS01-

2010, RV *Southern Surveyor*, Jan–Feb. 2010; Hassler et al., 2014). Seawater was sampled using non-contaminating procedures as per GEOTRACES recommendation using a Teflon double diaphragm pump (Wilden A100 with Teflon fittings; Kelair Pumps Australia Pty Ltd, Arndell Park, NSW, Australia) and acid-cleaned PE tubing, which delivered water directly to the clean room container under a laminar HEPA filter (ISO Class 5). The sampling hose was rinsed prior to collection by running water from the sampling depth for approximately 30 min, after which the water was passed through an acid-washed, 0.2-µm filter cartridge (Acropak 100, PALL, 0.2-µm with 0.8-µm pre-filter) and collected in acid-washed polycarbonate carboys under a HEPA filter (ISO Class 5 conditions). The filtered seawater was then stored at 4 °C in the dark for five days prior to addition of sodium azide followed by ultrafiltration.

4.1.1.3 Isolation of EPS from cultured phytoplankton and natural seawater

The ultrafiltration system used to isolate the EPS (Labscale TFF system, 10-kDa MWCO PES membrane (Pellicon R XL 50 Cassette, Millipore) was prepared by rinsing with 0.1 M HCl for 3-h and then with Milli-Q™ water until the pH of the permeate was that of Milli-Q™. Phytoplankton culture filtrates and seawater were diafiltered against Milli-Q™ water until the conductivity was no more than five times that of Milli-Q™. The retentate was then concentrated to 100-mL, frozen and freeze dried prior to weighing. The EPS yield was between 4.9 and 5.8 fg EPS per cell for both *P. antarctica* and *E. huxleyi*.

4.1.2 Analytical procedures

4.1.2.1 Crude chemical composition of EPS

A crude chemical composition of the EPS was determined as per Mancuso Nichols et al. (2005). Briefly, the EPS were dissolved in Milli-Q™ water (1 mg mL^{-1}) for use in subsequent colorimetric assays. Uronic acid content of the EPS was determined by the meta-hydroxydiphenyl method, using D-glucuronic acid (Sigma) as a standard. Protein content was determined by the bicinchoninic acid (BCA) protein assay, using bovine serum albumin as the standard (Sigma). Total neutral carbohydrate content was determined by the orcinol-sulfuric acid method, using D-glucose (Sigma) as a standard. The detection limits of the methods used were 25 mg glucuronic acid eq. L^{-1}, 100 mg protein L^{-1}, and 100 mg glucose eq. L^{-1}, respectively.

4.1.2.2 Physico-chemical characterisation of EPS

Physico-chemical characterisation of the bacterial and algal EPS was conducted at the department of Environmental Biogeochemistry and Ecotoxicology at the University of Geneva, using asymmetrical flow field-flow fractionation (AFIFFF; AF2000 Focus, Postnova Analytics GmbH, Landsberg am Lech, Germany) coupled with a diode array detector (UV), a fluorescence detector (Fluo), refractive index detector (RI) and inductively coupled plasma – mass spectrometry detector (ICP-MS, Agilent, 7700x; Agilent Technologies (Schweiz) AG, Basal, Switzerland). System control as well as data collection for RI was performed using the AFIFFF2000 Control software (version 1.1.011, Postnova Analytics). For UV and Fluo, the LC solution workstation software (Shimadzu, UK) was used for control and data collection. The EPS samples were resuspended in Milli-Q™ water to attain a concentration of 0.3 mg L^{-1}, and were then passed through 0.45-µm filters (syringe filters, Millopore) prior to injection into the system via a 1-mL sample loop. Trapezoidal channels of 350-µm thickness with 10-kDa cut-off, regenerated cellulose membrane (RC, Postnova Analytics) were utilised and a carrier solution of 100 mM NH_4NO_3 was used (Fluka, pH = 6, pre-filtered through 0.1-µm Teflon filters (Postnova analytics). Injection (focusing time = 10-min; inlet flow rate of 0.2-mL min^{-1}; focus flow rate (V_{foc}) of 3.88-mL min^{-1}; cross flow rate (V_{xf}) of 3.08-mL min^{-1}; outlet flow rate (V_{out}) of 1 mL min^{-1}) and a 1-min transition time always preceded a 40-min elution step. Here, two different procedures were used; one consisted of a linear cross flow gradient starting from 3-mL min^{-1} and ending at 0-mL min^{-1} while the second consisted of a constant cross flow of 0.2-mL min^{-1}. Each run was finished by a washing step of 10-min where no cross flow was applied (V_{xf} =0 mL min^{-1}; V_{out}= 1 mL min^{-1}).

The ^{56}Fe signal was obtained using ICP-MS (Agilent 7700x, He collision cell) connected to the AfIFFF outflow using a two channeled peristaltic pump, the first channel carrying the sample and the second an internal standard of Rh 1ppb in 4% HNO_3 (Backer suprapur). The two channels were connected to a mixing chamber before sample introduction into the ICP nebulizer.

For gradient V_{xf}, EPS molar masses (M_W) were calculated from a calibration curve of the log retention time vs log M_W (Reszat and Hendry, 2005) using 1-mL of 5 mg L^{-1} polystyrenesulfonates standards injections (PSS, Postnova Analytics; M_W ranging from 1.36- to 979-kDa). Molar mass dispersity ($Đ_M$), a measure of the spread of the molar mass distribution in a sample was also derived (Stepto, 2009);

$$Đ_M = Mw/Mn \qquad (1)$$

where *Mw* is the weight-average molar mass and *Mn* the number average molar mass. In addition, the molar mass at maximum peak intensity (*Mp*) was measured.

For comparison and discussion, the EPS colloidal distribution using this protocol was arbitrarily separated into three main pools of molar mass: 1) low molar mass components (LMM) from 0- to 300-kDa; 2) intermediate molar mass components (IMM, from 300- to 800-kDa); 3) high molar mass components (HMM) from 800- to 945-kDa plus any colloids > 945-kDa eluted rapidly once the cross flow was stopped.

For Vx = 0.2-mL. min^{-1}, colloids hydrodynamic radii (R_h) were evaluated using the elution theory as developed by Schimpf and co-authors (2000).

4.1.2.3 Trace element analysis

Trace element concentrations (Al, Cd, Co, Cu, Fe, Mn, Pb, Zn,) in EPS solutions (EPS in ultra-pure water) were determined using Sector Field Inductively Coupled Plasma Mass Spectrometry (Thermo Fisher ELEMENT 2, Bremen, Germany) at the Central Science Laboratory at the University of Tasmania. Measurements were made using both low resolution (nominally m/dm ~400, for ^{111}Cd, ^{208}Pb) and medium resolution (nominally m/dm > 4000; ^{27}Al, ^{55}Mn, ^{56}Fe, ^{59}Co, ^{63}Cu, ^{66}Zn). The use of increased spectral resolution allowed for essentially interference-free analysis. Potential sample matrix effects associated with the analysis of EPS containing samples were minimized through sample dilution, with indium added as an internal standard. Premixed external calibration standards (QCD Analysts, MISA suite of solutions, Spring Lake, USA) were used for instrument calibration. A similar analytical protocol has been reported by Bowie et al. (2010).

4.1.2.4 Chemical speciation of Fe-organic ligand complexes

Fe speciation was measured by Competitive Ligand Exchange – Adsorptive Cathodic Stripping Voltammetry (CLE-AdCSV) following the method of Croot and Johannson (2000). The instruments used were μAutolab II and III potentiostat (Ecochemie, Utrecht, Netherlands) with a hanging mercury (Hg) drop electrode (Hg, Sigma Aldrich, ACS reagent grade, 99.9995% trace metal basis; HMDE drop size 2, 0.4 mm^2 ±10%, VA 663 stand – Metrohm, Herisau, Switzerland), a glassy carbon rod counter electrode, and a double

junction, Ag/AgCl, reference electrode with a salt bridge filled with 3M KCl. The instruments were controlled using GPES software, version 4.7.

Samples were prepared in 0.2-µm filtered Tasman Sea surface seawater (seawater; GP13 GEOTRACES voyage, RV Southern Surveyor, May-June 2011, 30 00 °S 167 00 °E) collected using non-contaminating procedures as recommended by the GEOTRACES program, using Teflon-coated Niskin X-1010 bottles (General Oceanics, Miami, FL, USA) mounted on an autonomous rosette (Model 1018, General Oceanics, Miami, FL, USA) and deployed on a Kevlar rope (Strongrope, NSW, Australia).

EPS was added to the seawater to provide 1 nM dFe in addition to the 0.56 nM already present (measured by ICP-MS), giving a final dFe concentration of 1.56 nM. The solutions were then equilibrated at 4 °C in the dark for either 24-h or 9-wk (as per Hassler et al., 2011b). As in Hassler et al. (2011b), the longer equilibration time was used to investigate the fact that the Eigen–Wilkens mechanism predicts a slow equilibration of Fe with organic ligands (see Town and van Leeuwen, 2005). Samples were prepared for analysis by dispensing 10-mL of EPS enriched seawater into polypropylene tubes to which inorganic Fe at concentrations of 0–16 nM was added from a 1 µM standard (prepared daily; Fe as $FeCl_3$ in 0.5 M HCl, ICP grade, Fluka). The samples were buffered to a pH of 8.1 using 50-µl of 1 M EPPS (SigmaUltra) in 0.3M NH_4OH (Seastar, Baseline®). Samples were left to equilibrate at ambient temperature for 2-h, after which 10-µL of the exchange ligand 2-(2-Thiazolylazo)-p-cresol, TAC, (Sigma; 0.01 M dissolved in triple quartz distilled methanol, Mallinkrodt HPLC grade, prepared fortnightly) was added, and the samples left to equilibrate for a further 18–20-h at ambient temperature in the dark. This long reaction time was chosen considering the association of Fe with organic ligands. Labile Fe (Fe_{labile}) is defined as the proportion of Fe that is exchangeable with an exchange ligand, in this case TAC, over a determined period. If a small proportion of the Fe is labile in the presence of organic ligands, i.e. EPS, then it implies that the Fe-organic ligand complex is strong, and that if a weaker complex is formed then more labile Fe would be measured. As bacterially produced siderophores are often measured as part of the stronger L_1 group of ligands, the assumption was made that bacterial and algal EPS may have similar Fe-binding properties. With this in mind the approach of Hassler et al (2011a), who considered that stronger Fe-organic ligand association would require a longer reaction time with the exchange ligand, was taken and the longer 18–20-h equilibration time with TAC was used.

After equilibration, samples were analysed in polycarbonate titration cells and stirred continually (save for a period of quiescence when measuring) with an inbuilt PTFE rod

(1500 rpm). Dissolved oxygen was purged from the sample for 240-s using high purity argon (Air Liquide, Beresfield, NSW, Australia), followed by 120-s adsorption time onto the Hg drop. The sensitivity of the instrument(s) was determined by the slope of the peak height of the reduction current to the increase of iron addition when all organic ligands are saturated. Labile Fe concentrations ($[Fe]_{labile}$, i.e. $[Fe(TAC)_2]$ detected) could then be determined by dividing the peak height of the reduction current of the sample without Fe addition by the sensitivity of the instrument(s). The detection limit of both instruments was 0.05 nM Fe determined from three times the standard deviation of repeated measurements of a Southern Ocean seawater sample (*n*=8 for both instruments). The concentrations and conditional stability constants ($K_{Fe'L}$) of the Fe'-binding ligands present were determined from the speciation data using the non-linear fit method of (Gerringa et al, 1995). As a quality control of the data presented, the non-linear fit methods was checked to be within 10 % of the data using a linearization method (Harris, 1998). A conditional side reaction coefficient ($\alpha_{Fe'(TAC)2}$) of 627 ± 72 (10 µM TAC) was used for calculations (appendix 4). This coefficient was determined using UV photooxidised, 0.2-µm filtered Southern Ocean water in the presence of 10 nM inorganic iron and diethylenetriaminepentaacetic acid (DTPA, Sigma) using non-linear fit as per Croot and Johansson (2000) and Hassler et al (2013).

Analysis of the 0.2-µm filtered seawater used revealed that the organic ligands naturally present did not significantly affect the results obtained for the EPS as these were three to seven fold lower in concentration, and had a weak conditional stability constant in respect of Fe' binding when compared to the EPS experimental treatments.

4.1.2.5 Fe size fractionation and solubility

Stock solutions of synthetic seawater (Table 4.1) enriched with EPS and $^{55}FeCl_3$ (^{55}Fe-EPS; Perkin Elmer, 22.36 mCi mg^{-1} Fe at the time of use) were prepared and left for one week at 4 °C in the dark to allow the ^{55}Fe to equilibrate with the EPS. After equilibration, larger volumes of synthetic seawater was spiked with either $^{55}FeCl_3$ only or ^{55}Fe-EPS to give a 2 nM total Fe concentration across all experimental solutions. The samples were then incubated for a further 24-h at 4 °C in the dark. This low temperature was used as these experiments were run in parallel with bioavailability experiments using the Antarctic diatom *Chaetoceros simplex* (Hassler, Norman et al., in press). Samples were then size fractionated and collected as unfiltered, 0.2-µm and 0.02-µm filtrates (0.2-µm polycarbonate syringe filters, Millipore; 0.02-µm Anatop syringe filters, Whatman). 10 mL of scintillation cocktail was added (Ultima Gold, Perkin Elmer, Glen Waverley Melbourne, Australia) to the

radiolabeled solutions and the samples were analysed using a liquid scintillation counter (Tricarb 2810, Perkin Elmer, Glen Waverley Melbourne). Soluble Fe was defined as Fe present in the 0.02-µm filtered fraction (<0.02-µm) whereas, colloidal Fe was defined as any Fe present between > 0.02 to 0.2-µm. Experiments were run in duplicate.

4.1.2.6 Measurement of Fe(II) oxidation and Fe(III) reduction rates

4.1.2.6.1 Reagents and general information

Both Fe(II) oxidation rates and Fe(III) reduction rates were determined with UV-visible spectroscopy using the ferrozine (FZ) method. Ferrozine (FZ) was used for the these analyses as it does not bind Fe(III) to a significant degree (Pullin & Cabaniss, 2003), but reacts extremely rapidly with Fe(II) (Thompsen & Mottola, 1984; Lin & Kester, 1992). The purple complex formed, $Fe^{II}FZ_3$ is stable at pH 8 and has a maximum absorbance at 562 nm (Stookey, 1970; Viollier et al., 2000).

For Fe(II) oxidation analysis, a 50 mM stock solution of 3-(2-Pyridyl)-5-6-diphenyl-1,2,4-triazine-4',4"disulfonic acid sodium salt (ferrozine; Fluka analytical) was prepared by dissolving in ultra-pure water. From this a 1 mM working solution was prepared daily in synthetic seawater, and the pH adjusted to 8.09 to match the pH of the natural seawater used to prepare the samples. For Fe(III) reduction analysis the 50 mM FZ stock solution was prepared in synthetic seawater and adjusted to 8.09. Synthetic seawater was used as the carrier here as this stock solution was added directly to the samples without the need for a working solution.

Working 150 µM Fe stock solutions were prepared daily in 2 mM HCl. Fe(II) as ammonium iron(II) sulfate hexahydrate (Ajax Chemicals) was used for Fe(II) oxidation analysis, and Fe(III) as iron(III) chloride hexahydrate (Ajax Chemicals) was used for Fe(III) reduction analysis. The pH of these solutions was sufficient to prevent either Fe(II) oxidation or Fe(III) precipitation, yet low enough to prevent significant pH change in the samples (≤ 0.02 pH units) which could affect rate measurements.

Adjustments to pH were made using ultra-pure NaOH (Fluka), and pH was measured using a Hanna 9025 microprocessor pH meter combined with a glass electrode and Ag/AgCl reference which was calibrated daily using NBS scale NIST-traceable buffer solutions (pH 7.01, 10.01). During the period of analysis, the pH of the samples and reagents remained

within ± 0.02 pH units. All samples were prepared in triplicate in 0.2-µm filtered Tasman Sea surface water (seawater).

4.1.2.6.2 Determination of Fe(II) oxidation rates in the presence of model saccharides and natural bacterial and algal exopolymeric substances (EPS)

EPS from the sea ice bacteria, SAZ bloom, *E. huxleyi*, or a model ligand in the form of dextran (polysaccharide) or glucuronic acid (monosaccharide) was added to seawater to provide an Fe to ligand ratio (Fe:L) of 1:1.66. The volume of EPS used was based on concentration of Fe'-binding ligands measured by CLE-AdCSV, and the excess of these ligands present in respect of Fe in the EPS. To investigate the effect of concentration of organic ligands on a fixed concentration (30 nM) of Fe(II), samples containing dextran and glucuronic acid using concentrations ranging from 50 nM to 5000 nM (Fe:L from 1:66 to 1:166) were prepared. Once the organic material had been added to the seawater, the samples were left to equilibrate for 18 to 24-h at 4 °C in the dark. After equilibration the samples were allowed to come to ambient temperature (22 °C) before analysis, or measured on ice to maintain a temperature of 4 °C. Fe(II) at a concentration of 30 nM was added to the sample immediately prior to analysis. Once the Fe(II) had been added, the sample and FZ reagent were mixed at a T junction prior to being driven through a 1-m pathlength cell (or "waveguide", LWCC Type II, World Precision Instruments, Sarasota, FL, USA) by a peristaltic pump. The resulting $Fe^{II}FZ_3$ complex was measured colorimetrically at 562 nm using Ocean Optics spectrophotometry. A reference wavelength of 690 nm was used for baseline correction, and the system was zeroed before each run using a control sample (no Fe added) to take into account background absorbance of the sample and FZ solutions at 560 nm. The low temperature samples were maintained by placing the volumetric flask containing the sample in a bath of ice and water. The detection limit of the instrument at both 22 °C and 4 °C was 1 nM Fe(II) calculated as three times the standard deviation (SD) of the lowest calibration standard (n = 6; 10 nM Fe(II)).

4.1.2.6.3 Determination of Fe (III) reduction rates in the presence of model saccharides and natural bacterial and algal exopolymeric substances

Samples were prepared and equilibrated as for Fe(II) oxidation analysis using a Fe:L of 1:1.4 in respect of 50 nM Fe(III). As the volume of natural EPS available was limited, further samples using only the model ligands, dextran and glucuronic acid, were prepared which

would provide Fe:L of 1:10, 1:50 and 1:100 with respect to 50 nM Fe(III) to investigate the effect of high concentration. After equilibration the samples were allowed to come to room temperature, and two sample sets were prepared. To the first set, FZ was added to give a concentration of 1 mM and, after checking the pH, 50 nM Fe(III) was added and measurement started immediately. For the second set, Fe(III) was added to the equilibrated ligand sample and then left for a further 2-h at room temperature for the Fe(III) and ligand to equilibrate as per CLE-AdCSV analysis. After this second equilibration period, 1 mM FZ was added, the pH checked and analysis started. The sample was then driven through a single line to a 1-m pathlength cell (or "waveguide", LWCC Type II, World Precision Instruments, Sarasota, FL, USA) by a peristaltic pump, and any $Fe^{II}FZ_3$ complex formed was measured colorimetrically at 562 nm using Ocean Optics spectrophotometry and baseline correction with no Fe(III) present as before. Due to a limited volume of material, these analyses were carried out at 22 °C only, and measurements were taken every 10-min (semi-continuously) for 2.5-h. The detection limit of the instrument at 22 °C was 1 nM Fe(II) calculated as 3 times the SD of the lowest calibration standard (n = 6; 5 nM Fe(II)).

4.1.2.7 Humic substance-like material

Samples for the analysis of humic substance-like (HS-like) substances were prepared in synthetic seawater (Table 4.1) rather than 0.2-µm filtered seawater to remove any interference from HS-like material that may have been present in the seawater. The 2 nM background Fe measured in the synthetic seawater was not of consequence, as it would have been for Fe speciation analysis, because it is a requirement of the method that the natural organic matter is saturated with Fe. Determination of HS-like material was made using the voltametric method of Laglera et al (2007) as described in Chapter 2 (p 36) and using a 250-s sparge time and 300-s deposition time. Standard additions of Suwannee River Fulvic Acid (SRFA, Std 1; International Humic Substances Society, Denver, Colorado, USA) were made in 20 µg L^{-1} SRFA increments. The detection limit of the instruments was 1.56 µg L^{-1} (µAutolab II) and 1.31 µg L^{-1} (µAutolab III), determined from three times the standard deviation of 10 repeated measurements of a Southern Ocean seawater sample using purge and deposition times as per samples.

Table 4.1 Constituents of synthetic seawater used for humic substance-like analysis. Based on AQUIL media as per Price et al. (1989) using major salt only. Final pH = 8.00

Constituent	Concentration (M)
NaCl	4.20×10^{-1}
Na_2SO_4	2.88×10^{-2}
KCl	9.39×10^{-3}
$NaHCO_3$	7.14×10^{-3}
KBr	8.40×10^{-4}
H_3BO_3	1.46×10^{-3}
NaF	7.14×10^{-5}
$MgCl_2*6H_2O$	5.46×10^{-2}
$CaCi_2*2H_2O$	1.05×10^{-2}
$SrCl_2*6H_2O$	6.38×10^{-5}

4.1.2.8 Macronutrient analysis

The concentration of the major dissolved inorganic macronutrients, nitrate + nitrite (NO_X), nitrite (NO_2), ammonium (NH_4), and phosphate (PO_4) was determined by standard colorimetric methodology (Grasshoff et al. 1983) as adapted for flow injection analysis (FIA) on a four-channel LACHAT Instruments Quick-Chem 8500 autoanalyser (Hales et al. 2004). Samples were prepared in ultra-pure water (UPW) using a 1:20 (EPS:UPW) dilution factor.

4.1.2.9 Total Saccharides analysis

The total saccharide concentration of the four EPS isolates was determined semi-quantitatively using a modified version of the colorimetric method of Myklestad et al (1997). Briefly, total sugar concentration was determined after hydrolysis of an acidified sample (0.1 N HCl), which was contained in a sealed glass ampoule, at 120 °C for 1-h. After cooling, the sample was raised to a neutral pH and the-monosaccharides, or non-reducing sugars and polysaccharides made reducing by the hydrolysis of the glycosidic bonds, were subjected to an oxidation reaction during which Fe^{3+} is reduced to Fe^{2+}. The chromogen 2, 4, 6-tripyridyl-s-triazine (TPTZ) is added as a complexing agent which develops a violet

colour ($Fe(TPTZ)^{2+}_2$) that can be measured spectrophotometrically at 595 nm. Total sugar concentration (μmol C L^{-1}) was determined from a standard curve prepared from D-glucose in UPW. The detection limit of the method was 0.07 mg glucose eq L^{-1} (2.5 μmol C L^{-1}) calculated as three times the standard deviation of the lowest calibration standard (n = 6; 0.25 mg glucose L^{-1}). All glassware and reagents were prepared as described by Myklestad et al. (1997). Samples were prepared in UPW using a 1:200 (EPS:UPW) dilution factor.

4.1.3 Fe bioavailability and phytoplankton growth experiments

The diatom *Chaetoceros simplex* was selected as the model phytoplankton for this experiment as it represents an important species in Southern Ocean waters. The parent cultures were maintained, under trace-metal-clean conditions, in low Fe concentration (0.3 nM) Southern Ocean water, in exponential phase at 4 °C, on a 16:8-h light:dark cycle, at a light level of 60 μmol photons m^{-2} s^{-1} (details in Hassler et al 2011a). For Fe bioaccumulation and growth experiments, *C simplex* cells in exponential growth phase were isolated from the growth media by gravity filtration on to 2-μm polycarbonate filters (Millipore, Merck Millipore, Bayswater, VIC, Australia), and then rinsed once with trace-metal-clean oxalate solution (Tovar-Sanchez et al., 2003) and five times with an inorganic saline solution (0.6 M NaCl, 2.38 mM NaHCO3, Hassler at al., 2011a). The cells were then gently resuspended into 10-mL of synthetic seawater which was used to start the bioaccumulation and growth experiments. Cell density in this algal suspension was determined using a Coulter ® Multisizer II counter (Beckman, Lane Cove, NSW, Australia) with a 50-μm aperture tube.

4.1.3.1 Fe bioaccumulation experiments

Phytoplankton Fe uptake rates were used to estimate Fe bioavailability as per Hassler and Schoemann (2009) and Hassler et al. (2011a). The bioavailability of Fe associated with EPS (Fe-EPS) to *C. simplex,* was assessed by comparison of the internalisation rate constant (k_{int}) obtained in the presence of inorganic Fe only and in presence of Fe pre-equilibrated with the EPS for 1-wk. The calculation of k_{int} was obtained from the slope of the relationship between the measured intracellular Fe and increasing inorganic Fe.

Experimental solutions were spiked with inorganic $^{55}FeCl_3$ (Fe treatment, 31.75 mCi mg^{-1} Fe at the time of use; Perkin Elmer, Melbourne, VIC, Australia) or with ^{55}Fe pre-equilibrated with the EPS. A 2-mL sample was taken to determine the total initial ^{55}Fe content, and the

remaining solution was equilibrated for 24-h at 4 °C in the dark. Each treatment was prepared in triplicate. After equilibration, *C simplex* was spiked directly into the radiolabelled solutions to attain a cell density of 36,000 cells ml^{-1}, and was incubated at 4 °C at constant light (50 µmol photons m^{-2} s^{-1}) for a further 24-h. At the end of the incubation, the algal suspensions were gently filtered onto 0.45-µm nitrocellulose filters (Sartorius; Sartorius Stedim, Dandenong, South, VIC) for determination of intracellular Fe. After filtration, the filters were rinsed with oxalate solution (Tovar-Sanchez et al., 2003; Hassler and Schoemann, 2009), 5 x 3-mL at 2-min intervals, followed by three times 3-mL of 0.2-µm filtered seawater. The purpose of the oxalate wash was to remove any adsorbed Fe on cell surfaces. The initial radiolabelled solutions and final filters were collected in 20-mL scintillation vials, to which 10-mL of scintillation cocktail was added (Ultima Gold, Perkin Elmer, Melbourne, VIC, Australia). The samples were vortexed, and measured using a liquid scintillation counter (Tri-carb 2810 TR, Perkin Elmer, Melbourne, VIC, Australia) as per Hassler and Schoemann (2009). Given that soluble inorganic Fe is assumed to be 100 % bioavailable to diatoms (e.g., Shaked et al., 2005), its bioaccumulation in synthetic seawater can be used to determine the relationship between total Fe concentration and its bioavailability. Intracellular disintegrations per minute were transformed in Fe concentration using a custom-made quench curve, total initial radioactivity and dissolved Fe concentration (Hassler, Norman et al., in press).

4.1.3.2 Phytoplankton growth experiments

Filtered Tasman Sea surface water (seawater, 0.2-µm) was enriched with inorganic Fe (ICP standard, Fluka) or EPS to provide 1 nM Fe total (in addition to the 0.56 nM present in the natural seawater), and left to equilibrate at 4 °C in the dark for 24-h. After equilibration, the samples were transferred to 50-mL polycarbonate bottles to which Fe-limited *C. simplex* was added to attain a cell density of ~ 40, 000 cells-mL^{-1}. Each treatment was prepared in triplicate. A further treatment using unamended 0.2-µm filtered seawater was also prepared. The algal suspensions were incubated at 4 °C, at a continuous light level of 50 µmol photons m^{-2} s^{-1} for 187-h. Cell counts were made using an electronic particle counter (Multisizer II Coulter Counter, Beckman, Lane Cove, NSW, Australia) with a 50-µm aperture. Estimates of the maximum quantum yield (F_V/F_M) were made on phytoplankton cultures using a Pulse Amplitude Modulated fluorometer (Water-PAM; Walz GMBH, Effeltrich, Germany; Schreiber, 2004). A 3-mL sample was placed into a cylindrical quartz cuvette and dark-adapted for 15-min. Once the fluorescence signal was stable, a saturating pulse was

applied to give the dark-adapted maximum fluorescence (F_M). F_V/F_M was calculated as (F_M-Fo)/F_M (Schreiber, 2004).

4.1.4 Experimental precautions

All plasticware (LDPE and HDPE bottles, pipette tips and polycarbonate materials) were cleaned by first soaking in detergent (Citrinox acid detergent, 5% v/v) for 24-h, followed by rinsing five times in deionised water. The plasticware was then soaked for four weeks in 1 M HCl, except for polycarbonate which was soaked for one week to avoid deterioration. The equipment was then rinsed seven times in ultra-pure water, and then dried in an ISO Class 5 laminar flow hood. All trace-metal-clean items were sealed in triple bags until use, and experimental samples were sealed in triple bags during equilibration/incubation periods. All sample manipulations and reagent preparation was carried out in a ISO Class 5 laminar flow hood. All reagents were made up in ultra-pure water unless otherwise stated, and were passed through Chelex-100 resin (BioRad, conditioned as per Price et al., 1989) prior to use to minimise Fe contamination.

4.2 Results

4.2.1 Functional composition of EPS

All EPS isolates contained protein, uronic acid, neutral sugars and saccharides in varying proportions. The bacterial EPS was composed primarily of neutral sugars, with a small proportion of uronic acid, and comparatively little protein (Table 4.2). The composition of the two cultured algal isolates, *P. antarctica* and *E. huxleyi*, was very similar in terms of the relative concentration (%) of protein, uronic acid and neutral sugar content, however, the concentration of total saccharides in the *P. antarctica* EPS was 1.6-fold higher than that measured in the *E. huxleyi* EPS (Table 4.2). The SAZ bloom, which was dominated by coccolithophorids in a mixed algal and bacterial community, had the lowest relative or measured concentration of all constituents, with the relative concentrations of protein, uronic acid and neutral sugars being about half that of the two cultured algal isolates (Table 4.2).

Table 4.2 Composition of exopolymeric substances (EPS) isolated from an Antarctic sea ice bacteria, a natural sub-Antarctic zone bloom (SAZ bloom) and axenic algal cultures (*Phaeocystis antarctica* and *Emiliania huxleyi)*. Relative concentration (%) of protein, uronic acid and neutral sugars present are shown together with total hydrolysable saccharides (reported as mmol C g^{-1} EPS).

EPS origin	Protein %	Uronic acid %	Neutral sugar %	Total Saccharides (mmol C g^{-1} EPS)
Bacterial EPS				
Sea ice bacteria	3.0	22	74	6.4 ± 0.01
Algal EPS				
SAZ bloom	3.1	1.5	16	3.9 ± 0.01
Phaeocystis antarctica	5.8	3.6	28	7.5 ± 0.02
Emiliania huxleyi	8.5	3.6	27	4.6 ± 0.02

4.2.2 Size and molar mass distribution of EPS

The differential refractive index (RI) fractograms obtained showed that the algal EPS isolates from *P. antarctica* and *E. huxleyi*, and the EPS isolated from the SAZ bloom were made up of LMM material; whereas, the sea ice bacterial EPS was predominantly, if not entirely, made up of HMM components. The EPS isolated from *E. huxleyi* also contained a very small amount of IMM material at around 750 kDa (Fig. 4.1A-D).

Mass distribution parameters were calculated for the LMM region in all but the bacterial EPS, where very little LMM material was present (Table 4.3). Number-average molar masses obtained were 19 kDa for *P. antarctica*, 15 kDa for *E. huxleyi*, and 43 kDa for the SAZ bloom. Molar mass dispersity ($Đ_M$), a measure of the distribution of molar masses in a sample, was close to 2 in all cases indicating a non-uniform distribution (Table 4.3).

UV fractograms (Fig. 4.1A-D) followed the same trend as the RI fractogram (Fig. 4.1A-D). The maximum peak intensity (*Mp*) measured for both *P. antarctica* and *E. huxleyi* were low at ~8 kDa (Table 4.3, UV). In the SAZ bloom, two peaks were identified; the first with a similar molar mass to the two algal EPS of ~8 kDa, and the second giving a *Mp* of 24 kDa.

In the algal EPS from *P. antarctica* and SAZ bloom, the Fe distribution also followed the LMM trend of the RI with the *Mp* giving molar masses of ≤ 20 (Fig. 4.1B, D Table 4.3). The distribution of Fe in the *E.huxleyi* EPS was more complex as both LMM and HMM

components appeared to have equivalent proportions of Fe bound to them. A further peak was observed in the IMM region which, despite giving a much lower signal intensity, was not of negligible proportions (Fig 4.1C).

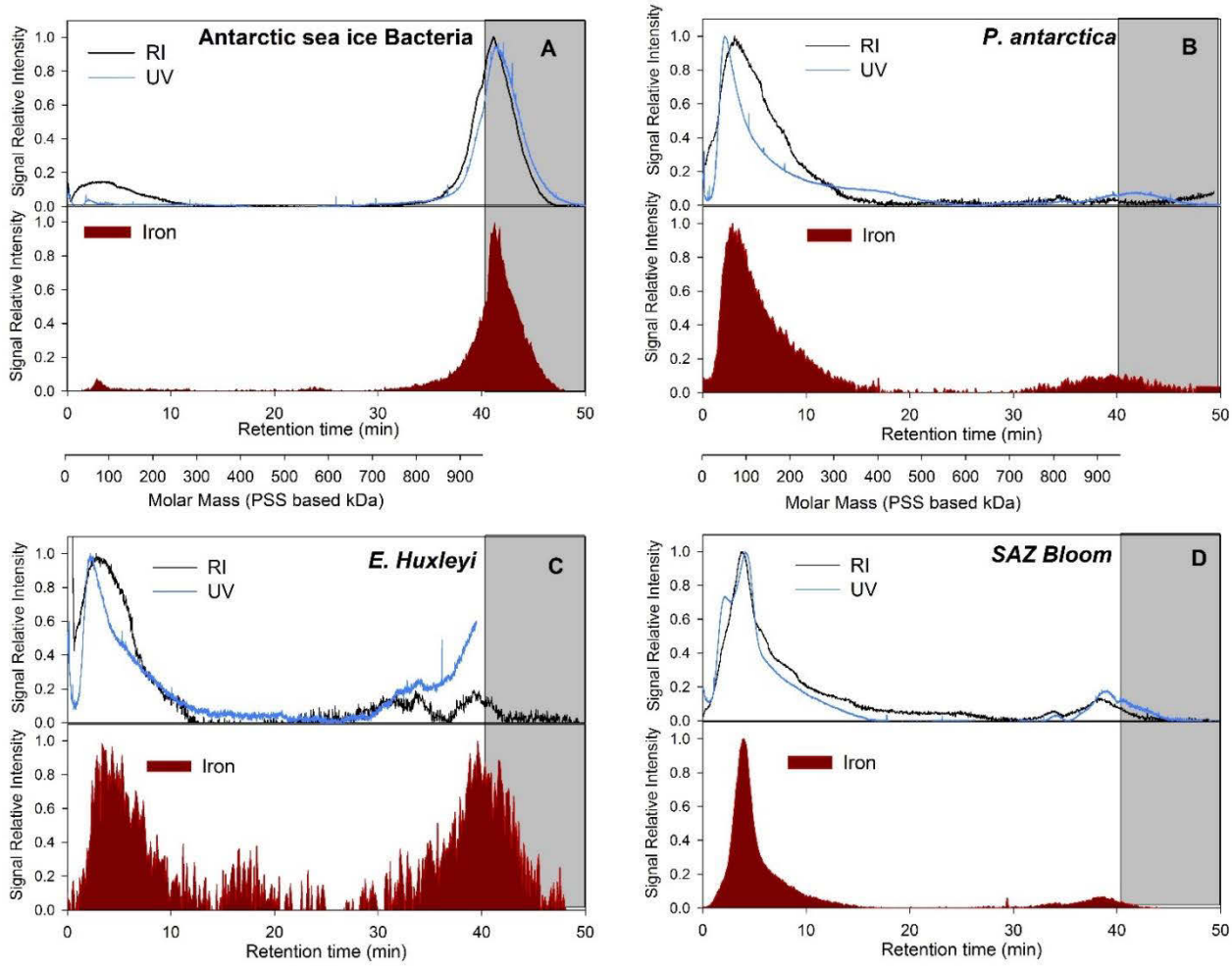

Figure 4.1 Molar mass distribution fractograms of exopolymeric substances (EPS) obtained by FFF-RI-UV-ICPMS using a linear decrease in cross-flow rate. Differential refractive index relative intensity, absorbance measured at λ = 254 nm (upper panel of each sub figure), and ^{56}Fe relative intensity (lower panel of each sub figure) from EPS isolated from Antarctic sea ice bacteria, sub-Antarctic zone bloom (SAZ bloom) and axenic algal cultures (*Phaeocystis antarctica* and *Emiliania huxleyi*) . The grey zone following 40-min elution time illustrates the end of applied cross flow and the end of the fractionation corresponding to elution of compounds > 950 kDa as determined using PSS molecular weight calibration.

Table 4.3 Mass distribution parameters for differential refractive index (DRI), UVD, and ^{56}Fe in the low molar mass (LMM) region of the respective signal fractograms exopolymeric substances (EPS) isolated from Antarctic sea ice bacteria, sub-Antarctic zone bloom (SAZ bloom) and axenic algal cultures (*Phaeocystis antarctica* and *Emiliania huxleyi*). *Mw* = weight average molar mass, *Mn* = number average molar mass, *Mp* = maximum peak intensity. Calculation for molar mass dispersity ($Đ_M$), *Đ = Mw/Mn.*

		Mw	***Mn***	***Mp***	*Đ*
SAZ Bloom	***RI***	43	24	21	1.8
	UV	34	19	24	1.8
	Iron	33	23	21	1.4
P. antarctica	***RI***	36	19	15	1.9
	UV	37	19	8	2.0
	Iron	37	22	13	1.7
E. huxleyi	***RI***	26	15	12	1.8
	UV	34	18	9	1.9
	Iron	29	15	15	2.0

The Fe signal eluograms for the sea ice bacteria and *P. antarctica* EPS appeared to follow the trends of RI, UV absorbance and fluorescence very well. The *E. huxleyi* and SAZ bloom EPS were less well matched in all parameters but a general agreement was still observed (Fig. 4.2). In the sea ice bacterial EPS, the Fe appears to be associated with EPS components of similar optical characteristics and distributed homogenously across components with a hydrodynamic radii (R_h) > 10 nm, with a maximum Fe peak intensity at 29 nm (Fig. 4.2A). Within the range of the data, three main components were found with R_h at peak maximums of 26 nm, 40 nm and 60 nm (Fig. 4.3). The EPS isolated from the SAZ bloom, *P. antarctica*, and *E. huxleyi* were predominantly components with R_h of < 10 nm (Fig. 4.2B, C, D), however there was a small proportion of Fe associated with components of R_h 10 to 70 nm present in the *E. huxleyi* EPS (Fig. 4.2C).

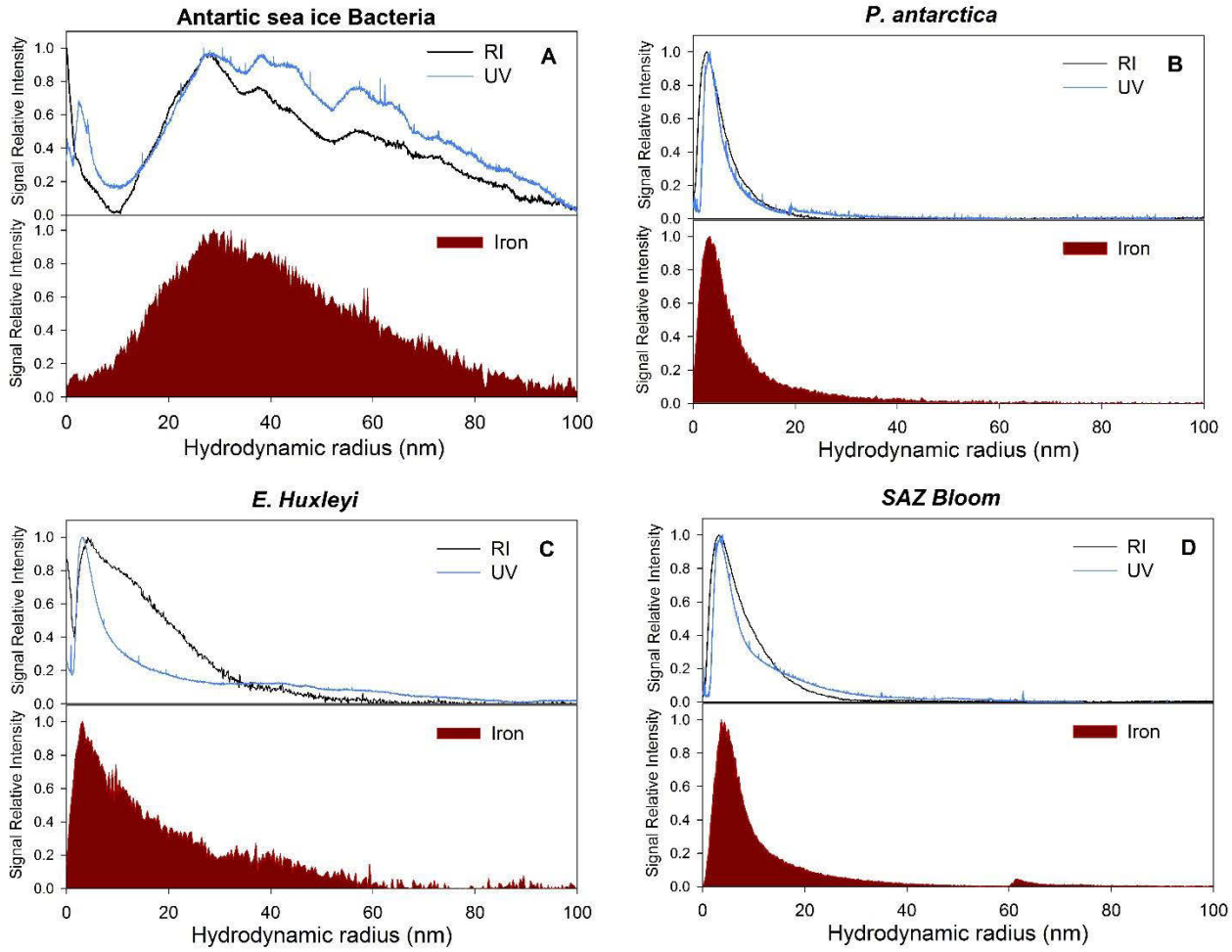

Figure 4.2 ^{56}Fe eluograms (lower panel of each sub figure) showing hydrodynamic radius (nm) of components of exopolymeric substances (EPS). For comparison refractive index relative intensity (lower panels), absorbance measured at λ = 254 nm (UV, upper panels), and fluorescence (fluo, upper panels) are shown. EPS were isolated from Antarctic sea ice bacteria, sub-Antarctic zone bloom (SAZ bloom) and axenic algal cultures (*Phaeocystis antarctica* and *Emiliania huxleyi*).

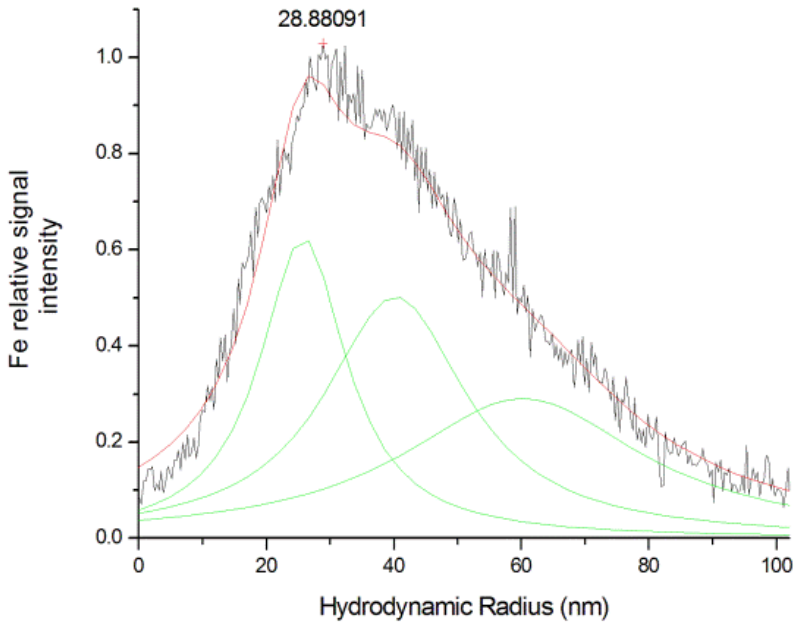

Figure 4.3 ^{56}Fe eluogram after *in silico* deconvolution of Fe distribution associated with Antarctic sea ice bacterial EPS. Maximum Fe signal intensity (red line) associated with components with hydrodynamic radii (R_h) of ~29 nm. Three further prominent components measured with R_h of ~ 26 nm, 40 nm and 60 nm (green lines).

4.2.3 Macronutrient and trace element composition of EPS

In all EPS isolates (bacterial and algal) ammonium (NH_4) was the dominant form of N present, which was measured in micromolar (g^{-1} EPS) concentrations in all isolates expect for the SAZ bloom (Table 4.4). PO_4 was also detected in all EPS isolates and was measured in micromolar concentrations (g^{-1} EPS) in the sea ice bacteria EPS and sub-micromolar concentrations (g^{-1} EPS) in all algal isolates. Of the algal isolates, *P. antarctica* contained the highest concentrations of all macronutrients, except for NO_2, and the SAZ bloom the lowest. The NO_X, NH_4 and PO_4 concentration in the *P. antarctica* EPS were 1.5 to 2.2-fold, 2.9 to 6.7-fold, and 1.1 to 1.7-fold higher, respectively, than those measured in the *E. huxleyi* and SAZ bloom EPS (Table 4.4).

ICP-MS analysis revealed that all EPS had measureable concentrations of Al, Co, Cu, Fe, Mn, and Zn, except for Co in the *E. huxleyi* EPS and Cu in the *P. antarctica* EPS (Table 4.5). In addition, the algal-EPS isolates (SAZ bloom, *P. antarctica* and *E. huxleyi*) also contained potentially toxic (Pb, Cd) trace metals, although concentrations were highly variable

between isolates (Table 4.5). Measured concentrations of Al and Mn and the more toxic metals Pb and Cd were substantially higher in the natural SAZ bloom EPS than all other algal-EPS isolates, likely reflecting a background concentration and subsequent uptake from the surrounding seawater.

Table 4.4 Concentration of macronutrients (NO_X, NO_2, NH_3, PO_4) present in exopolymeric substances (EPS) isolated from Antarctic sea ice bacteria, a sub-Antarctic zone bloom (SAZ bloom) and axenic algal cultures (*Phaeocystis antarctica* and *Emiliania huxleyi*). Data reported as nmol g^{-1} EPS.

EPS origin	NO_X	NO_2	NH_3	PO_4
Bacterial EPS				
Sea ice bacteria	994 ± 121	508 ± 183	8414 ± 922	2846 ± 171
Algal EPS				
SAZ bloom	271 ± 69	156 ± 57	689 ± 115	183 ± 49
Phaeocystis antarctica	606 ± 82	120	4684 ± 576	317 ± 90
Emiliania huxleyi	397 ± 125	180 ± 85	1590 ± 354	285 ± 129

Table 4.5 Concentration of trace metals present in exopolymeric substances (EPS) isolated from sea ice bacteria, a natural sub-Antarctic zone bloom (SAZ bloom) and axenic algal cultures (*Phaeocystis antarctica* and *Emiliania huxleyi*). Data reported as nmol g^{-1} EPS. <DL = below detection limit.

EPS origin	Al	Cd	Co	Cu	Fe	Mn	Pb	Zn
Bacterial EPS								
Sea ice bacteria	1537	< DL	9.8	182	393	14	< DL	35
Algal EPS								
SAZ bloom	16,543	3.8	8.9	98	2274	65	146	181
Phaeocystis antarctica	2277	< DL	3.2	< DL	7112	21	47.9	569
Emiliania huxleyi	798	< DL	< DL	100	5267	19	69.7	2996

4.2.4 Effect of EPS on Fe biogeochemistry

The relative concentration (%) of Fe_{labile} in the samples containing sea ice bacterial EPS and the two algal EPS, after both 24-h and 9-wk pre-equilibration, was less than 50% in all cases (Table 4.6). In the sample containing EPS from the SAZ bloom, Fe_{labile} was much greater at 63% after 24 h, and 98 % after 9-wk equilibration. Conditional stability constants for the sum of all ligands present (log $K_{Fe'\Sigma L}$) in the 24-h pre-equilibration samples all followed an inverse pattern of Fe_{labile}, where the SAZ bloom had the highest percentage of Fe_{labile} and the weakest log $K_{Fe'\Sigma L}$, and *P. antarctica* had the lowest percentage of Fe_{labile} and the strongest log $K_{Fe'\Sigma L}$ (Table 4.6).

A strong class of ligands (log $K_{Fe'L} \geq 12$ M^{-1}) was detected in all EPS save for the SAZ bloom. In addition, a further weaker ligand was detected in the EPS from both the sea ice bacteria and that of *E. huxleyi*. However, after 9-wk pre-equilibration just one ligand class was detected, except for in the SAZ bloom sample where no Fe′-binding ligands could be detected (Table 4.6). Of the log $K_{Fe'\Sigma L}$ calculated in the aged samples, all were slightly higher than those calculated after 24-h pre-equilibration, suggesting a degradation of the weaker ligands and a greater influence of the stronger ligands present.

Fe'-binding, HS-like material associated with the sea ice bacteria EPS was relatively low at < 2 mg SRFA eq g^{-1} EPS (Table 4.6). HS-like material was present in much higher concentrations in the algal-EPS isolates, with the *E. huxleyi* EPS having almost double the HS-like material compared to the SAZ bloom and *P. antarctica* EPS (Table 4.6). Analysis for heme signatures was conducted on all EPS isolates, however, none were detected (M. Gledhill, pers. comm.).

Table 4.6 Fe biogeochemistry associated with exopolymeric substances (EPS) isolated from an Antarctic sea ice bacteria, a natural sub-Antarctic Zone bloom (SAZ bloom) and axenic algal cultures (*Phaeocystis antarctica* and *Emiliania huxleyi*). The overall % of labile iron (Fe_{Labile}) and the concentration of ligands associated with strong binding affinities ($[L_1]$), weaker binding affinities ($[L_2]$) and the sum of all ligands ($[\Sigma L]$), together with the calculated conditional stability constant relative to inorganic iron ($\log K_{Fe'L1}$, $\log K_{Fe'L2}$ or $\log K_{Fe'sumL}$) is presented. Electrochemically detected humic substance-like (HS-like) material is also shown and expressed as Suwanee River Fulvic Acid (SRFA) equivalents. Results are from a sample set measured after 24 h equilibration, and a further set measured after 9 weeks. Both sets were equilibrated at 4 °C in the dark.

EPS origin	$[L_1]$ (µmol g^{-1} EPS)	log $K_{Fe'L1}$	$[L_2]$ (µmol g^{-1} EPS)	log $K_{Fe'L2}$	$[\Sigma L]$ (µmol g^{-1} EPS)	log $K_{Fe'\Sigma L}$	% Labile Fe	HA-like (mg g^{-1} EPS SRFA eq)
Bacterial EPS–24-h equilibration								
Sea ice bacteria	1.1 ± 0.09	12.12 ± 0.10	2.6 ± 0.24	11.44 ± 0.07	2.3 ± 0.26	11.56 ± 0.09	38	1.8 ± 0.2
Bacterial EPS–Aged for 9-wk								
Sea ice bacteria					1.24 ± 0.13	11.88 ± 0.08	21	
Algal EPS–24-h equilibration								
SAZ bloom					28.6 ± 9.71	11.17 ± 0.17	63	34 ± 0.9
Phaeocystis antarctica	23.1 ± 3.98	12.12 ± 0.15			30.9 ± 0.96	11.9 ± 0.03	25	38 ± 9.4
Emiliania huxleyi	17.7 ± 2.11	11.98 ± 0.11	29.7 ± 3.21	11.67 ± 0.10	36.9 ± 3.47	11.38 ± 0.08	37	60 ± 1.0
Algal EPS- Aged for 9-wk								
SAZ bloom					Not	detected	98	
Phaeocystis antarctica					21.6 ± 3.91	12.17 ± 0.15	21	
Emiliania huxleyi					26.4 ± 3.47	11.45 ± 0.08	47	

4.2.5 Effect of EPS on Fe solubility

The effect of EPS on Fe solubility was determined by the comparison of Fe size distribution, in the colloidal (> 0.02 to 0.2-µm) and soluble (< 0.02 µm) fractions, in the presence and absence of EPS. The presence of EPS, regardless of origin, significantly increased Fe solubility in both size fractions (Fig. 4.4). The presence of EPS from *P. antarctica* and the SAZ bloom enhanced soluble Fe to a greater degree than that derived from *P. antarctica*; whereas, colloidal Fe was enhanced to a greater degree by the *E. huxleyi* EPS (Fig. 4.4).

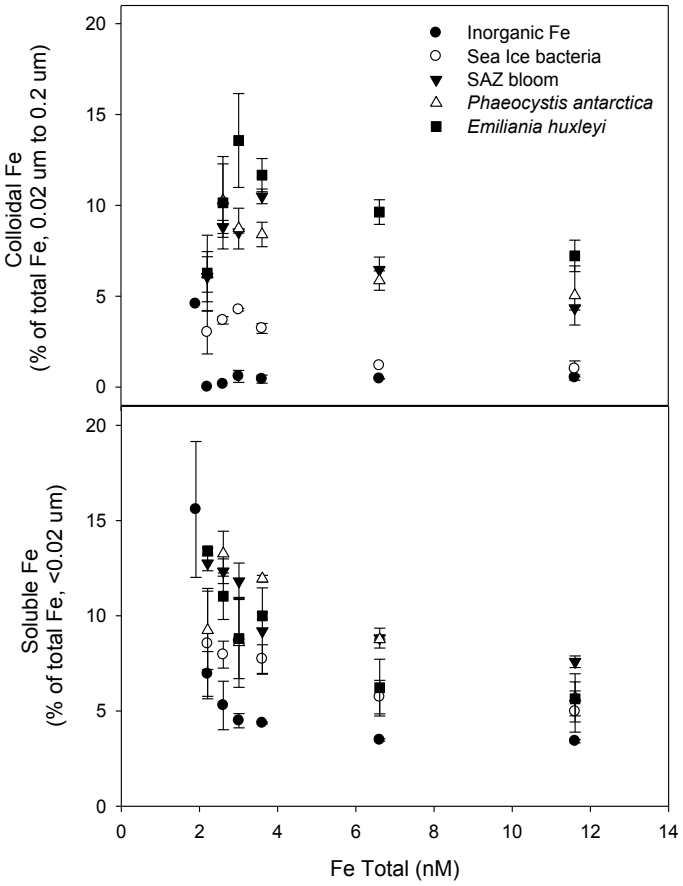

Fig. 4.4 The solubility of Fe in the presence or absence of bacterial or algal exopolymeric substances (EPS) in both the colloidal (0.02 um to 0.2 um) and soluble (<0.02 um) size fractions. EPS isolates were from an Antarctic sea ice bacteria, a natural phytoplankton bloom from the sub-Antarctic zone (SAZ bloom), and from axenic algal cultures of *Phaeocystis antarctica* and *Emiliania huxleyi*. An experimental control solution of inorganic Fe only is also presented. Experimental medium was synthetic seawater (pH 8.0). Error bars indicate half interval, n=2.

4.2.6 Effect of EPS and model saccharides on Fe redox chemistry

At 22 °C and pH 8.09, the oxidation rate of Fe(II) (30 nM) in the unamended 0.2-µm filtered Tasman Sea surface seawater (seawater) was extremely rapid, with the Fe(II) half-life being reached within 3-min. When identical samples were measured at 4 °C, the oxidation rate slowed and Fe(II) half-life was reached at 30-min, extending its half-life by a factor of 10. A similar temperature effect on Fe(II) oxidation was observed in the samples where EPS or model ligands had been added (Table 4.7). However, in treatments where EPS had been added, only the EPS isolated from *E. huxleyi* affected the oxidation rate and half-life of Fe(II) to a significant degree ($p = 0.001$) relative to the unamended seawater. At both temperatures, a faster oxidation rate and shorter half-life was observed compared to the seawater control (Table 4.7). At 22 °C, both of the equivalent model saccharides additions (Fe:L = 1:1.66) also gave significantly faster oxidation rates and shorter Fe(II) half-lives compared to the seawater control (dextran, $p < 0.005$, glucuronic acid, $p < 0.04$), with the dextran comparing very well to the *E. huxleyi* EPS (Table 4.7). However at 4 °C dextran significantly enhanced oxidation rate and decreased half-life ($p < 0.001$); whereas, the glucuronic acid did not. In contrast to the rates measured at 22 °C, at 4°C both oxidation rate and half-life were significantly decreased and increased, respectively, in the samples containing *E. huxleyi* EPS compared to the equivalent dextran addition ($p = <0.02$, Table 4.7).

Using the model saccharides, dextran and glucuronic acid, the ratio of organic ligand and Fe(II) was varied to investigate the effect of ligand concentration on Fe(II) oxidation. Fe(II) remained at 30 nM addition whilst organic ligand concentration was added at concentrations between 50 and 5000 nM (Fe:L 1:66 to 1:166). For both dextran and glucuronic acid, at ambient temperature (22 °C) and 4 °C, the rate of oxidation became increasingly faster and the half-life shorter as ligand concentration increased. However, the glucuronic acid did not show significant response difference from the seawater control until the highest concentration of 5000 nM (Fe:L = 1:166). Concentrations of dextran > 500 nM were trialled, but due to the increased viscosity of the samples, variability between replicate samples was too great to provide reliable results.

The effect of the presence of EPS on Fe reduction was also investigated. In solutions where EPS or a model saccharide (dextran or glucuronic acid) had been added to give a Fe:L of 1:1.4, no response above baseline interference was measured for the entire 2.5-h analysis period. An increase in ratio of dextran or glucuronic acid to Fe(III) up to 100 was also measured, but again no response above baseline interference was detected. These results

were consistent for samples analysed immediately after Fe(III) addition and also for those pre-equilibrated with Fe(III) for 2-h.

Table 4.7 Pseudo-first-order rate constant (k' s^{-1}) and half-life ($t_{½}$) for Fe(II) (30 nM) oxidation at ambient laboratory temperature (22 °C) and 4 °C in 0.2-µm filtered seawater only (pH 8.09 ± 0.02) and in the presence of model saccharides and isolated natural bacterial and algal exopolymeric substances (EPS). Model ligands = Dextran (DEX, polysaccharide) in concentrations 50 – 500 nM (Ligand-to Fe-ratio, L: Fe 1.66 to 16.6), and Glucuronic acid (GLU, monosaccharide) in concentrations 50–5000 nM (L: Fe 1.66 to 166). EPS isolates = Antarctic sea ice bacteria, natural phytoplankton bloom from the sub-Antarctic zone (SAZ bloom), axenic algal culture of *Emiliania huxleyi*. EPS were added at a concentration to give L:Fe of 1.66. Seawater only n = 12 (22 °C) and 6 (4 °C), all ligands n = 3 for both temperatures.

Added Organic Material	L: Fe	Oxidation rate k' s^{-1} (x 10^{-3}) 22 °C	Half-life min 22 °C	Oxidation Rate k' s^{-1} (x 10^{-3}) 4 °C	Half-life Min 4 °C
Seawater only		4.05 ± 0.346	2.87 ± 0.27	0.390 ± 0.031	30.18 ± 2.05
Sea Ice bacteria	1.4	4.13 ± 0.197	2.80 ± 0.14	0.402 ± 0.036	28.92 ± 2.60
SAZ bloom	1.4	4.10 ± 0.170	2.86 ± 0.05	0.407 ± 0.027	28.54 ± 2.74
Emiliania huxleyi	1.4	4.89 ± 0.262*	2.37 ± 0.12*	0.511 ± 0.030*	22.65 ± 1.38*
DEX 50 nmol	1.4	4.99 ± 0.078*	2.32 ± 0.04*	0.437 ± 0.017*	26.67 ± 0.71*
DEX 100 nmol	3.33	6.11 ± 0.622	1.90 ± 0.19	0.451 ± 0.026	25.69 ± 1.51
DEX 500 nmol	16.6	7.13 ± 0.304	1.62 ± 0.07	0.508 ± 0.010	22.73 ± 0.45
GLU 50 nmol	1.4	4.51 ± 0.130*	2.56 ± 0.07*	0.394 ± 0.033	29.80 ± 3.11
GLU 100 nmol	3.33	5.08 ± 0.251	2.28 ± 0.11	0.397 ± 0.055	29.08 ± 0.40
GLU 500 nmol	16.6	5.35 ± 0.166	2.16 ± 0.07	0.405 ± 0.061	28.55 ± 0.43
GLU 1000 nmol	33.3	5.47 ± 0.698	2.13 ± 0.25	0.422 ± 0.050	27.64 ± 3.33
GLU 5000 nmol	166	5.82 ± 0.182	1.98 ± 0.03	0.430 ± 0.015	26.87 ± 0.92†

* denotes where added organic material at a L: Fe ratio of 1.4 was significantly different from seawater

Dextran - all concentrations at both temperatures were significantly different from seawater.

Glucuronic acid – all concentrations at 22 °C were significantly different from seawater.

†Only 5000 nM (L:Fe = 166) was significantly different from seawater at 4 °C

4.2.7 Effect of EPS on phytoplankton growth and Fe bioavailability

The relative bioavailability of Fe associated with EPS (Fe-EPS) to the Southern Ocean diatom *C. simplex* was determined by comparing the uptake rate constants associated with each Fe-EPS incubation to that of the inorganic Fe incubation. In all Fe-EPS treatments Fe bioavailability to the Southern Ocean diatom *C. simplex* was > 50% (Table 4.8). In the treatments containing Fe-EPS from *P. antarctica* and *E. huxleyi* bioavailability was calculated to be > 100% (Table 4.8), suggesting a greater bioavailability of these Fe-EPS complexes than even inorganic Fe.

Growth rates calculated between 48 and 118 h, where all incubations were still in the exponential growth phase. This revealed that only the unamended seawater and the *C. simplex* incubated with Fe-EPS isolated from *E. huxleyi* were not significantly different to the inorganic Fe addition; all others showed a clear increase ($p \leq 0.03$, Table 4.8). After 141-h incubation, the *C. simplex* in the inorganic Fe and unamended seawater had clearly started to enter stationary growth phase. Whilst all treatments where Fe-EPS had been added, regardless of EPS origin, continued in the exponential growth phase for a further 24 to 48-h (Fig. 4.5A). Final cell densities showed that phytoplankton biomass (cells mL^{-1}) in all incubations containing Fe-EPS were significantly higher than inorganic Fe ($p \leq 0.03$, Table 4.8).

At T0, the F_V/F_M of the *C. simplex* cells was sub-optimal at 0.21 (Fig. 4.5B). A significant increase ($p < 0.05$) in F_V/F_M was measured in all treatments at 25-h, 48-h and 71-h reaching a maximum of 0.64 to 0.68 before steadily declining throughout the remaining time of the experiment. Despite the decline, final F_V/F_M measurements were still improved from T0 at 0.4 to 0.45. F_V/F_M did not differ significantly between treatments at any point during the experiment.

Table 4.8 The effect of Fe associated with EPS (Fe-EPS) on the growth of the Southern Ocean diatom, *C. simplex,* over 187-h incubation at 4 °C and 50 µmol photons m^{-2} s^{-1}. Fe concentration in the Tasman Sea surface seawater medium was 0.56 nM. The growth of *C simplex* in the presence of Fe bound to EPS was compared to both inorganic Fe and seawater control. Growth rate (µ d^{-1}, calculated between 48-h and 118-h when all incubations were in exponential growth phase), final biomass at 187-h (cells ml^{-1}), and the bioavailability (in %) of Fe-EPS relative to inorganic Fe (assumed 100% bioavailable) is presented. Additions of Fe-EPS and inorganic Fe provided an additional 1 nM Fe to the seawater medium. EPS isolates were from an Antarctic sea ice bacteria, a natural phytoplankton bloom from the sub-Antarctic zone (SAZ bloom), and from axenic algal cultures of *Phaeocystis antarctica and Emiliania huxleyi.* Errors represent the standard deviation of triplicate samples.

Fe Source	Growth rate (µ d^{-1})	Final biomass at 187 h (cells mL^{-1})	Bioavailable Fe (%)
Seawater control	0.40 ± 0.04	$1.66 \times 10^{+5} \pm 3.07 \times 10^{+4}$	
Inorganic Fe	0.40 ± 0.11	$1.75 \times 10^{+5} \pm 5.29 \times 10^{+3}$	100
Sea ice bacteria	0.43 ± 0.01 **	$2.34 \times 10^{+5} \pm 2.42 \times 10^{+4}$ *	88
SAZ bloom	0.45 ± 0.02 **	$2.25 \times 10^{+5} \pm 1.41 \times 10^{+4}$ *	50
Phaeocystis antarctica	0.44 ± 0.02 **	$2.18 \times 10^{+5} \pm 1.98 \times 10^{+4}$ *	122
Emiliania huxleyi	0.43 ± 0.03	$2.25 \times 10^{+5} \pm 2.70 \times 10^{+4}$ *	111

* indicates significant difference from inorganic Fe p = <0.03

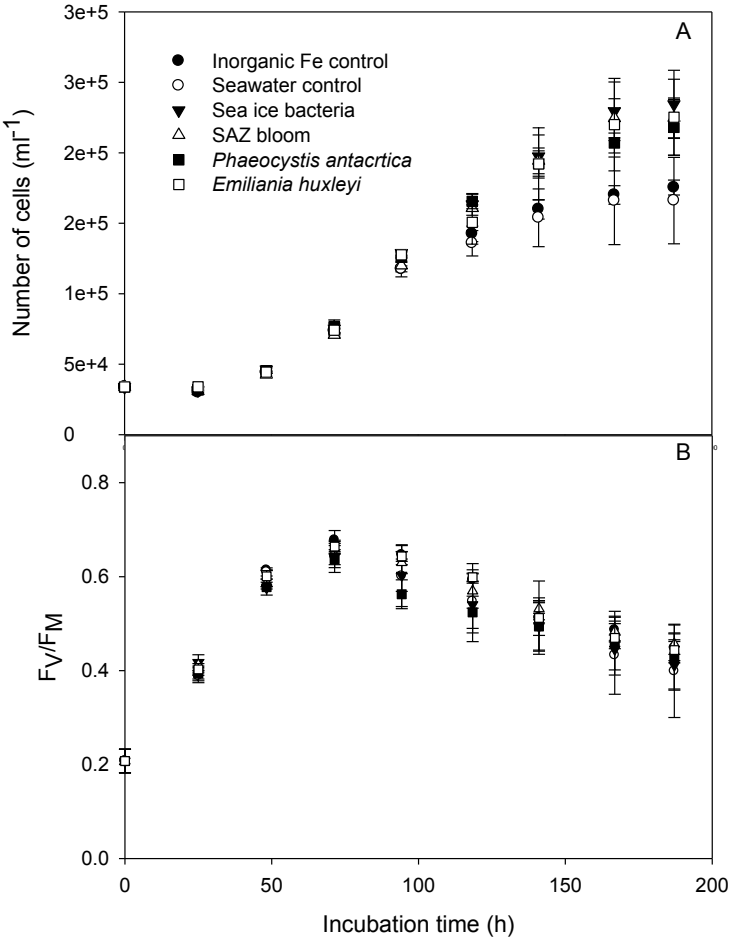

Fig. 4.5 The effect of Fe associated with EPS (Fe-EPS) on the growth of the Southern Ocean diatom, *C. simplex,* over 187-h incubation at 4 °C and at 50 µmol photons m^{-2} s^{-1}. Growth curve in terms of cells numbers (A) and maximum quantum yield (F_V/F_M, B) are presented. Fe concentration in the Tasman Sea surface seawater (seawater) medium was 0.56 nM. The growth of *C simplex* in the presence of Fe bound to EPS was compared to both inorganic Fe and seawater control. Additions of EPS and inorganic Fe provided an additional 1 nM Fe to the seawater medium. EPS isolates were from an Antarctic sea ice bacteria, a natural phytoplankton bloom from the sub-Antarctic zone (SAZ bloom), and from axenic algal cultures of *Phaeocystis antarctica and Emiliania huxleyi*. Error bars indicate standard deviation, *n*=3.

4.3 Discussion

4.3.1 Functional and molecular composition of EPS

Functional analysis revealed that all EPS contained uronic acids, neutral sugars and saccharides, which have been shown to weakly bind Fe and/or adsorb to Fe oxyhydroxides thereby preventing aggregation and, as a result, enhancing Fe reactivity and bioavailability (Croot & Johannson, 2000; Sreeram et al., 2004; Hassler and Schoemann, 2009; Benner, 2011; Hassler et al., 2011a, b). The sea ice bacterial EPS yielded similar relative concentrations of uronic acid and neutral sugar to EPS isolated from a pelagic bacterium (20% and 51%, respectively) grown under the same conditions (Hassler et al., 2011a; Mancuso Nichols et al., 2004, 2005). Additionally, in common with the sea ice bacterial EPS of this study, the pelagic bacterial EPS was also found to be of a high molecular mass (HMM; 2.48MDa, number average molar mass). The two cultured algal EPS isolates from *P. antarctica* and *E. huxleyi* had strikingly similar relative concentrations of uronic acid and neutral sugar, and all algal EPS were predominantly of low molecular weight (LMW), remaining after filtration on 0.45-µm. As with the bacterial EPS, the average number molar mass of the EPS from the two cultured algal isolates, *P. antarctica* and *E. huxleyi*, were very similar. The slightly higher average number molar mass of the SAZ bloom EPS may be indicative of the variability of material in the mixed community.

Direct comparisons between the bacterial and algal EPS are not possible as different growth media were used for the cultures. However, the difference in dominant molar mass between bacterial (HMM) and algal (LMM) EPS is interesting, as it suggests that there are compositional differences. Here again though, these comparisons should be viewed with caution as the molecular cut-off used for the bacterial EPS was different to that used for the algal EPS. The operational filtration made at 0.45-µm before injection should have removed undissolved material from the algal and SAZ bloom EPS. This at least indicated that the behaviour of algal EPS and other EPS are not the same in water and definitively rely on their different physico-chemical characteristics, properties and composition.

The molar mass distribution ($Đ_M$) of ~ 2 indicates that all EPS measured here have a non-uniform distribution; this was also the case for the pelagic bacteria measured by Hassler et al. (2011a) which had a $Đ_M$ 1.9. Considering the range of components that make up EPS, this heterogeneity is expected. The low absorbance *Mp* observed in both the *P. antarctica* and *E. huxleyi* EPS indicates that the majority of UV-absorbing compounds were of LMM, whilst

the occurrence of two peaks in the SAZ bloom EPS is likely indicative of a mixed community with a range of UV-absorbing compounds.

The distribution of Fe reflected the difference in molecular size of the algal and bacterial EPS, with the algal EPS Fe being associated with components with smaller hydrodynamic *radii* (R_h), for the most part < 10-um, than the bacterial EPS. The R_h of the three populations found in the sea ice bacteria EPS in this study (peaks at 26 nm, 40 nm and 60 nm) again compare very well with those obtained for the pelagic bacteria studied by Hassler et al. (2011a), who used a similar cross-flow analytical set-up, where R_h at peak maximum of 17-nm, 40 nm, and 55 nm were observed.

The EPS from the sea ice bacteria used in this study, and that from the pelagic bacteria used in the study of Mancuso Nichols et al (2004, 2005) and Hassler et al. (2011a), show similarities in functional and structural compositions, as do the two cultured algal isolates (*P. antarctica* and *E. huxleyi*) with each other, and suggests that these similarities may be common feature rather than an isolated observation. However, analysis of further bacterial and algal EPS isolates from different strains/species would be required in order to reveal any clear overriding similarities.

4.3.2 Association of EPS with macronutrients and trace elements

Inputs of atmospheric dust are known to periodically be deposited into the SAZ region (Bowie et al., 2009; Mongin et al., 2011; Cropp et al., 2012). The relatively high concentrations of Al, Mn, Pb and Cd measured in the SAZ bloom EPS, compared to those measured in the cultured algal EPS may, therefore, be the result of contamination from particulate matter from the surrounding waters in the SAZ (i.e. from colloidal clay particles), although dFe profiles (Hassler et al., 2014) did not provide evidence of enrichment of trace elements into surface waters of the sampling region. For the laboratory cultures, the growth media used for algal culture contained comparatively high concentrations of nutrients in order to attain sufficient biomass and it is possible that some of these nutrients may have been scavenged on to the EPS during culture. However, EPS is known to contain strong metal-binding groups and has the ability to form complexes with a wide variety of metals (Fe, Zn, Cu, Cd, Co, Mn, Mg, Ag, Ni, Pb) (Decho, 1990; Douchet et al., 2007). The association of EPS with nutrients in this study, and also in bacterial EPSs studied by Hassler et al. (2011b) and Gutierrez et al. (2012), may indicate that EPS not only have the ability to bind Fe, but also a suite of other constituents that are essential to phytoplankton growth. Hassler,

Norman et al. (in press) calculated a substantial enhancement of Zn, Co, and Cu, in field incubations that had been enriched with pelagic Southern Ocean bacterial EPS (Mancuso Nichols et al., 2004, 2005; Hassler et al., 2011a, b). The study (Hassler, Norman et al., in press) also observed an increase in NO_X concentration in bacterial EPS enriched incubations which was approximately 15-fold greater than that measured *in situ* in the low nutrient/low chlorophyll Tasman Sea (Hassler et al., 2014). The observations of Hassler, Norman et al. (in press) suggest that EPS may be efficient at sequestering/scavenging macronutrients, as well trace metals, from the water column. However, macronutrients are mainly anionic and are therefore unlikely to bind to EPS via the same mechanism as cationic trace elements, due to the net negative charge of EPS at the pH of seawater (McCarthy et al., 1996). For this study, direct comparison as to the acquisition efficiency of each EPS was not possible as the concentration of trace elements and macronutrients in solution varied between media and would be greatly enriched compared to *in situ* concentrations.

4.3.3 Effect of EPS on Fe biogeochemistry

The conditional stability constants in respect of inorganic Fe'-binding (log K'_{FeL}) of all EPS in this study fall within the range of previous open ocean measurements (log K'_{FeL} = 11 to 13.5 - Rue & Bruland, 1995, 1997; Boyé et al., 2001, 2005; Cullen et al., 2006; Frew et al., 2006; Kondo et al., 2008; Ibisanmi et all, 2011; see also table 1.1, chapter 1), suggesting that both bacterial and algal EPS are significant contributors to the organic ligand pool, particularly in the L_2 ligand class. In all EPS, except for the SAZ bloom, a smaller component of ligands, that would comparable to what is operationally defined as a L_1 class, or strong ligand ($K_{Fe'L} \geq 10^{12}$, Gledhill and Buck, 2012, and refs therein; Rue & Bruland, 1995, 1997), were measured after 24-h pre-equilibration. The contribution of the L_1 ligands to the total Fe-binding ligands measured in the EPS is small compared to the L_2 ligands, and the limited effect that EPS had on Fe(II) oxidations kinetics suggests that very strong Fe(III) binding ligands were absent. However, the $K_{Fe'L}$ measured for the L_1 ligands are also similar to that measured for bacterially produced siderophores (Vraspir and Butler, 2008 and refs therein), which are considered a key players in Fe complexation.

Although the log $K_{Fe'\Sigma L}$ were slightly higher in the aged (9-wk pre-equilibration) samples compared to the 24-h pre-equilibrated samples in all cases, except for the SAZ bloom, the stronger L_1 ligands measured in the sea ice bacterial EPS and *E. huxleyi* EPS after 24-h pre-equilibration were absent. This, together with lower measured concentration of ligands ([ΣL]), likely due, in part, to bacterial consumption during the aging period, suggests that all

ligands, both L_1 and L_2 classes, are degraded over time and likely to be highly reactive in surface waters. Despite the reduction in ligand concentration, Fe_{Labile} measured in the sea ice bacteria and *P. antarctica* was reduced after 9-wk compared to 24-h pre-equilibration, suggesting a stronger Fe-EPS association. This behaviour was also observed by Hassler et al. (2011a) in experiments using EPS isolated from a pelagic Southern Ocean bacteria, where [Fe_{Labile}] after 24-h pre-equilibration was 2.97nM but was decreased to 0.74 nM after 9-wk pre-equilibration. A control sample using unamended Southern Ocean seawater gave similar results ([Fe_{Labile}] = 2.92 nM and 0.84 nM after 24-h and 9-wk pre-equilibration, respectively). In addition, upon measurement by CLE-AdCSV both the samples containing EPS and the control displayed decreased sensitivity after 9-wk pre-equilibration compared to 24-h, a factor also observed during this experiment. The authors concluded that the decrease in sensitivity could not entirely be explained by the formation of inorganic Fe oxide, and Fe-EPS interaction also likely contributed (Hassler et al., 2011a).

In the sample containing EPS from the SAZ bloom, which had the lowest log $K_{Fe'\Sigma L}$ and high percentage of Fe_{Labile} after 24-h pre-equilibration, measurement by CLE-AdCSV did not detect any organic ligands after 9-wk pre-equilibration. Presumably any organic ligands present were too weak to be detected within the analytical window of the method. This loss of ligands suggests that the material in this 'mixed origin' sample maybe highly reactive in the natural environment; however, despite this, the importance of this material should not be overlooked. When compared to an *in situ* sample collected on the same day and location as the sample collected for EPS isolation, it was calculated that EPS (both bacterial and algal) likely accounted for the majority of organic ligands measured in the SAZ (*in situ*), and that the contribution of HS-like material from EPS can represent a substantial proportion of that measured in the euphotic zone, in this case ~ 14 % (Norman et al. in press).

The ability for organic ligands to outcompete others for Fe-binding is determined by both their concentration and conditional stability constant (Morel and Herring, 1993). Given the high log $K_{Fe'L}$ and/or high concentration of organic Fe-binding ligands measured for the *P. antarctica*, *E. huxleyi* and SAZ bloom EPS after 24-h incubation, this suggests that algal EPS may be particularly effective in competing for Fe in the presence of Fe-binding organic ligands. However, the mechanism by which both bacterial and algal EPS bind Fe is still unresolved. The conditional stability constants measured here are greater than those that have been measured for known functional components of EPS, i.e. uronic acid and, as such, may bind a portion of the Fe(III) present. In addition, the EPS may adsorb to very small Fe oxyhydroxide particles, resulting in prevention of aggregation of these particles thereby increasing Fe bioavailability. It is noteworthy that heme signatures, which have been

suggested as Fe-binding ligands (Gledhill and Buck, 2012) were not detected in any of the EPS isolates from this study.

The ability of organic ligands to improve and maintain Fe solubility in marine waters is well known (Johnson et al., 1997, Boyd and Ellwood, 2010), although mostly the organic ligands responsible for this behaviour are not identified. However, this study has shown both bacterial and algal EPS improve Fe solubility/filterability of both soluble and colloidal Fe. Furthermore, Fe solubility (or filterability as it recognised that the EPS may have acted to prevent aggregation of Fe oxyhydroxides), in the presence of algal EPS was greater in the colloidal fraction than that observed in the soluble fraction. This has important implications for Fe cycling in natural waters. Past studies have shown that colloidal Fe is often much more abundant in surface waters than soluble Fe, and despite the fact the soluble Fe is generally considered to be more biologically available to phytoplankton (Wu et al, 2001; Boye et al, 2010), there is some evidence that Fe bound to reactive newly formed colloids, particularly those of LMM, may be bioavailable to some phytoplankton (Chen & Wang, 2001; Chen et al., 2003). In addition, the aggregation and settling behaviour together with scavenging of colloidal Fe may in fact enhance Fe removal from surface waters (Wu et al., 2001; Boye et al. 2010).

Shipboard measurements of Fe(II) concentration have indicated slower than expected oxidation in some oceanic regions (Croot and Laan, 2002; Hansard et al., 2009, Roy et al., 2008). This has been attributed to low temperature, the presence of low concentrations of the oxidant H_2O_2 and/or the presence of Fe(II) binding organic ligands, although evidence of specific Fe(II) binding ligands in seawater is still debated (Croot and Laan, 2002; Roy et al, 2008; Miller et al., 2012). In this study, the Fe(II) half-life of the amended (i.e. EPS or model ligand added) and unamended 0.2-µm-filtered seawater measured at 22 °C were within the range of the 2-to 3-min predicted for seawater at pH 8, (15 and 25 °C; Millero et al. 1987). However, as shown in previous studies (Millero and Sotolongo, 1989; Croot et al., 2001, Roy et al., 2008), when measured at 4 °C the rate of Fe(II) oxidation slowed considerably, in this case extending the Fe(II) half-life to 30-min.

Much emphasis has been placed on the ability of organic ligands to slow Fe(II) oxidation, thereby, maintaining the availability of Fe(II) to phytoplankton for a longer period of time. In this study, a retardation in rate of Fe(II) oxidation was not observed. Indeed, in the presence of dextran, glucuronic acid or *E. huxleyi* EPS, Fe(II) oxidation was enhanced, and the presence of bacterial EPS and *P. antarctica* EPS had no effect. This may be evidence that

none of the EPS isolates or model ligands were binding Fe(II) to any measureable degree, or possibly that the complexes formed underwent rapid oxidation.

Variability in the effect of organic material on Fe(II) oxidation is not unusual. Under laboratory conditions, in NaCl solutions or seawater, the synthetic ligand ethylene glycol tetraacetic acid (EGTA) was observed to completely inhibit oxidation, salicylic acid decreased oxidation, but phthalic acid and ethylenediaminetetraacetic acid (EDTA, synthetic ligand) enhanced Fe(II) oxidation. Alanine and glutamic acid had a negligible effect (Santana-Casiano et al., 2000, 2004). Additionally, the same compound may behave differently depending on the experimental, or environmental, conditions to which it is subjected. For example, at pH 6, citrate has been shown to enhance Fe(II) oxidation, but at a higher pH (i.e. pH 8) Fe(II) oxidation decreased (Pham and Waite, 2008). This variation may be due to the stability of the Fe(III)-ligand complex formed; e.g. stronger complexes may enhance Fe(II) oxidation (T.D. Waite, pers comm), although the mechanism for this is not known, or that the organic ligand used mediated the production of an Fe(II) oxidant (i.e. H_2O_2 and superoxide).

In natural seawater from the sub-Arctic Pacific, Roy et al. (2008) demonstrated that, in UV-treated seawater, the half-life of Fe(II) was shorter than that measured in unamended seawater and that this behaviour was consistent over a range of temperatures (5 to 25 °C), indicating that the presence of organic ligands was retarding Fe(II) oxidation. However, a further study by Roy and Wells. (2011), again in the sub-Arctic Pacific, revealed a contrasting result where accelerated Fe(II) oxidation was observed in unamended seawater. The authors noted a clear relationship between enhanced Fe(II) oxidation and phytoplankton biomass, as this effect was most clearly apparent in the region of the chlorophyll maximum. They concluded that the presence of biologically produced strong Fe(III) binding ligands, specifically bacterially produced siderophores, may have been responsible for the increased Fe(II) oxidation rates.

Similarly, Millero et al (1987) observed that the half-life of Fe(II) in outflowing Biscayne Bay waters was two to five times greater than those found in Gulf Stream waters. This behaviour was attributed to the concentration of variable levels of organic ligands in the Bay waters, and that LMM ligands were partly responsible for this. Enhanced Fe(II) oxidation was certainly apparent in the presence of *E.huxleyi* EPS at both 22°C and 4°C; however, no significant effect was observed in the presence of SAZ bloom EPS or bacterial EPS at the excess ligand concentration used. Due to a limited amount of isolate in both cases, it was not possible to increase the concentration of EPS present, and so it is not possible to ascertain

whether a larger excess of these EPS would have resulted in a similar enhancement of Fe(II) oxidation. However, enhanced Fe(II) oxidation might be expected in the presence of a relatively strong Fe(III)-binding organic ligand, or Fe(II) oxidant (i.e. H_2O_2 and superoxide). Both the *E. huxleyi* and *P. antarctica* EPS were associated with L_1 and L_2 ligands, the stronger of which may have promoted the accelerated Fe(II) oxidation observed with the *E. huxleyi* EPS. Analysis for the presence of significant Fe(II) oxidising products was not conducted, nor was sufficient *P. antarctica* EPS available to enable further investigation of oxidation rate kinetics. Thus, the idea that the L_1 ligand components of EPS may, like siderophores, be responsible for Fe(II) removal cannot be confirmed without further experiments.

Although there was no evidence to suggest that EPS can enhance Fe (III) reduction in this study, previous studies have shown that high concentrations of (poly)saccharides, a ubiquitous component of bacterial and algal EPS, can enhance Fe(III) reduction through the production of photochemically produced superoxide (Rose et al., 2005; Morel et al., 2008; Steigenberger et al., 2010). More detailed experiments are required to confirm the role of EPS in Fe(III) reduction. It is possible that, like other forms of organic material, for example coloured dissolved organic matter, photochemically mediated transformations of EPS may be a pathway for the production of Fe(II).

4.3.4 Effect of EPS on phytoplankton growth and Fe bioavailability

All EPS used in this study resulted in Fe which was highly bioavailable to the Southern Ocean diatom *C. simplex,* a response also observed for Fe associated with saccharides (Hassler et al., 2011a, b). The Fe associated with the SAZ bloom EPS was the least bioavailable (although still 50%), which may be indicative of the varying composition of EPS within the sample; e.g. compositional differences in the EPS produced by the different strains/species present and also compositional changes by the same species during the various phases of the bloom . For comparison, all Fe-EPS from the phytoplankton isolates used in this study proved to be more bioavailable than the siderophore DFB (9%) and ferrichrome (7%, C. Hassler Pers. comm.), and all but the Fe-SAZ bloom EPS were more bioavailable than protoporphyrin IX (70%) and the polysaccharide dextran (84%, Hassler et al. 2011b). Hassler et al. (2011b) conducted similar bioaccumulation experiments using pelagic bacterial EPS and found the Fe associated with this EPS was 28% bioavailable. This is less than the Fe bound to the sea ice bacterial EPS used in this study, but the fact that the algal EPS is more bioavailable to *C. simplex* may be an indication that eukaryotic phytoplankton can more readily utilise algal material rather than bacterial material. However, Fe bound to

bacterial EPS was more accessible than bacterial-siderophore-bound Fe, which has been shown to be mostly poorly available to phytoplankton (Hassler and Schoemann, 2009; Buck et al., 2010). The enhanced bioavailability of EPS-bound Fe demonstrated here is likely due to improved Fe solubility and the possible formation of Fe species that are bioavailable to *C. simplex* (Hassler et al., 2011b).

During the growth experiments, the incubations to which Fe-EPS had been added showed a prolonged period of exponential growth, between 24 and 48 h longer, and an enhanced biomass compared to the incubations where Fe was supplied as unbound inorganic Fe. From these experiments, it is clear that Fe bound to EPS sustained the uptake and growth of *C. simplex*, and relieved Fe stress from a previously Fe-limited culture (Hassler, Norman et al., in press). This effect appears not to be limited to single species laboratory experiments. Field experiments using two natural phytoplankton assemblages, one from the Tasman Sea and the other from the SAZ, demonstrated that the addition of EPS isolated from a pelagic bacteria was highly bioavailable and promoted the growth of two very different phytoplankton communities (Chapter 3 of this thesis; Hassler, Norman et al., in press). The enhanced growth from Fe-EPS complexes compared to inorganic Fe is to be expected, as the EPS will maintain the Fe in a less aggregated and potentially more bioavailable form. Using F_V/F_M as an indicator of cell health, the sub-optimal T0 value likely reflects the fact that the *C. simplex* cells were Fe limited at the start of the experiment, as was desired. All incubations, regardless of treatment, improved their F_V/F_M as the added Fe became available, with the Fe-EPS treatments comparing extremely well with the inorganic Fe addition.

4.4 Conclusion

Until now EPS have been an under-studied group of Fe-binding organic ligands. This study has highlighted many, previously unknown, functional and molecular properties of bacterial and algal EPS, as well as demonstrating the significant effect that EPS may have on Fe biogeochemistry. Much of the previous research investigating bioavailability and Fe complexation with organic ligands has focused on bacterially produced siderophores. This study shows that Fe bound to EPS enhances Fe solubility (and/or perhaps prevents Fe oxyhydroxide aggregation). It is likely to have the capacity to compete for Fe with bacterially produced siderophores, due to both the high binding affinities and the concentrations at which Fe-binding ligands associated with EPS occur, but may also enhance the removal of

Fe(II) from surface waters. Moreover, EPS-bound Fe appears to be more bioavailable to phytoplankton, both under laboratory conditions and to natural phytoplankton communities, than siderophore-bound Fe (Hassler, Norman et al., in press).

The association of EPS with other vital macronutrients and trace elements may have important biogeochemical implications for phytoplankton in nutrient-poor regions of the ocean where primary productivity is limited by nutrients other than Fe (i.e. other trace elements, N, P and Si). Laboratory experiments have shown that the rate of EPS production increases in some diatom species under N and/or P limitation, although the rate of production varies considerably between species (Myklestad, 1995; Penna, 1999).This indicates that EPS may also play a role in sequestering macronutrients from the water column, although, as stated above, the mechanism for this remains unknown, and thus, the production and function of EPS may help to alleviate a degree of nutrient stress. In addition, measurements of bacterial abundance and remineralisation of DOM and DOC during phytoplankton blooms and non-bloom periods indicates that EPS may also provide heterotrophic bacteria with a source of organic carbon (Amon and Benner, 1994, 1996; Morán et al., 2001; Obernoster et al., 2008). This cannot be over-looked as Fe remineralised through the grazing and viral lysis of bacteria has been found to be highly bioavailable to phytoplankton and may make a substantial contribution to the dFe pool in remote ocean regions (Hutchins & Bruland., 1994; Barbeau et al., 1996; Poorvin et al., 2004; Strzepek et al., 2005; Sarthou et al., 2008).

Whilst siderophores are an extremely important part of the organic ligand pool, this study demonstrates that the role of EPS in Fe biogeochemistry, and consequently Fe bioavailability, is also significant. In order to further our understanding of the dynamics of Fe-limited oceans, and also improve existing biogeochemical models so that oceanic carbon fixation can be accurately predicted, the role of both bacterial and algal EPS in Fe biogeochemical cycling deserves further consideration.

CHAPTER 5:

OCEANIC IRON ENRICHMENT FROM AUSTRALIAN MINERAL DUST: FROM CHEMISTRY TO BIOAVAILABILITY.

Note and acknowledgements

The data presented in this chapter were obtained from a set of dust enrichments experiments conducted at UTS and the University of Geneva by myself and Prof. Christel Hassler. Analyses that I carried out myself were: Fe chemical speciation, Fe-binding humic substance-like (HS-like) material, macronutrients, and total hydrolysable saccharides. I also assisted Prof. Hassler with the analysis of Fe size fractionation, Fe solubility, bioavailability and phytoplankton growth experiments. I am grateful to colleagues listed below who provided materials, analysis, data, and methodologies.

Prof. Grant McTainsh (Griffith University, QLD) – Providing the processed dust.

Dr Michael Ellwood (ANU) – Total metal analysis.

Dr. Laurie Burn-Nunes (Curtin University, WA) – Collection and provision of rainwater.

Dr. Veronique Schoemann (University of Brussels) – Determination of total acidic leachable Fe present in the dust.

5.0 Introduction

Atmospherically transported continental dust is a major source of iron (Fe), as well as a source of other macronutrients (nitrogen (N) and phosphorous (P)) and trace elements (i.e. Zn, Cu) (Baker et al., 2003, 2007; Buck et al., 2013), and represents the largest global input of Fe deposited into the oceans (Duce & Tindale, 1991, Jickells et al., 2005, Mahowald et al., 2005). However, dust inputs into the South Pacific and Southern Ocean regions are highly episodic due to the seasonal variability of wind patterns, storm events and precipitation (Mackie at al., 2008). The primary dust source for these ocean areas is thought to be the arid regions of Australia (Duce & Tindale, 1991; Jickells et al., 2005; Li et al., 2008), which model estimates predict provide approximately 100 - 120 Tg y^{-1}, or ~5% of the total global dust input (Li et al., 2008; Mitchell et al., 2010). However, most of the dust is deposited into the South Pacific with just a small fraction (~7 Tg Y^{-1}) transported to the Southern Ocean (Li et al., 2008).

Many factors influence the bioavailability of dust-borne Fe to phytoplankton, both before it enters the ocean and after. At source, the geology and soil types vary with region, as do wind erosion properties, the proportion of anthropogenic material, and more importantly, the Fe content (McTainsh et al., 1990; Fung et al., 2000; Mackie et al., 2008). This gives rise to varying proportions of reactive and refractory Fe (Mackie et al., 2008), which in turn determines Fe solubility (Sholkovitz et al., 2012).

Once in the atmosphere, the dust particles are exposed to a number of poorly characterised physical and chemical processes during transport which can determine the solubility and species of Fe delivered to the ocean. For example, during cloud processing the particles are repeatedly exposed to low pH conditions (pH 1 to 5, Jickells and Spokes, 2001), increasing the lability of the Fe-(hydr)oxides contained in the aerosols (Spokes and Jickells, 1996). In addition, exposure to UV radiation initiates photochemical reduction of both particulate and colloidal Fe(III) (hydr)oxides, to Fe(II) (Jickells and Spokes, 2001). Fe-binding organic ligands, such as formate, acetate, oxalate, and humic substances (contained in the soil/crustal material) have been reported to be present in cloud and rain water and atmospheric aerosols (Erel et al., 1993; Pehkonen et al., 1993; Hegg et al., 2002; Willey et al., 2008; Paris and Desboeufs, 2013). Also relevant to Fe availability once the dust is deposited into the ocean, is complexation with organic ligands. This complexation has been shown to aid the production of the reductant H_2O_2, and the photochemical reduction of Fe(III) to Fe(II) (Baker and Croot, 2010), and also to retard the oxidation of Fe(II) for several hours (Willey et al., 2008).

Deposition into the surface ocean is either via dry deposition (gravitational settling and turbulent deposition), which is the dominant deposition mechanism close to source (Mahowald et al., 2005), or wet deposition (through precipitation events), which is the dominant mechanism in remote ocean regions (Duce and Tindale, 1991; Sarthou et al: 2003; Schulz et al., 2012). Dissolution of Fe into seawater from dry deposition is very low; however, from wet deposition (pH 4 to 7) up to 14% of the Fe may be in solution (Jickells and Spokes, 2001). Thus, wet deposition is considered to be a more efficient way of introducing nutrients into surface water as a significant fraction of the dust is already dissolved in the water droplets (Paris and Desbeoufs, 2013). Dust source, the atmospheric conditions to which the dust particles are exposed, and the mode of supply to the ocean are, therefore, key determinants to the lability of the Fe supplied, and potentially its bioavailability to phytoplankton.

Due to atmospheric processing, dust-borne Fe will be deposited in the surface ocean in both oxidised and reduced forms (Buck et al., 2013). A significant proportion of the Fe deposited is in the form of Fe(II) (Majestic et al., 2007), which has traditionally been considered a highly bioavailable form of Fe (Shaked and Lis., 2012), but Fe(II) oxidises rapidly in seawater to form less biologically available Fe-(oxy)hydroxides (Kuma and Matsunaga, 1995). However, before oxidation occurs much of the Fe will become complexed with organic ligands present in the water column (Gledhill & van den Berg, 1994; Wu & Luther, 1994; van den Berg, 1995; Rue & Bruland, 1995) which, as with the organic ligands present in the atmosphere, have been shown to be extremely important for maintaining Fe solubility (Kuma et al., 1996; Lui & Millero., 2002; Chen et al., 2004). This organic complexation can also enhance the bioavailability of Fe(III) to bacterio- and phytoplankton (Hutchins et al., 1999; Maldonado and Price, 2001; Rose & Waite, 2003; Chen et al., 2004; Maldonado et al., 2005; Hassler et al., 2011b).

A causative link between phytoplankton blooms and dust deposition, particularly in relation to Fe input, is not always clear (Cropp et al., 2013). Elevated dFe concentrations have been reported following large wet deposition events (Hanson et al., 2001); however, the extent of the bioavailability of the newly delivered Fe is generally not known. Some field studies report a positive biological response (Gabric et al., 2002; Moore et al., 2006; Shi et al., 2012), whilst others report very weak or absence of response (Johnson et al., 2003; Boyd et al; 2004; Mackie et al., 2008).

The Southern Ocean represents the largest HNLC region in the global ocean, with dFe generally measured at sub-nanomolar concentrations (Boye et al., 2001, 2005; de Jong et

al., 2008; Lannuzel et al., 2008). In addition, areas where Fe is a co-limiting factor with other nutrients (e.g. N, P, and Si) are known to occur in the Tasman Sea (Sedwick et al., 1999; Hutchins et al., 2001; Law et al., 2011). Australian mineral dust may, therefore, represent an important source of Fe, and other nutrients, for these regions as any increases in dust deposition and Fe supply could have a large effect on Fe-limited phytoplankton (Mahowald et al. (2005). However, little is known about how the Fe delivered with dust affects Fe chemistry in seawater, its bioavailability and its subsequent effect on phytoplankton growth.

Laboratory experiments that examine the chemistry, bioavailability and biological effect of Fe in atmospheric dust are limited. Visser et al. (2003) investigated the impact of dust deposition on the growth rate of two Southern Ocean diatom species (*Thalassiosira* sp. and *Actinocyclus* sp.) using dusts with different physico-chemical properties from Namibia and Mauritania. They reported that the growth rates were positively correlated with the reactivity/dissolution of the Fe in seawater; however, not all of the dissolved Fe was bioavailable to the phytoplankton when compared to inorganic $FeCl_3$ (0.7 to 2 % for *Thalassiosira* sp. and 6 to 30% for *Actinocyclus* sp.).

In the experiments described here, we simulate a wet deposition event(s), typical of remote ocean waters such as the Southern Ocean and Tasman Sea, to investigate the impact of atmospheric dust deposition on the environmentally and geographically relevant Southern Ocean diatom, *Chaetoceros simplex*. This dust was selected not only because it represents dust from a source periodically deposited into the Tasman Sea and Southern Ocean, but also because it was used in a previous study which indicated that it affects the growth of various phytoplankton groups (C. Hassler, unpublished data; Chapter 3). As photochemical transformations play an important role in determining Fe speciation, likely generating bioavailable forms of Fe, the effect of UV exposure on Fe chemistry, together with the bioavailability of the Fe produced was also investigated.

5.1 Materials and methods

For the Fe chemical speciation section, three experiments using the same experimental set-up were conducted. As the results gained from the second experiment were very different from the first, a third experiment was run twelve days later. The results of the third experiment confirmed that it was likely that the first experiment had been compromised (Fe contamination) and so the results presented here are predominantly from the latter two

experiments, referred to as Exp 2 and Exp 3. The data presented are, therefore, from replicate experiments and the results for each experiment are shown separately rather than as pooled data. During the first experiment (Exp 1), analyses for retention of organic material on C_{18} Sep-Pak resin were also undertaken, as were Fe bioavailability and phytoplankton growth experiments. These were conducted in a different medium and were not compromised and, therefore, the data is reported here. Samples were also taken from Exp 2 and Exp 3 and stored in order to repeat the bioavailability and growth experiments. These will be conducted at the University of Geneva upon the acquisition of a suitable ^{55}Fe source.

5.1.1 Experimental procedure and precautions

The mineral dust used in this experiment was collected during a dust storm on 26th September 2009, using a High Volume Air Sampler (HVS) situated on the roof (4th floor) of the Environmental Sciences building at Griffith University, Nathan Campus, Brisbane, QLD, Australia. The source origin of the dust was the Buronga region, NSW. Total acid leachable iron concentration of the dust was determined by ICP-MS, using a dust concentration of 0.50 mg L^{-1} resuspended in 0.2-µm-filtered, Tasman Sea surface water. The sample was acidified (2 mL L^{-1} qHCL, Seastar) for nine months prior to analysis (V. Schoemann, pers comm.), and yielded an iron concentration of 372.1 nM. This acidification pre-treatment was undertaken to solubilise any Fe present. In order to mimic a wet deposition event, the dust was resuspended in rainwater (pH 5.36; Orion 3 star benchtop pH meter), collected in the Tasman Sea (31°35.849'S 178°00.00'E, GP13 GEOTRACES voyage, 27/05/2011). The rainwater contained 1.26 µM Fe (unfiltered; Table 5.1).

The enriched rainwater was then shaken vigorously to disperse, and then left to equilibrate in the dark for 30-min. After equilibration the enriched rainwater was dispensed into 3 acid-cleaned quartz tubes, and the tops sealed with a Teflon cap to minimise metal contamination. To mimic exposure to natural atmospheric radiation, the tubes were exposed to a full light spectrum measured between 250 to 700 nm with a Spectrilight ILT950 spectroradiometer (International light technologies, Peabody, MA, USA) under one of three treatments: (1) 2000 µE with a UV filter (VIS), (2) 2000 µE without UV filter (UV), (3) dark, for 1-h. During exposure the tubes were placed in a water bath to maintain a steady ambient temperature (21–22 °C). After 1-h exposure, the enriched rainwater was then dispensed into synthetic seawater to achieve a final dust enrichment of ~0.50 mg L^{-1} (Exp 2 = 0.56 mg L^{-1}, Exp 3 = 0.52 mg L^{-1}). The dFe originally present in the unfiltered rainwater

accounted for a 2.22 nM dFe (unfiltered) contribution to experimental solution once added to the synthetic seawater medium (Table 5.1). The experimental solutions were then left to equilibrate for a further 30 min before sub-sampling for the analyses and biological experiments detailed below.

All plasticware (LDPE and HDPE bottles, pipette tips, forceps and polycarbonate containers) were cleaned by first soaking in detergent (Citrinox acid detergent, 5% v/v) for 24 h, followed by rinsing five times in deionised water. The plasticware was then soaked for four weeks in 1M HCl, except for polycarbonate bottles, which were soaked for one week to avoid deterioration. The equipment was then rinsed seven times in ultra-pure water (UPW; 18.2 MΩ cm^{-1}, Arium 611UV, Sartorius Stedim, Melbourne, VIC, Australia), and then dried in an ISO Class 5 laminar flow hood. All trace metal clean items were sealed in triple zip lock plastic bags until use. Polycarbonate filters (0.02- and 0.2-µm, 47-mm, nuclepore, Milipore; Merck Millipore, Bayswater, VIC, Australia) were immersed in 1 M ultrapure HCl (Seastar) for one week before gentle rinsing seven times in UPW, and stored in UPW until use. All sample manipulations and reagent preparation was carried out in an ISO Class 5 laminar flow hood. All reagents were made up in UPW unless otherwise stated, and were passed through Chelex-100 resin (BioRad, conditioned as per Price et al., 1989) prior to use to minimise Fe contamination.

Table 5.1. Constituents of synthetic seawater (SS) based on AQUIL media as per Price et al. (1989) using major salts only. Final pH = 8.00. Background dissolved Fe = 0.73 ± 0.02 nM, n = 4

Constituent	Concentration (M)
NaCl	4.20×10^{-1}
Na_2SO_4	2.88×10^{-2}
KCl	9.39×10^{-3}
$NaHCO_3$	7.14×10^{-3}
KBr	8.40×10^{-4}
H_3BO_3	1.46×10^{-3}
NaF	7.14×10^{-5}
$MgCl_2*6H_2O$	5.46×10^{-2}
$CaCi_2*2H_2O$	1.05×10^{-2}
$SrCl_2*6H_2O$	6.38×10^{-5}

5.1.2 Analytical procedures

5.1.2.1 Trace element determination in atmospheric dust and rainwater

Trace elements (Fe, Cu, Zn, Ni,) were determined in 0.2-µm and-0.02 µm filtered samples by ICP-MS (Element XR, Thermo-scientific, Australia), using organic extraction with isotope dilution based on the method of Sohrin et al. (2008) but using Toyopearl AF-Chelate-650M resin in place of Nobias Chelate-PA1 resin, as per Milne et al (2010). Samples were spiked with enriched isotopes of ^{57}Fe (>95%), ^{67}Zn (>90%), ^{65}Cu (>99%), and ^{61}Ni (>99%). The sample pH was buffered to around 7.0 which helped to overcome Mo loading on the resin, thereby reducing Mo interferences. All samples were spiked with an internal standard (Sc, Yb and In) that was used as a check on resin performance. The detection limits for Fe, Zn, Cu and Ni are estimated to be 0.05, 0.02, 0.02 and 0.1 nM for these elements, respectively.

5.1.2.2 Chemical speciation of Fe-binding organic ligand complexes in wet deposited atmospheric dust and rainwater

Iron speciation of 0.2-µm and 0.02-µm filtered samples was measured by Competitive Ligand Exchange Adsorptive – Cathodic Stripping Voltammetry (CLE-AdCSV) following the method of Croot and Johannson (2000). The instruments used were µAutolab II and III potentiostat (Ecochemie, Utrecht, Netherlands) with a hanging mercury (Hg) drop electrode (Hg, Sigma Aldrich, ACS reagent grade, 99.9995% trace metal basis; HMDE drop size 2, 0.4 mm^2 ±10%, VA 663 stand – Metrohm, Herisau, Switzerland), a glassy carbon rod counter electrode, and a double junction, Ag/AgCl, reference electrode with a salt bridge filled with 3M KCl. The instruments were controlled using GPES software, version 4.7. The sample were prepared as detailed in Chapter 3 (p. 82). The Fe titration range was 0 to 24 nM for these analyses. The detection limit of the instruments was 0.05 nM and 0.04 nM Fe determined from 3 times the standard deviation of repeated measurements of a Southern Ocean seawater sample (n=8 for both instruments). The conditional side-reaction coefficient between Fe and TAC in synthetic seawater ($\alpha Fe'(TAC)_2$) of 210 was used to calculate ligand concentration and conditional stability constants ($K_{Fe'L}$) calculations (Hassler et al, 2011b).

5.1.2.3 Assessment of organic material in atmospheric dust and rainwater

Assessment of the nature of the organic material associated with the rainwater and dust was determined by the solid-phase extraction method developed by Abbasse et al (2002) using Sep-Pak C18 cartridges (Waters), as described in Hassler et al. (2009). For these analyses, unfiltered samples were spiked with radiolabelled iron (^{55}Fe, as $FeCl_3$ in 0.5M HCl, Perkin Elmer) at a final activity of 0.7 nCi/mL, corresponding to 0.6-nM iron addition, and then left to equilibrate for 24-h in the dark at 4 °C. After equilibration, the samples were filtered through 0.2- and 0.02-um syringe filters (0.2-µm – Millipore, 25 mm; 0.02-µm – Whatman Anatop, 25 mm). Prior analysis, the C_{18} cartridges were preconditioned by successive passages of 10-mL of 100% methanol (ACS reagent, Sigma Aldrich), 10 mL of ultra-pure water (UPW, 18.2 $M\Omega cm^{-1}$, Arium 611UV, Sartorius Stedim) 10-mL of 2 M nitric acid (ACS grade), 20-mL of UPW, and 15-mL of 0.01 M ammonium acetate, at a flow rate of 6 – 7-mL min^{-1}. After preconditioning, 10-mL of sample was passed through the cartridges at a flow rate of 3-4-mL min^{-1}. The resin was then rinsed with 10-mL of ammonium acetate (0.01 M), to remove the saline matrix, and the retained Fe was eluted with 10-mL of nitric acid (2 M). Finally, any remaining organic ligands were eluted with 5-mL of 100% methanol. Two mL of each of the radiolabelled solutions were collected in 20-mL scintillation vials, to which 10-mL of scintillation cocktail was added (Ultima Gold, Perkin Elmer). The samples were vortexed, and measured using a liquid scintillation counter (Perkin Elmer, Tri-carb 2810 TR). A mass balance considering all fractions compared to initial radioactivity demonstrated an Fe recovery of 112 ± 6 % (n=8).

5.1.2.4 Analysis of humic substances-like material in atmospheric dust and rainwater

Humic substance-like material (HS-like) in unfiltered, 0.2-µm and 0.02-µm-filtered samples was determined using the voltammetric method of Laglera et al. (2007), and as detailed in Chapter 2 (p. 36). For these analyses, the final pH of the samples was 8.21. Analysis of an unamended sample (i.e. no Suwannee River Fulvic Acid (SRFA) added) indicated that the background concentration of HS-like material was very low, and so a purge time of 250 s and adsorption time of 300 s was used. The detection limit of the instruments was 1.49 µg L^{-1} and 1.36 µg L^{-1} determined from three times the standard deviation of ten repeated measurements of an unamended Southern Ocean seawater sample using the same purge and deposition times as for the samples.

5.1.2.5 Total saccharides analysis of atmospheric dust and rainwater

Total hydrolysable saccharide concentration was determined semi-quantitavely in the 0.2- and 0.02-µm-filtered samples from each treatment (UV, VIS, Dark), and also rainwater in synthetic seawater (experimental dilution). Analysis was conducted as detailed in Chapter 4 (p. 130) using the colorimetric method of Myklestad et al (1997). The detection limit of the method was 0.07 mg glucose equivalents L^{-1} (2.5 µmol C L^{-1}) calculated as three times the standard deviation of the lowest calibration standard (n = 6; 0.25 mg glucose L^{-1}). All glassware and reagents were prepared as described by Myklestad et al. (1997).

5.1.2.6 Macronutrient analysis of atmospheric dust and rainwater dust

The concentration of the major dissolved inorganic macronutrients, nitrate + nitrite (NO_X), nitrite (NO_2), silicate ($SiOH_4$), and phosphate (PO_4) was determined by standard colorimetric methods (Grasshoff et al. 1983) as adapted for flow injection analysis (FIA) on a 4 channel LACHAT Instruments Quick-Chem 8500 autoanalyser (Hales et al. 2004).

5.1.3 Fe bioavailability and phytoplankton growth experiments

The diatom *Chaetoceros simplex* was selected as the model phytoplankton for this experiment as it is easy to enumerate using an electronic particle counter and small diatoms are important species in Southern Ocean (Sarthou et al., 2005). The parent cultures were maintained in exponential phase under trace-metal-clean conditions in Southern Ocean water at low Fe concentration (0.3 nM), 4 °C, and a light level of 60 µmol photons m^{-2} s^{-1}, on 16:8-h light:dark cycle (details in Hassler et al 2011a). To start the bioaccumulation and growth experiments, exponentially growing *C simplex* cells were isolated from the growth medium by gravity filtration on to 2-µm polycarbonate filters (Millipore, Merck Millipore, Bayswater, VIC, Austrailia), and then rinsed once with trace-metal-clean oxalate solution and five times with an inorganic saline solution (0.6 M NaCl, 2.38 mM NaHCO3, Tovar-Sanchez et al. 2003; Hassler at al., 2011a). The cells were then gently resuspended into 10 mL of synthetic seawater (table 1), which was used to inoculate incubation bottes for the bioaccumulation and growth experiments. The cell density of this algal suspension was determined using a Coulter ® Multisizer II counter (Beckman, Lane Cove, NSW, Australia) with a 50-µm aperture tube.

5.1.3.1 Iron bioaccumulation experiments – the bioavailability of wet-deposited, dust-borne Fe

To avoid interference from dust particles during analysis, 0.2-µm filtered rather than unfiltered experimental solution (UV, VIS, or Dark exposed dust + inorganic Fe control) was used for the bioaccumulation study. The experimental solution (growth medium) was dispensed into 1-L polycarbonate containers and then spiked with radiolabelled Fe (^{55}Fe, as $FeCl_3$ in 0.5M HCl, Perkin Elmer) to reach a final specific activity of 0.7 nCi/mL, corresponding to 0.6-nM Fe enrichment. For each treatment, a 2-mL subsample was taken to determine the total initial ^{55}Fe content, and the remaining solution was equilibrated for 24-h at 4 °C in the dark. Each treatment (UV, VIS, Dark treated dust/rainwater solutions) was prepared in triplicate. After equilibration, *C simplex* was spiked directly into the radiolabelled solutions to reach a cell density of 36,000 cells mL^{-1}, and cells were incubated at 4 °C at constant light (60 µmol photons m^{-2} s^{-1}) for a further 24-h. At the end of the incubation the algal suspensions were gently filtered onto 0.45-µm nitrocellulose filters (Sartorius) for determination of intracellular Fe. After filtration, the filters were rinsed with oxalate solution (Tovar-Sanchez et al., 2003; Hassler and Schoemann, 2009), five times 3-mL at 2-min intervals, followed by three times 3-mL of 0.2-µm-filtered seawater. Two mL of the initial radiolabelled solutions and the filters were collected in 20-mL scintillation vials, to which 10-mL of scintillation cocktail was added (Ultima Gold, Perkin Elmer). The samples were vortexed, and measured using a liquid scintillation counter (Tri-carb 2810 TR, Perkin Elmer, Melbourne, VIC, Australia) as per Hassler and Schoemann (2009). Fe bioavailability of Fe associated with dust was estimated from a parallel incubation of *C. simplex* in synthetic seawater with 0.1–1.2 nM $FeCl_3$ addition (0.1 to 1.4 nCi/mL) in absence of dust. Given that inorganic Fe is assumed to be 100 % bioavailable to diatoms (e.g., Shaked et al., 2005), its bioaccumulation in synthetic seawater can be used to determine the relationship between total Fe concentration and its bioavailability.

5.1.3.2 Growth experiments – The effect of wet-deposited dust-borne Fe on phytoplankton growth

To assess the impact of dust on phytoplankton growth, filtered Southern Ocean seawater (0.2 µm; SAZ-Sense voyage, RV *Aurora Australis*, 153 1 °E 45 3 °S, 11/02/2007, dFe 0.3 nM) was spiked with aliquots of each of the dust-enriched rainwater treatments (final concentration 0.5 mg L^{-1}, as for all other parameters) and left to equilibrate at 4 °C in the dark for 24-h. An inorganic Fe control (1 nM) was also prepared and equilibrated under the same conditions. After 24-h, the samples were filtered and dispensed in 50-mL

polycarbonate bottles. *C simplex* was added to attain a starting cell density of ~ 40,000 cells mL^{-1}. Each treatment was prepared in triplicate. The algal suspensions were incubated at 4 °C, in continuous light, at a light level of 50 µmol photons m^{-2} s^{-1} for 13-d. Cell counts and estimates of the maximum quantum yield of photosystem II (F_V/F_M) were taken daily. F_V/F_M was measured using a water-PAM (pulse amplitude modulated) fluorometer (Walz GmbH, Effeltrich, Germany). A 2-mL aliquot of sample was transfer to a quartz cuvette following 10-min of dark adaptation. The minimum fluorescence (F_0) was measured, and then a saturating light pulse was applied to determine maximum fluorescence. F_V/F_M was then determined using the equation, $(F_M\text{-}F_0)/F_M$ (Schreiber, 2004).

5.2 Results

5.2.1 The concentration of macronutrients and trace elements in atmospheric dust and rainwater

Analysis for the determination of macronutrients revealed that the undiluted rainwater contained 0.78 µM $Si(OH)_4$, and 2.2 µM NO_X, however, the concentration of PO_4 was below the limit of detection. At experimental dilution, all macronutrients were below the limit of detection and did not, therefore, contribute to the experimental dust treatments.

In the dust-enriched samples, NO_X was not detected in measurable concentrations, however, low concentrations of PO_4 (all < 0.6 µM) were measured in both experiments and in all treatments and size fractions (0.2-µm and 0.02-µm-filtered samples; Table 5.2). Silicic acid ($Si(OH)_4$) was measured in much higher concentrations with the 0.2 µM filtered samples ranging between 24 and 43 µM, and for the 0.02-µm size fraction between 12 and 29 µM (Table 5.2). No pattern in concentrations were observed between treatments but, as with PO_4, $Si(OH)_4$ was present in all samples. A comparison of size fractions showed that between 63 and 76% of the PO_4 and 43% to 78% of the $Si(OH)_4$ present in the 0.2-µm fraction passed through a 0.02-µm filter.

ICP-MS analysis (after isotopic spiking) of trace elements Fe, Zn, Ni, and Cu revealed that the rainwater contributed to the concentration of Fe (1.63 nM) and Cu (0.27 nM) in the experimental treatments, but not to Zn or Ni (Table 5.2). In the dust-treated samples (rainwater + dust trace element contribution) Fe was measured in all samples and varied between the two experiments and across treatments, but in all cases dFe was present in both the 0.2-µm and 0.02-µm filtered samples (Table 5.2). Zn was measured in all Exp 2 0.2-µm treatments, but not in the 0.02-µm fraction, or in any of the Exp 3 samples (Table 5.2).

The UV- and Dark-treated samples had very similar Zn concentrations (2.86 nM and 2.60 nM, respectively) whereas in the VIS treatment it was considerably lower, by ~45% (Table 5.2). Although present in much lower concentrations (< 0.5 nM, all cases) Cu was present in all treatments and size fractions from both experiments. Ni was not detected in measureable concentrations in any experimental sample. A comparison of size fractions showed that between 20 and 80% of the Fe and 45% to 100% of the Cu present in the 0.2-µm fraction passed through a 0.02-µm filter. Overall, the proportion of soluble Fe (< 0.02 µm) was greater in Exp 3, whereas, soluble Cu was greater in Exp 2 (Table 5.2).

Table 5.2 Concentration of macronutrients (phosphate (PO_4), silicic acid ($Si(OH)_4$; µM) and trace elements (Iron (Fe), zinc (Zn) and copper (Cu); nM) present in filtrates of experimental samples simulating the wet deposition of Australian mineral dust into the Southern Ocean. The dust used was collected during a large dust storm over Brisbane, QLD., and resuspended in rainwater collected in the Tasman Sea (31°35.849'S 178°00.00'E, GP13 GEOTRACES voyage, 27/05/2011) before being exposed to UV + visible light (UV, 2000 µE), visible light only (VIS, 2000 µE), or kept in darkness (Dark). Resuspended, treated dust was added to synthetic seawater to give a dust enrichment of 0.5 mg L^{-1}. Data for single 0.2 µm and 0.02 µm filtered samples are presented. **Bold type** = Exp 2, non-bold type = Exp 3. Errors for PO_4 and $Si(OH)_4$ are the standard deviation of triplicate samples. Fe, Zn and Cu data is from a single sample. Concentrations measured in the dust treatments are the combined contribution of rainwater and dust. < DL = below detection limit.

	Macronutrients		**Trace Elements**		
Treatment	**PO_4 (µM)**	**$Si(OH)_4$ (µM)**	**Fe (nM)**	**Zn (nM)**	**Cu (nM)**
Diluted Rainwater – 0.2 µm filtered	< DL	< DL	1.63	< DL	0.27
UV 0.2 µm filtered	**0.46 ± 0.03**	**24.0 ± 8.9**	**2.69**	**2.86**	**0.41**
	0.33 ± 0.02	38.0 ± 1.6	2.30	< DL	0.27
UV 0.02 µm filtered	**0.35 ± 0.09**	**12.7 ± 3.6**	**0.81**	**< DL**	**0.30**
	0.23 ± 0.02	29.7 ± 3.0	1.45	< DL	0.19
VIS 0.2 µm filtered	**0.55 ± 0.05**	**37.5 ± 7.3**	**3.49**	**1.51**	**0.28**
	0.30 ± 0.04	28.9 ± 3.3	2.19	< DL	0.42
VIS 0.02 µm filtered	**0.41 ± 0.01**	**16.1 ± 1.3**	**0.70**	**< DL**	**0.21**
	0.19 ± 0.04	18.0 ± 2.2	1.77	< DL	0.19
Dark 0.2 µm filtered	**0.45 ± 0.04**	**43.1 ± 9.1**	**4.20**	**2.60**	**0.29**
	0.32 ± 0.01	37.5 ± 8.1	1.16	< DL	0.32
Dark 0.02 µm filtered	**0.35 ± 0.04**	**25.4 ± 7.3**	**3.61**	**< DL**	**0.29**
	0.20 ± 0.04	22.3 ± 5.3	2.24	< DL	0.16

5.2.2 Solubility of dust-borne Fe and Fe in rainwater

The total acid-leachable Fe concentration of 372.1 nM in the Buronga (QLD) dust sample was used to calculate overall Fe solubility and the proportion of Fe present in the soluble (< 0.02-µm), colloidal (0.02- to 0.2-µm) and particulate (> 0.2-µm) size fraction during Exp 1. Overall solubility of dFe was very low in all cases at < 1.1%. Calculation of the relative proportion of Fe present in the soluble (< 0.02-µm), colloidal (0.02- to 0.2-µm) and particulate (> 0.2-µm) size fractions revealed that in all treatments the majority of Fe (> 98 %) was present in the particulate fraction (Table 5.3). The Dark treated samples contained the highest proportion of soluble Fe, although this was still < 1%, and very little colloidal Fe (Table 5.3). The proportion of soluble Fe in the UV and VIS treatments was < 0.46% with the remaining fraction being colloidal (Table 5.3).

Table 5.3 Fe size fractionation (soluble < 0.02-µm, colloidal 0.02- to 0.2-µm and particulate > 0.2-µm) of Fe associated with rainwater and Australian continental dust in experimental samples from two replicate experiments simulating the wet deposition of Australian mineral dust into the Southern Ocean. Solubilities of each size fraction are calculated using the total acid leachable concentration (372.1 nM) of Fe present in 0.5 mg L^{-1} dust. Treatments were as per Table 5.2. Relative concentrations (%) are presented. **Bold type** = Exp I, non-bold type = Exp II.

Treatment	Soluble Fe <0.02 µm (%)	Colloidal Fe 0.02 to 0.2 µm (%)	Particulate Fe >0.2 µm (%)
UV	**0.20**	**0.51**	**99.29**
	0.37	0.23	99.40
VIS	**0.17**	**0.75**	**99.08**
	0.46	0.11	99.43
Dark	**0.95**	**0.16**	**98.89**
	0.59	0.00	99.70

5.2.3 Fe chemical speciation of dust-borne Fe and rainwater

The background dissolved Fe (dFe) present in synthetic seawater was 0.73 ± 0.02 nM (determined by CLE-AdCSV after 45-min UV oxidation), 100 % of which was labile. Titration for the determination of organic ligands in the synthetic seawater was linear with no ligands detected, and the concentration of humic substance-like (HS-like) substances was below the detection limit of the instrument.

Of the 1.63 nM total dFe measured in the 0.2-µm-filtered rainwater (experimental dilution in synthetic seawater), 73% was labile. The concentration of organic Fe'-ligands in undiluted 0.2-µm filtered rainwater was 1.35 ± 0.31 µM, which amounted to a contribution of 2.31 ± 0.74 nM to the experimental treatments, and the calculated conditional stability constant (log $K_{Fe'L}$) for these ligands was 10.66 ± 0.06. The concentration of HS-like substances was below the detection limit of the instrument and did not contribute to that measured in the experimental treatments.

The data presented for dFe and Fe_{Labile} (Fig. 5.1) were corrected for the contribution of Fe from the synthetic seawater, but experiments aimed to simulate dust-borne Fe delivered via wet deposition, the contribution from the rainwater was included. However, for the determination of organic ligand concentration and conditional stability constant (log $K_{Fe'L}$) total dFe values were used (Fig. 5.2).

The concentration of Fe_{Labile} (after synthetic seawater correction) was below the detection limit in the UV (Exp 3) and VIS (Exp 2 and 3) 0.02-µm filtered samples, but was present in the Dark 0.02-µm samples and all 0.2-µm samples (Fig 5.1). Where Fe_{Labile} was measured, the relative concentration was < 25% in all samples, except for Exp 3 Dark 0.02-µm filtered, where 45 % of the Fe was labile. The UV and Dark treatments displayed similar relative Fe_{Labile} concentrations in the 0.2 µm filtered samples (16 to 23%), whereas Fe_{Labile} was considerably less in the VIS samples (Fig. 5.1).

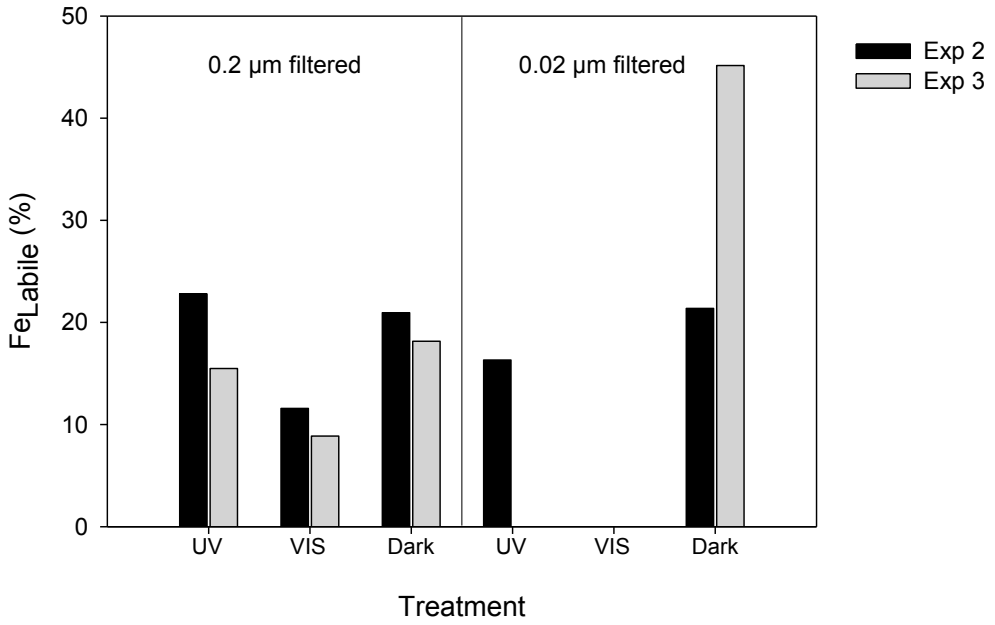

Fig. 5.1 Relative concentration of 10 µM TAC-Labile Fe (Fe_{Labile}) as a percentage of the total dissolved Fe measured in the 0.2-µm and 0.02-µm filtered fractions of experimental samples from two replicate experiments simulating the wet deposition of Australian mineral dust into the Southern Ocean. The dust used was collected during a large dust storm over Brisbane, QLD., and resuspended in rainwater collected in the Tasman Sea (31° 35.849'S 178° 00.00'E, GP13 GEOTRACES voyage, 27/05/2011) before being exposed to UV + visible light (UV, 2000 µE), visible light only (VIS, 2000 µE), or kept in darkness (Dark). Resuspended, treated dust was added to synthetic seawater to give a dust enrichment of 0.5 mg L^{-1}. Where no bars are present the concentration of Fe_{Labile} was below detection limit (0.05 nM) after synthetic seawater Fe correction.

Ligand concentration (ΣL) varied between 4.13 ± 0.30 nM (UV) and 6.74 ± 0.51 nM (VIS) in the 0.2-µm fractions, and between 3.15 ± 0.06 nM (VIS) and 5.13 ± 0.70 nM (UV) in the 0.02-µm fractions (Fig. 5.2A). Comparison between size fractions revealed that in the UV and Dark treatments the ligand concentration and log $K_{Fe'L}$ were similar between size fractions, suggesting that the majority of Fe'-binding ligands were associated with 0.02-µm fraction (Fig. 5.2A, B). However, this was not the case for the VIS treatment where, in both experiments, the Fe'-binding ligands in the < 0.02-µm fraction represented 50 to 70% of that measured in the < 0.2-µm fraction, as opposed to > 85% for the UV and Dark treatments (Fig. 5.2A).

The strongest ligands were measured in the Exp 2 Dark treatment, with both the < 0.2-µm and < 0.02-µm fractions having a log $K_{Fe'L}$ > 11.55 (Fig. 5.2B). However, the log $K_{Fe'L}$ of the

Exp 3 Dark treatment was lower than the other treatments and contained much weaker ligands (~10.7) (Fig. 5.2B). For both experiments, the UV and VIS treatments all had lower log $K_{Fe'L}$ (< 11.5) than the Exp 2 Dark treatment, and were similar between treatments and size fractions, except for Exp 2 UV 0.02-µm which was considerably lower at Log $K_{Fe'L}$ 10.80 ± 0.18 (Fig. 5.2B).

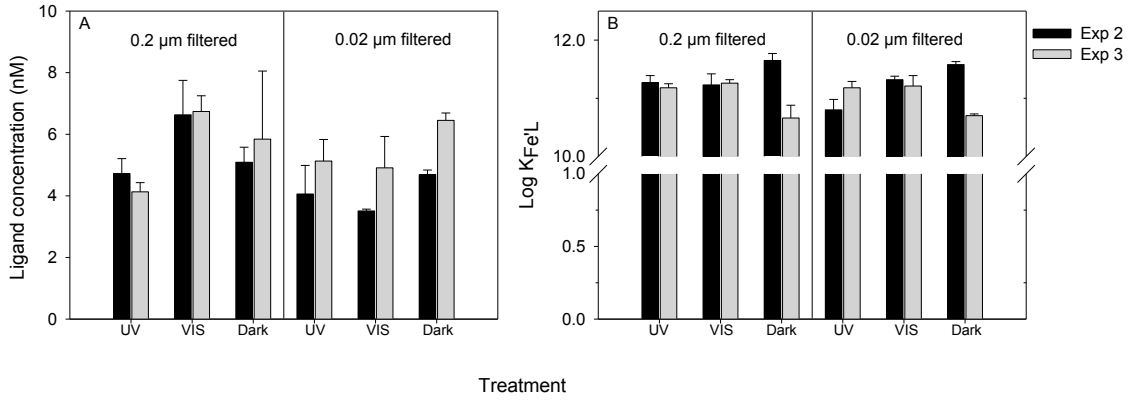

Fig. 5.2 Concentration of Fe'-binding organic ligands (nM; A) and conditional stability constants (Log $K_{Fe'L}$; B) in the 0.2-µm and 0.02-µm-filtered fractions of experimental samples from two replicate experiments simulating the wet deposition of Australian mineral dust into the Southern Ocean. Treatments were as per Fig. 5.1. Ligand concentration and Log $K_{Fe'L}$ were calculated using total dissolved Fe concentrations.

5.2.4 The concentration of HS-like material in atmospheric dust and rainwater

The concentration of electrochemically detected Fe'-binding HS-like material was low regardless of treatment, with all samples containing < 6 µg L^{-1} SRFA eq. and followed the order (from highest to lowest concentration) Dark > VIS > UV in all size fractions, except for VIS and UV 0.02-µm filtered where HS-like concentration was below the detection limit of the instruments (Fig. 5.3).

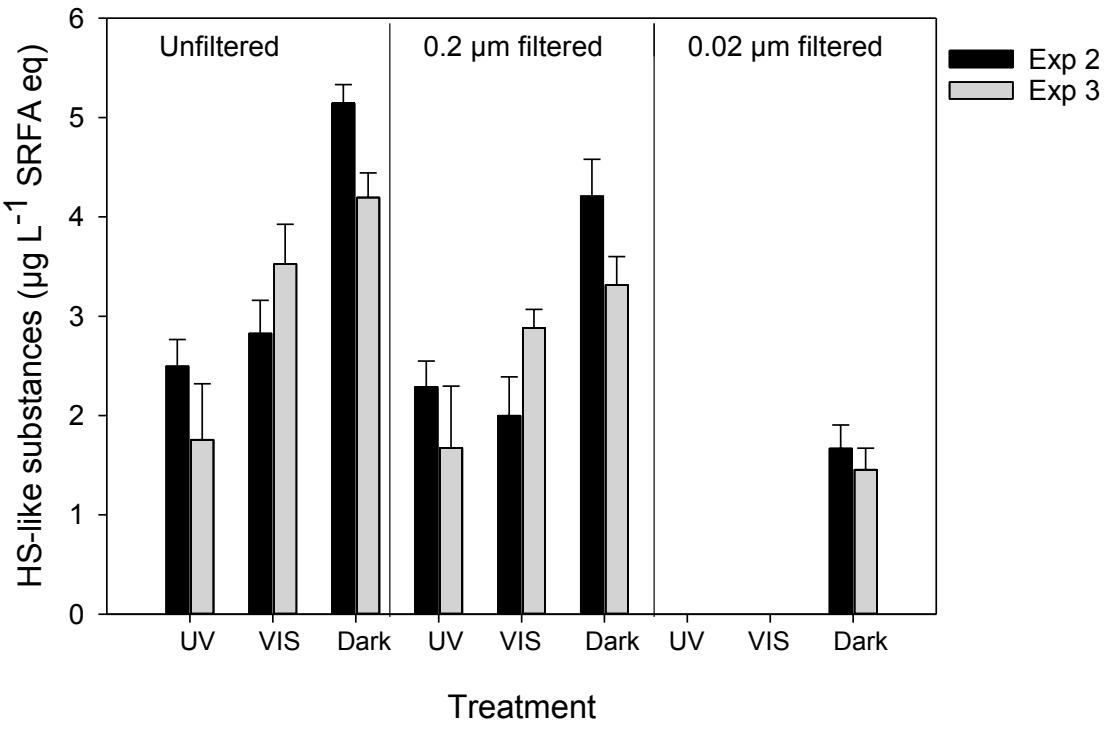

Fig. 5.3 Concentration of electrochemically detected Fe'-binding humic substance-like material (HS-like; µg L^{-1} SRFA equivalent) in unfiltered, 0.2-µm and 0.02-µm filtered fractions of experimental samples from two replicate experiments simulating the wet deposition of Australian mineral dust into the Southern Ocean. Treatments were as per Fig. 5.1. Errors = standard deviation of triplicate samples. Where no bars are present the concentration of HS-like was below detection limit (1.49 µg L^{-1} SRFA Eq.).

The distribution of HS-like material varied considerably between size fractions. The proportion of HS-like material in the particulate fraction (> 0.2-µm) of the VIS and Dark samples was 2.1 to 4.1 fold greater than that in the UV-treated particulate samples (Table 5.4). Only the Dark-treated samples contained HS-like material in the soluble phase (< 0.02-µm) which amounted to ~30%. The greatest proportion of HS-like material was present in the colloidal fraction (0.02- to 0.2-µm) for all treatments. However, the relative concentrations were quite different between treatments and followed the order UV (> 90%) > VIS (70 to 80%) > Dark (45 to 50%) (Table 5.4).

Table 5.4 Relative size distribution (%) of humic substance-like (HS-like) material in experimental samples from two replicate experiments simulating the wet deposition of Australian mineral dust into the Southern Ocean. Particulate = > 0.2-µm, Colloidal = 0.02- to 0.2-µm, soluble = < 0.02-µm. Treatments were as per Table 5.2. **Bold type** = Exp 2, non-bold type = Exp 3.

Treatment	HS particulate (%)	HS colloidal (%)	HS soluble (%)
UV	**8.4**	**91.6**	**0**
	5.1	94.9	0
VIS	**29.3**	**70.7**	**0**
	18.4	81.6	0
Dark	**18.1**	**49.4**	**32.5**
	21.0	44.5	34.5

Fe retention by the C_{18} resin, measured in the UV and Dark treated samples during Exp 1, was high at 96 to 100%, (Table 5.5). The measured Fe retentions of all treatments and size fractions was between ∽ 30% (for HA, DFB, GLU) and ∽80% (for DTPA) higher than any of the model ligands used.

Table 5.5 Relative retention of Fe on C_{18} resin of Fe associated with Australian mineral dust. For comparison model ligands (humic acid (HA); desferrioxamine B (DFB), 15 nM; DTPA, 100 nM; glucuronic acid (GLU), 100 nM) are presented. Experimental medium was synthetic seawater (pH 8.0). UV- and Dark-treated dust enrichments are presented. Unfiltered, 0.2-µm filtered and 0.02-µm filtered were measured to assess the nature of the organic ligands in each size fraction.

Treatment	Retention %
UV unfilt.	96
UV 0.2 µm filt.	100
UV 0.02 µm filt.	99
Dark unfilt.	101
Dark 0.2 µm filt.	100
Dark 0.02 µm filt.	98
HA	60.7
DFB	66.0
DTPA	21.8
GLU	67.2

5.2.5 The concentration of total hydrolysable saccharides in atmospheric dust and rainwater

The concentration of total hydrolysable saccharides in the rainwater was to 1.4 mM C, which amounted to a contribution of 2.40 ± 0.05 µM C to the experimental treatments.

In all dust-enrichment treatments, the total saccharide concentration (rainwater + dust contribution) was greater than that of the rainwater alone. In both experiments (Exp 2 and 3), saccharide concentration in the 0.2-µm filtered, UV-treated samples was significantly lower than both the VIS and Dark samples ($p \leq 0.002$; Fig. 5.4). In Exp 2, saccharide concentration was also significantly elevated in the VIS treatment compared to the Dark treatment ($p = 0.003$); however, for Exp 3 these treatments did not differ significantly from each other (Fig. 5.4). A comparison between size fractions revealed that the distribution of colloidal (0.02- to 0.2-µm) and soluble (< 0.02-µm) material varied between treatments. In the UV-treated samples > 90% of the material passed through a 0.02-µm filter into the soluble phase (both experiments), whereas less was present in this size fraction for the VIS and Dark treated samples (60 to 80%) (Fig. 5.4).

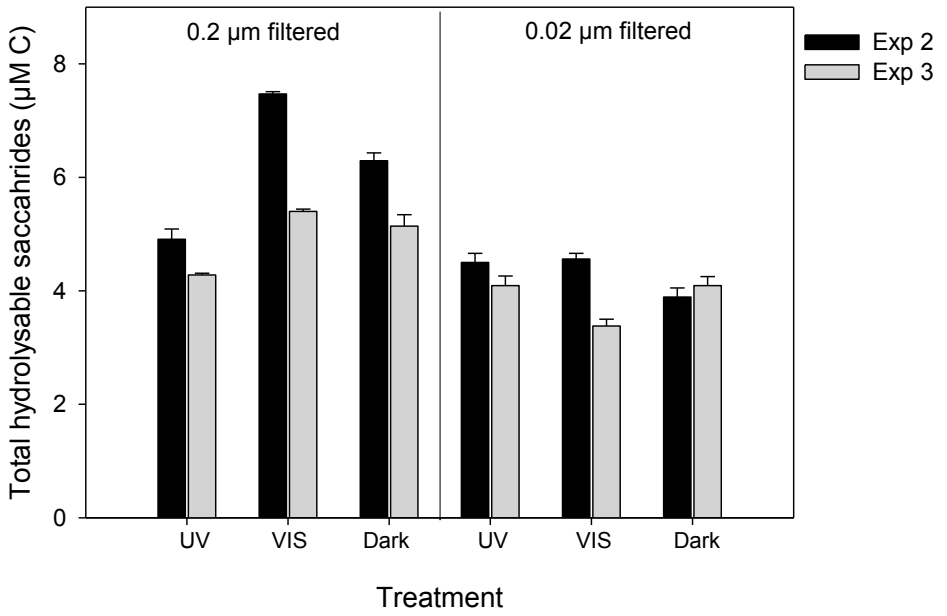

Fig. 5.4 Concentration of total hydrolysable saccharides (reported as µM C) measured in 0.2-µm and 0.02-µm filtered experimental samples from two experiments simulating the wet deposition of Australian mineral dust into the Southern Ocean. Treatments were as per Fig. 5.1. Error = standard deviation of triplicate samples.

5.2.6 Effect of dust-borne Fe on phytoplankton growth and Fe bioavailability

The effect of dust-borne Fe on phytoplankton growth and Fe bioavailability was assessed during Exp 1. Growth rates of *C. simplex* were calculated between 136-h and 232-h when all incubations were in exponential phase. The cells in the VIS incubation had the fastest growth rate compared to any other treatment, including the inorganic Fe control ($p \leq 0.001$ in all cases; Table 5.6). However, the inorganic Fe incubation entered the exponential growth phase almost two days (46-h) before the dust incubations and continued exponential growth until the end of the incubation period, whereas the dust incubations appeared to enter stationary growth at ~ 250-h. This was most apparent in the VIS incubation despite the elevated growth rate (Fig. 5.5A). The result of the extended period of exponential growth in the inorganic Fe incubation was a significantly higher final biomass than the dust incubations ($p = \leq 0.001$; Table 5.6, Fig. 5.5A). The elevated exponential growth of the cells in the VIS incubation was reflected in the final biomass, which was significantly higher than both the UV and Dark incubations ($p = \leq 0.001$). The UV and Dark incubations exhibited very similar growth rates and final biomass (Table 5.6, Fig. 5.5A).

Table 5.6 The effect of Fe associated with Australian desert dust on the growth of the Southern Ocean diatom *C. simplex.* Bioavailability (%) of Fe associated with Australian mineral dust relative to inorganic Fe (assumed 100% bioavailable) measured after 24-h. Growth rate (μ d^{-1}, calculated between 136-h and 232-h when all incubations were in exponential phase) and final biomass after 326-h incubation period at 4 °C and 50 µmol photons m^{-2} s^{-1} are also presented. Treatments were as per Table 5.2. Error = standard deviation of triplicate samples.

Treatment	Exponential phase growth rate (μ d^{-1})	Final biomass at 326-h (cells $mL^{-1} \times 10^5$)	Bioavailability (%) after 24-h
Inorganic Fe	0.18 ± 0.001	12.7 ± 0.35	100*
UV	0.21 ± 0.020	8.4 ± 0.22	42.6 ± 3.4
VIS	0.26 ± 0.005	10.3 ± 0.27	21.1 ± 5.4
Dark	0.21 ± 0.010	8.5 ± 0.47	31.4 ± 4.3

* Inorganic Fe assumed to be 100% bioavailable to diatoms (Shaked et al., 2005).

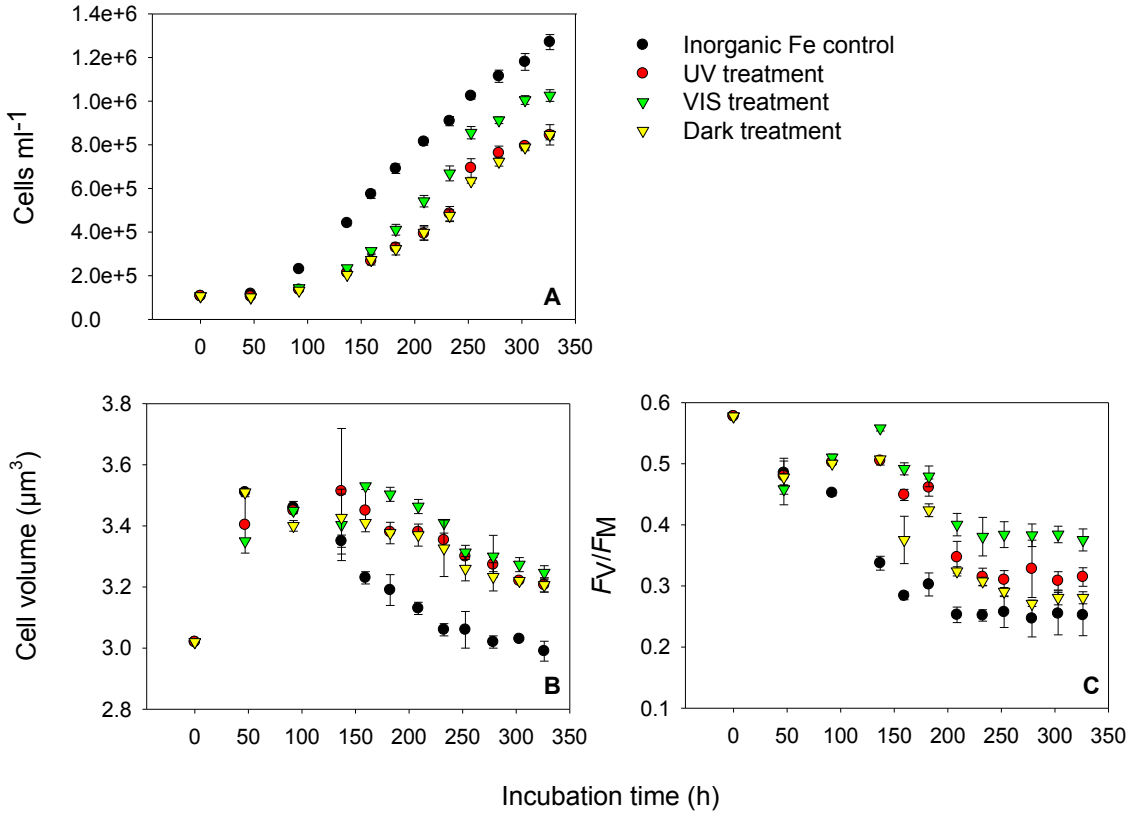

Figure 5.5 The effect of Fe associated with Australian mineral dust on the growth of the Southern Ocean diatom *C. simplex* over 326-h incubation period at 4 °C and 50 µmol photons m^{-2} s^{-1}. Growth curves (A), Cell volume, μm^3 (B) and F_V/F_M (C) were compared to an inorganic Fe (1 nM) incubation. The dust used was collected during a large dust storm over Brisbane, QLD., and resuspended in rainwater collected in the Tasman Sea (31°35.849'S 178°00.00'E, GP13 GEOTRACES voyage, 27/05/2011) before being exposed to UV + visible light (UV, 2000 µE), visible light only (VIS, 2000 µE), or kept in darkness (Dark). Resuspended, treated dust was added to synthetic seawater to give a dust enrichment of 0.5 mg L^{-1}. Error = standard deviation of triplicate samples.

Average cell volume at T0 was 3.02 μm^3. After an initial peak of 3.51 μm^3 at 46 h, the cell diameter of *C. simplex* in the inorganic Fe control declined rapidly and was significantly smaller ($p \leq 0.002$) than any of the dust treatments from ~140-h to the conclusion of the experiment (Fig 5.5B). Final measurements showed that the cells in the inorganic Fe control were of similar size (2.99 ± 0.03 μm^3) to that measured at T0. Peak cell diameter in the dust incubations occurred at different time points. Cells in the Dark treatment reached a maximum diameter of 3.51 μm^3 at 46-h, whereas the UV and VIS treatments took longer to attain maximum diameter at ~140-h and ~160-h, respectively (Fig. 5.5B). The decline in cell volume in the dust treatments was less rapid than was observed in the inorganic Fe control, and at the conclusion of the incubation cell volume was still significantly larger than

at T0 (~3.21 µm all treatments). Cell volume was significantly larger in the VIS treatment only during the exponential growth phase ($p \leq 0.002$) compared with the UV and Dark, which were similar during the experimental period (Fig. 5.5B).

The maximum quantum yield of *C. simplex* cells at the start of the experiment was 0.6 ± 0.002. However, all incubations displayed a 15 to 20% decline in F_V/F_M during the first 100-h. After this point, save for a short recovery to initial F_V/F_M at ~ 140-h by the VIS incubation, all dust incubations displayed a steady decline before maintaining an F_V/F_M of between 0.25 to 0.4 from ~ 250h until the end of the incubation (Fig. 5.5C). The cells in the VIS incubation maintained the highest F_V/F_M of all treatments. Although the inorganic Fe incubation exhibited high growth rate and biomass, the cells displayed the lowest F_V/F_M of all treatments, diverging from the dust incubations at ~ 92-h when exponential growth started in this incubation (Fig. 5.5C). This was followed by a sharp decline from 0.45 to 0.33 between 92-h and 136-h. After this point the cells in the inorganic Fe incubation followed a similar trend to the dust incubations, but maintained the lowest F_V/F_M (Fig. 5.5C).

The bioavailability of the Fe associated with the dust to the Southern Ocean diatom *C. simplex* was determined by comparing the uptake rates of each incubation to that of inorganic Fe, which is assumed to be 100% bioavailable (Shaked et al., 2005). Although the Fe in the dust treatments was not as bioavailable to *C. simplex* as inorganic Fe, the Fe associated with dust exposed to UV light was significantly more bioavailable than either the VIS or Dark treatments ($p = < 0.02$). The Dark treatment was more bioavailable than the VIS treatment; however, this was not statistically significant (Table 5.6).

5.3 Discussion

5.3.1 Fe Chemistry of dust-borne Fe and Fe in rainwater

5.3.1.1 Contribution of rainwater to the ocean dFe and organic ligand pool

There are few measurements of dFe in rainwater from remote ocean regions available; however, concentrations of between 0.04 µM and 1.47 µM are reported for rainwater collected in coastal and marine areas (see review by Deguillaume et al., 2005; Cheize et al., 2012). The concentration of dFe measured in the rainwater sample used in this study (1.26 µmol L^{-1}) was close to the upper values of this range. Assuming that this concentration is consistent with that of other precipitation events in the Tasman Sea, and using the average

solubility of Fe measured by Heimberger et al (2013; 85%) and a 100-mm × 100-mm collection funnel, a contribution to soluble Fe of 10.71 μM m^{-2} per rain event can be calculated. The annual input would therefore be dependent on the number rain events that occur; of which there were very few during the voyage on which the rainwater samples were collected (∽ one per week). Although rainfall would vary seasonally, considering one rain event per week to be an average for this region, then the contribution of soluble Fe would be just 1.53 μM m^{-2} d^{-1}, assuming that the Fe remained in a soluble form upon deposition into the surface ocean.

Fe′-binding organic ligands present in the ocean are generally measured in excess of dFe; however, the concentration of ligands measured in the rainwater sample was only slightly in excess of the dFe (1.36 μM and 1.26 μM, respectively). This almost 1:1 ratio of Fe to ligand was also measured by Cheize et al. (2012), not only in filtered rainwater samples, but in unfiltered samples also. However, the concentration of both Fe and organic ligands in the unfiltered samples was ∽ 3-fold greater compared to the filtered samples (Cheize et al. (2012), indicating that as only 0.2-μm-filtered rainwater was analysed in the study reported here, a relatively high proportion of ligands originally present were not measured.

The conditional stability constants in respect of Fe-binding (log $K_{Fe'L}$) of the organic ligands present the rainwater were generally lower than those measured in rainwater by Cheize et al. (2012). The method used by Cheize et al. (2012) was a CLE-AdCSV method similar to that used here, but which was specifically adapted to measure rainwater at a more natural pH (5.52 -6.20). From this method Cheize et al. (2012) calculated the $K_{Fe'L}$ of one sample to be $10^{11.1}$, similar to many of the samples from this study, but all other samples (both 0.45-μm filtered and unfiltered) had a $K_{Fe'L}$ in the range of L_1 ligands of between $10^{12.4}$ and $10^{12.8}$. However, rainwater is known to be associated with organic acids, many of which have lower conditional stability constants than those measured by Cheize et al. (2012) and, in some cases, can have a $K_{Fe'L} < 10^{10}$ (Okochi and Brimblecombe, 2001; Paris and Desboeufs, 2013; Wozniak et al., 2013). In addition, the organic ligands present in the rainwater sample used are likely to have been subjected to a degree of atmospheric processing before collection, and so the measured $K_{Fe'L}$ may reflect the photo-degradation and/or acid destruction of a stronger ligand (Barbeau et al., 2001, 2003; Baker and Croot, 2010). The weak $K_{Fe'L}$ suggests that the organic ligands associated with the rainwater, whilst contributing to the oceanic ligand pool, are likely to have a less important role in Fe biogeochemistry once they are deposited into the ocean.

5.3.1.2 The contribution of dFe and organic ligands to the ocean from atmospheric dust

Fractional solubilities from Fe-laden aerosols of between <1% to 80% have been reported although, as Baker et al. (2006) and Sedwick et al. (2007) point out, the diverse range of techniques used to calculate these solubilities may contribute to this variability. However, calculated solubility of the Fe from this dust compares very well with that generally measured in mineral (lithogenic) sourced dust, which is often ≤ 1% (Jickells and Spokes, 2001; Jickells et al., 2005, Mahowald et al., 2009, Sholkovitz et al 2012). There are many factors that affect the solubility of aerosol Fe. Baker and Jickells (2006) suggest that the primary factor controlling dust-borne Fe solubility is particle size. The increase in the surface-to-volume ratio of small particles results in a greater proportion of the Fe close to the surface of the particle, and therefore, exposes more Fe for dissolution (Baker and Jickell, 2006; Trapp et al; 2010). In addition, the low solubility measured here may indicate that there was very little anthropogenic material incorporated into the dust or rainwater during the original atmospheric transit, as the Fe from anthropogenic sources (i.e. from combustion products/biomass burning) is generally more soluble than lithogenic Fe (2% to 19%; Bonnet and Guieu, 2004; Guieu et al., 2005; Sedwick et al., 2007; Luo et al., 2008).

Anthropogenic aerosols often contain organic acids, nitrates, sulphates and HS that can increase the solubility of Fe (Trapp et al., 2010; Paris and Desboeufs, 2013). More recently Kadar et al (2014) have demonstrated that exopolymeric substances (EPS), produced by most bacterio- and phytoplankton, are particularly efficient in enhancing both the Fe solubility and colloidal stability of Fe associated with nanoparticles derived from the mineral dusts that have undergone atmospheric processing. Although the enhanced dissolution may be in part due to photoreductive processes, it may also be that the polyanionic nature of the EPS stabilises Fe in low-molecular-weight fractions (< 3 kDa; Kadar et al., 2014).

The higher concentration of ligands and higher log $K_{Fe'L}$ of the dust-enriched samples, compared to the rainwater sample, indicates that the presence of organic material associated with the dust that has an Fe'-binding affinity in the mid-range of L_2 ligands ($\geq 10^{8.8}$ to 10^{12}; Rue & Bruland, 1995 & 1997; Croot & Johansson, 2000), similar to those often measured in open water samples. However, the contribution of dust-derived organic ligands to the oceanic ligand pool is likely to be small. Dust deposition in this region of the Tasman Sea is highest during the summer months and so, considering the average ligand concentration measured in the dust from this study of 5.16 ± 1.06 nM, a contribution of 0.05 nM d^{-1} can be calculated. Using the sub-surface ligand concentrations measured in the

profiles from the PINTS voyage (Chapter 2), this would equate to ∽2 % of the total ligands measured in this region.

5.3.1.3 Nature of Fe-binding ligands in rainwater and atmospheric dust

Although the provenance of the Fe'-binding material is not known it is likely that a number of Fe'-binding organic ligands were present, including HS-like substances (Laglera and van den Berg, 2007, 2009) which were measured in the dust-enriched samples, and saccharides (Hassler et al., 2011, Chapter 3) which were measured in both the dust-enriched samples and the rainwater. Like the organic acids present in rainwater, these compounds can contain hydroxyl and carboxylic groups that can bind Fe (Croot & Johansson, 2000; Sreeram et al., 2004; Benner 2011; Paris and Desboeufs, 2013; Wozniak et al., 2013). Interestingly, the majority of Fe-binding organic ligands and saccharides measured in all treatments were present as soluble ligands, whereas HS-like material was mostly present in the colloidal fraction.

The contribution of HS-like material to the organic ligand pool measured would be dependent on the nature of the material. Assuming that HS-like materials were mostly FA and HA, similar to Suwannee River reference materials, which binds 16.7 nmol Fe mg^{-1} FA and 32 nM Fe mg^{-1} HA (Laglera and van den Berg, 2009), then the contribution of HS-like material to the ligand pool can be estimated. This contribution would be only marginal, < 2.6 % in all treatments, with the highest contribution occurring in the dark treatments (0.38 to 2.6 %), and the light treatments having an overall smaller contribution (0.5 to 1.5 %). The measurable concentrations of HS-like material present in all but two 0.02-µm samples indicates that a very small proportion of the electrochemically detected colloidal HS-like material measured in open ocean regions is sourced from atmospheric aerosols. Assuming that the HS-like material present in the samples was of a similar molecular size to SRFA (generally measured as < 15kDa, Chin et al., 1993; Perminova et al., 2003), then one would expect that if the HS-like substances were present as intact material then the majority would be present in the soluble fraction. The Dark sample, which was not affected by photodegradation, indicates that this was not the case and that the much of the HS-like material was present as adsorbed colloids.

Saccharides are known to weakly bind Fe (Croot and Johannson, 2000; Rue and Bruland, 2001), and have been shown to enhance Fe bioavailability to phytoplankton (Hassler et al., 2011b). Like marine surface waters, carbohydrates/saccharides can make a significant

component of the DOM present in rainwater and aerosols, particularly in the spring and summer months (Medeiros et al., 2006; Seaton et al., 2013). The total hydrolysable saccharide concentration of the rainwater sample used in this study was approximately two orders of magnitude higher (1.4 mM C, undiluted sample) than the concentrations measured in surface seawater samples (2.5 to 27 μM C; Benner et al., 1992; Pakulski and Benner, 1994; Wang et al., 2006). In addition, both the total saccharide concentrations for the rainwater and dust-enriched samples were an order of magnitude higher than their respective total Fe-binding ligand concentrations. This suggests that only a small proportion of the saccharides present in both the rainwater and dust had an affinity for Fe-binding. As the individual components that make up the ligand matrices in these samples is not known it is not possible to confirm the contribution of Fe-binding saccharides to the total ligand pool measured in the rainwater and dust. However, whilst not all saccharides will contribute to the oceanic Fe-binding ligand pool, they will also be contributing to the carbon (C) pool and providing a C source to heterotrophic bacteria (Obernosterer et al., 2008). The magnitude of this input will, however, be dependent on the frequency and intensity of precipitation and/or dust storm events.

As stated above although the contribution of saccharides to the ligands measured is not known, given the concentration range of 2.4 to 7.5 μM (as μM C) measured in the dust-enriched samples one might expect that these compounds would make up a high proportion of the Fe-binding ligands present, and thus, the ligands might be more hydrophilic in nature. However, the high retention of Fe from all dust treatments on to the Sep-Pack C_{18} resin (>96% in all cases) indicates that the ligands associated with the rainwater and dust were in fact of a more hydrophobic nature (Hassler at al., 2009). Natural organic matter, including humic substances, is known to be amphiphilic (containing both hydrophilic and hydrophobic groups; Thurman, 1985; Buffle, 1990). In addition, significant quantities of hydrophobic organic material have been measured in rainwater, cloud water, aerosols and fog (Kieber et al., 2006; Duarte et al., 2007), some of which have been suggested as source of Fe(II)-stabilising ligands (Willey et al., 2008). Although the source of the hydrophobic material cannot be confirmed, the fact that there was little variation in retention between treatments or size fractions suggests that the nature (i.e. hydrophobicity) of the organic ligands present was not affected by the different light exposures.

5.3.1.4 Effect of light on Fe Chemistry

Ligand and HS-like concentration measured during this study were both higher in the 0.02-µm-filtered Dark samples compared to the UV and VIS samples, which were likely affected by photolytic processes. These results indicate that the higher proportion of Fe present in the soluble (< 0.02-µm) fraction of the Dark treated samples compared to the UV and VIS samples is likely due to a higher concentration of soluble Fe stabilising organic ligands in the Dark samples. Exposure to both visible and UV light also resulted in a reduction of the log $K_{Fe'L}$ associated with the Fe'-binding organic ligands in these treatments. This was particularly apparent in the samples from Exp 2, and slightly enhanced in the UV treatments. Although not all organic ligands exhibit this behaviour, photoreduction often produces a photoproduct of a weaker Fe-binding affinity, and α-hydroxy-carboxylic acid groups found in some siderophores have certainly been found to be photo-sensitive (Barbeau et al., 2001, 2003; Hassler et al., 2012). In addition, the photochemical reduction of colloidal and organically bound Fe(III) is a known reduction pathway (Waite and Morel, 1984; Barbeau et al., 2001), as is the production of the reductant superoxide from the photodegradation of organic material (Rose and Waite, 2005, 2006). It is possible that the UV exposure initiated such reductive process during these experiments, and that the variation in bioavailability between light exposure treatments was due to different forms of Fe released under different light regimes.

The high aromaticity of humic material suggests that it is readily degraded by photochemical processing, particularly by UV light (Thurman, 1985; Obernosterer and Herndl, 2000), and this was very well demonstrated in these experiments. Overall, the Dark samples contained up to 50% more HS-like material in all size fractions (soluble, colloidal and particulate) than those samples that had been exposed to light, with UV exposure generally having a greater effect. Our results highlighted the high sensitivity to light (UV and VIS) of HS-like material associated with atmospheric dust, in all size fractions, but particularly in the soluble fraction where no HS-like material was measured in either the UV or VIS samples. In the larger size fractions, presumably some of the HS-like material originally present in the particulate fraction underwent photolytic processing resulting in the production of smaller colloids.

5.3.2 Biological response to dust-borne Fe

The bioaccumulation experiments indicate that the Fe delivered in the UV-treated dust enrichment was the most bioavailable to *C. simplex*. The lower log $K_{Fe'L}$ of the UV treatments, likely as a result of photodegradation, indicates the formation of weaker ligands that may make the complexed Fe more accessible to the phytoplankton. This may be either available for direct uptake, or, in natural communities, by enabling their own biologically produced Fe-binding ligands, for example EPS, (Hassler, Norman et al. in press; Norman et al., in press; chapter 4 of this thesis), to compete for the complexed Fe.

With the relative proportion (%) of bioavailable Fe in all the treatments ranging between 20% and 40%, when compared to Fe bound to hydroxymate siderophores DFB (9%) or ferrichrome (7%; C. S. Hassler pers. comm.), the Fe delivered with the dust and rainwater could be considered highly bioavailable to this diatom, regardless of the type of light exposure. However, no dust treatments were as bioavailable to *C. simplex* as inorganic Fe, or inorganic Fe bound to ProtoporpyrinIX (70%) or the saccharides dextran (84%; Hassler et al. 2011b) and glucuronic acid (120%). As inorganic Fe bound to bacterial EPS has been shown to be extremely bioavailable to *C. simplex* (28 %, Hassler et al., 2011b; 50 %, Hassler, Norman et al, in press), it is possible that, as suggested by Kadar et al. (2013), complexation with EPS produced by natural communities may further enhance dust-borne Fe bioavailablity.

Although the cells in the dust treatments appeared to respond more positively to the dust-borne Fe than the inorganic Fe, it was not as efficient in sustaining growth, in terms of biomass yield, over the experimental period, and so the results of the Fe bioavailability and growth experiments appear somewhat contradictory. However, one should consider that the bioavailability experiment reflects a short 24 h response rather than a longer term one, in this case days. Unfortunately, the first growth measurements after T0 were not taken until ~48-h incubation, at which point very little difference between dust treatments was observed. In the VIS treatment, the higher proportion of organic ligands present in the < 0.2-µm fraction, compared to the UV treatment indicates that colloidal Fe was likely to be the dominant form of Fe available to *C. simplex* in those incubations. Whilst colloidal Fe is generally less bioavailable to phytoplankton, utilisation of this form has been demonstrated in the diatom *Thallasiosira psuedonana* (Chen and Wang, 2001, 2003). The fact the phytoplankton exposed to the VIS-treated dust were better sustained in the longer term suggests that, despite reduced bioavailability, colloidal Fe becomes an increasing important Fe source over time, at least to some diatom species.

The difference in short- and longer-term phytoplankton response to this particular dust has also been shown in experiments conducted during the PINTS voyage. For these experiments natural phytoplankton communities from two contrasting sites in the Tasman Sea (P1, northern and P3, southern Tasman Sea) were used, and the dust introduced at the same concentration as for this study but as a dry deposition event (Chapter 3; Hassler et al., 2014). Size-fractionated bioavailability results showed that at P1 the >10 μm size fraction (microphytoplankton) had the greatest response after 24-h, whereas, at P3 the greatest response was measured in the 0.7- to 2-μm size fraction (picophytoplankton, C. Hassler, unpublished data). However, longer-term (4-d) chl-*a* results (biomass indicator) showed that the dust-borne Fe had not benefitted any size fraction and had, in fact, supressed the picophytoplankton relative to inorganic Fe. In contrast, at P3 the microphytoplankton were the greatest beneficiaries. As described in Chapter 3, a community shift was also observed at both sites. The cyanobacteria that originally dominated at P1 were supressed and a small increase in diatoms observed, and at P3 prasinophytes and dinoflagellates increased. The PINTS results suggest that the dust-borne Fe was more accessible to some species than others, although electrochemical detection of Fe-binding organic ligands by CLE-AdCSV indicated an added input of likely biologically produced ligands for both P1 and P3, which suggested that some species were responding to the added dust-borne Fe.

An example of species-specific dust utilisation can be found in the diazotroph *Trichodesmium*. The process of N_2 fixation necessitates a high Fe requirement and this species is often Fe limited (Kutska et al., 2003). Like most phytoplankton species *Trichodesmium* utilises only dissolved Fe (Rubin et al. 2011). However, Rubin et al. (2011) have demonstrated that this species has the ability to accelerate the dissolution rates of dust-borne Fe and increase their cellular uptake rates, although the mechanisms used in this process are unknown. Blooms of *Trichodesmium* are common in the waters north of Australia and in the north Coral Sea (Law et al., 2011), which is an area of seasonal dust deposition.

Mixed biological responses, such as that of the PINTS experiments are well reported (Gabric et al., 2002; Johnson et al., 2003; Boyd et al; 2004; Moore et al., 2006; Shi et al., 2012; Mackie et al., 2008) and is likely due to the fact that seasonal dust deposition does not always coincide with the nutritional requirement or bloom periods of phytoplankton species or communities – hence, the reason as to why some studies report a response and others do not (Cropp et al., 2013). Additionally, the concentration of bioavailable Fe delivered with

the dust may, or may not, be enough to enhance the concentration of bioavailable Fe present so that the biological demand of the community is satisfied.

If we consider an average annual dust deposition of 0.5 mg L^{-1}, with deposition concentrated mainly in the summer months, it is possible to estimate the contribution of bioavailable Fe delivered with this dust to the surface waters of the Tasman Sea and areas of the Southern Ocean. The total Fe deposited would be approximately 41 nmol m^{-2} d^{-1}, of which ~1% would be soluble (0.41 nM m^{-2} d^{-1} soluble Fe). The Fe considered bioavailable for biological uptake amounts to 0.12 nmol m^{-2} d^{-1}, assuming that 35% of the total soluble Fe is bioavailable. Using the biogeochemical Fe budget calculated for similar waters by Bowie et al (2009), the contribution of new Fe from this dust is extremely small. Bowie et al. calculate that biologically remineralised Fe accounts for the largest Fe flux (~2913 nmol m^{-2} d^{-1}), with lateral advection providing 124 nmol m^{-1} d^{-1}. Vertical diffusion accounted for a further 31 nmol m^{-2} d^{-1} and 213 nmol m^{-2} d^{-1} was exported downwards. With the Fe uptake rate calculated to be ~4062 nmol m^{-2} d^{-1} the Fe supply, new or remineralised, was not enough to satisfy the Fe biological requirement. We can see that the new Fe supplied by this dust alone would not be sufficient to stimulate or sustain a phytoplankton bloom. However, this considers a steady supply of dust-borne Fe, and deposition events are, in reality, highly episodic rather than continuous. The results of this study and those of PINTS voyage and Rubin et al (2011) suggest that large dust storm events or repetitive episodic supply of Fe (and other nutrients) would likely be beneficial to some phytoplankton species. However, should the beneficiaries of this new Fe be mostly diazotrophs this could lead to an increase of N into the mixed layer and possible P limitation of other phytoplankton species (Ellwood et al., 2013).

5.4 Conclusion

The experiments conducted during this study demonstrate that light exposure, and particularly UV light, can have a substantial effect on a) Fe chemistry of iron-laden atmospheric desert dust by lowering log $K_{Fe'L}$ and altering the size distribution of both Fe and organic ligands (including HS-like material and saccharides) and b) Fe bioavailability to phytoplankton, either as a direct result of the formation of weaker ligands or by photoreductive processes.

Although dust inputs are secondary in magnitude to upwelling as a source of Fe to the surface waters of the Southern Ocean and Tasman Sea (Watson, 2001; Chapter 1), dust-borne Fe originating from the Australian continent represents an important periodic source of Fe, and other vital macronutrients and trace elements, to these ocean regions (Hesse, 1994; Hesse and McTainsh, 2003; Mackie et al., 2008; Gabric et al., 2010; Cropp et al, 2013). A significant increase in dust mobilisation has been observed across the major Australian source region of the Lake Eyre Basin during the peak activity period for dust transport which, together with predictions of future climatic variations that may alter seasonal transport, deposition processes, and an increase the frequency of storm events, will probably have corresponding changes in the atmospheric deposition (Mahowald et al., 2005; Hobday et al., 2008; Mitchell et al., 2010). These events are likely to result in a greater deposition of Fe-rich dust into the Coral Sea, Tasman Sea and Southern Ocean, which represent areas of Fe-limitation or co-limitation (Martin et al., 1990, 1994; Moore at al., 2009; Boyd and Ellwood, 2010; Law et al., 2011).

The results of this study indicate that wet, dust-deposition events may provide vital nutrients, particularly $Si(OH)_4$, PO_4, Fe and Zn, required for phytoplankton growth, together with a range of Fe-binding ligands that help to maintain Fe solubility and enhance Fe reduction processes, both during atmospheric transport and upon deposition to the surface ocean. When the results of the PINTS companion experiments are also considered (Chapter 3; Hassler et al., 2014) the dust-borne Fe provides bioavailable forms of Fe to some phytoplankton species over both short and longer time periods, suggesting that Fe remains bioavailable in both soluble and colloidal forms, despite the low fractional solubility calculated here. However, the solubilities calculated were from dust-enriched rainwater diluted in synthetic seawater (no ligands present), and it should be remembered that the ultimate solubility of dust-borne Fe will be determined upon deposition by the nature of the Fe-binding ligands present in the surface waters (Baker and Jickells, 2006). That considered, solubility does not always guarantee that the Fe is bioavailable to phytoplankton; it is the form/species of Fe delivered that is more important to bioavailability, and this can be very species specific (Hutchins et al., 1999; Visser et al., 2003; Maldonado et al., 2005; Maldonado et al., 2006, Rubin et al., 2011). The enhanced bioavailability observed in this study may have been due to the stabilising effect of complexing ligands that were measured in both the rainwater and dust-enriched samples, or organic ligands produced by the phytoplankton (i.e. EPS), and/or the formation of a more bioavailable form of Fe via direct and indirect UV-light-mediated reduction processes (Waite and Morel, 1984; Barbeau et al., 2001; Rose and Waite, 2005, 2006).

Although Australian desert dust may provide the surface waters of the Tasman Sea, Coral Sea and Southern Ocean with bioavailable forms of Fe, possibly in increasing quantities, the impact that dust-borne Fe will have on a natural phytoplankton community will ultimately be dependent on duration and intensity of the deposition event, and most importantly the nutritive state of the community and the composition of the community present (Boyd et al., 2007; Cropp et al., 2013).

CHAPTER 6:

GENERAL DISCUSSION

6.0 General discussion

The work presented in this thesis investigated a range of organic and inorganic Fe sources to determine how organic complexation affected Fe solubility, chemistry, and bioavailability, and which sources had the biggest influence on Fe bioavailability to phytoplankton. Results obtained provided new information about the distribution of Fe-binding organic ligands, including HS-like material, in the Tasman Sea and sub-Antarctic Zone (SAZ), which is pertinent to the international GEOTRACES programme. Perturbation experiments also highlighted sources of Fe that appear to be key to the phytoplankton communities in these regions. This study also found that bacterial and algal EPS are significant contributors to Fe biogeochemistry, and revealed many previously unknown functional and molecular characteristics. Furthermore, experiments demonstrated that photochemical processes have a significant effect on Fe and organic ligands associated with dust from the Australian continent, and that this may affect the bioavailability of dust-borne Fe.

6.1 Distribution and effect of HS-like material in the Tasman Sea and SAZ

Humic substances (HS) are known to bind Fe (and other nutrients) and have been suggested as a contributor to the weaker L_2 ligand pool (Laglera et al., 2007; Laglera & van den Berg, 2009). The generally low concentrations of Fe-binding HS-like material measured in coastal and offshore regions of the EAC and Tasman Sea (mostly < 100 μg L^{-1}; Chapters 2 and 3) indicate that in these regions, HS-like material accounts for a very small fraction of the Fe-binding organic ligand pool. However, one continental shelf and two river plume samples were in excess of this concentration, which might indicate that at times of peak river flow a greater concentration of HS-like material may be transported onto the shelf. The reported strengthening of the EAC (Ridgway and Hill, 2009) could result in such an enhancement of HS delivery at the shelf, which has the potential to alter the nutrient dynamics and affect the growth of phytoplankton (Price et al., 1988; Hutchins et al., 1998, 2002; Doblin et al., 1999; Imai et al., 1999). However, the perturbation experiments (Chapters 2 and 3), conducted using contrasting phytoplankton communities (EAC, cyclonic cold core eddy (CCE), northern and southern Tasman Sea), indicated that overall growth was not affected, but that C fixation may be reduced by the presence of HS in the EAC community (Chapter 2). Whether this result was due to a concentration effect (the EAC received 600 μg L^{-1} and the CCE 200 μg L^{-1} SRFA), and/or due to the composition of the phytoplankton community is unclear. A

strengthening of the EAC will transport cyanobacteria-dominated communities (i.e. *Synechococcus* sp. and *Prochlorococcus* sp.) into regions previously inhabited by a greater abundance of diatoms and dinoflagellates, together with warm, nutrient-poor water (Baird et al., 2008; Thompson et al., 2009). Factors such as modifications to currents other than the EAC (e.g. ACC, Equatorial currents), or variability in the strength and trajectory of dust-carrying winds from the Australian continent may also influence community distribution, however, the resulting communities may become mixtures of the two regions and potentially more diverse. An increase in the distribution of cyanobacteria in the Tasman Sea may itself have implications for C fixation, as the total C that cyanobacteria fix is small in comparison to diatoms. Furthermore, C fixation by cyanobacteria could be further limited by increased concentrations of HS (Chapter 2). However, an added input of HS will also enrich the nutrient pool of this region that is generally considered to be N and/or Fe limited (Ellwood et al. 2013; Hassler et al., 2014). The greater microbial consumption of HS-like material measured in the EAC, together with photochemical processes, are remineralisation pathways that would provide these nutrients to the resident phytoplankton.

Although it is accepted that marine HS is largely composed of degraded algal products, the direct production of HS-like material by phytoplankton has been debated. The perturbation experiments indicated that, in addition to the microbial communities, the phytoplankton themselves contribute to the HS-like pool. Using fluorescence measurements Romera-Castillo and co-workers (2010, 2011) showed that phytoplankton of the genera *Chaetoceros, Skeletonema, Prorocentrum* and *Micromonas* all produced marine HS-like material. Whilst this marine phytoplankton-produced HS-like material was not characterised, it is likely to contain exudates such as EPS, which has an affinity for Fe-binding, as both newly produced material and as an aged, degraded product. The presence of EPS in marine HS may, in part, account for the higher concentrations of Fe-binding HS-like material that were generally found at, or adjacent to, the chlorophyll maximum (Cmax) in the natural samples. Despite this, there was little correlation between HS-like material and Chl-*a* (Chapters 2 and 3). As observed with other DOM products excreted by phytoplankton (i.e. DOC) this lack of correlation indicates that there is a decoupling between HS-like concentration and phytoplankton biomass. The composition of HS-like material in offshore waters explains much of this decoupling. Although there is a proportion of newly produced material (i.e. EPS), it is also composed of degraded algal matter and exudates, representing past rather than present primary productivity (Andrews et al., 2000), together with organic material associated with the co-occurring microbial community and grazers. However, like dissolved organic carbon (DOC), HS is likely to exist as semi-labile, semi-refractory, and refractory

material (Hansell et al., 2012). Correlations with phytoplankton biomass may also depend on the relative proportions of these fractions, which will vary depending on the degree of microbial or photochemical degradation and the physical movement of HS-like material.

6.2 Distribution of organic ligands in the Tasman Sea and SAZ

There are few previous measurements of organic ligand concentrations and conditional stability constants in the Tasman Sea and SAZ; however, the results from this thesis (Chapter 3) are consistent with previous studies in the Southern Ocean (Boye et al., 2001, 2005; Frew et al., 2006) and SAZ (Boye et al., 2001; Ibisanmi et al., 2011). Furthermore, the distribution of organic ligands throughout the water column was also as expected, with higher conditional stability constants measured in the upper water column (above 200m), particularly at, or adjacent to the Cmax, and lower conditional stability constants at depth. As with previous studies, ligand concentration was also in excess of dissolved Fe throughout the water column, but there does not appear to be any correlation between the two parameters (Ibisanmi et al., 2011).

The conditional stability constants measured showed that the majority of organic ligands present were in the L_2 class. L_1 ligands only occur in the upper water column (i.e., top 200 m; Rue & Bruland., 1997; Cullen et al., 2006; Ibisanmi et al., 2011), and in the profiles measured here (Chapter 3), only one sample (collected in the top 50 m of the water column), contained L_1 ligands. The CLE-AdCSV technique used to measure Fe speciation does not allow determination of the origin of the strong ligands measured, but generally bacterial siderophores are proposed as the source (Gledhill and Buck, 2012 and refs therein). However this study has revealed that algal and bacterial EPS are also associated with both L_1 and L_2 ligands (Norman et al., in press; Chapter 4). Given that EPS are likely to be present in much higher concentrations than siderophores (Hassler et al., 2011a), it is possible that a proportion of the L_1 ligands previously measured in the oceans were associated with EPS.

6.3 Important Fe sources in the Tasman Sea and SAZ

The organic ligands selected for the PINTS voyage Fe enrichment experiments (Chapter 3) represent those that are found throughout the oceans (siderophores, saccharides, excreted algal products, HS). The perturbation experiments in the EAC, CCE and north and south Tasman Sea (Chapters 2 and 3) demonstrated the important role that organic ligands

(including HS-like material) play in regulating the nutrient dynamics of marine systems. However, the responses of the phytoplankton communities were varied. The experiments in Chapters 2 and 3 reinforce the observation that not all species or size classes utilise the same nutrient sources, and that the bioavailability of Fe to phytoplankton is dependent on the various Fe species and Fe sources (i.e., inorganic or organically bound; Sunda and Huntsman, 1995; Wilhelm, 1995; Hassler et al, 2011a). Fe bound to bacterial EPS showed the greatest enhancement of phytoplankton growth across all size classes compared to all other sources, whilst the dust-borne Fe present in D1 altered phytoplankton community structure. This was observed at both the northern and southern Tasman Sea sites (P1 and P3). However, whilst specific taxa appear to better equipped to access some forms of Fe over others, the community as a whole is able to utilise almost all forms of Fe input. This effect is likely to be enhanced via recycling through the microbial community and grazers.

6.3.1 Bacterial and Algal EPS

EPS can enhance Fe solubility/filterability in both the soluble and colloidal phases (Hassler et al., 2011b; Chapter 4) which can extend the retention time of Fe in the dissolved phase, thereby, making Fe more available to phytoplankton for longer (Whitfield, 2001). This is unlikely to be the sole reason for the enhanced phytoplankton growth measured in the PINTS experiments (Chapter 3) because other organic ligands, including DFB and glucuronic acid, also exhibit this behaviour (Hassler et al., 2011b). The weak conditional stability constants measured in the EPS incubations (log $K_{Fe'L}$ 10.43 to 11.03; Chapter 3) compared to the other enrichments would also have played a role, as Fe bound to weaker ligands is generally more accessible to phytoplankton (Sunda and Huntsman, 1998). Fe-EPS complexes have been shown to be highly bioavailable to phytoplankton (Hassler et al., 2011b, Hassler, Norman et al., in press; Chapter 4), and Fe bioaccumulation experiments show that Fe uptake in the PINTS EPS and glucuronic acid (GLU), which forms a weak complex, treatments were very similar (Hassler, Norman et al., in press). However, laboratory experiments using the diatom *C. simplex* indicated that the Fe bound to the pelagic bacterial EPS used in the PINTS experiments was less bioavailable than the saccharides GLU and dextran (DEX; Hassler et al., 2011b). EPS are also associated with other essential macronutrients and trace elements, although the mechanism for this association is unclear (Hassler et al., 2011a; Norman et al., in press; Chapter 4), which could benefit nutrient-limited phytoplankton communities such as those in the Tasman Sea and SAZ. It is possible, therefore, that a combination of extra nutrients associated with the EPS, as well as

weakly bound, soluble Fe, accounted for the enhanced biomass observed in the EPS incubation (Chapter 3).

The conditional stability constants measured for the pelagic bacterial EPS used in the perturbation experiments (Chapter 3) were much weaker than those measured in sea ice bacterial EPS used for the laboratory experiments (log $K_{Fe'L1}$ 12.12, Log $K_{Fe'L2}$ 11.44, log $K_{Fe'SumL}$ 11.56; Chapter 4). Although difference in Fe-binding affinity may be a reflection of the composition of the pelagic bacterial EPS used in the PINTS experiments, the functional and physico-chemical analyses indicate that the two EPS were, in fact, very similar in composition (Hassler et al., 2011a; Chapter 4). The variability in conditional stability constants may be due to the exposure of the pelagic bacterial EPS to photochemical and biological processes during the PINTS experiments, which can result in the formation of a photoproduct that has a weaker conditional stability constant than the original ligand. During the laboratory experiments, the sea ice bacterial EPS was not exposed to these processes. UV light was excluded from the PINTS incubations, due to the use of polycarbonate bottles and so biological degradation is likely to have a greater influence than UV oxidation. However, as observed in the dust experiments (Chapter 5) visible light may also influence Fe-organic ligand complex stability.

Whilst Fe-EPS complexes appear to be highly bioavailable to phytoplankton, the mechanism by which EPS is associated with Fe is not yet resolved. EPS contains functional groups such as saccharides and uronic acid that have previously been associated with Fe-binding (Croot and Johansson, 2000; Hassler and Schoemann, 2009; Hassler et al., 2011a, b). However, whether EPS, and possibly other organic ligands, weakly bind Fe or prevent the aggregation of very small oxyhydroxide particles, or perhaps both, remains unresolved. However, EPS may accelerate Fe(II) oxidation, and thus, Fe(II) removal from the system, although whether it can also enhance Fe(III) reduction requires further investigation.

6.3.2 Atmospheric dust

The two dust samples used in this study displayed many similarities, but the different community responses (Chapter 3) indicate that their composition was different. It is possible that the samples had different mineralogies (data not available) and that the atmospheric processing they underwent before collection resulted in different Fe species and size fractions. This may have resulted in the delivery of Fe species that were more bioavailable to some phytoplankton species than others, as evidenced by the suppression

of cyanobacteria in the D1 enrichment (Chapter 3). However, the bioavailability of dust-borne Fe may not only be dependent on the form of Fe delivered, but may also depend on organic ligands present in surface waters. Evidence that nanoparticulate dust-EPS complexes enhance the solubility and colloidal stability of the associated Fe (Kadar et al., 2014) suggests that bioavailability, possibly to other phytoplankton species, may be increased. Whether this is true also for other organic ligands (saccharides, siderophores, HS) has yet to be investigated.

Ligands with high conditional stability constants were measured in the D1 incubations (Chapter 3). The dust itself contains organic ligands (Chapter 5) but these are much weaker, and whilst they would have contributed to the L_2 ligands present they would not have been associated with the L_1 class. It is, therefore, likely that the strong ligands were biologically produced i.e., siderophores or L_1 components of EPS. In the natural environment, the contribution that ligands associated with dust and rainwater (in the case of wet deposition events) make to the organic ligand pool of the surface ocean may be very small (Chapter 5), but will vary depending the intensity and duration of deposition events. However, their role in Fe biogeochemistry during atmospheric transport is extremely important because, like Fe-ligand complexation in the oceans, complexation during atmospheric transport can mediate the production of H_2O_2 and the photochemical reduction of Fe(III) to Fe(II) (Baker and Croot, 2010). Furthermore, this complexation may help to stabilise Fe(II) and retard its oxidation (Willey et al., 2008). Thus, Fe-ligand complexation, together with atmospheric processing (i.e. acid reduction) will determine the species of Fe delivered to the surface ocean.

Dust (Chapter 3 and 5) and rainwater (Chapter 5) are also associated with other nutrients and trace elements that are beneficial to phytoplankton. D1 contained P, Si and Zn but no detectable N (Chapter 5) and so, whilst the added P and Si may benefit diatoms, the degree of utilisation may also depend on their N requirement and *in situ* availability. However, using the P and Si concentrations and estimated number of wet deposition events from Chapter 5, and the vertical supply calculations of Ellwood et al. (2013), the contribution of P (m^{-1} d^{-1}) would be negligible, and the Si contribution would amount to just 4 % of the vertical supply (m^{-1} d^{-1}). Thus, as with Fe content (Chapter 5), the nutrients present, the concentration in which they occur, and the effect they have on the biology of the surface ocean will depend on the dust source, and the intensity and duration of deposition.

6.4 Future research

This thesis has provided new information on the distribution and origins of Fe-binding organic ligands, and gives insight into the role these ligands play in Fe biogeochemistry. The results also highlight areas of research that could continue to improve our understanding of Fe biogeochemistry and its link with Fe bioavailability. These include:

- The current technique used for the analysis of organic ligands (CLE-AdCSV) allows for the determination of 1, or occasionally 2, classes of ligands. The detection window, set by the concentration of the competing ligand used, determines which ligands can be measured. It is clear that there are many ligands present in seawater and there is a continued need for the development of techniques that allow for the detection of more ligand classes within the same detection window. Furthermore, CLE-AdCSV does not distinguish between inorganic colloidal Fe and organically bound Fe. The development of techniques that could differentiate between Fe hydroxides, adsorbed Fe hydroxides and organic ligands would help to establish the role that organic ligands play in Fe biogeochemistry (i.e. Fe-binding or the prevention of aggregation through adsorption).
- A greater emphasis should be placed on the functional and physico-chemical characterisation of natural ligands (as conducted with the EPS in this thesis). Novel technologies such as metabolomics, which seeks to identify and quantify metabolites (Fiehn, 2001, Kind and Fiehn, 2006), NMR (Nuclear magnetic resonance spectroscopy), Advanced FTIR (Fourier transform infrared spectroscopy) and FT-IT-MS (Fourier transform ion trap mass spectrometry), which may give insight into the configuration/conformation aspects of chelation, are promising techniques. These, in parallel with more sensitive Fe speciation analysis, may assist in unravelling the origins of ligands in natural waters. This would give greater insight into the contribution each ligand makes to the Fe biogeochemistry of the study region.
- Although this work has focused on the regulation of Fe by natural organic ligands it should be noted that many other transition metals (e.g. Cu, Mn, Zn) can be bound, to a greater or lesser extent, to the same organic ligands as those studied here. The development of the techniques highlighted above may, therefore, assist in furthering our knowledge regarding the regulation of both beneficial and toxic trace elements by organic material.
- It is known that the effect of photochemistry on organic material varies. Often photochemistry degrades the organic ligand, and/or initiates Fe(III) reduction,

however, some ligands are not photosensitive (i.e. hydroxamate siderophores). Furthermore, the reduction of Fe(III) or Fe(III)-ligand complexes can be mediated via direct photoreduction, or the through the production of chemical reductants following photodegradation of organic material. Although EPS were seen to degrade over time, generally the conditional stability constants changed little and the association with Fe strengthened, indicating that some EPS may be less reactive than others. However, the effect of photochemistry on the association of Fe with EPS needs to be addressed as this may affect both Fe chemistry and bioavailability, and would give greater insight into how Fe-EPS complexes behave in natural waters.

- Further to the work by Kadar et al. (2014) who demonstrated that EPS can enhance the solubility and colloidal stability of Fe associated with atmospherically processed dust nanoparticles, experiments that investigate the bioavailability of dust-borne Fe-EPS, and other ligand complexes should be undertaken.
- Dust deposition in the global ocean varies in intensity and duration. The concentration of dust deposited may affect the distribution of Fe (i.e. proportions of soluble or colloidal Fe) as higher concentrations are likely to enhance aggregation and scavenging. Given the prediction of enhanced dust deposition into the Tasman Sea in the future, such concentration effects should be explored to test the hypothesis that more Fe will be present in the soluble fraction at low dust concentrations (i.e. 0.05 mg L^{-1}), whereas higher concentrations (i.e. 5 mg L^{-1}) will favour the formation of colloids. Although some phytoplankton can utilise colloidal Fe, it is generally considered to be much less available. Whilst the results in this thesis (Chapters 3 and 5) indicate that dust-borne Fe is highly bioavailable to some phytoplankton species (i.e. diatoms and haptophytes), an increase in the intensity and frequency of deposition events may, in fact, lower bioavailability due to the removal of Fe from surface waters via aggregation and scavenging.
- Finally, given that the Tasman Sea and Southern Ocean are predicted to be severely affected under climate-change scenarios (Hobday et al., 2008), the effect of lowered pH on Fe chemistry, i.e., changes to Fe-binding affinities and solubility of organic ligands, and the subsequent effects to Fe bioavailability need to be addressed.

6.5 Conclusion

It is widely accepted that the complexation of Fe with organic compounds is the primary factor that regulates Fe reactivity and its bioavailability to phytoplankton in the open ocean

(See recent reviews Vraspir and Butler, 2009; Hassler et al., 2012; Gledhill and Buck, 2012; Shaked and Lis, 2012). Despite considerable efforts to unravel the provenance of the many organic ligands present in the 'ligand soup' and to determine their contribution to Fe chemistry and bioavailability, much of this pool remains largely unresolved. This thesis has improved our knowledge of the impact that Fe and organic ligand source has on Fe biogeochemistry, particularly in the Tasman Sea. However, there are many other regions, i.e. coastal waters and polar regions, where the contributions of the various Fe and organic ligand sources will be very different. For example, coastal regions may be more dependent on Fe from river input and atmospheric dust (Coale et al., 1996; Jickells et al., 2005; Mahowald et al., 2005), whereas remote oceans and polar regions will be more dependent on remineralised Fe (Watson, 2001; Poorvin et al., 2004, 2011; Strzepek et al., 2005). In coastal regions, HS may have a greater contribution to the ligand pool, whilst biologically produced organic ligands will be critical in remote oceans. Furthermore, the endemic phytoplankton and microbial communities also need to be considered, as does their nutritional status. In order to improve our overall understanding of Fe biogeochemistry, the relative importance of each Fe and organic ligand source needs to be addressed for the various oceanic regions. This will move towards a better understanding of how Fe chemistry affects Fe-limitation and co-limitation observed in both HNLC and LNLC regions, and will allow for more accurate model predictions to be made as to the fate of the oceans under climate change scenarios.

APPENDICES

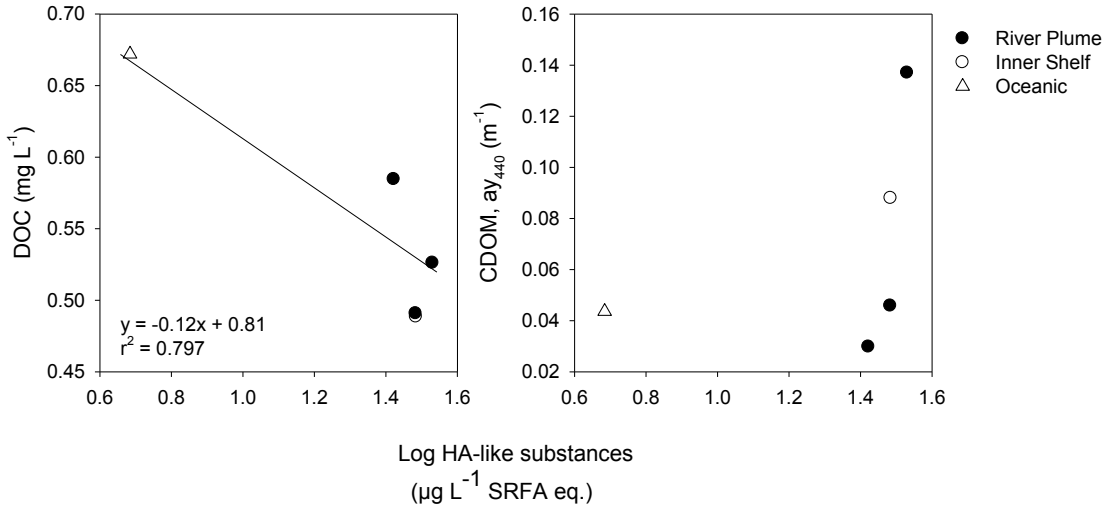

Appendix 1 Relationships between the concentration of humic substance-like (HS-like) material, DOC (mg L^{-1}) and CDOM (ay_{440} m^{-1}) from 5 samples taken during the SS2010-V09 Tasman Sea voyage (*RV Southern Surveyor*, 15th to 31st October 2010, austral spring). Data comprised three River Plume, one Inner Shelf, and one Oceanic samples. HS-like concentration data was log transformed to allow for clearer graphical representation.

Appendix 2 Individual marginal tests for environmental predictor variables used in distance-based redundancy analysis investigating the drivers of HS-like material concentration in the EAC incubations (Chapter 2).

Marginal Test	Pseudo-F	P	Prop
TChl-a	1.411	0.275	0.124
But-fucoxanthin	3.820	0.085	0.276
Fucoxanthin	2.647	0.148	0.209
Hex-fucoxanthin	0.017	0.889	0.002
Diadinoxanthin	1.623	0.235	0.140
NH4	0.001	0.977	<0.001
NO3	1.099	0.323	0.099
P04	61.735	0.001	0.861
dFe	42.321	0.005	0.809
Bacteria	1.233	0.326	0.109
Synechococcus	0.978	0.352	0.089
Prochlorococcus	1.364	0.282	0.120
Small eukaryotes	1.453	0.252	0.127
Large eukaryotes	0.277	0.557	0.027

Appendix 3 Individual marginal tests for environmental predictor variables used in distance-based redundancy analysis investigating the drivers of HS-like material concentration in the CCE incubations (Chapter 2).

Marginal Test	Pseudo-F	P	Prop
TChl-a	0.060	0.795	0.006
Peridinin	0.455	0.504	0.044
But-fucoxanthin	0.423	0.502	0.041
Fucoxanthin	0.129	0.705	0.013
Hex-fucoxanthin	0.231	0.640	0.023
Diadinoxanthin	0.051	0.822	0.005
NH4	3.132	0.115	0.239
NO3	0.144	0.722	0.014
P04	0.241	0.602	0.024
dFe	0.065	0.810	0.006
Bacteria	1.485	0.234	0.129
Synechococcus	0.331	0.553	0.032
Prochlorococcus	0.877	0.379	0.081
Small eukaryotes	0.687	0.428	0.064
Large eukaryotes	0.065	0.802	0.006

Appendix 4 Determination of the conditional side-reaction coefficient ($\alpha_{Fe'(TAC)2}$) (Chapters 3 and 4).

The analytical window of the CLE-AdCSV technique is set by the concentration of the competing ligand used (in this case TAC) and the $\alpha_{Fe'(TAC)2}$, which is a measure of the Fe-binding affinity of the TAC taking into account side reactions for other elements i.e. Ca and Mg that may also bind with the competing ligand. The $\alpha_{Fe'(TAC)2}$ is derived from the conditional cumulative stability constant, $\beta'_{Fe'(TAC)2}$

$$\beta'_{Fe'(TAC)2} = \frac{[Fe(TAC)_2]}{[Fe'][TAC]^2} \quad (2)$$

$$\alpha_{Fe'(TAC)2} = [TAC]^2 * \beta'_{Fe'(TAC)2} \quad (3)$$

Although the CLE-AdCSV method is constrained by the analytical window, it can generally detect ligands that are within ± 10 units of the log $\alpha_{Fe'(TAC)2}$ (Donet and van den Berg, 1992).

As different waters are likely to have different matrices an $\alpha_{Fe'(TAC)2}$ should be calculated for each water mass or sample type. Using the method of Croot and Johansson (2000), a competitive equilibrium was prepared between a fixed concentration of Fe (10 nM as $FeCl_3$ in 0.5M HCl, ICP grade, Fluka) in UV-digested seawater (or other sample matrix), and increasing concentrations of DTPA, (Diethylenetriaminepentaacetic acid, Sigma) in concentrations between 0 and 5000 nM. DTPA was used as an α_{DTPA} of $10^{7.95}$ in respect of Fe and a log $K'_{Fe'DTPA}$ of $10^{8.65}$ has previously been calculated (Croot and Johansson, 2000). The prepared titration was left to equilibrate overnight to allow for the slow equilibrium, due to the high side binding of Ca and Mg, to be completed. After equilibration 10 µM of TAC was added and the samples left to further equilibrate for 18 to 20 h. The samples were then analysed, as per the standard protocol, from high to low DTPA concentration and the concentration of $Fe(TAC)_2$ (i.e.Fe_{Labile}) can been seen to increase with decreasing DTPA concentration.

To calculate $\alpha_{Fe'(TAC)2}$ and therefore set the analytical window, the ratio (*X*) of the reduction current measured in the presence (i_p) and absence (i_0) of DTPA is plotted against log [DTPA′] and the values fitted to a 4-parameter logistic Hill curve (Sigma Plot, version 12) as per Hassler et al. (2013). Using the method of Hassler et al. (2013) the predicted values of X

and [DTPA′] from the linear portion of the Hill curve are used to derive $\beta'_{Fe'(TAC)2}$ (3) and $\alpha_{Fe'(TAC)2}$ (2).

$$\beta'_{Fe'(TAC)2} = \frac{X * K'_{Fe'DTPA} * [DTPA']}{[TAC]^2 - X * [TAC]^2} \quad (3)$$

The $\alpha_{Fe'(TAC)2}$ calculated for the seawater from the PINTS voyage (636 ± 48) and for the seawater used for the EPS experiments (627 ± 72) were considerably higher than the $\alpha_{Fe'(TAC)2}$ calculated by Croot and Johansson (2000; $\alpha_{Fe'(TAC)2}$ = 250) and Hassler et al (2013; 236 ±22) for the same TAC concentration. However, variability in $\alpha_{Fe'(TAC)2}$ values are not unusual and may be due to the use of different batches of TAC and DTPA, and also the sample matrix. Despite this difference, the calculated log $K_{Fe'(TAC)2}$ of 12.22 (PINTS) and 12.79 (EPS) are in good agreement with that calculated by Croot and Johansson (2000) of 12.4. Thus, the $\alpha_{Fe'(TAC)2}$ values calculated during these studies could be confidently used to calculate the ligand concentrations and conditional stability constants resulting from the CLE-AdCSV analyses.

REFERENCES

Abbasse, G., Ouddane, B., Fischer, J-C., 2002. Determination of total and labile fraction of metals in seawater using solid phase extraction and inductively coupled plasma atomic emission spectrometry (ICP-AES). *J. Anal. Atom. Spectrom*. 17, 1354–1358. doi: 10.1039/b203407g

Aluwihare, L.I., Repeta, D.J., 1999. A comparison of the chemical characteristics of oceanic DOM and extracellular DOM produced by marine algae. *Mar. Ecol. Prog. Ser*. 186, 105–117.

Amador, J. A., Milne, P. J., Moore, C. A., Zika, R.G. 1990. Extraction of Chromophoric Humic Substances from Seawater. *Mar. Chem*. 29, 1–7

Amin, S.A. Green, D.H., Hart, M.C., Küpper, F.C., Sunda, W.G., Carrano, C.J. 2009. Photolysis of iron–siderophore chelates promotes bacterial–algal mutualism. *PNAS.* 106: 17071–17076.

Amon, R. M. W., Benner, R. 1994. Rapid cycling of high-molecular-weight dissolved organic matter in the ocean. *Nature*. 369, 549–552.

Amon, R. M. W., Benner, R. 1996. Photochemical and microbial consumption of dissolved organic carbon and dissolved oxygen in the Amazon River system. *Geochim. Cosmochim. Acta* 60, 1783–1792.

Anderson, M.J., Gorley, R.N. Clarke, K.R. 2008. PERMANOVA A+ for PRIMER, Guide to software and statistical methods: PRIMER-E Ltd.

Andrews, S. S., Caron, S., Zafiriou, O. C. 2000. Photochemical oxygen consumption in marine waters: A major sink for colored dissolved organic matter. *Limnol. Oceanogr*. 45, 267–277.

Anesio, A.M., Granéli, W., Aiken, G.R., Kieber, D.J., Mopper, K. 2005. Effect of humic substance photodegradation on bacterial growth and respiration in lake water. *Appl. Environ. Microb*. 71, 6267–6275.

Azam, F. 1998. Microbial control of oceanic carbon flux: The plot thickens. *Science* 280, 694–696

REFERENCES

Baird, M.E., Timko, P.G., Middleton, J.H., Mullaney, T.J., Cox, D.R., Suthers, I.M. 2008. Biological properties across the Tasman Front off southeast Australia. *Deep-Sea Res. I*. 55, 1438–1455.

Baker, A. R., Kelly, S.D., Biswas, K.F., Witt, M., Jickells, T.D. 2003. Atmospheric deposition of nutrients to the Atlantic Ocean, *Geophys. Res. Lett.* 30, 2296 doi:10.1029/2003GL018518.

Baker, A.R., Jickells, T.D. 2006. Mineral particle size as a control on aerosol iron solubility. *Geophys. Res. Lett*. 33, L17608.

Baker, A.R., Jickells, T.D., Witt, M., Linge, K.L. 2006. Trends in the solubility of iron, aluminium, manganese and phosphorus in aerosol collected over the Atlantic Ocean. *Mar. Chem*. 98, 43–58.

Baker, A.R., Croot, P.L. 2010. Atmospheric and marine controls on aerosol iron solubility in seawater. *Mar. Chem*. 120, 4–13.

Barbeau, K., Moffett, J. W., Caron, D. A., Croot, P. L., Erdner, D. L. 1996. Role of protozoan grazing in relieving iron limitation of Phytoplankton. *Nature*. 380, 61–64.

Barbeau, K., Rue, E.L., Bruland, K.W., Butler, A. 2001. Photochemical cycling of iron in the surface ocean mediated by microbial iron(III)-binding ligands. *Nature.* 413**,** 409–413.

Barbeau, K., Rue, E.L., Trick, C.G., Bruland, K.W., Butler, A. 2003. Photochemical reactivity of siderophores produced by marine heterotrophic bacteria and cyanobacterial based on characteristic Fe(III) binding groups. *Limnol. Oceanogr.* 48, 1069–1078.

Barlow R.G., Mantoura R. F.C., Gough M.A., Fileman T.W. 1993. Pigment signatures of the phytoplankton composition in the north-eastern Atlantic during the 1990 spring bloom, *Deep Sea Res. II*. 40, 459–477.

Behrenfeld, M. J., Milligan, A. J. 2013. Photophysiological expression of iron stress in Phytoplankton. *Annu. Rev. Mar. Sci.* 5, 217–246. doi:10.1146/ANNUREV-MARINE-121211-172356.

REFERENCES

Belzile, C., Roesler, C. S., Christensen, J. P., Shakhova, N., Semiletov, I. 2006. Fluorescence measured using the WETstar DOM fluorometer as a proxy for dissolved matter absorption. *Estuar. Coast. Shelf. Sci.* 67, 441–449.

Benner, R., Pakulski, J.D., McCarthy, M., Hedges, J.I., Hatcher, P.G., 1992. Bulk chemical characteristics of dissolved organic matter in the ocean. *Science*. 255, 1561–1564.

Benner, R. and Ziegler, S. 1999. Do photochemical transformations of dissolved organic matter produce biorefractory as well as bioreactive substances? In: *Proceedings of the 8th International Symposium on Microbial Ecology*. Eds. C. R. Bell, M. Briylinsky and P. Johnson-Green. Atlantic Canada Society for Microbial Ecology, Halifax, Canada.

Benner, R. 2002. Chemical composition and reactivity: In: *Biogeochemistry of marine dissolved organic matter*. Eds. Hansell, D. A., Carlson, C. A. Academic Press, Elsevier Science, New York. pp 59–90.

Benner, R., 2011. Loose ligands and available iron in the ocean. *Proc. Natl. Acad. Sci.* 108, 893–894.

Berman, T., Bronk, D.A**.** 2003. Dissolved Organic Nitrogen: a dynamic participant in aquatic ecosystems. *Aquat. Microb. Ecol*. 31, 273–305.

Blough, N.V., Del Vecchio, R. 2002. Chromophoric DOM in the coastal environment. In; *Biogeochemistry of Marine Dissolved Organic Matter*. Eds. Hansell, D. A. and Carlson, C. A. Academic Press, Elsevier Science, New York. pp. 509–546.

Bonnet, S., Guieu, C. 2010. Dissolution of atmospheric iron in seawater. *Geophys. Res. Lett*. 31, L03303, doi:10.1029/2003GL018423.

Bowie, A.R., Lohan, M.C. 2009. Determination of iron in seawater. In, *Practical guidelines for the analysis of seawater.* Ed.O. Wurl. CRC Press, Taylor and Francis Group, London, UK.

REFERENCES

Bowie, A. R., Lannuzel, D., Remenyi, T. A., Wagener, T., Lam, P. J.,Boyd, P. W., Guieu, C., Townsend, A. T., and Trull, T. W. 2009. Biogeochemical iron budgets of the Southern Ocean south of Australia: decoupling of iron and nutrient cycles in the subantarctic zone by the summertime supply. *Global Biogeochem. Cy.* 23, GB4034. doi:10.1029/2009GB003500.

Bowie, A.R., Townsend, A.T., Lannuzel, D., Remenyi, T.A., van der Merwe, P., 2010. Modern sampling and analytical methods for the determination of trace elements in marine particulate material using magnetic sector inductively coupled plasma–mass spectrometry. *Anal. Chim. Acta*. 676, 15–27.

Bowie, A.R., Griffiths, F.B., Dehairs, F., Trull, T.W. 2011. Oceanography of the subantarctic and Polar Frontal Zones south of Australia during summer: Setting for the SAZ-Sense study. *Deep-Sea Res. II.* 58, 2059–2070.

Boyd, P., Newton, P. 1999. Does planktonic community structure determine downward particulate organic carbon flux in different oceanic provinces? *Deep Sea Res I.* 46: 63–91.

Boyd, P.W., Watson, A.J., Laws, C.S., Abraham, E.R., Trull, T., Murdoch, R., Bakker, D.C.E., Bowie, A.R., Buesseler, K.O., Chang, H., Charette, M., Croot, P., Downing, K., Frew, R., Gall, M., Hadfield, M., Hall, J., Harvey, M., Jameson, G., LaRoche, J., Liddicoat, M., Ling, R., Maldonaldo, M.T., McKay, R.M., Nodder, S., Pickmere, S., Pridmore, R., Rintoul, S., Safi, K., Sutton, P., Strzepek, R., Tanneberger, K., Turner, S., Waite, A., Zeldis, J. 2000. A mesoscale phytoplankton bloom in the polar Southern Ocean stimulated by iron fertilization. *Nature* 407: 695–702.

Boyd, P.W., McTainsh, G., Sherlock, V., Richardson, K., Nichol, S., Ellwood, M., Frew, R. 2004. Episodic enhancement of phytoplankton stocks in New Zealand subantarctic waters: Contribution of atmospheric and oceanic iron supply. *Global Biogeochem. Cy*. 18, GB1029, doi:10.1029/2002GB002020.

REFERENCES

Boyd**,** P.W., Jickells, T., Law, C.S., Blain, S., Boyle, E.A., Buesseler, K.O., Coale, K.H., Cullen, J.J., de Baar, H.J.W.. Follows, M., Harvey, M., Lancelot, C., Levasseur, M., Owens N. P. J., Pollard, R., Rivkin, R.B., Sarmiento, J., Schoemann, V., Smetacek, V., Takeda, S., Tsuda, A., Turner, S., Watson, A.J. 2007. Mesoscale iron enrichment experiments 1993-2005: Synthesis and future directions. *Science* 315**,** 612–617.

Boyd, P.W., Ellwood, M.J. 2010. The biogeochemical cycle of iron in the ocean. *Nature Geosci.* 3, 675–682.

Boyd, P.W., Strzepek, R., Chiswell, S., Chang, H., DeBruyn, J.M., Ellwood, M., Keenen, S., King, A.L., Maas, E.W., Nodder, S., Sander, S.A., Sutton, P., Twining, B.S., Wilhelm, S.W., Hutchins, D.A. 2012. Microbial control of diatom bloom dynamics in the open ocean. *Geophys. Res. Lett*. 39, L18601, doi: 10.1029/2012GL053448.

Boye, M., van den Berg, C.M.G. 2000. Iron availability and the release of iron-complexing ligands by *Emiliania huxleyi*. *Mar. Chem*. 70, 277–287.

Boye, M., van den Berg, C.M.G., de Jong, J.T.M., Leach, H., Croot, P., de Baar, H.J.W. 2001. Organic complexation of iron in the Southern Ocean. *Deep-Sea Res. I*. 48, 1477–1497.

Boye, M., Nishioka, J., Croot, P.L., Laan, P., Timmermans, K.R., de Baar, H.J.W. 2005. Major deviations of iron complexation during 22 days of a mesoscale iron enrichment in the open Southern Ocean. *Mar. Chem*. 96, 257–271.

Boye, M., Nishioka, J., Croot, P., Laan, P., Timmermans, K.R., Strass, V.H., Takeda, S., de Baar, H.J.W. 2010. Significant portion of dissolved organic Fe complexes in fact is Fe colloids. *Mar. Chem.* 122, 20–27.

Breitbarth**,** E., Achterberg, E.P., Ardelan, M.V., Baker, A.R., Bucciarelli, E., Chever, F., Croot, P.L., Duggen, S., Gledhill, M., Hassellöv, M., Hassler, C.S., Hoffmann, L.J., Hunter, K.A., Hutchins, D.A., Ingri, J., Jickells, T., Lohan, M.C., Nielsdóttir, M.C., Sarthou, G., Schoemann, V., Trapp, J.M.,Turner, D.R., Ye., Y. 2009. Iron biogeochemistry across marine systems – progress from the past decade. *Biogeosciences Discuss.* 6, 6635–6694.

REFERENCES

Bronk, D. A. 2002. Dynamics of dissolved organic nitrogen. In; B*iogeochemistry of Marine Dissolved Organic Matter*. Eds. Hansell, D. A. and Carlson, C. A. Academic Press, Elsevier Science, New York. pp. 153–247.

Bronk, D. A., See, J.H., Bradley, P., Killberg, L. 2007. DON as a source of bioavailable nitrogen for phytoplankton. *Biogeosciences*. 4, 283–296.

Bruland, K.W., Orians, K.J., Cowen, J.P. 1994. Reactive trace metals in the stratified central North Pacific. *Geochem. Cosmochim. Acta,* 58, 3171–3182.

Bruland, K.W., Rue, E.L., Smith, G.J. 2001. Iron and macronutrients in California coastal upwelling regimes: Implications for diatom blooms. *Limnol. Oceanogr.* 46, 1661–1674.

Buck, K., Selph, K.E., Barbeau, K.A. 2010. Iron-binding ligand production and copper speciation in an incubation experiment of Antarctic Peninsula shelf waters from the Bransfield Strait, Southern Ocean. *Mar. Chem.* 122, 148–159.

Buck, C.S., Landing, W.M., Resing, J. 2013. Pacific Ocean aerosols: Deposition and solubility of iron, aluminium, and other trace elements. *Mar. Chem*. 157, 117–130.

Buffle, J. 1990. The analytical challenge posed by fulvic and humic compounds. *Anal. Chim*. *Acta.* 232, 1–2.

Buma, A.G.J., de Baar, H.J.W., Nolting, R.F., van Bennekom, A.J. 1991. Metal enrichment experiments in the Weddell-Scotia Seas: effect of iron and manganese on various plankton communities. *Limnol. Oceanogr.* 36, 1865–1878.

Bushaw, B. L., Zepp, R. G., Tarr, M. A., Schulzjander, D., Bourbonniere, R. A., Hodson, R. E., Miller, W. L., Bronk, D. A., Moran, M. A. 1996. Photochemical release of biologically available nitrogen from aquatic dissolved organic matter. *Nature*. 381, 404–407.

Calace, N., Casagrande, A., Mirante, S., Petronio, B.M., Pietroletti, M. 2010. Distribution of humic substances dissolved and particulated in water column in Ross Sea, Antarctica. *Microchem. J*. 96, 218–224.

REFERENCES

Carlsson, P., Granéli, E. 1993. Availability of humic bound nitrogen for coastal phytoplankton. *Est. Coast. Shelf. Sci*. 36, 433–447.

Cheize, M., Sarthou, G., Croot, P. L., Bucciarelli, E., Baudoux, A.-C., and Baker, A. R. 2012. Iron organic speciation determination in rainwater using cathodic stripping voltammetry. *Anal. Chim. Acta,* 736, 45–54.

Chen, M., Wang, W-X. 2001. Bioavailability of natural colloid-bound iron to marine plankton: Influences of colloidal size and aging. *Limnol. Oceanogr.* 46, 1956–1967.

Chen, M., Dei., R.C.H., Wang, W-X., Guo, L.D. 2003. Marine diatom uptake of iron bound with natural colloids of different origins. *Mar Chem.* 81, 177–189.

Chen, M., Wang, W-X., Guo, L. 2004. Phase partitioning and solubility of iron in natural seawater controlled by dissolved organic matter. *Global. Biogeochem. Cy.* 18, GB 4013, doi:10.1029/2003GB00216o.

Chen, M., Wang, W-X. 2008. Accelerated uptake by phytoplankton of iron bound to humic acids. *Aqua. Biol.* 3, 155–166.

Chisolm, S. 2000. Stirring times in the Southern Ocean. *Nature*. 407, 685–687.

Coale, K.H., Fitzwater, S.E., Gordon. R.M., Johnson, K.S., Barber, R.T. 1996. Control of community growth and export production by upwelled iron in the equatorial Pacific Ocean. *Nature.* 379, 621–624.

Coale, K. H., Johnson, K. S., Chavez, F. P., Buesseler, K. O., Barber, R. T., Brzezinski, M. A., Cochlan, W. P., Millero, F. J., Falkowski, P. G., Bauer, J. E., Wanninkhof, R. H., Kudela, R. M., Altabet, M. A., Hales, B. E., Takahashi, T., Landry, M. R., Bidigare, R. R., Wang, X., Chase, Z., Strutton, P. G., Friederich, G. E., Gorbunov, M. Y., Lance, V. P., Hilting, A. K., Hiscock, M. R., Demarest, M., Hiscock, W. T., Sullivan, K. F., Tanner, S. J., Gordon, R. M., Hunter, C. N., Elrod, V. A., Fitzwater, S. E., Jones, J. L., Tozzi, S., Koblizek, M., Roberts, A. E., Herndon, J., Brewster, J., Ladizinsky, N., Smith, G., Cooper, D., Timothy, D., Brown, S. L., Selph, K. E., Sheridan, C. C., Twining, B. S., and Johnson, Z. I. 2004. Southern Ocean iron enrichment experiment: carbon cycling in high- and low-Si waters. *Science.* 304, 408–414.

REFERENCES

Croot, P.L., Bowie, A.R., Frew, R.D., Maldonado, M.T., Hall, J.A., Safi, K.A., La Roche, J., Boyd, P.W., Law, C.S. 2001. Retention of dissolved iron and Fe^{II} in an iron induced Southern Ocean phytoplankton bloom. *Geophys Res Lett*. 28, 3425–3428.

Croot, P.L., Johansson, M. 2000. Determination of iron speciation by cathodic stripping voltammetry in seawater using the competing ligand 2-(-Thiazolylazo)-p-crestol (TAC). *Electroanalysis.* 12: 565–576.

Croot, P.L., Bowie, A.R., Frew, R.D., Maldonado, M.T., Hall, J.A., Safi, K.A., La Roche, J., Boyd, P.W., Law, C.S., 2001. Retention of dissolved iron and Fe(II) in an iron induced Southern Ocean phytoplankton bloom. *Geophys. Res. Lett*. 28, 3425–3428.

Croot, P.L., Laan, P. 2002. Continuous shipboard determination of Fe(II) in polar waters using flow injection analysis with chemiluminescence detection. *Anal. Chim.Acta*. 466, 261–273.

Cowley, R., Critchley, G., Eriksen, R., Latham, V., Plaschke, R., Rayner, M., Terhell, D. 1999. Hydrochemistry operations manual, Rep. 236, 106 pp., CSIRO Mar. Lab., Hobart, Tasmania, Australia.

Cropp, R. A., Gabric, A. J., Levasseur, M., McTainsh, G. H., Bowie, A., Hassler, C. S., Law, C. S., McGowan, H., Tindale, N., Viscarra Rossel, R. 2013. The likelihood of observing dust-stimulated phytoplankton growth in waters proximal to the Australian continent. *J. Marine Syst.* 117-118, 43–52. doi:10.1016/J.JMARSYS.2013.02.013

Crosby. S.A., Glasson. D.R., Cutler. A.H., Butler. I., Turner. D.R., Whitfield. M., Millward, G.E. 1983. Surface areas and porosities of Fe(III)- and Fe(II)-derived oxyhydroxides. *Environ. Sci. Tech.* 17, 709–713.

Cullen, J.T., Bergquist, B.A., Moffett, J.W. 2006. Thermodynamic characterization of the partitioning of iron between soluble and colloidal species in the Atlantic Ocean. *Mar. Chem*. 98, 295–303.

REFERENCES

Cutter, G., Andersson, P., Codispoti, L., Croot, P., Fracois, R., Lohan, M., Obata, H., and van der Loeff, M. R. (2010). Sampling and sample handling protocols for GEOTRACES Cruises. Available at www.geotraces.org/libraries/documents/Intercalibration/Cookbook.pdf (Verified 21 June 2014)

de Baar, H.J.W., de Jong, J.T.M., Bakker, D.C.E., Loscher, B.M., Veth, C., Bathmann, U., Smetacek. 1995. Importance of iron for phytoplankton blooms and carbon dioxide drawdown in the Southern Ocean. *Nature.* 373, 412–415.

de Baar, H.J.W., de Jong, J.T.M. 2001. Distributions, sources and sinks of iron in seawater. In: *The biogeochemistry of iron in seawater.* Eds. D.R. Turner, K.A. Hunter. John Wiley & Sons, UK. pp 123–254.

de Baar, H.J.W., La Roche, J. 2003. Trace metals in the oceans: evolution, biology and global change. In *Marine Science Frontiers for Europe*. Eds G. Wefer, F. Lamy, F. Mantoura. Springer, Berlin. pp 79–105.

de Baar, H.J.W., Boyd, P.W., Coale, K.H., Landry, M.R., Tsuda, A., Assmy, P., Bakker, D.C.E., Bozec, M.R., Barber, R.T., Brezezinski, M.A., Buesseler, K.O., Boyé, M., Croot, P.L., Gervais, F., Gorbunov, M.Y., Harrison, P.J., Hiscock, W.T., Laan, P., Lancelot, C., Law, C.S., Levasseur, M., Marchetti, A., Millero, F.J., Nishioka, J., Nojiri, Y., van Oijem, T., Riebesell, U., Rijkenberg, M.J.A., Saito, H., Takada, S., Timmermans, K.R. Veldhuis, M.J.W., Waite, A.M., Wong, C-S. 2005. Synthesis of iron fertilization experiments: From the Iron Age in the Age of Enlightenment. *J. Geophys. Res.* 110: C09S16, doi:10.1029/2004JC002601.

de Jong, J.T.M., den Dasa, J., Bathmann, U., Stolla, S.H.C. Kattner, C., Nolting, R.F., de Baar, H.J.W. 1998. Dissolved iron at subnanomolar levels in the Southern Ocean as determined by ship-board analysis. *Anal. Chim. Acta.* 377, 113–124.

de Jong, J., Schoemann, V., Mattielli,N., Lannuzel, D., 2008. High-accuracy determination of iron in seawater by isotope dilution multiple collector inductively coupled plasma mass spectrometry (ID-MC-ICP-MS) using nitrilotriacetic acid chelating resin for preconcentration and matrix separation. *Anal. Chim. Acta*. 623, 126–139. doi:10.1016/j. aca.2008.06.013.

REFERENCES

Decho, A.W. 1990. Microbial exopolymer secretions in ocean environments: Their role(s) in food webs and marine processes. In, Oceanography and Marine Biology Annual Review. Ed., M. Barnes. Aberdeen Univ Press, Aberdeen, Scotland. 28, 73–153.

Deguillaume, L., Leriche, M., Desboeufs, K., Mailhot, G., George, C., Chaumerliac, N., 2005. Transition metals in atmospheric liquid phases: sources, reactivity, and sensitive parameters. *Chem. Rev.*105, 3388–3431.

Devol, A.H., Dos Santos, A., Forsberg, B.R., Zaret, T.M. 1984. Nutrient addition experiments in Lago Jacarentinga, Central Amazon, Brazil: 2. The effect of humic and fulvic acids. *Hydrobiologia*. 109, 97–103.

Dignac, M.F., Urbain, V., Rybacki, D., Bruchet, A., Snidaro, D., Scribe, P. 1998. Chemical description of extracellular polymers: Implication on activated sludge floc structure. *Wat. Sci. Tech.* 38, 45–53.

DiTullio, G.R., Grebmeier, J.M., Arrigo, K.R., Lizotte, M.P., Robinson, D.H., Leventer, A., Barry, J.P., Van Woert, M.L., Dunbar, R.B. 2000. Rapid and early export of *Phaeocystis antarctica* blooms in the Ross Sea, Antarctica. *Nature.* 404, 595–598.

Doblin, M.A., Blackburn, S.I. and Hallegraeff, G.M. 1999. Growth and biomass stimulation of the toxic dinoflagellate *Gymnodinium catenatum* (Graham) by dissolved organic substances. *J. Exp. Mar. Biol. Ecol.* 236, 33–47.

Doblin, M. A., Ralph, P. J., Petrou, K. L., Shelly, K., Westwood, K., van den Enden, R., Wright, S., and Griffiths, B. (2011). Diel variation of chlorophyll-a fluorescence, phytoplankton pigments and productivity in the Sub-Antarctic and Polar Front Zones south of Tasmania, Australia. *Deep-sea Res. II.* 58, 2189–2199. doi:10.1016/J.DSR2.2011.05.021.

Donat, J.R., van den Berg, C.M.G., 1992. A new cathodic stripping voltammetric method for determining organic copper complexation in seawater. *Mar. Chem*. 38, 69–90.

Douchet., F.J., Lead, J.R., Santschi., P.H. 2007. Colloid – Trace element interactions in aquatic systems. In; *Environmental Colloids and Particles: Behaviour, Separation and Characterisation.* Eds: K.J. Wilkinson, J. R. Lead. Wiley. pp 95–157.

REFERENCES

Duarte, R. M. B. O., Santos, E.B.H., Pio, C.A., Duarrte, A.C. 2007. Comparison of structural features of water-soluble organic matter from atmospheric aerosols with those of aquatic humic substances. *Atmos. Environ.* 41, 8100–8113.

Duce, R.A., Tindale, N.W. 1991. Atmospheric transport of iron and it's deposition in the ocean. *Limnol. Oceanogr.* 36, 1715–1726.

Duggen, S., Olgun, N., Croot, P., Hoffman, L., Dietze, H., Delmelle, P., Teschner. 2010. The role of airborne volcanic ash for the surface ocean biogeochemical iron-cycle: a review. *Biogeosciences* 7, 827–844.

Elrod, V.A., Berelson, W.M., Coale, K.H., Johnson, K.S. 2004. The flux of iron from continental shelf sediments: A missing source for global budgets. *Geophys. Res. Lett.* 31, L12307, doi:10.1029/2004GL020216.

Ellwood, M.J., Law, C.S., Hall, J., Woodward, E.M.S., Strzepek, R., Kuparinen, J., Thompson, K., Pickmere, S., Sutton, P., Boyd, P.W. 2013. Relationships between nutrient stocks and inventories and phytoplankton physiological status along an oligotrophic meridional transect in the Tasman Sea. *Deep-Sea Res I*. 72, 102–120.

Engel, A., Thoms, S., Riebesell, U., Rochelle-Newall, E., Zondervan, I. 2004. Polysaccharide aggregation as a potential sink of marine dissolved organic carbon. *Nature.* 428, 929–932.

Erel, Y., Pehkonen, S.O., Hoffmann, M.R., 1993. Redox chemistry of iron in fog and stratus clouds. *J. Geophys. Res*. 98, 18423–18434.

Esteves, V.I., Otero, M., Duarte, A.C. 2009. Comparative characterization of humic substances from the open ocean, estuarine water and fresh water. *Org. Geochem*. 40, 942–950.

Falkowski, P.G. 1994. The role of phytoplankton photosynthesis in global biogeochemical cycles. *Photosyn. Res*. 39, 235–258.

Falkowski, P.G., Barber, R.T., Smetacek, V. 1998. Biogeochemical controls and feedbacks on ocean primary production. *Science*. 281, 200–206.

REFERENCES

Fiehn, O 2001. Combining genomics, metabolome analysis, and biochemical modelling to understand metabolic networks. *Comp Funct Genom* 2, 155–168.

Flemming, H.-C., Wingender, J., Mayer, C., Körstgens, V. and Borchard, W. 2000. Cohesiveness in biofilm matrix polymers. In: *Community Structure and Co-operation in Biofilms*. Eds: H.M. Lappin-Scott, P. Gilbert, M. Wilson and D. Allison. SGM symposium 59. Cambridge University Press, Cambridge, UK. pp. 87–105.

Frew, R.D., Hutchins, D.A., Nodder, S., Sanudo-Wilhelmy, S., Tovar-Sanchez, A., Leblanc, K., Hare, C.A., Boyd. P.W., 2006. Particulate iron dynamics during FeCycle in subantarctic waters southeast of New Zealand. *Global. Biogeochem. Cy*. 20, GB1S93. doi: 10.1029/2005GB002558.

Fung, I.Y., Meyn, S.K., Tegen, I., Doney, S.C., John, J.G., Bishop, J.K.B. 2000. Iron supply and demand in the upper ocean. *Glob. Biogeochem. Cy.* 14, 281–295.

Gabric, A.J., Cropp, R., Ayers, G.P., McTainsh,G., Braddock, R., 2002. Coupling between cycles of phytoplankton biomass and aerosol optical depth as derived from SeaWiFS time series in the Subantarctic Southern Ocean. *Geophy. Res. Lett*. 29, 1112. doi: 10.1029/2001GL013545.

Gagnon, R., Levasseur, M., Weise, A.M., Fauchot, J., Campbell, P.G.C., Weissenboeck, B.J., Merzouk, A., Gosselin, M., Vigneault, B. 2005. Growth stimulation of Alexandrium Tamarense (Dinophyceae) by humic substances from the Manicouagan River (Eastern Canada). *J. Phycol*. 41, 489–497.

Garg, S., Rose, A.L., Godrant, A., Waite, T.D. 2007. Iron uptake by the ichthyotoxic *Chattonella Marina* (Raphiophyceae): impact of superoxide generation. *J. Phycol.* 43, 978–991.

Gerringa, L.J.A., Herman, P.M.J., Poortvliet, T.C.W. 1995. Comparison of the linear van den Berg/Ružić transformation and a non-linear fit of the Langmuir isotherm applied to Cu speciation data in the estuarine environment. *Mar. Chem.* 48, 131–142.

REFERENCES

Gerringa, L.J.A., de Baar, H.J.W., Timmermans, K.R. 2000. A comparison of iron limitation of phytoplankton in natural oceanic waters and laboratory media conditioned with EDTA. *Mar. Chem*. 68, 335–346.

Giesy, J.P. 1976. Stimulation of growth in *Scenedesumus obliquus* (Chlorophtceae) by humic acids under iron limited conditions. *J. Phycol*. 12, 172–179.

Ginoux, P., Ramaswamy, V. 2008. Distribution, transport, and deposition of mineral dust in the Southern Ocean and Antarctica: Contribution of major sources. *J. Geophys. Res.* 113, D10207. doi: 10.1029/2007JD009190

Gledhill, M., van den Berg, C.M.G. 1994. Determination of the complexation of iron(III) with natural organic complexing ligands in seawater using cathodic stripping voltammetry. *Mar. Chem*. 47, 41–54.

Gledhill, M., McCormack, P., Ussher, S., Achterberg, E.R., Fauzi, R., Mantoura, C., Worsford, P.J. 2004. Production of siderophore type chelates by mixed bacterioplankton populations in nutrient enriched seawater incubations. *Mar. Chem.* 88, 75–83.

Gledhill M., Buck, K.N. 2012. The organic complexation of iron in the marine environment: a review. *Front Microbio.* 3, 69. doi: 10.3389/fmicb.2012.00069.

Gordon, R.M., Coale, K.H., Johnson, K.S. 1997. Iron distribution in the equatorial Pacific: Implications for new production. *Limnol. Oceanogr*. 42, 419–431.

Grasshoff, K.M., Ehrhardt, M., Kremling, K., 1983. Methods of Seawater Analysis. Verlag Chemie, Weinheim, Germany.

Guieu, C., Bonnet, S., Wagener, T. 2005. Biomass burning as a source of dissolved iron to the open ocean? *Geophys. Res. Lett*. 32, L19608, doi:10.1029/2005GL022962.

Gutierrez, T., Biller, D.V., Shimmield, T., Green, D.H., 2012. Metal binding properties of the EPS produced by *Halomonas* sp. TG39 and its potential in enhancing trace element bioavailability to eukaryotic phytoplankton. *Biometals*. 25, 1185–1194.

REFERENCES

Hales, B., van Greer, A., Takahashi, T., 2004. High-frequency measurements of seawater chemistry: Flow-injection analysis of macronutrients, *Limnol. Oceanogr. Methods*. 2, 91–101, doi:10.4319/lom.2004.2.91.

Hansard, S.P., Landing, W.M., Measures, C.I., Voelker, B.M., 2009. Dissolved iron(II) in the Pacific Ocean: Measurements from the PO2 and P16N CLIVAR/CO_2 repeat hydrography expeditions. *Deep-Sea Res. I.* 56, 1117–1129.

Hansell, D.A., Carlson, C.A., 2002. *Biogeochemistry of marine dissolved organic matter.* Academic Press, San Diego.

Hansell, D.A., Carlson, C.A., Schlitzer, R. 2012. Net removal of major marine dissolved organic fractions in the subsurface ocean. *Global. Biogeochem.Cy*. 26, GB1016, doi:10.1029/2011GB004069.

Hanson, A.K., Tindale, N.W., Abdel-Moati, M.A.R. 2001. An Equatorial Pacific rain event: influence on the distribution of iron and hydrogen peroxide in surface waters. *Mar. Chem*. 75, 69–88

Harris, D.C., 1998. Nonlinear least-squares curve fitting with Microsoft Excel Solver. *J. Chem. Educ.* 75, 119–121.

Harrison, G.I., Morel, F.M.M. 1986. Response of the marine diatom *Thalassiosira weissflogii* to iron stress. *Limnol. Oceanogr.* 31, 989–997.

Hassler, C.S., Schoemann, V. 2009a. Bioavailability of organically bound iron in controlling Fe to model phytoplankton of the Southern Ocean. *Biogeosciences.* 6, 2281–2296.

Hassler, C.S., Havens S.M., Bullerjahn G.S., Michael, R., McKay, L., Twiss, M.R. 2009b. An evaluation of iron bioavailability and speciation in western Lake Superior with the use of combined physical, chemical, and biological assessment. *Limnol. Oceanogr*. 54, 987–1001

Hassler, C.S., Alasonati, E., Mancuso Nichols, C.A., Slaveykova, V.I. 2011a. Exopolysaccharides produced by bacteria isolated from the pelagic Southern Ocean – Role in Fe binding, chemical reactivity, and bioavailability. *Mar. Chem.* 123, 88–98.

Hassler, C.S., Schoemann, V., Mancuso Nichols, C., Butler, E.C.V., Boyd, P.W. 2011b. Saccharides enhance iron bioavailability to Southern Ocean phytoplankton. *PNAS.* 108, 1076–1081.

Hassler, C., Djajadikarta, R.J., Doblin, M.A., Everett, J.D., Thompson, P. 2011c. Characterisation of water masses and nutrient limitation of phytoplankton in the separation zone of the East Australian Current in spring 2008. *Deep-Sea Res II.* 58, 664–677.

Hassler, C.S., Schoemann, V., Boye, M., Tagliabue, A., Rozmarynowycz, M., McKay, R.M. 2012. Iron bioavailability in the Southern Ocean. *Oceanogr. Mar. Biol.* 50, 1–64.

Hassler, C.S., Legiret, F-E., Butler, E.C.V. 2013. Measurement of iron speciation in seawater at 4 °C: The use of competitive ligand exchange-adsorptive cathodic stripping voltammetry. *Mar. Chem.* 149, 63–73.

Hassler, C.S., Ridgeway, K.R., Bowie, A.R., Butler, E.C.V., Clementson, L.A., Doblin, M.A., Davies, D.M., Law, C., Ralph, P.J., van der Merwe, P., Watson, R., Ellwood, M.J. 2014. Primary productivity induced by iron and nitrogen in the Tasman Sea – An overview of the PINTS expedition. *Mar. Freshwater Res.* 65, 517–537. doi. Org/10.1071/MF13137

Hassler, C.S., Norman, L., Angles, E., Mancuso Nichols, C.A., Clementson, L.A., Robinson, C., Watson, R.J., Doblin, M.A. 2014. Exopolymeric substances can relieve iron limitation in oceanic phytoplankton. *Mar. Chem*. **In press**.

Heimberger, A. Losno, R., Triquet, S. 2013. Solubility of iron and other trace elements in rainwater collected on the Kergulen Island (South Indian Ocean). *Biogeosciences*. 10, 6617–6628.

Hegg, D., Gao, S., Jonsson, H., 2002. Measurements of selected dicarboxylic acids in marine cloud water. *Atmos. Res*. 6, 1–10.

Hesse, P. P. 1994. The record of continental dust from Australia in Tasman Sea sediments. *Quaternary Sci. Rev.* 13, 257–272. doi:10.1016/0277-3791(94)90029-9.

Hesse, P. P., and McTainsh, G. H. 2003. Australian dust deposits: modern processes and the Quaternary record. *Quaternary Sci. Rev.* 22, 2007–2035, doi:10.1016/S0277-3791(03)00164-1.

REFERENCES

Hiemstra, T., van Riemsdijk, W.H. 2006. Biogeochemical speciation of Fe in ocean water. *Mar. Chem.* 102, 181–197.

Hobday, A., Poloczanska E.S., Matear R.J. 2008. *Report to the Australian Greenhouse Office.*

Hoagland, K.D., Rosowski, J.R., Gretz, M.R., Roemer, S.C. 1993. Diatom extracellular polymeric substances: function, fine structure, chemistry, and physiology. *J. Phycol.* 29, 537–566.

Hudson, R. J. M., Covault, D. T., Morel, F. M. M. 1992. Investigations of iron coordination and redox chemistry reactions in seawater using 59Fe radiometry and ion-pair solvent extraction of amphiphilic iron complexes. *Mar. Chem.* 38, 209–235

Hudson, R.J.M., Morel, F.M.M. 1993. Trace metal transport by marine microorganisms: implications of metal coordination kinetics. *Deep-sea Res*. 40, 129–151.

Hunter, K.A., Boyd, P.W. 2007. Iron-binding ligands and their role in the ocean biogeochemistry of iron. *Environ. Chem.* 4, 221–232. Doi:10.1071/EN01012

Hutchins, D.A., DiTullio, G.R., Bruland, K.W. 1993. Iron and regenerated production: Evidence for biological iron recycling in two marine environments, *Limnol. Oceanogr.* 38, 1242–1255.

Hutchins, D. A. and Bruland, K. W. 1998. Iron-limited diatom growth and Si:N uptake ratios in a coastal upwelling regime. *Nature*. 393, 561–564.

Hutchins, D.A., DiTullio, G.R., Zhang, Y., Bruland, K.W. 1998. An iron limitation mosaic in the California upwelling regime. *Limnol. Oceanogr*. 43, 1037–1054.

Hutchins, D.A., Witter, A., Butler, A., Luther III, G.W. 1999. Competition among marine phytoplankton for different chelated iron species. *Nature.* 400, 858–861.

Hutchins, D.A., Sedwick, P.N., DiTullio, G.R., Boyd, P.W., Quéguiner, B., Griffiths, F.B., Crossley, C. 2001. Control of phytoplankton growth by iron and silicic acid availability in the subantarctic Southern Ocean: Experimental results from the SAZ Project. *J. Geophys. Res.* 106 (C12), 31559–31572.

Hutchins, D.A., DiTullio, G.R., Alm, M.B., Riseman, S.F., Maucher, J.M., Geesey, M.E., Trick, C.G., Smith, G.J., Rue, E.L., Conn, J., Bruland, K.W. 2002. Phytoplankton iron limitation in the Humboldt Current and Peru Upwelling. *Limnol. Oceanogr*. 47, 997–1011.

Ibisanmi, E., Sander, S.G., Boyd, P.W., Bowie, A.R., Hunter, K.A., 2001. Vertical distributions of iron-(III) complexing ligands in the Southern Ocean. *Deep-Sea Res. II.* 58, 2113–2125.

Imai, A., Fukushima, T., Matsushige, K., 1999. Effects of iron limitation and aquatic humic substances on the growth of Microcystis aeruginosa. *Can. J. Fish. Aquat. Sci*. 56, 1929–1937.

Inaba, K., Sekine, T., Tomioka, N., Yagi, O. 1996. Seasonal and longitudinal changes in copper and iron in surface water of shallow eutrophic Lake Kasuigaura, Japan. *Wat. Res*. 2, 280–286.

IPCC 2007. 'The Physical Science Basis. Contribution of Working Group 1 to the Fourth assessment Report of the Intergovernmental Panel on Climate Change.' (Eds S. Solomon, D. Qin, M. Manning, Z. Chen, M.C. Marquis, K. Averyt, M. Tignor and H.L. Miller.) (Intergovernmental Panel on Climate Change: Cambridge, New York).

Jackson, T.A., Hecky, R.E. 1980. Depression of primary productivity by humic matter in lake and reservoir waters of the boreal forest zone. *Can. J. Fish. Aquat*. Sci. 37, 2300–2317.

Janse, I., van Rijssel, M., Gottschal, J.C., Lancelot, C., Gieskes, W.W.C. 1996. Carbohydrates in the North Sea during spring blooms of Phaeocystis. *Aquat. Microb. Ecol*. 10, 97–103.

Jickells, T.D., Spokes, L.J. 2001. Atmospheric iron inputs to the ocean. In *The biogeochemistry of iron in seawater.* Eds. D.R. Turner, K.A. Hunter. John Wiley & Sons, Chichester, UK. pp 85–123.

Jickells, T.D., An, Z.S., Anderson, K.K., Baker, A.R., Bergametti, G., Brooks, N., Cao, J.J., Boyd, P.W., Duce, R.A., Hunter, K.A., Kawahata, H., Kubilay, N., La Roche, J., Liss, P.S., Mahowald, N., Prospero, J.M., Ridgwell, A.J. Tegen, I., Torres, R. 2005. Global Iron Connections between Desert Dust, Ocean Biogeochemistry, and Climate. *Science.* 308, 67–71.

Johnson, K.S., Coale, K.H., Elrod, V.A., Tindale, N.W. 1994. Iron photochemistry in the equatorial Pacific. *Mar. Chem.* 46, 319–334.

REFERENCES

Johnson, K.S., Gordon, R.M., Coale, K.H. 1997. What controls dissolved iron concentrations in the world ocean? *Mar. Chem.* 57, 137–161.

Johnson, K.S., Chavez, F.P., Friederich, G.E. 1999. Continental-shelf sediment as a primary source of iron for coastal phytoplankton. *Nature*. 398, 697–700.

Johnson, K. S., Elrod, V.A., Fitzwater, S.E., Plant, J.N., Chavez, F.P., Tanner, S.J., Gordon, R.M., Westphal, D.L., Perry, K.D., Wu, J., Karl, D.M. 2003. Surface ocean-lower atmosphere interactions in the Northeast Pacific Ocean Gyre: Aerosols, iron, and the ecosystem response. *Global Biogeochem. Cy*. 17, 1063, doi: 10.1029/2002GB002004.

Johnson, K.S., Elrod, V., Fitzwater, S., Plant, J., Boyle, E., Bergquist, B., Bruland, K., Aguilar-Ialas, A., Buck, K., Loham, M., Smith G.J., Sohst, B., Coale, K., Gordon, M., Tanner, S., Measures, C., Moffett, J., Barbeau, K., King., A., Bowie, A., Chase, Z., Cullen, J., Laan, P., Landing, W., Mendez, J., Milne, A., Obata, H., Doi, T., Ossiander, L., Sarthou, G., Sedwick, P., van den Berg, S., Laglera-Baquer, L., Wu, J-F., Cai, Y. 2007. Developing standards for dissolved iron in seawater. *Eos*. 88, 131–132.

Jorand, F., Boué-Bigne, F., Block, J.C., Urbain, V., 1998. Hydrophobic/hydrophilic properties of activated sludge exopolymeric substances. *Wat. Sci. Tech*. 37, 307–315.

Kadar, E., Cunliffe, M., Fisher, A., Stolpe, B., Lead, J., Shi, Z. 2014. Chemical interaction of atmospheric mineral dust-derived nanoparticles with natural seawater - EPS and sunlight-mediated changes. *Sci. Total Environ*. 468–469, 265–271.

Karl, D.M., Björkman, K.M. 2002. Dynamics of DOP. In: *Biogeochemistry of marine dissolved organic matter*. Eds. Hansell, D.A and Carlson, C.A. Academic Press, New York, USA. pp. 249–366

Kieber, D. J., McDaniel, J., Mopper, K. 1989. Photochemical source of biological substrates in sea water: implications for carbon cycling. *Nature*. 341, 637–639.

Kieber, D.J. 2004. Photochemical production of biological substrates. In: *The effects of UV radiation in the marine environment.* Eds. S. de Mora, S. Demers, M. Vernet. Cambridge University Press, Cambridge, UK. pp. 130–148

REFERENCES

Keiber, R.J., R. F. Whitehead D, J. D. Willey, S. Reid, Seaton, P.J. 2006. Chromophoric dissolved organic matter (CDOM) in rainwater collected in southeastern North Carolina, USA. *J. Atmos. Chem.* 54, 21–41.

Kind, T., Fiehn, O. 2006. Metabolomic database annotations via query of elemental compositions: Mass accuracy is insufficient even at less than 1 ppm. *BMC Bioinformatics.* 7, 234.

Kirk, J. T. O. 1994. *Light and photosynthesis in aquatic ecosystems.* 2nd Ed. Cambridge University Press, Cambridge, UK.

Kogut, M.B., Voelker, B.M., 2001. Strong copper-binding behavior of terrestrial humic substances in seawater. *Environ. Sci. Technol*. 35, 1149–1156.

Koprivnjak, J.-F., Pfromm, P.H., Ingall, E., Vetter, T.A., Schmitt-Kopplin, P., Hertkorn, N., Frommberger, M., Knicker, H., Perdue, E.M., 2009. Chemical and spectroscopic characterization of marine dissolved organic matter isolated using coupled reverse osmosis–electrodialysis. *Geochim. Cosmochim. Acta*. 73, 4215–4231.

Kondo, Y., Takeda, S., Nishioka, J., Obata, H., Furuya, K., Johnson, W.K., Wong, C.S. 2008. Organic iron(III) complexing ligands during an iron enrichment experiment in the western subarctic North Pacific. *Geophys. Res. Lett.* 35, L12601, doi: 10.1029/2008GL033354.

Kondo, Y., Takeda, S., Nishioka, J., Sato, M., Saito, H., Suzuki, K., Furuya, K. 2013. Growth stimulation and inhibition of natural phytoplankton communities by model ligands in the Western subarctic Pacific. *J. Oceanogr*. 69, 97–115.

Kosakowska, A., Nedzi, M., Pempkowiak, J. 2007. Responses of the toxic cyanobacterium *Microcystis aeruginosa* to iron and humic substances. *Plant Physiol. Bioch*. 45, 365–370.

Kowalezuk, P., Copper, W. J., Whitehead, R. F., Durako, M. J., Sheldon, W. 2003. Characterisation of CDOM in an organic rich river and surrounding coastal ocean in the South Atlantic Bight. *Aquat. Sci.* 65, 381–398.

Kuma, K., Matsunaga, F.L. 1995. Availability of colloidal ferric oxides to coastal marine phytoplankton. *Mar. Biol*. 122, l–11.

REFERENCES

Kuma, K., Nishioka, J., Matsunaga, K. 1996. Controls on iron(III) hydroxide solubility in seawater: The influence of pH and natural organic chelators. *Limnol. Oceanogr.* 41, 396–407.

Kuma, K., Katsumoto, A., Kawakami, H., Takatori, F., Matsunaga, K. 1998. Spatial variability of Fe(III) hydroxide solubility in the water column of the northern North Pacific Ocean. *Deep-Sea. Res. I.* 45, 91–113.

Kuma, K., Tanaka, J., Matsunaga. K. 1999. Effect of natural and synthetic organic-Fe(III) complexes in an estuarine mixing model on iron uptake and growth of a coastal marine diatom, *Chaetoceros sociale*. *Mar. Biol.* 134, 761–769.

Kutska, A.B., Shaked, Y., Milligan, A.J., King, D.W., Morel, F.M.M. 2005. Extracellular production of superoxide by marine diatoms: Contrasting effects on iron redox chemistry and bioavailability. *Limnol. Oceanogr.* 50, 1172–1180.

Laglera, L.M., Battaglia, G.,van den Berg, C.M.G. 2007. Determination of humic substances in natural waters by cathodic stripping voltammetry of their complexes with iron. *Anal. Chim. Acta.* 599, 58–66

Laglera, L.M., van den Berg, C.M.G. 2009. Evidence for geochemical control of iron by humic substances in seawater. *Limnol. Oceanogr.* 54, 610–619.

Laglera, L.M., Battaglia, G., van den Berg, C.M.G. 2011. Effect of humic substances on the iron speciation in natural waters by CLE/CSV. *Mar. Chem*. 127, 134-143.

Lam, P.J., Bishop, J.K.B., Henning, C.C., Marcus, M.A., Waychunas, G.A., Fung, I.Y. 2006. Wintertime phytoplankton bloom in the subarctic Pacific supported by continental margin iron. *Glob. Biogeochem. Cy.* 20, GB1006, doi:10.1029/2005GB002557

Lannuzel, D. Schoemann, V., de Jong, J., Tison, J-L., Chou, L. 2007 Distribution and biogeochemical behaviour of iron in the East Antarctic sea ice. *Mar. Chem.* 106, 18–32.

Lannuzel, D., Schoemann, V., de Jong, J., Chou, L., Delille, B., Becquevort, S., Tison, J-L. 2008. Iron study during a time series in the western Weddell pack ice. *Mar. Chem.* 108: 85–95.

Lavery, T.J., Roudnew, B., Gill, P., Seymour, J., Seuront, L., Johnson, G., Mitchell, J.G. & Smetacek, V. 2011. Iron defecation by sperm whales stimulates carbon export in the Southern Ocean. *Proceedings of the Royal Society B* 277, 3527–3531, doi: 10.1098/rspb.2010.0863.

Law, C. S., Ellwood, M., Woodward, E. M. S., Marriner, A., Bury, S., Safi, K. 2011. Response of surface nutrient inventories and nitrogen fixation to a tropical cyclone in the South-West Pacific. *Limnol. Oceanogr.* 56, 1372–1385. doi:10.4319/LO.2011.56.4.1372.

Lee, J., Park, J.H., Shin, Y.S., Lee, B.C., Chamg, N.I., Cho, J., Kim, S.D. 2009. Effect of dissolved organic matter on the growth of algae, *Pseudokirchneriella subcapitata*, in Korean lakes: The importance of complexation reactions. *Ecotox. Environ. Safe*. 72, 335–343.

Li, F., Ginoux, P., and Ramaswamy, V. 2001. Distribution, transport, and deposition of mineral dust in the Southern Ocean and Antarctica: Contribution of major sources, J. Geophys. Res., 113, D10207, doi:10.1029/2007JD009190, 2008.

Lin, J., Kester, D.R., 1992. The kinetics of Fe(II) complexation by ferrozine in seawater. *Mar. Chem*. 38, 283–301.

Liu, X., Millero, F.J., 2002. The solubility of iron in seawater. *Mar. Chem*. 77, 43–54.

Loscher, B.M., de Baar, H.J.W., de Jong, J.T.M., Veth, C., Dehairs, F. 1997. The distribution of Fe in the Antarctic Circumpolar Current. *Deep-Sea. Res. II.* 44, 143–187.

Lumpkin, R., Speer, K. 2007. Global ocean meridional overturning. *J. Phys. Oceanogr.* 37, 2550–2562.

Luther III, G. W., Rozan, T.F., Witter, A., Lewis, B. 2001. Metal-organic complexation in the marine environment. *Geochem Trans*. 2, 65. doi:10.1186/1467-4866-2-65.

Luo, C., Mahowald, N., Bond, T., Chuang, P., Artaxo, P., Siefert, R., Chen, Y., Schauer, J. 2008. Combustion iron distribution and deposition. *Glob. Biogeochem. Cy.* 22, GB1012

Mackie, D.S., Boyd, P.W., McTainsh, G.H., Tindale, N.W., Westberry, T.K., Hunter, K.A. 2008. Biogeochemistry of iron in Australian dust: From eolian uplift to marine uptake. *Geochem. Geophys. Geosys*. Q03Q08. doi: 10.1029/2007GC001813.

REFERENCES

Mahowald. N.M., Baker. A.R., Bergametti. G., Brooks, N., Duce. R.A., Jickells. T.D., Kubilay. N., Prospero. J.M., Tegen. I. 2005. Atmospheric global dust cycle and iron inputs to the ocean. *Glob. Biogeochem. Cy*. 19, GB4025, doi: 10.1029/2004GB002402.

Mahowald, N.M., Engelstaedter, S., Luo, C., Sealy, A., Artaxo, P., Benitez-Nelson, C., Bonnet, S., Chen, Y., Chuang, P.Y., Cohen, D.D., Dulac, F., Herut, B., Johansen, A.M., Kubilay, N., Losno, R., Maenhaut, W., Paytan, A., Prospero, J.M., Shank, L.M., Siefert, R.L. 2009. Atmospheric iron deposition: Global distribution, variability, and human perturbations. *Annu. Rev. Mar. Sci.* 1, 245–78

Majestic, B.J., Schauer, J.J., Shafer, M.M. 2007. Application of synchrotron radiation for measurement of iron red-ox speciation in atmospherically processed aerosols. *Atmos. Chem. Phys.* 7, 2475–2487.

Malcolm, M.L. 1990. The uniqueness of humic substances in each of soil, stream and marine environments. *Anal. Chim. Acta.* 232, 19–30.

Maldonado, M.T., Price, N.M. 1999. Utilization of iron bound to strong organic ligands by plankton communities in the subarctic Pacific Ocean. *Deep-Sea. Res.* 46, 2447–2473.

Maldonado, M.T. Price, N.M. 2001. Reduction and transport of organically bound iron by *Thalassiosira oceanica. J Phycol*. 37, 298–310

Maldonado, M.T., Hughes, M.P., Rue, E.L., Wells, M.L. 2002. The effect of Fe and Cu on growth and domoic acid production by *Pseudo-nitzschia multiseries* and *Pseudo-nitzschia australis. Limnol. Oceanogr*. 47, 515–526

Maldonado, M.T., Strzepek, R.F., Sander, S., Boyd, P.W. 2005. Acquisition of Fe bound to strong organic complexes, with different Fe binding groups and photochemical reactivities, by plankton communities in Fe-limited subantarctic waters. *Glob. Biogeochem. Cycles*. 19, GB4S23. doi:10.1029/2005GB002481.

Maldonado, M.T., Allen, A.E., Chong, J.S., Lin, K., Leos, D., Karpenko, N., Harris, S.L. 2006. Copper-dependent iron transport in coastal and oceanic diatoms. *Limnol. Oceanogr.* 51, 1729–1743.

REFERENCES

Mancuso Nichols, C.A., Garon, S., Bowman, J.P., Raguénès, G., Guézennec, J. 2004. Production of exopolysaccharides by Antarctic marine bacterial isolates. *J. Applied. Microbiol.* 96, 1057–1066 doi:10.1111/j.1365-2672.2004.02216.x

Mancuso Nichols, C., Lardière, S.G., Bowman, J.P., Nichols, P.D., Gibson, J., Guézennec, J. 2005. Chemical characterization of exopolysaccharides from Antarctic marine bacteria. *Microb. Ecol*. 49, 578–589.

Mantoura, R.F.C., Dickson, A., Riley, J.P. 1978. The Complexation of Metals with Humic Materials in Natural Waters. *Est. Coast. Marine. Sci.* 6, 387–408.

Mantoura R. F.C., Llewellyn C.A. 1983. The rapid determination of algal chlorophyll and carotenoid pigments and their breakdown products in natural waters by reverse-phase high-performance liquid chromatography. *Anal. Chim. Acta*. 151, 297–314.

Maranger, R., Bird, D.F., Price, N.M. 1998. Iron acquisition by photosynthetic marine phytoplankton from ingested bacteria. *Nature,* 396, 248–151.

Marchetti, A., Parker, M.S., Moccia, L.P., Lin, E.O., Arrieta, A.L., Ribalte, F., Murphy, M.E.P., Maldonado, M.T., Armbrust, E.V. 2009. Ferritin is used for iron storage in bloom forming marine pennate diatoms. *Nature* 457, 467–470.

Marinov, I., Gnanadesikan, A., Toggweiler, J.R., Sarmiento, J.L. 2006. The Southern Ocean biogeochemical divide. *Nature.* 441, 964–967. doi:10.1038/nature04883.

Marinov, I., Gnanadesikan, A., Sarmiento, J.L., Toggweiler, J.R., Follows, M., Mignone, B.K. 2008. Impact of oceanic circulation on biological carbon storage in the ocean and atmospheric *p*CO2. *Global Biogeochem. Cy.* 22, GB3007, doi:10.1029/2007GB002958

Marshall, J.A., de Salas, M., Oda, T. & Hallegraeff, G. 2005. Superoxide production by marine microalgae. *Mar. Biol.* 147, 533–540.

Martin, J.H., Fitzwater, S.E. 1988. Iron deficiency limits phytoplankton growth in the north-east Pacific subarctic. *Nature.* 331, 341–343.

REFERENCES

Martin, J.H., Gordon, R.M. 1988. Northeast Pacific iron distributions in relation to phytoplankton productivity. *Deep-Sea Res*. 35, 177–l 96.

Martin, J.H., Gordon, R.M., Fitzwater, S., Broenkow, W.W. 1989. VERTEX: phytoplankton/iron studies in the Gulf of Alaska. *Deep-Sea. Res.* 36, 649–680.

Martin, J.H. 1990. Glacial-interglacial CO_2 change: the iron hypothesis, *Paleoceanography.* 5, 1–13.

Martin, J.H., Gordon, R.M., Fitzwater, S.E. 1991. The case for iron. *Limnol. Oceanogr.* 36, 1793–1802.

Martin, J.H., Coale, K.H., Johnson, K.S., Fitzwater, S.E., Gordon, R.M., Tanner, S.J., Hunter, C.N., Elrod, V.A., Nowick, J.L. Coley, T.L., Barber, R.T., Lindley, S., Watson, A.J., van Scoy, K., Law, C.S., Liddicoat, M.I., Ling, R., Stanton, T., Stockel, J., Collins, C., Anderson, A., Bidigare, R., Ondrusek, M., Latasa, M., Millero, F.J., Lee, K., Yao, W., Zhang, J.Z., Friedrich, G., Sakamoto, C., Chavez, F., Buck, K., Kobler, Z., Greene, R., Falkowski, P., Chisholm, S.W., Hoge, F., Swift, R., Yungel, J., Turner, S., Nightingale, P., Hatton, A., Liss, P., Tindale, N.W. 1994. Testing the iron hypothesis in ecosystems of the equatorial Pacific Ocean. *Nature* 371, 123–129.

Mawji, E., Gledhill, M., Milton, J.A., Tarran, G.A., Ussher, S., Thompson, A., Wolff, G.A., Worsford, P.J., Achterberg, E.P. 2008. Hydroxamate siderophores: Occurrence and importance in the Atlantic Ocean. *Environ. Sci. Technol.* 42, 8675–8680.

Mawji, E., Gledhill, M., Milton, J.A., Zubkov, M.V., Thompson, A., Wolff, G.A., Achterberg,E.P. 2011. Production of siderophore type chelates in Atlantic Ocean waters enriched with different carbon and nitrogen sources. *Mar. Chem.* 124, 90–99.

McKay, R.M.L., Wilhelm, S.W., Hall, J., Hutchins, D.A., Al-Rshaidat, M.M.D., Mioni, C.E., Pickmere, S., Porta, D., Boyd, P.W. 2005. Impact of phytoplankton on the biogeochemical cycling of iron in subantarctic waters southeast of New Zealand during FeCycle. *Global Biogeochem Cy.* 19, GB4S24.

McTainsh, G.H., Burgess, R., Pitblado, J.R. 1990. Wind erosion in eastern Australia. *Aust. J. Soil. Res.* 28, 323–339.

REFERENCES

Measures, C.I., Vink, S. 1999. Seasonal variations in the distribution of Fe and Al in the surface waters of the Arabian Sea. *Deep-Sea Res. II*. 46, 1597–1622.

Medeiros, P.M., Conte, M.H., Weber, J.C., Simoneit, B.R.T. 2006. Sugars as source indicators of biogenic organic carbon in aerosols collected above the howland experimental forest, Maine*. Atmos. Environ*. 40, 1697–1705.

Miller, W.L., Zepp, R.G. 1995. Photochemical production of dissolved inorganic carbon from terrestrial organic matter: Significance to the oceanic coastal organic carbon cycle. *Geophys. Res.* 22,417-420, doi:10.1029/94GL03344.

Miller, C.J., Rose, A.L., Waite, T.D. 2009. Impact of natural organic matter on H_2O_2-mediated oxidation of Fe(II) in a simulated freshwater system. *Geochim. Cosmochim. Acta*. 73, 2758–2768.

Miller, C.J., Lee, S.M.V., Rose, A.L. and Waite, T.D. 2012. Impact of natural organic matter on H_2O_2-mediated oxidation of Fe(II) in seawater. *Environ. Sci. Technol*. 46, 11078–11085.

Millero, F.J., Sotolongo, S., Izaguirre, M. 1987. The oxidation kinetics of Fe(II) in seawater, *Geochim. Cosmochim. Acta*, 51, 793–801.

Millero, F.J. 1998. Solubility of Fe(III) in seawater. *Earth. Plan. Sci. Let.* 154, 323–329.

Millero, F.J., Sotolongo, S. 1989. The oxidation of Fe(II) with H_2O_2 in seawater. *Geochim. Cosmochim. Acta*. 51, 1867–1873.

Mitchell, R.M., Campbell, S.K., Qin, Y. 2010. Recent increase in aerosol loading over the Australian arid zone. *Atmos. Chem. Phys.* 10, 1689–1699.

Mongin, M., Matear, R., Chamberlain, M. 2011. Seasonal and spatial variability of remotely sensed chlorophyll and physical fields in the SAZ-Sense region. *Deep-Sea Res. II.* 58, 2082–2093. doi:10.1016/J.DSR2.2011.06.002.

Moore, K.M., Doney, S.C., Glover, D.M., Fung, I.Y. 2001. Iron cycling and nutrient–limitation patterns in surface waters of the World Ocean. *Deep-Sea Res. II*. 49, 463–507.

REFERENCES

Moore, C.M., Mills, M.M., Milne, A., Langlois, R., Achterberg, E.P., Lochte, K., Geider, R.J., Roche, J. 2006. Iron limits primary productivity during spring bloom development in the central North Atlantic. *Global Change Biol*. 12, 626–634, doi: 10.1111/j.1365-2486.2006.01122.x

Moore, C.M. Mills, M.M. Achterberg, E.P., Geider, R.J., La Roche, J., Lucus, M.I., McDonagh, E.L., Pan, X., Poulton, A.J., Rijkenberg, M.J.A., Suggett, D.J., Ussher, S.J., Woodward, E.M.S. 2009. Large-scale distribution of Atlantic nitrogen fixation controlled by iron availability. *Nature Geosci*. 2, 867–871.

Mopper, K., Stubbins, A., Ritchie, J.D., Bialk, H.M., Hatcher, P.G. 2007. Advanced instrumental approaches for characterization of marine dissolved organic matter: extraction techniques, mass spectrometry, and nuclear magnetic resonance spectroscopy. *Chem. Rev*. 107, 419–442.

Moran, M. A., Hodson, R. E. 1989. Formation and bacterial utilization of dissolved organic carbon derived from detrital lignocellulose. *Limnol. Oceanogr*. 34, 1034–1047.

Moran. M. A., Hodson, R. E. 1990. Bacterial production on humic and nonhumic components of dissolved organic carbon. *Limnol. Oceanogr*. 35, 1744–1756.

Moran, M.A., Hodson, R.E. 1994. Support of bacterioplankton production by dissolved humic substances from three marine environments. *Mar. Ecol. Prog. Ser*. 110, 241–247.

Morán, X.A.G., Gasol, J.M., Pedrós-Alió, C., Estrada, M. 2001. Dissolved and particulate primary production and bacterial production in offshore Antarctic waters during austral summer: coupled or uncoupled? *Mar. Ecol. Prog. Ser*. 222, 25–39.

Morel, F.M.M., Hering, J.G., 1993. *Principles and Applications of Aquatic Chemistry*, Wiley, New York.

Morel, N.M., Price, F.M.M. 1998. Biological cycling of iron in the ocean. *Metal Ions in Biological Systems*. 35, 1–36.

Morel, F.M.M., Price, N.M. 2003. The biogeochemical cycles of trace metals in the oceans. *Science.* 300, 944–947.

REFERENCES

Morel, F.M.M., Kustka, A.B., Shaked, Y. 2008. The role of unchelated Fe in the Fe nutrition of phytoplankton. *Limnol. Oceanogr*. 53, 400–404.

Myklestad, S.M. 1995. Release of extracellular products by phytoplankton with special emphasis on polysaccharides. *Sci. Total. Environ*. 165, 155–164.

Myklestad, S.M., Skånøy, E., Hestmann, S. 1997. A sensitive and rapid method for analysis of mono- and polysaccharides in seawater. *Mar. Chem*. 56, 279–286.

Naito, K., Matsui, M., Imai, I. 2005. Ability of marine eukaryotic red tide microalgae to utilise insoluble iron. *Harmful Algae*. 4, 1021–1032.

Nanninga, H. J., Ringenaldus, P., Westbroek, P. 1996. Immunological quantification of a polysaccharide formed by *Emiliania huxleyi*. *J. Mar. Syst*. 9, 67–74.

Neilands, J.B. 1981. Iron-absorption and transport in microorganisms. *Ann. Rev. Nutr.* 1, 27–46.

Nelson, N. B., Siegel, D. A., Michaels, A. E. 1998. Seasonal dynamics of colored dissolved organic matter in the Sargasso Sea. *Deep-Sea Res. I* 45, 931–957.

Neu, T.R., Lawrence, J.R., 2009. Extracellular polymeric substances in microbial biofilms. In: *Microbial glycobiology: Structures, relevance and applications*. Eds. Moran, A., Brennan, P., Holst, O., von Itzstein, M. Elsevier, San Diego. pp 735–758.

Nicol, S., Bowie, A., Jarman, S., Lannuzel, D., Meiners, K.M., van der Merwe, P. 2010. Southern Ocean iron fertilization by baleen whales and Antarctic krill. *Fish & Fisheries*. 11, 203–209.

Norman, L., Cabanes, D.J.E., Blanco-Ameijeras, S., Moisset, S.A.M., Hassler, C.S. 2014. Iron Biogeochemistry in aquatic systems: from source to bioavailability. *Chimia*. 68, 764–771.

Norman, L., Worms, I.A.M., Angles, E., Bowie, A.R., Mancuso Nichols, C., Pham, A.N., Townsend, A.T., Waite, T.D., Hassler, C.S. The role of bacterial and algal exopolymeric substances (EPS) in iron (Fe) chemistry. *Mar. Chem*. **In press**.

Obata, H., Karatani, H., and Nakayama, E. 1993. Automated determination of iron in seawater by chelating resin concentration and chemiluminescence detection. *Anal. Chem.* 65, 1524–1528. doi:10.1021/AC00059A007.

Obata, H., van den Berg, C.M.G. 2001. Determination of picomolar levels of iron in seawater using catalytic cathodic stripping voltammetry. *Anal. Chem*. 73, 2522–2528.

Obernosterer, I., Herndl, G. J. 2000. Differences in the optical and biological reactivity of the humic and non-humic dissolved organic carbon component in two contrasting coastal marine environments. *Limnol. Oceanogr*. 45, 1120–1129.

Obernosterer, I., Christaki, U., Lefèvre, D., Catala, P., Van Wambeke, F., Lebaron, P. 2008. Rapid bacterial mineralization of organic carbon produced during a phytoplankton bloom induced by natural fertilization in the Southern Ocean. *Deep-Sea Res. II*. 55, 777–789.

Oke, P.R., Middleton, J.H. 2000. Topographically induced upwelling off Eastern Australia*. J. Phys. Oceanogr*. 30, 512–531.

Okochi, H. and Brimblecombe, P. 2002. Potential trace metal–organic complexation in the atmosphere. *Sci. World J.* 2, 767–786, doi:10.1100/tsw.2002.132.

Opsahl, S., and Benner, R. 1998. Photochemical reactivity of dissolved lignin in river and ocean waters. *Limnol. Oceanogr.* 43**,** 1297–1304.

Orians, K.J., Bruland, K.W. 1985. Dissolved aluminium in the central North Pacific. *Nature.* 316, 427–429.

Öztürk, M., Croot, P.L., Bertilsson, S., Abrahamsson, K., Karlson, B., David, R., Fransson, A., Sakahaug, E. 2004. Iron enrichment and photoreduction of iron under UV and PAR in the presence of hydroxycarboxylic acid: implications for phytoplankton growth in the Southern Ocean. *Deep-Sea. Res. II.* 51, 2841–2856.

Pakulski, D.J., Benner, R. 1994. Abundance and distribution of carbohydrates in the ocean. *Limnol Oceanogr.* 39, 930–940.

REFERENCES

Panagiotopoulos, C., Sempéré, R. 2005. Analytical methods for the determination of sugars in marine samples: a historical perspective and future directions. *Limnol. Oceanogr-Meth. 3*, 419–454.

Parekh, P., Follows, M.J., Boyle, E. 2004. Modeling the global ocean iron cycle. *Global Biogeochem. Cy*. 18, GB1002, doi:10.1029/2003GB002061.

Paris, R., Desboeufs, K.V. 2013. Effect of atmospheric organic complexation on iron-bearing dust solubility. *Atmos. Chem*. Phys. 13, 4895–4905.

Pehkonen, S.O., Slefert, R., Erel, Y., Webb, S., Hoffmann, M.R. 1993. Photoreduction of iron oxyhydroxides in the presence of important atmospheric organic compounds. *Environ. Sci. Technol.* 27, 2056–2062.

Penna, A., Berluti, S., Penna, N., Magnani, M. 1999. Influence of nutrient ratios on the in vitro extracellular polysaccharide production by marine diatoms from the Adriatic Sea. *J. Plankton. Res.* 21, 1681–1690.

Perminova, I.V., Frimmel, F.H., Kudryavtsev, A.V., Kulikova, N.A., Abbt-Braun, G., Hesse, S.Petrosyant, V.S. 2003. Molecular weight characteristics of humic substances from different environments as determined by size exclusion chromatography and their statistical valuation. *Environ. Sci. Technol*. 37, 2477–2485.

Pham, A.N., Waite, T.D. 2008. Oxygenation of Fe(II) in natural waters revisited: Kinetic modeling approaches, rate constant estimation and the importance of various reaction pathways. *Geochim. Cosmo. Acta*. 72, 3616–3630

Pollard, R.T., Salter, I., Sanders, R.J., Lucas, M.I., Moore, C.M., Mills, R.A., Statham, P.J., Allen, J.T., Baker, A.R., Bakker, D.C.E., Charette, M.A., Fielding, S., Fones, G.R., French, M., Hickman, A.E., Holland, R.J., Hughes, J.A., Jickells, T.D., Lampitt, R.S., Morris, P.J., Nédélec, F.H., Nielsdottir, M., Planquette, H., Popova, E.E., Poulton, A.J., Read, J.F., Seeyave, S., Smith, T., Stinchcombe, M., Taylor, S., Thomalla, S., Venables, H.J., Williamson, R. & Zubkov, M.V. 2009. Southern Ocean deep-water carbon export enhanced by natural iron fertilisation. *Nature.* 457, 577–580.

REFERENCES

Pomeroy, L.R. 1974. The oceans food web; a changing paradigm. *Biol. Sci.* 24, 499–504.

Poorvin, L., Rinta-Kanto, J.M., Hutchins, D.A., Wilhelm, S.W. 2004. Viral release of iron and its bioavailability to marine plankton. *Limnol Oceanogr*. 49, 1734–1741.

Poorvin, L., Sander, S.G., Velasquez, I., Ibisanmi, E., LeCleir, G.R., Wilhelm, S.W. 2011. A comparison of Fe bioavailability and binding of a catecholate siderophore with virus-mediated lysates from the marine bacterium *Vibrio alginolyticus* PWH3a. *J. Exp. Mar. Biol. Ecol.* 399, 43–47.

Price, N.M., Harrison, G.I., Hering, J.G., Hudson, R.J., Nirel, P.M.V., Palenik, B., Morel, F.M. 1989. Preparation and chemistry of the artificial algal culture medium AQUIL. *Biol. Oceanogr*. 6, 443–361.

Price**,** N.M., Ahner, B.A., Morel, F.M.M. 1994. The equatorial Pacific Ocean: Grazer-controlled phytoplankton populations in an iron-limited ecosystem. *Limnol. Oceanogr*. 39, 520–534.

Price, N.M., Morel, F.M.M. 1998. Biological cycling of iron in the ocean. In, *Metal ions in biological systems.* Eds. A Sigel & H Sigel. 35, 1–36, Marcel Dekker, New York, USA.

Prospero, J.M., Ginoux, P., Torres, O., Nicholson, S.E., Gill, T.E. 2001. Environmental characterization of global sources of atmospheric soil dust identified with the Nimbus 7 Total Ozone Mapping Spectrometer (TOMS) absorbing aerosol product, *Rev. Geophys. 40*, 1002, doi:10.1029/2000RG000095, 2002.

Pullin, J.M., Cabaniss, S.E. 2003. The effects of pH, ionic strength, and iron-fulvic acid interactions on the kinetics of non-photochemical iron transformations. II. The kinetics of thermal reduction. *Geochim. Cosmochim. Acta.* 67, 4079–4089.

Quigley, M.S., Santschi, P.H., Hung, C.C., Gau L.D., Honeyman, B.D. 2002. Importance of acid polysaccharides for Th-234 complexation to marine organic matter. *Limnol. Oceanogr*. 47, 367–377.

Raiswell, R., Tranter, M., Benning, L. G., Siegert, M., De'ath, R., Huybrechts, P., Payne, T. 2006. Contributions from glacially derived sediment to the global iron (oxyhydr)oxide cycle:

Implications for iron delivery to the oceans. *Geochim. Cosmochim. Acta.* 70, 2765–2780, doi:10.1016/j.gca.2005.12.027.

Raiswell, R., Benning, L. G., Tranter, M., and Tulaczyk, S. 2008. Bioavailable iron in the Southern Ocean: the significance of the iceberg conveyor belt, *Geochem. Trans*. 9, doi:10.1186/1467-4866-9-7, 2008.

Reszat, T.N, Hendry, M.J. 2005. Characterizing dissolved organic carbon using asymmetrical flow field-flow fractionation with on-line UV and DOC detection. *Anal Chem*. 77, 4194–4200.

Reynolds, S., Navidad, A. 2012. 'SS2010/01 - Role of iron and other micronutrients in controlling primary productivity in the Tasman Sea: bioavailability, biogeochemical cycling and sources.' (CSIRO Marine National Facility, unpublished voyage hydrochemistry report, October 2012: Hobart, Tasmania.)

Ridgway, K.R., Godfrey, J.S. 1997. Seasonal cycle of the East Australia Current. *J. Geophys. Res*. 102, 22921-22936.

Ridgway, K.R., Hill, K. 2009. The East Australian Current. Marine climate change in Australia: Impacts and adaptation responses, 2009 report card. Available at; http://www.oceanclimatechange.org.au/content/images/uploads/EAC.pdf. (verified 21/06/2014)

Rijkenberg, M.J.A., Gerringa, L.J.A., Carolus, V.E., Velzeboer, I., de Baar, H.J.W., 2006. Enhancement and inhibition of iron photoreduction by individual ligands in open ocean seawater. *Geochim. Cosmochim. Acta.* 70, 2790–2805.

Rijkenberg, M.J.A., Gerringa, L.J.A., Timmermans, K.R., Fischer, A.C., Kroon, K.J., Buma, A.G.J., Wolterbeek, B.T., de Baar, H.J.W., 2008. Enhancement of the reactive iron pool by marine diatoms. *Mar. Chem*. 109, 29–44.

Romera-Castillo, C., Sarmento, H., Alvarez-Salgado, X.A., Gasol, J.M., Marrasé, C. 2010. Production of chromophoric dissolved organic matter by marine phytoplankton. *Limnol. Oceanogr.* 55, 446–454.

REFERENCES

Romera-Castillo, C., Sarmento, H., Alvarez-Salgado, X.A., Gasol, J.M., Marrasé, C. 2011. Net production and consumption of fluorescent colored dissolved organic matter by natural bacterial assemblages growing on marine phytoplankton exudates. *Appl. Environ. Microb.* 77, 7490–7498, doi: 10.1128/AEM.00200-11.

Rose, A.L., Waite, T.D. 2002. Kinetic Model for Fe(II) Oxidation in seawater in the absence and presence of natural organic matter. *Environ. Sci. Technol*. 36, 433–444.

Rose, A.L., Waite, T.D. 2003. Kinetics of iron complexation by dissolved natural organic matter in coastal waters. *Mar. Chem*. 84, 85–103.

Rose, A.L., Waite, T.D. 2005. Reduction of organically complexed ferric iron by superoxide in a simulated natural water. *Environ. Sci. Technol.* 39, 2645–2650.

Rose, A.L., Salmon, T.P., Lukondeh, T., Neilan, B.A., Waite, T.D. 2005. Use of superoxide as an electron shuttle for iron acquisition by the marine cyanobacterium *Lyngbya majuscule Environ. Sci. Technol*. 39, 3708–3715.

Rose, A.L., Waite, T.D. 2005. Reduction of organically complexed ferric iron by superoxide in a simulated natural water. *Environ. Sci. Technol.* 39, 2645–2650.

Rose, A.L., Waite, T.D. 2006. Role of superoxide in the photochemical reduction of iron in seawater. *Geochim. Cosmochim. Acta.* 70, 3869–3882.

Roughan, M., Middleton, J.H. 2002. A comparison of observed upwelling mechanisms off the east coast of Australia. *Cont. Shelf Res*. 22, 2551–2572.

Roughan, M., Middleton, J. 2004. On the East Australia Current: variability, encroachment and upwelling. *J. Geophys. Res*. 109, C07003

Roy, E.G., Wells, M.L., King, D.W. 2008. Persistence of iron(II) in surface waters of the western subarctic Pacific. *Limnol. Oceanogr.* 53, 89–98.

Roy, E.G., Wells, M.L. 2011. Evidence for regulation of Fe(II) oxidation by organic complexing ligands in the Eastern Subarctic Pacific. *Mar. Chem*. 127, 115–122.

REFERENCES

Rubin, M., Berman-Frank, I., Shaked, Y. 2011. Dust- and mineral-iron utilization by the marine dinitrogen-fixer Trichodesmium. *Nat. Geosci.* doi: 10.1038/NGEO1181.

Rue**,** E.L., Bruland, K.W. 1995. Complexation of iron(III) by natural organic ligands in the Central North Pacific as determined by a new competitive ligand equilibration/adsorptive cathodic stripping voltammetric method. *Mar. Chem*. 50, 117–138.

Rue**,** E.L., Bruland, K.W. 1997. The role of organic complexation on ambient iron chemistry in the equatorial Pacific Ocean and the response of a mesoscale iron addition experiment. *Limnol. Oceanogr.* 42, 901–910.

Rue**,** E.L., Bruland, K.W. 2001. Domoic acid binds iron and copper: a possible role for the toxin produced by the marine diatom *Pseudo-nitzschia. Mar. Chem*. 76, 127–134.

Saito, M.A., Moffett, J.W., Chisholm, S.W., Waterbury, J.B. 2002. Cobalt limitation and uptake in *Prochlorococcus*. *Limnol. Oceanogr*. 47, 1629–1636.

Salmon, T.P., Rose, A.L., Neilan, B.A., Waite, T.D. 2006. The FeL model of iron acquisition: nondissociative reduction of ferric complexes in the marine environment. *Limnol Oceanogr*. 51, 1744–1754.

Santana-Casiano, J.M., González-Davila, M., Rodriguez, M.J., Millero, F.J. 2000. The effect of organic compounds in the oxidation kinetics of Fe(II). *Mar. Chem*. 70, 211–222.

Santana-Casiano, J.M., González-Davila, M., Millero, F.J. 2004. The oxidation of Fe(II) in NaCl-HCO^-_3 and seawater solutions in the presence of phthalate and salicylate ions: a kinetic model. *Mar. Chem*. 85, 27–40.

Sarthou, G., Timmermans, K.R., Blain, S., Treguer, P. 2005. Growth physiology and fate of diatoms in the ocean: a review. *J. Sea Res*. 53: 25–42.

Sarthou, G., Vincent, D., Christaki, U., Obernosterer, I., Timmermans, K. R., and Brussaard, C. P. D. 2008. The fate of biogenic iron during a phytoplankton bloom induced by natural fertilisation: Impact of copepod grazing. *Deep-Sea Res*. 55, 734–751. doi:10.1016/j.dsr2.2007.12.033.

Schimpf, M., Caldwell, K., Giddingd, J.C., 2000. Field-flow fractionation handbook. Wiley Interscience, New York.

Schreiber, U. 2004. Pulse-amplitude modulation (PAM) fluorometry and saturation pulse method: An overview. In: *Chlorophyll fluorescence: A signature of photosynthesis.* Eds GS Papageorgiou, Govindjee. Springer, Netherlands.

Schaule, B.K., Patterson, C.C. 1981. Lead concentrations in the northeast Pacific: evidence for global anthropogenic perturbations. *Earth. Planet. Sci. Lett.* 54, 97–116.

Schulz, M., Prospero, J.M., Baker, A.R., Dentener, F., Ickes, L., Liss, P.S., Mahowald, N.M., Nickovic, S., Pérez García-Pando, C., Rodríguez, S., Sarin, M., Tegen, I., Duce, R.A. 2012. Atmospheric transport and deposition of mineral dust to the ocean: Implications for research needs. *Environ. Sci. Technol*. 46, 10390-10404, doi, 10/1021/es300073u.

Seaton, P.J., Kieber, R.J., Willey, J.D., Brooks Avery Jr, G., Dixon, J.L. 2013. Seasonal and temporal characterization of dissolved organic matter in rainwater by proton nuclear magnetic resonance spectroscopy. *Atmos. Environ*. 65, 52–60.

Sedwick, P.J., DiTullio, G.R., Hutchins, D.A., Boyd, P.W., Griffiths, F.B., Crossley, A.C., Trull, T.W., Quéguiner, B. 1999. Limitation of algal growth be iron deficiency in the Australian Subantarctic region. *Geophys. Res. Lett*. 26, 2865–2868.

Sedwick, P.N., Sholkovitz, E.R., Church, T.M. 2007. Impact of anthropogenic combustion emissions on the fractional solubility of aerosol iron: evidence from the Sargasso Sea. *Geochem. Geophys. Geosys*. 8, Q10Q06.

Sedwick, P.N., Bowie, A.R. & Trull, T.W. 2008. Dissolved iron in the Australian sector of the Southern Ocean (CLIVAR-SR3 section): meridional and seasonal trends. *Deep-Sea Res. I.* 55, 911–925.

Seymour, J. R., Doblin, M. A., Jeffries, T. C., Brown, M. V., Newton, K., Ralph, P. J., Baird, M., and Mitchell, J. G. 2012. Contrasting microbial assemblages in adjacent water-masses associated with the East Australian Current. *Environ. Microbiol. Rep.* 4, 548–555. doi:10.1111/J.1758-2229.2012.00362.X

REFERENCES

Shaked, Y., Kustka, A.B., Morel, F.M.M. 2005. A general kinetic model for iron acquisition by eukaryotic phytoplankton. *Limnol. Oceanogr.* 50, 872–882.

Shaked, Y., Lis, H. 2012. Disassembling iron availability to phytoplankton. *Front. Micro. Biol*. doi: 10.3389/fmicb.2012.00123.

Shi, J-H., Gao, H-W., Zhang, J., Tan, S-C., Ren, J-L., Liu, C-G., Liu, Y., Yao, X. 2012. Examination of causative link between a spring bloom and dry/wet deposition of Asian dust in the Yellow Sea, China. *J. Geophys. Res.* 117, D17304, doi:10/1029/2012/JD017983.

Sholkovitz, E. R. 1976. Flocculation of dissolved organic and inorganic matter during mixing of river water and seawater. *Geochim. Cosmochim. Acta.* 40, 831–845.

Sholkovitz, E.R., Copeland, D. 1980. The coagulation, solubility and adsorption properties of Fe, Mu, Cu, Ni, Cd, Co and humic acids in a river water. *Geochim. Cosmochim. Acta.* 45, 181–189.

Sholkovitz, E.R., Sedwick, P.N., Church, T.M. 2009. Influence of anthropogenic combustion emissions on the deposition of soluble aerosol iron to the ocean: Empirical estimates for island sites in the North Atlantic. *Geochim. Cosmochim. Acta.* 73, 3981–4003.

Sholkovitz, E.R., Sedwick, P.N., Church, T.M., Baker, A.R., Powell, C.F. 2012. Fractional solubility of aerosol iron: Synthesis of a global-scale data set. *Geochim. Cosmochim. Acta.* 89, 173–189

Smetacek, V. 2008. Are declining Antarctic krill stocks a result of global warming or the decimation of the whales? In: *The Impact of Global Warming on Polar Ecosystems*. Ed. C Duarte. Fundacion BBVA, Spain, pp. 46–83.

Smith, W.O., Nelson, D.M. 1985. Phytoplankton bloom produced by a receding ice edge in the Ross Sea – spacial coherence with the density field. *Science*. 227, 163–166.

Sohrin, Y., Urushihara, S., Nakatsuka, S., Kono, T., Higo, E., Minami, T., Norisuye, K., Umetani, S. 2008. Trace metals in seawater by ICPMS after preconcentration using an ethylenediaminetracetic acid chelating resin. *Anal. Chem.* 80, 6267–6273.

REFERENCES

Soria-Dengg, S., Horstmann, U. 1995. Ferrioxamines B and E as iron sources for the marine diatom *Phaeodactylum tricornutum*. *Mar. Ecol. Prog. Ser.* 127, 269–277.

Soria-Dengg, S., Reissbrodt, R., Horstmann, U. 2001. Siderophores in marine coastal waters and their relevance for iron uptake by phytoplankton: experiments with the diatom *Phaeodactylum tricornutum*. *Mar. Ecol. Prog. Ser.* 220, 73–82.

Spokes, L.J., Jickells, T.D. 1996. Factors controlling the solubility of aerosol trace metals in the atmosphere and on mixing into seawater. *Aquatic. Geochem.* 1, 355–374.

Sreeram, K.J., Yamini Shrivastava, H., Nair, B.U. 2004. Studies on the nature of interaction of iron(III) with alginates. *Biochim. Biophys. Acta*. 1670, 121–125.

Steigenberger, S., Statham, P.J., Völker, C., Passow, U. 2010. The role of polysaccharides and diatom exudates in the redox cycling of Fe and the photoproduction of hydrogen peroxide in coastal seawaters. *Biogeosciences.* 7, 109–119.

Stepto, R.F.T. 2009. Dispersity in polymer science. *Pure Appl. Chem.* 81, 351–353.

Stookey, L.L. 1970. Ferrozine – a new spectrophotometric reagent for iron. *Anal Chem*. 42, 779–781.

Strzepek, R. F., Maldonado, M. T., Higgins, J. L., Hall, J., Safi, K., Wilhelm, S. W., and Boyd, P. W. 2005. Spinning the "Ferrous Wheel": The importance of the microbial community in an iron budget during the FeCycle experiment. *Global Biogeochem Cycles*. 19: GB4S26, 10.1029/2005GB002490.

Stumm, W., Morgan, J. 1996. *Aquatic Chemistry: chemical equilibria and rates in natural water.* John Wiley & Sons, New York.

Sunda WG. 1988. Trace metal interactions with marine phytoplankton. *Biol Oceanogr*. 6, 411–442.

Sunda, W.G., Swift, D.G., Huntsman, S.A. 1991. Low iron requirement for growth in oceanic phytoplankton. *Nature*. 351, 55–57.

REFERENCES

Sunda, W.G., Huntsman, S.A. 1995. Iron uptake and growth limitation in oceanic and coastal phytoplankton. *Mar. Chem.* 50, 189–206.

Sunda, W. G., Huntsman, S. A. 1998. Processes regulating cellular metal accumulation and physiological effects: Phytoplankton as a model system, *Sci. Total Environ*. 219, 165–181.

Sunda, W.G. 2001. Bioavailability and bioaccumulation of iron in the sea. In*, The biogeochemistry of iron in seawater.* Eds. D.R. Turner and K.A. Hunter. John Wiley & Sons, Ltd, New York.

Tagliabue, A., Arrigo, K.R. 2006. Processes governing the supply of iron to phytoplankton in stratified seas. *J Geophys Res*. 111, C06019.

Tagliabue, A., Bopp, L., Aumont, O., Arrigo, K.R. 2009. Influence of light and temperature on the marine iron cycle: from theoretical to global modeling. *Global Biogeochem. Cy*. 23, 2017.

Tang, D., Morel, F.M.M., 2006. Distinguishing between cellular and Fe-oxide-associated trace elements in phytoplankton. *Mar. Chem*. 98, 18–30.

Taylor, S.R. 1964. Abundance of chemical elements in the continental crust: a new table. *Geochim. Cosmochim. Acta*. 28, 1273–1285.

Thomas, D.N. 2003. Iron limitation in the Southern Ocean. *Science.* 302, 565.

Thomas, D.N., Papadimitriou, S, Michel, C. 2010. Biogeochemistry of sea ice. In; *Sea ice*, 2nd edition. Eds. D.N. Thomas and G.S. Dieckmann. Wiley-Blackwell. pp. 425–468.

Thompsen, J.C., Mottola, H.A. 1984. Kinetics of the complexation of iron(II) with ferrozine. *Anal. Chem*. 56, 755–757.

Thompson, P.A., Baird, M.E.., Ingleton, T., Doblin, M.A. 2009. Long-term changes in temperate Australian coastal water: implications for phytoplankton. *Mar. Ecol. Prog. Series*. 394, 1–19

Thompson, P.A., Bonham, P., Waite, A.M., Clementson, L.A., Cherukuru, N., Hassler, C.S., Doblin, M.A. 2011. Contrasting oceanographic conditions and phytoplankton communities on the east and west coasts of Australia. *Deep-Sea Res II.* 58, 645–663.

REFERENCES

Thurman, E.M. Malcolm, R.L. 1981. Preparative isolation of aquatic humic substances. *Environ. Sci. Technol*. 15, 463–466.

Thurman, E.M. 1985. Aquatic humic substances. In: *Organic geochemistry of natural waters*. Ed. E. M. Thurman. pp. 273–361. Springer, Dortrecht, Netherlands.

Tovar-Sanchez, A., Sañudo-Wilhelmy, S.A., Garcia-Vargas, M., Weaver, R.S., Popels, L.C. & Hutchins, D.A. 2003. A trace metal clean reagent to remove surface-bound iron from marine phytoplankton. *Mar. Chem.* 82, 91–99.

Trapp, J.M., Millero, F.J., Prospero, J.M. 2010. Trends in the solubility of iron in dust-dominated aerosols in the equatorial Atlantic trade winds: Importance of iron speciation and sources. *Geochem. Geophys. Geosys*. 11, Q03014, doi:10.1029/2009GC002651.

Tsuda, A., Takeda, S., Saito, H., Nishioka, J., Nojiri, Y., Kudo, I., Kiyosaea, H., Shiomoto, A., Imai, K., Ono, T., Shimamoto, A., Taumune, D., Yoshimura, T., Aono, T., Hinuma, A., Kinugasa, M., Suzuki, K., Sohrin, Y., Noiri, Y., Tani, H., Deguchi, Y., Tsurushima, N., Ogawa, H., Fukami, K., Kuma, K., Saino, T. 2003. A Mesoscale Iron Enrichment in the Western Subarctic Pacific Induces a Large Centric Diatom Bloom. *Science.* 300, 958-961.

Turner, S.M., Nightingale, P.D., Spokes, L.J., Liddicoat, M.I., Liss, P.S. 1996. Increased dimethyl sulphide concentrations in sea-water from in-situ iron enrichment. *Nature.* 383, 513–517.

van den Berg, C.M.G.1995. Evidence for organic complexation of iron in seawater. *Mar. Chem.* 50, 139–157.

Van Heukelem, L., Thomas, C. 2001. Computer assisted high performance liquid chromatography method development with applications to the isolation and analysis of phytoplankton pigments. *J. Chromatogr. A* 910, 31–49. doi:10.1016/S0378-4347(00)00603-4

Van Trump, J.I., Rivera Vega, F.J., Coates, J.D. 2013. Natural organic matter as a global antennae for primary production. *Astrobiology*. 13, 476-482, doi: 10.1089/ast.2012.0912.

REFERENCES

Velasquez, I., Nunn, B.L., Ibisanmi, E., Goodlett, D.R., Hunter, K.A. Sander, S.G. 2011. Detection of hydroxamate siderophores in coastal and Sub-Antarctic waters off the South Eastern Coast of New Zealand. *Mar. Chem*. 126, 97–107.

Veldhuis, M., de Baar, H.J.W. 2005. Iron resources and oceanic nutrients: advancement of global environment simulations. *J Sea Res.* 53, 1–6.

Verdugo. 2004. The role of marine gel-phase on carbon cycling in the ocean. *Mar. Chem.* 92, 65–66.

Viollier, E., Inglett, P.W., Hunter, K., Roychoudhury, A.N., van Cappellen, P. 2000. The ferrozine method revisited: Fe(II)/Fe(III) determination in natural waters. *App. Geochem*. 15, 785–790.

Visser, F., Gerringa, L.J.A., Van der Gaast, S.J., de Baar, H.J.W., Timmermans, K.R. 2003. The role of the reactivity and content of iron of aerosol dust on growth rates of two Antarctic diatom species. *J. Phycol.* 39, 1085–1094.

Vodacek, A., Blough, N. V., DeGrandpre, M. D., Peltzer, E. T., and Nelson, R. K. 1997. Seasonal variation of CDOM and DOC in the Middle Atlantic Bight: Terrestrial inputs and photooxidation. *Limnol. Oceanogr* 42, 674–686.

Vong, L., Laës, A., Blain, S. 2007. Determination of iron–porphyrin-like complexes at nanomolar levels in seawater. *Anal. Chim. Acta.* 588, 237–244.

Vraspir, J.M., Butler, A. 2009. Chemistry of marine ligands and siderophores. *Annu. Rev. Mar. Sci.* 1, 43–63.

Waite, T.D., Morel, F.M.M. 1984. Photoreductive dissolution of colloidal iron oxides in natural waters. *Environ. Sci. Technol.* 18, 860–868

Waite, T.D., Torikov, A., Smith, J.D. 1986. Photo assisted dissolution of colloidal iron-oxides by thiol-containing compounds 1. Dissolution of hematite (alpha-Fe2O3). *J. Colloid Interface Sci*. 112, 412–420.

REFERENCES

Waite, T.D. 2001. Thermodynamics of the iron system in seawater. In *The biogeochemistry of iron in seawater.* Eds. D.R. Turner, K.A. Hunter. John Wiley & Sons, UK. pp 291–342.

Watson, A.J. 2001. Iron limitation in the oceans. In *The biogeochemistry of iron in seawater.* Eds. D.R. Turner, K.A. Hunter. John Wiley & Sons, UK. pp 9–40.

Wells, M.L., Price, N.M., Bruland, K.W. 1995. Iron chemistry in seawater and its relationship to phytoplankton: a workshop report. *Mar. Chem.* 48, 157–182.

Wells, M. 1998. Marine colloids: A neglected dimension. *Nature.* 319, 530–531.

Wells, M. 1999. Manipulating iron availability in nearshore waters. *Limnol. Oceanogr.* 44, 1002–1008

Wells, M.L., Trick, C.G., Cochlan, W.P., Beall, B. 2009. Persistence of iron limitation in the Western subarctic Pacific SEEDS II mesoscale fertilization experiment. *Deep-Sea Res. II*. 56, 2910–2821.

Whitfield, M. 2001. Interactions between phytoplankton and trace metals in the ocean. *Adv. Mar. Biol.* 41, 3–128.

Wilhelm, S. W., Trick, C.G. 1994. Iron-limited growth of cyanobacteria: Multiple siderophore production is a common response. *Limnol. Oceanogr.* 39, 1979–1984.

Wilhelm, S. W. 1995. Ecology of iron-limited cyanobacteria: A review of physiological responses and implications for aquatic systems. *Aquat. Microb. Ecol*. 9, 265–303.

Wilhelm, S. W., Suttle , C.A. 1999 . Viruses and nutrient cycles in the sea, *Bio Science*, 49, 781–788.

Witter, A.E., Hutchins, D.A., Butler, A., Luther III, G.W. 2000. Determination of conditional stability constants and kinetic constants for strong model Fe-binding ligands in seawater. *Mar. Chem.* 69, 1–17.

Witter, A.E., Lewis, B.L., Luther III, G.W. 2000. Iron speciation in the Arabian Sea. *Deep-Sea. Res. II.* 47, 1517–1539.

REFERENCES

Willey, J.D., Kieber, R.J., Seaton, P.J., Miller, C. 2008. Rainwater as a source of Fe(II)-stabilizing ligands to seawater. *Limnol. Oceanogr*. 53, 1678–1684

Worms, I., Simon, D.F., Hassler, C.S., Wilkinson, K.J. 2006. Bioavailability of trace metals to aquatic microorganisms: importance of chemical, biological and physical processes on biouptake. *Biochemie.* 88, 1721–1731.

Wozniak, A.S., Shelley, R.U. Sleighter, R.L., Abdulla, H.A.N., Morton, P.L., Landing, W.M., Hatcher, P.G. 2013. Relationships among aerosol water soluble organic matter, iron and aluminum in European, North African, and Marine air masses from the 2010 US GEOTRACES cruise. *Mar. Chem.* 154, 24–33.

Wu, J., Luther III, G.W.1994. Size-fractionated iron concentrations in the water column of the western North Atlantic Ocean. *Limnol. Oceanogr.* 39, 1119–1129.

Wu, J.F. & Luther, G.W. 1995. Complexation of Fe(III) by natural organic ligands in the Northwest Atlantic Ocean by a competitive ligand equilibration method and a kinetic approach. *Mar. Chem.* 50, 159–177.

Wu, J., Boyle, E., Sunda, W., Wen, L-S. 2001. Soluble and colloidal iron in the oligotrophic North Atlantic and North Pacific. *Science.* 293, 847–849.

Wu, L., Cai, W., Zhang, L., Nakamura, H., Timmermann, A., Joyce, T., McPhaden, M.J., Alexander, M., Qiu, B., Visbeck, M., Chang, P., Giese, B. 2012. Enhanced warming over the global subtropical western boundary currents. *Nature Climate Change*. DOI:10.1038/nclimate1353.

Yang, R., van den Berg, C.M.G. 2009. Metal complexation by humic substances in seawater. *Environ. Sci. Technol.* 43, 7192–7197.

Ziegler, S., Benner, R. 2000. Effects of solar radiation on dissolved organic matter cycling in a subtropical seagrass meadow. *Limnol. Oceanogr*. 45, 257–266.